

University of Montana

## ScholarWorks at University of Montana

---

Graduate Student Theses, Dissertations, &  
Professional Papers

Graduate School

---

2003

### Poly(alkylene D-aldaramides) and their corresponding esters: Synthesis and conformational studies

Jinsong Zhang

*The University of Montana*

Follow this and additional works at: <https://scholarworks.umt.edu/etd>

**Let us know how access to this document benefits you.**

---

#### Recommended Citation

Zhang, Jinsong, "Poly(alkylene D-aldaramides) and their corresponding esters: Synthesis and conformational studies" (2003). *Graduate Student Theses, Dissertations, & Professional Papers*. 9481. <https://scholarworks.umt.edu/etd/9481>

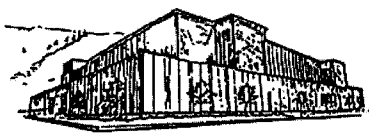
This Dissertation is brought to you for free and open access by the Graduate School at ScholarWorks at University of Montana. It has been accepted for inclusion in Graduate Student Theses, Dissertations, & Professional Papers by an authorized administrator of ScholarWorks at University of Montana. For more information, please contact [scholarworks@mso.umt.edu](mailto:scholarworks@mso.umt.edu).

# NOTE TO USERS

This reproduction is the best copy available.

**UMI**<sup>®</sup>





**Maureen and Mike  
MANSFIELD LIBRARY**

The University of

**Montana**

---

Permission is granted by the author to reproduce this material in its entirety, provided that this material is used for scholarly purposes and is properly cited in published works and reports.

**\*\*Please check "Yes" or "No" and provide signature\*\***

Yes, I grant permission

X

No, I do not grant permission

Author's Signature: \_\_\_\_\_

Date: \_\_\_\_\_

12/31/2003

Any copying for commercial purposes or financial gain may be undertaken only with the author's explicit consent.

---



# Poly(alkylene D-aldaramides) and their Corresponding Esters

## – Synthesis and Conformational Studies

by

Jinsong Zhang

M. S. Chinese Academy of Sciences, Beijing, China, 1997

B. S. Shandong Normal University, Jinan, China, 1994

Presented in partial fulfillment of the requirements

for the degree of

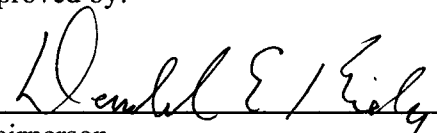
Doctor of Philosophy

Department of Chemistry

The University of Montana

2003

Approved by:

  
Chairperson

  
Dean, Graduate School

1-12-04  
Date

UMI Number: 3115915

Copyright 2004 by  
Zhang, Jinsong

All rights reserved.

### INFORMATION TO USERS

The quality of this reproduction is dependent upon the quality of the copy submitted. Broken or indistinct print, colored or poor quality illustrations and photographs, print bleed-through, substandard margins, and improper alignment can adversely affect reproduction.

In the unlikely event that the author did not send a complete manuscript and there are missing pages, these will be noted. Also, if unauthorized copyright material had to be removed, a note will indicate the deletion.

**UMI**<sup>®</sup>

---

UMI Microform 3115915

Copyright 2004 by ProQuest Information and Learning Company.

All rights reserved. This microform edition is protected against unauthorized copying under Title 17, United States Code.

ProQuest Information and Learning Company  
300 North Zeeb Road  
P.O. Box 1346  
Ann Arbor, MI 48106-1346

**Poly(alkylene D-aldaramides) and their Corresponding Esters – Synthesis and Conformational Studies****Director: Donald E. Kiely** DEK.

Poly(alkylene D-aldaramides) and the corresponding monomer alkylendiammonium D-aldarate salts/amic acid salts were synthesized. These novel salts/amic acid salts can undergo a two step polycondensation to afford poly(alkylene D-aldaramides). The 1:1 molar ratio of the acid and amine units was employed to fulfill the stoichiometry requirement of polycondensation reactions. This improved new method to prepare polyhydroxypolyamides is a valuable contribution to the exciting blend of carbohydrate and polymer chemistry.

A gel permeation chromatography method to determine molecular weights and molecular weight distribution of poly(alkylene D-aldaramides) was established. Refractive index, light scattering and viscometric detectors were applied for conventional and universal calibration. It was shown that both the simplified  $^1\text{H}$  NMR end-group analysis and the GPC measurement give valuable molecular weight information, with the GPC measurements giving more detailed information, e.g., molecular weight distribution.

Molecular mechanics calculations were applied to conformational studies of 2,3,4,5-tetra-*O*-acyl-*N,N'*-dialkyl-D-glucaramides and the corresponding polymer. A “model building” approach and Monte Carlo dihedral angle search method were both applied.  $^1\text{H}$  NMR coupling constant information provided a preliminary assignment of the corresponding conformation of the glucaryl unit. “Building blocks” were generated according to the chirality and the structural components of the target molecule. The results from this model building approach were compared with those from the “systematic search” results and X-ray crystallography results.

A Monte Carlo – Molecular Mechanics conformational search package was generated with a random, automated, dihedral angle generator, the MM3 (92) molecular mechanics program, and an analysis program embedded in a Unix Script file. These programs were written in FORTRAN 77, and application of the package is reported.



**To my parents, Guangyin Zhang and Juanfeng Sun**

**To my husband, Jing Tao**

## ACKNOWLEDGEMENTS

I wish to show my deepest gratitude to my advisor, Dr. Donald E. Kiely, with whom I have had the pleasure of working for the past 4 years, for his guidance, support and friendship. Dr. Kiely's active involvement with all of his students and his personable nature has made working in the Kiely group both challenging and enjoyable.

Thanks are also expressed to the members of the dissertation committee: Dr. Nigel D. Priestley, Dr. Richard J. Field, Dr. Holly Thompson and Dr. J. Stephen Lodmell for their patience to me, concern with my project, and all the prompt response to any of my questions.

I wish to thank the entire Kiely group, Dr. Arvind Viswanathan, Kylie Kramer, Jay Brand and Christopher Timko, for the wonderful collaboration, discussion and friendship, Dr. Meryllyn Manley-Harris, for her demonstration of scientific dedication, Judith Kiely and Bobbi Offill for their patience and help, and Mrs. Doren Shafidadeh for the encouragement and financial support.

I would like to thank Dr. Kenneth I. Hardcastle at Emory University Crystallography Laboratory, Department of Chemistry, Emory University for the X-ray crystal structure determination for the compound in chapter 1. I would like to extend my thanks to Dr. Susan D. Styron, a previous graduate student of Dr. Kiely, for her help in conformational study, Dr. Michael Dowd and Jing Tao to write the Monte Carlo simulation program, Dr. John Gerdes to provide workstations for the complicated calculation, and his students, for technique support and help. I'd like to thank Dr. Earle Adams for the help in NMR operation and collaboration.

I would like to thank all the faculty and staff members of the Department of Chemistry at the University of Montana for their instruction, encouragement, help and friendship. Without them, I could not finish my study as successful as I did.

Finally, I express my highest gratitude to my parents, sister, Huiquan, and my husband, Jing, who have supported me through never-ending love, encouragement, generosity and friendship.

## TABLE OF CONTENTS

ABSTRACT.....	ii
DEDICATION.....	iii
ACKNOWLEDGMENT.....	iv
LIST OF TABLES.....	vi
LIST OF ILLUSTRATIONS.....	xii
CHAPTER 1 .....	1
CHAPTER 2 .....	76
CHAPTER 3 .....	113
CHAPTER 4 .....	158
CHAPTER 5 .....	182
APPENDIX 1.....	215
APPENDIX 2.....	248

## LIST OF TABLE

### Chapter 1. Conformational and X-ray Crystallographic Studies of 2,3,4,5-tetra-*O*-Acetyl-*N,N'*-Dimethyl-*D*-Glucaramide – Molecular Mechanics Using a Model Building Approach

<b>Table 1</b>	Chemical shifts ( $\delta$ , ppm) and coupling constants (J, Hz) for compounds <b>2</b> ~ <b>7e</b>	9
<b>Table 2</b>	Dihedral angle ( $\omega$ , °) set for 2,3,4,5-tetra- <i>O</i> -acetyl- <i>N,N'</i> -dimethyl- <i>D</i> -glucaramide ( <b>7a</b> )	10
<b>Table 3</b>	Torsion angles varied in MM3 studies of 2,3,4,5-tetra- <i>O</i> -acetyl- <i>N,N'</i> -dimethyl- <i>D</i> -glucaramide ( <b>7a</b> )	12
<b>Table 4</b>	Variable dihedral angles and starting conformations for systematic conformational study	14
<b>Table 5</b>	Minimized conformations <b>A</b> of <i>N</i> -methylacetamide used to establish a conformational model for O9-C1-N7-H19 and O14-C6-N8-H22 dihedral angle ( $\omega$ , °) of <b>7a</b>	16
<b>Table 6</b>	O9-C1-C2-O10 Dihedral angles of C1-C2 Model: ( <i>2R</i> )- <i>N</i> -methyl-2-acetoxypropanamide ( <b>B</b> )	19
<b>Table 7</b>	O13-C5-C6-O14 Dihedral angles of C5-C6 Model: ( <i>2S</i> )- <i>N</i> -methyl-2-acetoxypropanamide ( <b>D</b> )	20
<b>Table 8</b>	Dihedral angles ( $\omega$ , °) of atoms attached to C1 and C2 in the <b>B1</b> and <b>B3</b> conformations of ( <i>2R</i> )- <i>N</i> -methyl-2-acetoxypropanamide after MM3 minimization and <b>D1</b> and <b>D2</b> of ( <i>2S</i> )- <i>N</i> -methyl-2-acetoxypropanamide	21
<b>Table 9</b>	Minimized conformations ( <b>F</b> ) of methyl acetate used to establish a conformational model for the C2-O10-C44-O92, C3-O11-C53-O93, C4-O12-C62-O94, and C5-O13-C71-O95 dihedral angles ( $\omega$ , °) of <b>7a</b>	23
<b>Table 10</b>	Torsion angles ( $\omega$ , °) before and after MM3 calculation and final energies (kcal/mol) of ( <i>2S,3S</i> )-2,3-diacetoxybutane to determine the orientation of two adjacent acetoxy groups on C2, C3 with a dihedral angle of 60.0° between H15 and H16	26
<b>Table 11</b>	Conformations (minima) of ( <i>2S,3S</i> )-2,3-diacetoxybutane <b>G</b> (H15-C2-C3-H16 ca. -60.0°)	27
<b>Table 12</b>	Dihedral angles (°) of atoms attached to O10 and C2 of conformations <b>G3</b> , <b>G9</b> and <b>G6</b> of ( <i>2S,3S</i> )-2,3-diacetoxybutane (H15-C2-C3-H16 -60.0°)	29
<b>Table 13</b>	Torsion angles ( $\omega$ , °) before and after MM3 calculation and final energies (kcal/mol) of ( <i>2S,3S</i> )-2,3-diacetoxybutane to determine the orientation of two adjacent acetoxy groups on C2, C3 with a dihedral angle of 60.0° between H15 and H16	30

<b>Table 14</b>	Conformations (minima) of (2 <i>S</i> ,3 <i>S</i> )-2,3-diacetoxybutane <b>J</b> (H15-C2-C3-H16 ca. +60.0°)	31
<b>Table 15</b>	Torsion angles ( $\omega$ , °) before and after MM3 calculation and final energies (kcal/mol) of (2 <i>S</i> ,3 <i>R</i> )-2,3-diacetoxybutane to determine the orientation of two adjacent acetoxy groups on C4, C5 with a dihedral angle of -60.0° between H17 and H18	33
<b>Table 16</b>	Conformations (minima) of (2 <i>S</i> ,3 <i>R</i> )-2,3-diacetoxybutane <b>K</b> (H17-C4-C5-H18 ca. -60.0°)	34
<b>Table 17</b>	Torsion angles ( $\omega$ , °) before and after MM3 calculation and final energies (kcal/mol) of (2 <i>S</i> ,3 <i>R</i> )-2,3-diacetoxybutane model <b>L</b> to determine the orientation of two adjacent acetoxy groups on C4, C5 with a dihedral angle +60.0° between H17 and H18	35
<b>Table 18</b>	Conformations (minima) of (2 <i>S</i> ,3 <i>R</i> )-2,3-diacetoxybutane <b>L</b> (H17-C4-C5-H18 ca. +60.0°)	38
<b>Table 19</b>	Torsion angles ( $\omega$ , °) before and after MM3 calculation and final energies (kcal/mol) of (2 <i>R</i> ,3 <i>R</i> )-2,3-acetoxybutane <b>M</b> to determine the orientation of two adjacent acetoxy groups on C3, C4 with a dihedral angle of 180.0° between H16 and H17	40
<b>Table 20</b>	Minima of (2 <i>R</i> ,3 <i>R</i> )-2,3-acetoxybutane <b>M</b> (H16-C3-C4-H17 ca. 180.0°)	41
<b>Table 21</b>	Dihedral angles (°) of some minima of (2 <i>R</i> ,3 <i>R</i> )-2,3-acetoxybutane <b>M</b> (H16-C3-C4-H17 ca. 180.0°)	41
<b>Table 22</b>	Sixteen possible conformations of every rotamer of 2,3,4,5-tetra- <i>O</i> -acetyl- <i>N,N'</i> -dimethyl-D-glucaramide ( <b>7a</b> )	44
<b>Table 23</b>	MM3 calculated energies (kcal/mol) of different 2,3,4,5-tetra- <i>O</i> -acetyl- <i>N,N'</i> -dimethyl-D-glucaramide ( <b>7a</b> ) rotamers	46
<b>Table 24</b>	Calculated torsion angles ( $\omega$ , °) of the final four low energy rotamers of <b>7a</b> as compared to the torsion angles suggested by the model studies	48
<b>Table 25</b>	Energy distribution for low-energy conformations <b>1m</b> - <b>4m</b> of 2,3,4,5-tetra- <i>O</i> -acetyl- <i>N,N'</i> -dimethyl-D-glucaramide ( <b>7a</b> ) using MM3 at dielectric constant 1.0	51
<b>Table 26</b>	MM3 calculated dihedral angles ( $\omega$ , °) of 2,3,4,5-tetra- <i>O</i> -acetyl- <i>N,N'</i> -dimethyl-D-glucaramide ( <b>7a</b> )	52
<b>Table 27</b>	Vicinal coupling constants (J, Hz) of 2,3,4,5-tetra- <i>O</i> -acetyl- <i>N,N'</i> -dimethyl-D-glucaramide ( <b>7a</b> ) (Karplus/Altona calculated and <sup>1</sup> H NMR).	53
<b>Table 28</b>	Distances (Å) of amide hydrogens and oxygen atoms (either carbonyl O or ester O) of low energy minima ( <b>1m</b> – <b>4m</b> ) of <b>7a</b>	55

**Chapter 2. Application of A Model Building Approach to Molecular Mechanics (MM3) for Calculating Low Energy Conformations of Tetra-*O*-Acyl-*N,N'*-Dialkyl-D-Glucaramides to Predict Corresponding Polyamide Secondary Structures**

<b>Table 1</b>	Calculated torsion angles ( $\omega$ , °) of building blocks for <b>1</b>	78
<b>Table 2</b>	Conformational study of methyl propanate ( <b>A</b> ) to determine the O92=C44-C48-C96, O93=C53-C57-C101, O94=C62-C66-C106 and O95=C71-C75-C111 dihedral angle ( $\omega$ , °)	82
<b>Table 3</b>	Relevant dihedral angles ( $\omega$ , °) along C44-C48 bond of methyl propanate ( <b>A</b> ) minima	83
<b>Table 4</b>	Conformational study of methyl 2-methylpropanate ( <b>B</b> ) to determine the O92=C44-C48-C128, O93=C53-C57-C133, O94=C62-C66-C138, and O95=C71-C75-C143 dihedral angles ( $\omega_1$ , °) and the O92=C44-C48-C96, O93=C53-C57-C101, O94=C62-C66-C116, and O95=C71-C75-C111 dihedral angles ( $\omega_2$ , °)	85
<b>Table 5</b>	Relevant dihedral angles ( $\omega$ , °) along C44-C48 bond of methyl 2-methylpropanate ( <b>B</b> ) minima	86
<b>Table 6</b>	Conformational study of <i>N</i> -ethyl formamide ( <b>D</b> ) to determine the C1-N7-C27-C96 and C6-N8-C33-C112 dihedral angle ( $\omega$ , °)	88
<b>Table 7</b>	Relevant dihedral angles ( $\omega$ , °) along C27-N7 bond of <i>N</i> -ethyl formamide ( <b>D</b> ) minima	89
<b>Table 8</b>	Conformational study of <i>N</i> -ethyl acetamide ( <b>E</b> ) to determine the C1-N7-C27-C96 and C6-N8-C33-C112 dihedral angle ( $\omega$ , °)	90
<b>Table 9</b>	MM3 calculated energies (kcal/mol) of different 2,3,4,5-tetra- <i>O</i> -propanyl- <i>N,N'</i> -dimethyl-D-glucaramide ( <b>2</b> ) rotamers	92
<b>Table 10</b>	Energy distribution for low-energy conformations 1 – 4 of 2,3,4,5-tetra- <i>O</i> -propanyl- <i>N,N'</i> -dimethyl-D-glucaramide ( <b>2</b> ) using MM3 at dielectric constant 1.0	93
<b>Table 11</b>	Torsion angles ( $\omega$ , °) suggested by Propanate Model (methyl propanate ( <b>A</b> )) and the low energy conformations of rotamer 1 to 4 of <b>2</b>	95
<b>Table 12</b>	MM3 calculated energies (kcal/mol) of different 2,3,4,5-tetra- <i>O</i> -(2-methylpropanyl)- <i>N,N'</i> -dimethyl-D-glucaramide ( <b>3</b> ) rotamers	96
<b>Table 13</b>	Energy distribution for low-energy conformations 1 – 4 of 2,3,4,5-tetra- <i>O</i> -(2-methylpropanyl)- <i>N,N'</i> -dimethyl-D-glucaramide ( <b>2</b> ) using MM3 at dielectric constant 1.0	97
<b>Table 14</b>	Torsion angles ( $\omega$ , °) suggested by Isobutanate Model (methyl 2-methylpropanate ( <b>B</b> )) and the low energy conformations of rotamer 1 to 4 of <b>3</b>	98

<b>Table 15</b>	MM3 calculated energies (kcal/mol) of different rotamers of 2,3,4,5-tetra- <i>O</i> -(2,2-dimethylpropanyl)- <i>N,N'</i> -dimethyl-D-glucaramide ( <b>4</b> )	99
<b>Table 16</b>	Energy distribution for low-energy conformations 1 – 4 of 2,3,4,5-tetra- <i>O</i> -(2,2-dimethylpropanoyl)- <i>N,N'</i> -dimethyl-D-glucaramide ( <b>2</b> ) using MM3 at dielectric constant 1.0	100
<b>Table 17</b>	MM3 calculated dihedral angles ( $\omega$ , °) for 2,3,4,5-tetra- <i>O</i> -acyl- <i>N,N'</i> -dimethyl-D-glucaramide ( <b>1 - 4</b> )	101
<b>Table 18</b>	Calculated and experimental ( <sup>1</sup> H NMR) coupling constants (J, Hz) from global minima of 2,3,4,5-tetra- <i>O</i> -acyl- <i>N,N'</i> -dimethyl-D-glucaramides ( <b>1 - 4</b> )	101
<b>Table 19</b>	MM3 calculated energies (kcal/mol) of different rotamers of 2,3,4,5-tetra- <i>O</i> -acetyl- <i>N,N'</i> -dihexyl-D-glucaramide ( <b>5</b> )	102
<b>Table 20</b>	Energy distribution for low-energy conformations 1 – 4 of 2,3,4,5-tetra- <i>O</i> -acetyl- <i>N,N'</i> -dihexyl-D-glucaramide ( <b>5</b> ) using MM3 at dielectric constant 1.0	103
<b>Table 21</b>	MM3 calculated dihedral angles ( $\omega$ , °) of 2,3,4,5-tetra- <i>O</i> -acetyl- <i>N,N'</i> -dihexyl-D-glucaramide ( <b>5</b> )	105
<b>Table 22</b>	Vicinal coupling constants (J, Hz) for 2,3,4,5-tetra- <i>O</i> -acetyl- <i>N,N'</i> -dihexyl-D-glucaramide ( <b>5</b> ) (Karplus/Altona <sup>[4]</sup> calculated and <sup>1</sup> H NMR results)	105
<b>Table 23</b>	Hydrogen bonding of global minima <b>1</b> to <b>5</b> indicated by distances (Å) between amide hydrogen and ester oxygen atoms	106

### Chapter 3. Preparation of salts of selected D-alдарic acids and a new procedure for stereochemically random hydroxylated nylons preparation

<b>Table 1</b>	Formation of hexamethylenediammonium D-glucarate ( <b>2c</b> ) and amic acid salts <b>3c</b> and <b>4c</b> under different reaction conditions	122
<b>Table 2</b>	Formation of <b>2c</b> , <b>3c</b> and <b>4c</b> over a temperature range at different time intervals	123
<b>Table 3</b>	Preparation of poly(alkylene D-glucaramide) from alkylenediammonium D-glucarate and the corresponding amic acid salts	129
<b>Table 4</b>	Different ratios of DMSO to MeOH as solvent used to prepare poly(hexamethylene D-glucaramide) ( <b>7c</b> )	131
<b>Table 5</b>	Ethylene glycol and methanol as solvent for pre-polymerization of <b>7c</b>	133
<b>Table 6</b>	Effect of triethylamine on polymerization (prepolymer) of poly(hexamethylene D-glucaramide) ( <b>7c</b> )	135
<b>Table 7</b>	Reaction conditions and the corresponding polymers ( <b>7c</b> ) after postpolymerization	137

#### Chapter 4. GPC Study to Determine the Molecular Weight and Molecular Weight Distribution of Some Polyhydroxypolyamides

<b>Table 1</b>	GPC analysis results of molecular weight and molecular weight distribution of acetates (2) derived from the same poly(hexamethylene D-glucaramide) (1) prepolymer acetylated using the pyridine method (JZ040440 and <i>N</i> -methylimidazole method (JZ04047) with Waters – conventional calibration	170
<b>Table 2</b>	Reaction conditions for preparation of poly(hexamethylene D-glucaramide) (1) prepolymer samples and the GPC analysis of the corresponding acetates using the Viscotek instrument – universal calibration and conventional calibration methods	172
<b>Table 3</b>	GPC analysis of the acetates (2) of poly(hexamethylene D-glucaramide) (1) prepolymer (JZ04050_1) and postpolymer (JZ04050_2) pair (Waters – conventional calibration)	173
<b>Table 4</b>	GPC analysis of the poly(hexamethylene D-glucaramide) prepolymer (JZ04083) and postpolymer (JZ04084) acetates (2) (Viscotek – universal calibration)	177
<b>Table 5</b>	GPC analysis of poly(tetramethylene tetra- <i>O</i> -acetyl-D-glucaramide) (4) with Waters – conventional calibration and Viscotek – universal and conventional calibration	178
<b>Table 6</b>	GPC analysis results of acetates (4) from poly(tetramethylene D-glucaramide) prepolymer (JZ04081) and postpolymer (JZ04082) (Viscotek – universal calibration and conventional calibration)	179
<b>Table 7</b>	GPC analysis of poly(3,6-dioxa-1,8-octamethylene tetra- <i>O</i> -acetyl galacataramide) (6) (Viscotek – universal and conventional calibration)	179
<b>Table</b>	<b>8.</b> GPC analysis results of poly(dodecamethylene tetra- <i>O</i> -acetyl galacataramide) (8) (Viscotek – universal calibration and conventional calibration)	180

#### Chapter 5. Monte Carlo Dihedral Angle Search and Molecular Mechanics Study. Method and Application

<b>Table 1</b>	Atom types in MM3 (92)	197
<b>Table 2</b>	Selected torsion parameters of MM3 (92)	198
<b>Table 3</b>	Total steric energies ( <i>E</i> , kcal/mol) and torsion angles ( $\omega$ , °) of butane minima at dielectric constant 1.5	204
<b>Table 4</b>	Total steric energy ( <i>E</i> , kcal/mol) and torsion angles ( $\omega$ , °) of <i>N</i> -methylacetamide (2) minima	205
<b>Table 5</b>	Number of new conformations found for MC-MM3 study of 3	207



<b>Table 6</b>	Four low energy conformations obtained from MC-MM3 study of <b>3</b> , total steric energy (E, kcal/mol) and backbone torsion angles ( $\omega$ , °)	208
<b>Table 7</b>	Comparison of global minimum obtained from two different conformational analysis approaches (“model-building approach” and Monte Carlo dihedral angle search)	210

## LIST OF ILLUSTRATION

### Chapter 1. Conformational and X-ray Crystallographic Studies of 2,3,4,5-tetra-*O*-Acetyl-*N,N'*-Dimethyl-*D*-Glucaramide – Molecular Mechanics Using a Model Building Approach

<b>Figure 1</b>	Three classes of stereochemically different poly(alkylene <i>D</i> -glucaramides)	2
<b>Figure 2</b>	<sup>1</sup> H NMR spectra (CDCl <sub>3</sub> ) of poly(hexamethylene 2,3,4,5-tetra- <i>O</i> -acetyl- <i>D</i> -glucaramide) ( <b>3</b> ) and the model compound 2,3,4,5-tetra- <i>O</i> -acetyl- <i>N,N'</i> -dihexyl- <i>D</i> -glucaramide ( <b>5a</b> ). Protons H15 – H18	3
<b>Figure 3</b>	1,3-Interactions between the acetoxy groups on C2 and C4 on diamides <b>5a</b> and <b>7a</b> and polyamide <b>3</b>	6
<b>Figure 4</b>	The extended conformation and four starting rotamers of <b>7a</b>	11
<b>Figure 5</b>	Numbering system for compound <b>7a</b>	13
<b>Figure 6</b>	“Building blocks” (A - M) for conformational study of tetra- <i>O</i> -acetyl- <i>N,N'</i> -dimethyl- <i>D</i> -glucaramide ( <b>7a</b> )	15
<b>Figure 7</b>	End C Model of <b>7a</b> : <i>N</i> -methylacetamide	16
<b>Figure 8</b>	Lower energy ( <b>A3</b> ) and higher energy ( <b>A1</b> ) conformations of <i>N</i> -methylacetamide	17
<b>Figure 9</b>	C1-C2 Model of <b>7a</b> : ( <i>2R</i> )- <i>N</i> -methyl-2-acetoxypropanamide ( <b>B</b> ) and C5-C6 Model of <b>7a</b> : ( <i>2S</i> )- <i>N</i> -methyl-2-acetoxypropanamide ( <b>D</b> )	18
<b>Figure 10</b>	Newman projections of <b>B1</b> and <b>B3</b> of ( <i>2R</i> )- <i>N</i> -methyl-2-acetoxypropanamide looking down the C1-C2 bond, and <b>D1</b> and <b>D2</b> of ( <i>2S</i> )- <i>N</i> -methyl-2-acetoxypropanamide looking down the C6-C5 bond	20
<b>Figure 11</b>	Acyloxy Rotamer Model of <b>7a</b> : methyl acetate	22
<b>Figure 12</b>	The lower energy ( <b>F1</b> , left) and higher energy ( <b>F3</b> , right) conformations of methyl acetate – Acyloxy Rotamer Model	23
<b>Figure 13</b>	Vicinal Acyloxy Model I for C2, C3 vicinal acetyl groups of <b>7a</b> , rotamers 3 and 4: [( <i>2S,3S</i> )-2,3-diacetoxybutane <b>G</b> (H15-H16: -60.0°)]	25
<b>Figure 14</b>	Newman projection formula of <b>G3</b> , <b>G9</b> and <b>G6</b> of ( <i>2S,3S</i> )-2,3-diacetoxybutane (H15-C2-C3-H16 -60.0°) looking down the O10-C2 bond (R = -C(O)CH <sub>3</sub> , R' = -CH(CH <sub>3</sub> )OC(O)CH <sub>3</sub> )	27
<b>Figure 15</b>	Vicinal Acyloxy Model II [( <i>2S,3S</i> )-2,3-diacetoxybutane (H15-H16: 60.0°)] for C2, C3 vicinal acetoxy groups of <b>7a</b> : rotamers 1 and 2.	29
<b>Figure 16</b>	Vicinal Acyloxy Model III: [( <i>2S,3R</i> )-2,3-diacetoxybutane <b>K</b> (H17-H18: -60.0°)] for C4, C5 vicinal acetoxy groups of <b>7a</b> , rotamers 1 and 3	32

<b>Figure 17</b>	Vicinal Acyloxy Model IV: [(2 <i>S</i> ,3 <i>R</i> )-2,3-diacetoxybutane <b>L</b> (H17-C4-C5-H18 ca. +60.0°)] for vicinal C3, C4 acetoxy groups of <b>7a</b> , rotamers 1 - 4	37
<b>Figure 18</b>	Vicinal Acyloxy Model V of <b>7a</b> : (2 <i>R</i> ,3 <i>R</i> )-2,3-acetoxybutane <b>M</b> (H16-H17: 180.0°)	39
<b>Figure 19</b>	Newman projections of (2 <i>R</i> ,3 <i>R</i> )-2,3-acetoxybutane <b>M</b> (H16-C3-C4-H17 180.0°) to compare conformations <b>M1</b> , <b>M3</b> and <b>M2</b> with O12 in the front and C4 in the back	42
<b>Figure 20</b>	Low-energy conformations <b>1m</b> – <b>4m*</b> derived from starting rotamers 1 - 4 ( <b>7a</b> )	50
<b>Figure 21</b>	Minimum energy (MM3) rotamer <b>3m</b> ( <b>7a</b> ) (Tubes and Spheres-and-Sticks rendering)	52
<b>Figure 22</b>	Intramolecular hydrogen bonding of rotamer <b>3m</b> ( <b>7a</b> , the distance of C71=O95···H22-N8 is 1.954 Å and the distance of C6=O14···H19-N7 calculated to be 1.921 Å)	54
<b>Figure 23</b>	Superimposed conformations of global minima of both tetra- <i>O</i> -acetyl <i>N,N'</i> -dimethyl-D-glucaramide ( <b>7a</b> , rotamer <b>3m</b> , numbered carbons) and D-glucaramide (conformation <b>8-1a</b> ). The numbers the figure are for tetra- <i>O</i> -acetyl- <i>N,N'</i> -dimethyl-D-glucaramide ( <b>7a</b> , rotamer <b>3m</b> )	57
<b>Figure 24</b>	X-ray crystal structure of 2,3,4,5-tetra- <i>O</i> -acetyl- <i>N,N'</i> -dimethyl-D-glucaramide ( <b>7a</b> )	59
<b>Figure 25</b>	Intermolecular hydrogen bonding between pairs of <b>7a</b> in the solid state	60
<b>Figure 26</b>	A comparison of the crystal structures of 2,3,4,5-tetra- <i>O</i> -acetyl- <i>N,N'</i> -dimethyl-D-glucaramide ( <b>7a</b> ) and <i>N,N'</i> -dimethyl-D-glucaramide	61
<b>Figure 27</b>	Low energy conformations (dielectric constant 1.0) of 2,3,4,5-tetra- <i>O</i> -acetyl- <i>N,N'</i> -dimethyl-D-glucaramide ( <b>7a</b> , rotamer <b>3m</b> ) and the X-ray crystal structure of sodium potassium D-glucarate	62

**Chapter 2. Application of A Model Building Approach to Molecular Mechanics (MM3) for Calculating Low Energy Conformations of Tetra-*O*-Acyl-*N,N'*-Dialkyl-D-Glucaramides to Predict Corresponding Polyamide Secondary Structures**

<b>Figure 1</b>	2,3,4,5-Tetra- <i>O</i> -acetyl- <i>N,N'</i> -dimethyl-D-glucaramide ( <b>1</b> )	76
<b>Figure 2</b>	Four starting rotamers of <b>1</b> , generated according to vicinal H15, H16, H17 and H18 <sup>1</sup> H NMR coupling constants information	78
<b>Figure 3</b>	The compounds modeled in the previous chapter ( <b>1</b> ) and this study ( <b>2</b> - <b>5</b> ) and their H16-H17 couplings (in parentheses)	80
<b>Figure 4</b>	Propanate Model ----- methyl propanate ( <b>A</b> )	81

<b>Figure 5</b>	Newman projections along C44-C48 bond of methyl propanate (A) minima (R = -OCH <sub>3</sub> )	83
<b>Figure 6</b>	Isobutanate Model – methyl 2-methylpropanate (B)	85
<b>Figure 7</b>	Newman projection of methyl 2-methylpropanate (B) minima: along C44-C48 bond	86
<b>Figure 8</b>	2,3,4,5-tetra- <i>O</i> -Acetyl- <i>N,N'</i> -dihexyl-D-glucaramide (5), <i>N</i> -ethylformamide (D) and <i>N</i> -ethylacetamide (E)	88
<b>Figure 9</b>	Newman projections along the N7-C27 bond of the <i>N</i> -ethylformamide (D) minima [R = C(O)H]	89
<b>Figure 10</b>	Lowest energy conformations for the minimized conformations of the 2,3,4,5-tetra- <i>O</i> -acyl- <i>N,N'</i> -dimethyl-D-glucaramides 1 – 4 (the upper row, from left to right are 1 and 2; the bottom row, from left to right are 3 and 4, respectively)	94
<b>Figure 11</b>	2,3,4,5-Tetra- <i>O</i> -acetyl- <i>N,N'</i> -dihexyl-D-glucaramide (5) low energy rotamer 3 (Tubes and Spheres-and-Sticks rendering)	104
<b>Figure 12</b>	Hydrogen bonds of global minima of 1 – 5	107
<b>Figure 13</b>	Repeating oligomer 3G6G6G6G3 (composed of four acetylated glucaryl units, with two <i>N</i> -propyl terminals, and three repeating hexamethylene units between the acetylated glucaryl units), as a segment of a stereoregular, repeating <i>head, tail</i> - poly(hexamethylene 2,3,4,5-tetra- <i>O</i> -acetyl-D-glucaramide)	108
<b>Figure 14</b>	Repeating oligomer 3G6G6G6G3 (top, represent repeating <i>head, tail</i> - poly(hexamethylene 2,3,4,5-tetra- <i>O</i> -acetyl-D-glucaramide)) and alternating oligomer 3G'6G'6G'6G'3 (bottom, composed of four acetylated glucaryl units, with two <i>N</i> -propyl terminals, and three repeating hexamethylene units between the acetylated glucaryl units), as a segment of a alternating <i>head, tail</i> – <i>tail, head</i> - poly(hexamethylene 2,3,4,5-tetra- <i>O</i> -acetyl-D-glucaramide)	109

### Chapter 3. Preparation of salts of selected D-aldaric acids and a new procedure for stereochemically random hydroxylated nylons preparation

<b>Scheme 1</b>	Nylon 66 and hydroxylated nylons	115
<b>Scheme 2</b>	Aminolysis of an ester with a herero atom at the $\alpha$ position (Rate enhancement according to Ogata et al <sup>[15]</sup> )	117
<b>Scheme 3</b>	Preparation of hexamethylenediammonium D-glucarate (2c)	120
<b>Scheme 4</b>	Disalt (2c) and <i>N</i> -(6-aminohexyl)-D-glucar-6-amic acid salt (3c) formation in the reaction of a diamine (hexamethylenediamine) with an acid/lactone form of D-glucaric acid	124
<b>Scheme 5</b>	Preparation of alkylenediammonium D-glucarate (2a – 2g) and the corresponding amic acid salt (3a – 3g and 4a – 4g)	126

<b>Scheme 6</b>	Preparation of alkylenediammonium D-aldarate ( <b>5a – 5c</b> , <b>5e – 5h</b> and <b>6c</b> )	127
<b>Scheme 7</b>	Preparation of poly(alkylene D-glucaramide)	130
<b>Scheme 8</b>	Post-polymerization for random poly(alkylene D-glucaramide)	136

#### Chapter 4. GPC Study to Determine the Molecular Weight and Molecular Weight Distribution of Some Polyhydroxypolyamides

<b>Figure 1</b>	Distribution of molecular weight in a typical polymer <sup>[1]</sup>	159
<b>Figure 2</b>	Development and detection of size separation by GPC <sup>[10]</sup>	163
<b>Figure 3</b>	Schematic of a GPC system <sup>[10]</sup>	164
<b>Figure 4</b>	Chromatograms of acetates <b>2</b> derived from same prepolymer <b>1</b> using the pyridine method (top) and <i>N</i> -methylimidazole method (bottom)	171
<b>Figure 5</b>	Chromatogram of poly(hexamethylene D-glucaramide) prepolymer and postpolymer acetates – Waters RI instrument	174
<b>Figure 6</b>	Viscotek chromatograms (RI chromatograms) of acetylated poly(hexamethyl-ene D-glucaramide) pre (top) and post (bottom) polymers	175
<b>Figure 7</b>	Viscotek chromatograms (RI and viscometry) of acetylated poly(hexamethyl-ene D-glucaramide) pre (top) and post (bottom) polymers	176

#### Chapter 5. Monte Carlo Dihedral Angle Search and Molecular Mechanics Study. Method and Application

<b>Figure 1</b>	Schematic representation of the four key contributions to a molecular mechanics force field: bond stretching, angle bending, torsional terms and non-bonded interactions	185
<b>Scheme 1</b>	Flow diagram of MC-MM3	201
<b>Figure 2</b>	Newman projection of three minima of butane ( <b>1</b> ) along C2-C3 bond, from left to right are <b>1A</b> ( <i>gauche</i> ), <b>1B</b> ( <i>anti</i> ) and <b>1C</b> ( <i>gauche</i> ), respectively	204
<b>Figure 3</b>	Minima of <i>N</i> -methylacetamide ( <b>2</b> )	204
<b>Figure 4</b>	<b>C250</b> , the lowest energy conformation of <b>3</b> , tubing and spheres-and-sticks rendering ( <sub>2</sub> G <sup>-</sup> )	208
<b>Figure 5</b>	Global minimum ( <b>3m</b> ) generated from “model building” approach with the Tripos MM3 force field and <b>C250</b> generated from Monte Carlo dihedral angle search with MM3 (92) Allinger force field	210

## Appendix 1. Spectra of Compounds in Chapter 1 and Chapter 2

<b>Figure 1</b>	<sup>1</sup> H NMR (DMSO-d <sub>6</sub> ) spectrum of methyl D-glucarate 1,4-lactone ( <b>1</b> )	215
<b>Figure 2</b>	<sup>1</sup> H NMR (DMSO-d <sub>6</sub> ) spectrum of methyl D-glucarate 1,4-lactone ( <b>1</b> )	216
<b>Figure 3</b>	<sup>1</sup> H NMR (CDCl <sub>3</sub> ) spectrum of poly(hexamethylene D-glucaramide) ( <b>2</b> )	217
<b>Figure 4</b>	<sup>1</sup> H NMR (CDCl <sub>3</sub> ) spectrum of poly(hexamethylene tetra- <i>O</i> -acetyl-D-glucaramide) ( <b>3</b> )	218
<b>Figure 5</b>	<sup>1</sup> H NMR (DMSO-d <sub>6</sub> ) spectrum of <i>N,N'</i> -dihexyl-D-glucaramide ( <b>4</b> )	219
<b>Figure 6</b>	<sup>1</sup> H NMR (DMSO-d <sub>6</sub> ) spectrum of <i>N,N'</i> -dihexyl-D-glucaramide ( <b>4</b> ) 3.4 – 8.2 ppm	220
<b>Figure 7</b>	<sup>1</sup> H NMR (DMSO-d <sub>6</sub> ) spectrum of <i>N,N'</i> -dihexyl-D-glucaramide ( <b>4</b> , add 2 drops D <sub>2</sub> O)	221
<b>Figure 8</b>	<sup>1</sup> H NMR (DMSO-d <sub>6</sub> ) spectrum of <i>N,N'</i> -dihexyl-D-glucaramide ( <b>4</b> , add 2 drops D <sub>2</sub> O) 3.58 – 4.12 ppm	222
<b>Figure 9</b>	<sup>1</sup> H NMR (CDCl <sub>3</sub> ) spectrum of tetra- <i>O</i> -acetyl- <i>N,N'</i> -dihexyl-D-glucaramide ( <b>5a</b> )	223
<b>Figure 10</b>	<sup>1</sup> H NMR (CDCl <sub>3</sub> ) spectrum of tetra- <i>O</i> -acetyl- <i>N,N'</i> -dihexyl-D-glucaramide ( <b>5a</b> ) 5.00 – 6.40 ppm	224
<b>Figure 11</b>	Mass (TOF electron spray) spectrum of tetra- <i>O</i> -acetyl- <i>N,N'</i> -dihexyl-D-glucaramide ( <b>5a</b> )	225
<b>Figure 12</b>	<sup>1</sup> H NMR (CDCl <sub>3</sub> ) spectrum of tetra- <i>O</i> -propanyl- <i>N,N'</i> -dihexyl-D-glucaramide ( <b>5b</b> )	226
<b>Figure 13</b>	<sup>1</sup> H NMR (CDCl <sub>3</sub> ) spectrum of tetra- <i>O</i> -propanyl- <i>N,N'</i> -dihexyl-D-glucaramide ( <b>5b</b> ) 5.00 – 6.50 ppm	227
<b>Figure 14</b>	Mass (TOF electron spray) spectrum of tetra- <i>O</i> -propanyl- <i>N,N'</i> -dihexyl-D-glucaramide ( <b>5b</b> )	228
<b>Figure 15</b>	<sup>1</sup> H NMR (CDCl <sub>3</sub> ) spectrum of tetra- <i>O</i> -methylpropanyl- <i>N,N'</i> -dihexyl-D-glucaramide ( <b>5c</b> )	229
<b>Figure 16</b>	<sup>1</sup> H NMR (CDCl <sub>3</sub> ) spectrum of tetra- <i>O</i> -methylpropanyl- <i>N,N'</i> -dihexyl-D-glucaramide ( <b>5c</b> ) 5.00 – 6.50 ppm	230
<b>Figure 17</b>	Mass (TOF electron spray) spectrum of tetra- <i>O</i> -methylpropanyl- <i>N,N'</i> -dihexyl-D-glucaramide ( <b>5c</b> )	231
<b>Figure 18</b>	Mass (TOF electron spray) spectrum of tetra- <i>O</i> -dimethylpropanyl- <i>N,N'</i> -dihexyl-D-glucaramide ( <b>5d</b> )	231
<b>Figure 19</b>	<sup>1</sup> H NMR (CDCl <sub>3</sub> ) spectrum of tetra- <i>O</i> -benzoyl- <i>N,N'</i> -dihexyl-D-glucaramide ( <b>5e</b> )	233
<b>Figure 20</b>	<sup>1</sup> H NMR (CDCl <sub>3</sub> ) spectrum of tetra- <i>O</i> -benzoyl- <i>N,N'</i> -dihexyl-D-glucaramide ( <b>5e</b> ) 5.50 – 6.80 ppm	234
<b>Figure 21</b>	Mass (TOF electron spray) spectrum of tetra- <i>O</i> -benzoyl- <i>N,N'</i> -dihexyl-D-glucaramide ( <b>5e</b> )	235

<b>Figure 22</b>	<sup>1</sup> H NMR (DMSO-d <sub>6</sub> ) spectrum of dimethyl-D-glucaramide ( <b>6</b> )	236
<b>Figure 23</b>	<sup>1</sup> H NMR (DMSO-d <sub>6</sub> ) spectrum of dimethyl-D-glucaramide ( <b>6</b> ) 3.00 – 8.50 ppm	237
<b>Figure 24</b>	<sup>1</sup> H NMR (DMSO-d <sub>6</sub> ) spectrum of dimethyl-D-glucaramide ( <b>6</b> , add 6 drops D <sub>2</sub> O)	238
<b>Figure 25</b>	<sup>1</sup> H NMR (DMSO-d <sub>6</sub> ) spectrum of dimethyl-D-glucaramide ( <b>6</b> , add 6 drops D <sub>2</sub> O) 3.60 – 4.20 ppm	239
<b>Figure 26</b>	<sup>1</sup> H NMR (DMSO-d <sub>6</sub> ) spectrum of tetra- <i>O</i> -acetyl- <i>N,N'</i> - dimethyl-D-glucaramide ( <b>7a</b> )	240
<b>Figure 27</b>	<sup>1</sup> H NMR (DMSO-d <sub>6</sub> ) spectrum of tetra- <i>O</i> -acetyl- <i>N,N'</i> - dimethyl-D-glucaramide ( <b>7a</b> ) 4.50 – 8.50 ppm	241
<b>Figure 28</b>	Mass (TOF electron spray) spectrum of tetra- <i>O</i> -acetyl- <i>N,N'</i> - dimethyl-D-glucaramide ( <b>7a</b> )	242
<b>Figure 29</b>	<sup>1</sup> H NMR (CDCl <sub>3</sub> ) spectrum of tetra- <i>O</i> -propanyl- <i>N,N'</i> - dimethyl-D-glucaramide ( <b>7b</b> )	243
<b>Figure 30</b>	Mass (TOF electron spray) spectrum of tetra- <i>O</i> -propanyl- <i>N,N'</i> - dimethyl-D-glucaramide ( <b>7b</b> )	244
<b>Figure 31</b>	<sup>1</sup> H NMR (CDCl <sub>3</sub> ) spectrum of tetra- <i>O</i> -methylpropanyl- <i>N,N'</i> - dimethyl-D-glucaramide ( <b>7c</b> )	245
<b>Figure 32</b>	<sup>1</sup> H NMR (CDCl <sub>3</sub> ) spectrum of tetra- <i>O</i> -benzoyl- <i>N,N'</i> -dimethyl- D-glucaramide ( <b>7e</b> )	246
<b>Figure 33</b>	Mass (TOF electron spray) spectrum of tetra- <i>O</i> -benzoyl- <i>N,N'</i> - dimethyl-D-glucaramide ( <b>7e</b> )	247

## Appendix 2. Spectra of Compounds in Chapter 3

<b>Figure 1</b>	<sup>1</sup> H NMR (DMSO-d <sub>6</sub> ) spectrum of D-glucaric acid, D-glucaro- 6,3-lactone and D-glucaro-1,4-lactone mixture ( <b>1</b> )	248
<b>Figure 2</b>	<sup>1</sup> H NMR (D <sub>2</sub> O) spectrum of D-glucaric acid, D-glucaro-6,3- lactone and D-glucaro-1,4-lactone mixture ( <b>1</b> )	249
<b>Figure 3</b>	<sup>1</sup> H NMR (D <sub>2</sub> O) spectrum of ethylenediammonium D-glucarate ( <b>2a</b> ) / <i>N</i> -(2-aminoethyl)-D-glucar-6-amic acid salt ( <b>3a</b> ) / <i>N</i> -(2- aminoethyl)-D-glucar-1-amic acid salt ( <b>4a</b> ) mixture	250
<b>Figure 4</b>	<sup>1</sup> H NMR (D <sub>2</sub> O) spectrum of tetramethylenediammonium D- glucarate ( <b>2b</b> ) / <i>N</i> -(4-aminobutyl)-D-glucar-6-amic acid salt ( <b>3b</b> ) / <i>N</i> -(4-aminobutyl)-D-glucar-1-amic acid salt ( <b>4b</b> ) mixture	251
<b>Figure 5</b>	<sup>1</sup> H NMR (D <sub>2</sub> O) spectrum of hexamethylenediammonium D- glucarate ( <b>2c</b> )	252
<b>Figure 6</b>	<sup>13</sup> C NMR (D <sub>2</sub> O) spectrum of hexamethylenediammonium D- glucarate ( <b>2c</b> )	253
<b>Figure 7</b>	<sup>13</sup> C NMR DEPT (D <sub>2</sub> O) spectrum of hexamethylenediammonium D-glucarate ( <b>2c</b> )	254

<b>Figure 8</b>	<sup>1</sup> H NMR (D <sub>2</sub> O) spectrum of hexamethylenediammonium D-glucarate ( <b>2c</b> ) / <i>N</i> -(6-aminobutyl)-D-glucar-6-amic acid salt ( <b>3c</b> ) / <i>N</i> -(6-aminobutyl)-D-glucar-1-amic acid salt ( <b>4c</b> ) mixture	255
<b>Figure 9</b>	<sup>1</sup> H NMR (D <sub>2</sub> O) spectrum of octamethylenediammonium D-Glucarate ( <b>2d</b> ) / <i>N</i> -(8-aminobutyl)-D-glucar-6-amic acid salt ( <b>3d</b> ) / <i>N</i> -(8-aminobutyl)-D-glucar-1-amic acid salt ( <b>4d</b> ) mixture	256
<b>Figure 10</b>	<sup>1</sup> H NMR (D <sub>2</sub> O) spectrum of 3,6-dioxaoctamethylenediammonium D-glucarate ( <b>2f</b> ) / <i>N</i> -(8-amino-3,6-dioxa-octyl)-D-glucar-6-amic acid salt ( <b>3f</b> ) / <i>N</i> -(8-amino-3,6-dioxa-octyl)-D-glucar-1-amic acid salt ( <b>4f</b> ) mixture	257
<b>Figure 11</b>	<sup>1</sup> H NMR (D <sub>2</sub> O) spectrum of <i>m</i> -xylylenediammonium D-glucarate salt ( <b>2g</b> ) / <i>N</i> -( <i>m</i> -amino-xylylene)-D-glucara-6-amic acid salt ( <b>3g</b> ) / <i>N</i> -( <i>m</i> -amino-xylylene)-D-glucara-1-amic acid salt ( <b>4g</b> ) mixture	258
<b>Figure 12</b>	<sup>1</sup> H NMR (D <sub>2</sub> O) spectrum of ethylenediammonium D-galacatarate ( <b>5a</b> )	259
<b>Figure 13</b>	<sup>1</sup> H NMR (D <sub>2</sub> O) spectrum of tetramethylenediammonium D-galacatarate ( <b>5b</b> )	260
<b>Figure 14</b>	<sup>1</sup> H NMR (D <sub>2</sub> O) spectrum of hexamethylenediammonium D-galacatarate ( <b>5c</b> )	261
<b>Figure 15</b>	<sup>1</sup> H NMR (D <sub>2</sub> O) spectrum of 3,6-dioxaoctamethylenediammonium D-galacatarate ( <b>5f</b> )	262
<b>Figure 16</b>	<sup>1</sup> H NMR (D <sub>2</sub> O) spectrum of <i>m</i> -xylylenediammonium D-galacatarate ( <b>5g</b> )	263
<b>Figure 17</b>	<sup>1</sup> H NMR (D <sub>2</sub> O) spectrum of 3,3'-diamino- <i>N</i> -methyl diisopropylammonium D-galactarate ( <b>5h</b> )	264
<b>Figure 18</b>	<sup>1</sup> H NMR (D <sub>2</sub> O) spectrum of hexamethylenediammonium D-xylarate ( <b>6c</b> )	265
<b>Figure 19</b>	<sup>1</sup> H NMR (DMSO- <i>d</i> <sub>6</sub> ) spectrum of <i>random</i> poly(ethylene D-glucaramide) ( <b>7a</b> ) prepolymer	266
<b>Figure 20</b>	<sup>1</sup> H NMR (DMSO- <i>d</i> <sub>6</sub> ) spectrum of <i>random</i> poly(tetramethylene D-glucaramide) ( <b>7b</b> ) prepolymer	267
<b>Figure 21</b>	<sup>1</sup> H NMR (DMSO- <i>d</i> <sub>6</sub> ) spectrum of <i>random</i> poly(tetramethylene D-glucaramide) ( <b>7b</b> ) postpolymer	268
<b>Figure 22</b>	<sup>1</sup> H NMR (DMSO- <i>d</i> <sub>6</sub> ) spectrum of <i>random</i> poly(hexamethylene D-glucaramide) ( <b>7c</b> ) prepolymer	269
<b>Figure 23</b>	<sup>1</sup> H NMR (DMSO- <i>d</i> <sub>6</sub> ) spectrum of <i>random</i> poly(hexamethylene D-glucaramide) ( <b>7c</b> ) postpolymer	270
<b>Figure 24</b>	<sup>1</sup> H NMR (DMSO- <i>d</i> <sub>6</sub> ) spectrum of <i>random</i> poly(3,6-dioxa-1,8-octamethylene D-glucaramide) ( <b>7f</b> ) prepolymer	271
<b>Figure 25</b>	<sup>1</sup> H NMR (DMSO- <i>d</i> <sub>6</sub> ) spectrum of <i>random</i> poly( <i>m</i> -xylylene D-glucaramide) ( <b>7g</b> ) prepolymer	272
<b>Figure 26</b>	<sup>1</sup> H NMR (DMSO- <i>d</i> <sub>6</sub> ) spectrum of <i>random</i> poly(hexamethylene D-galacataramide) ( <b>8c</b> ) prepolymer	273



<b>Figure 27</b>	<sup>1</sup> H NMR (D <sub>2</sub> O) spectrum of <i>random</i> poly(dodecamethylene D-galacataramide) ( <b>8e</b> ) prepolymer	274
<b>Figure 28</b>	<sup>1</sup> H NMR (D <sub>2</sub> O) spectrum of <i>random</i> poly(3,6-dioxa-1,8-octamethylene D-galacataramide) ( <b>8f</b> ) prepolymer	275

# Chapter 1. Conformational and X-ray Crystallographic Studies of 2,3,4,5-tetra-*O*-Acetyl-*N,N'*-Dimethyl-*D*-Glucaramide – Molecular Mechanics Using a Model

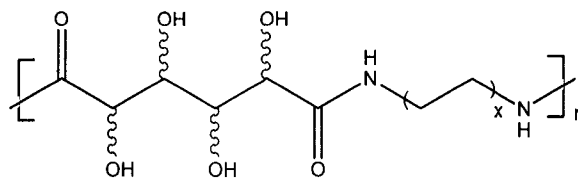
## Building Approach

### Introduction

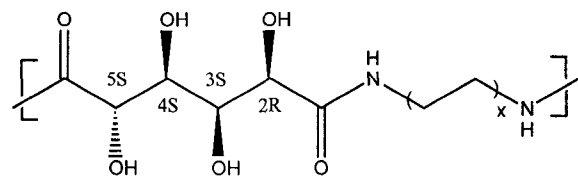
*D*-Glucaric acid, an available diacid from the oxidation of *D*-glucose, has been used to make polyhydroxypolyamides (PHPAs), “hydroxylated nylons”, in the Kiely labs for a number of years.<sup>[1-14]</sup> Since *D*-glucaric acid, [(2*R*,3*S*,4*S*,5*S*)-tetrahydroxyhexanedioic acid], has four chiral centers, three classes of stereochemically different poly(alkylene *D*-glucaramides) have been synthesized; “randomly aligned” polyamides, repeating *head, tail* - polyamides, and alternating *head, tail* - *tail, head* - polyamides (Figure 1).

Knowledge of the conformations of the different polyamides can help in understanding their properties and potential applications.

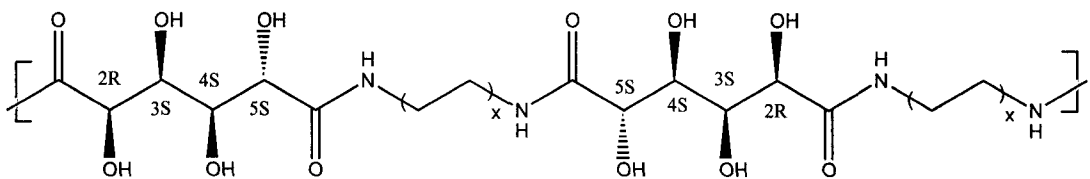
The <sup>1</sup>H NMR spectra (CDCl<sub>3</sub>) of the glucaryl backbone protons for both poly(hexamethylene 2,3,4,5-tetra-*O*-acetyl-*D*-glucaramide) (**3**) and 2,3,4,5-tetra-*O*-acetyl-*N,N'*-dihexyl-*D*-glucaramide (**5a**) are shown in Figure 2. Comparison of the two spectra indicate that the proton chemical shifts on the polymer (**3**) and the corresponding model compound (**5a**) are comparable, and that the <sup>1</sup>H NMR spectrum of model compound (**5a**) can provide added coupling information to the repeating *D*-glucaryl unit of the polymer (**3**).



"Random" poly(alkylene D-glucaramide)



Stereoregular repeating *head, tail* - poly(alkylene D-glucaramide)



Stereoregular alternating *head, tail - tail, head* - poly(alkylene D-glucaramide)

$x = 1, 2, 3, 4, 5, \text{ or } 6$

**Figure 1.** Three classes of stereochemically different poly(alkylene D-glucaramides).

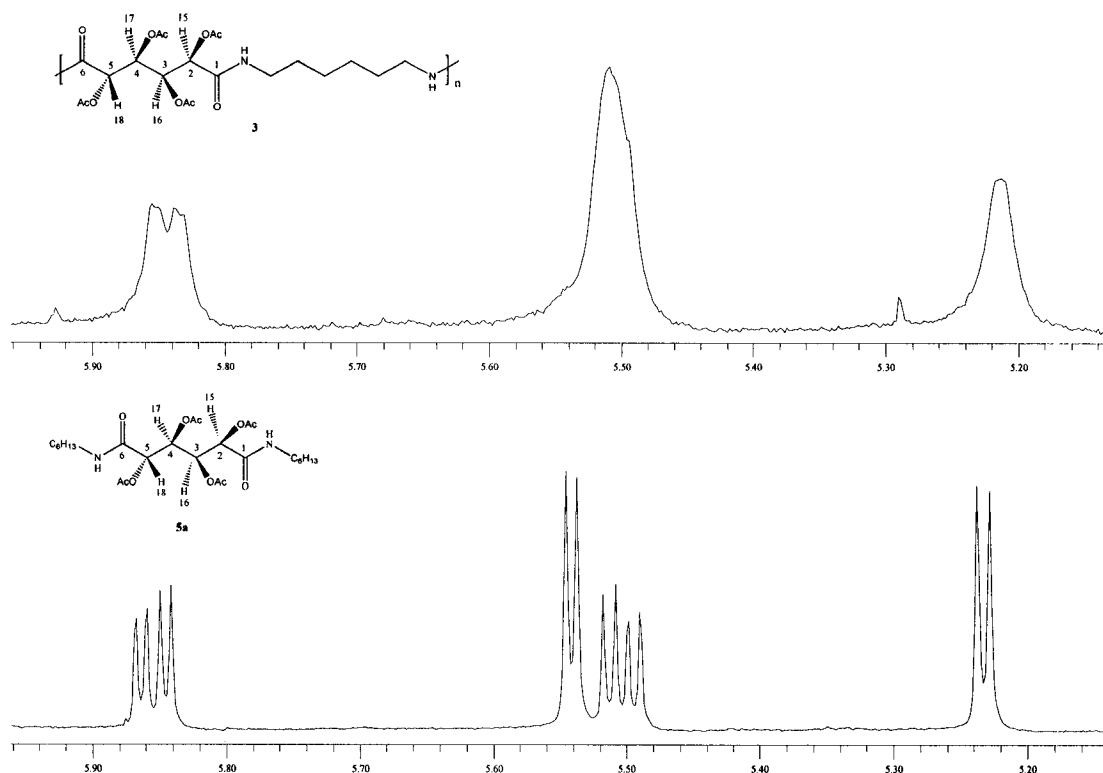


**Figure 2.**  $^1\text{H}$  NMR spectra ( $\text{CDCl}_3$ ) of poly(hexamethylene 2,3,4,5-tetra-*O*-acetyl-*D*-glucaramide) (**3**) and the model compound 2,3,4,5-tetra-*O*-acetyl-*N,N'*-dihexyl-*D*-glucaramide (**5a**). Protons H15 – H18.

The  $^1\text{H}$  NMR spectra of 2,3,4,5-tetra-*O*-acetyl-*N,N'*-dihexyl-*D*-glucaramide (**5a**) and 2,3,4,5-tetra-*O*-acetyl-*N,N'*-dimethyl-*D*-glucaramide (**7a**) have also been compared. It was found that in the glucaryl unit proton region, the two spectra are quite similar, indicating that the structurally simpler 2,3,4,5-tetra-*O*-acetyl-*N,N'*-dimethyl-*D*-glucaramide (**7a**) can also serve as a model compound to study the conformation of the *D*-glucaryl unit in the polymer **3**.

For nylon 6,6, an extended, planar zig-zag, arrangement of carbon atoms is considered to be the favored conformation.<sup>[36]</sup> However, with four hydroxyl groups or esterified

hydroxyl groups attached to the adipic acid unit, the conformation of the diacid unit is not extended.<sup>[18-24]</sup> Previous studies of the unprotected D-glucaramide unit indicated postulated “bent” or “sickle” conformations resulting from the relief of sterically unfavorable nonbonded interactions between parallel substituents on  $\beta$ -related carbon atoms, or so called 1,3-parallel interactions. Sweeting et al.<sup>[18]</sup> investigated six peracetylated hexonitriles in solution utilizing  $^1\text{H}$  NMR spectroscopy. For penta-*O*-acetyl-D-mannonitrile and penta-*O*-acetyl-D-galactonitrile, which do not have parallel 1,3-interaction of substituents, their proton-proton coupling constants were consistent with a zig-zag conformation in which the cyano group lies in the plane of the other carbon atoms of the chain. In contrast, the “sickle” conformation of penta-*O*-acetyl-D-gluconitrile was favored in order to alleviate 1,3-interaction of acetoxy groups on C2 and C4. Angyl and coworkers<sup>[19,20]</sup> also conducted  $^1\text{H}$  NMR conformational studies on various derivatives of glucose. In particular, they found that hexa-*O*-acetyl-D-glucitol prefers a “sickle” conformation ( ${}_2\text{G}^-$  and  ${}_3\text{G}^+{}_4\text{G}^+$ ) over an extended conformation. Horton et al.<sup>[22]</sup> reported a “sickle” conformation for 3,4-di-*O*-acetyl-1,2:5,6-bis(thioanhydro)-D-glucitol ( ${}_3\text{G}^-$ ) and a “sickle” conformation for penta-*O*-acetylalohexose diethyl dithioacetal having a D-gluco configuration ( ${}_2\text{G}^-$  and  ${}_5\text{G}^+$ ). Here,  ${}_2\text{G}^-$  Denotes the sickle conformation obtained by  $120^\circ$  clockwise rotation of the remote atom (C3) along the C2-C3 bond;  ${}_3\text{G}^+$  denotes the sickle obtained by  $120^\circ$  counterclockwise rotation of the remote atom (C4) along the C3-C4 bond;  ${}_3\text{G}^-$  denotes the sickle obtained by  $120^\circ$  clockwise rotation of the remote atom (C4) along the C3-C4 bond;  ${}_4\text{G}^+$  denotes the sickle obtained by  $120^\circ$  counterclockwise rotation of the remote atom (C5) along the C4-C5 bond;  ${}_5\text{G}^+$

denotes the sickle obtained by 120° counterclockwise rotation of the remote atom (C6) along the C5-C6 bond.<sup>[22]</sup> The role of 1,3-interactions in determining acyclic carbohydrate conformations is clearly important, and it was expected that this phenomenon might contribute to the distribution of conformations observed in the present modeling study.

Most of the previous acyclic monosaccharide derivative conformational studies were based on <sup>1</sup>H NMR analysis, with the assumption that proton coupling constants of <4 Hz represents vicinal protons in a *gauche* orientation, and that coupling constants of >7 Hz indicated principally an *anti* orientation of the vicinal protons.<sup>[18,25]</sup> These limits reflect the broad implications of the Karplus equation.<sup>[25]</sup>

Looking at the extended conformations of diamides **5a** and **7a** and polyamide **3** (Figure 3), sterically unfavorable 1,3-interactions are seen between the acetoxy groups on C2 and C4. To relieve this steric strain, counterclockwise rotation around C3-C4 bond for 120° gives a “sickle” conformation.

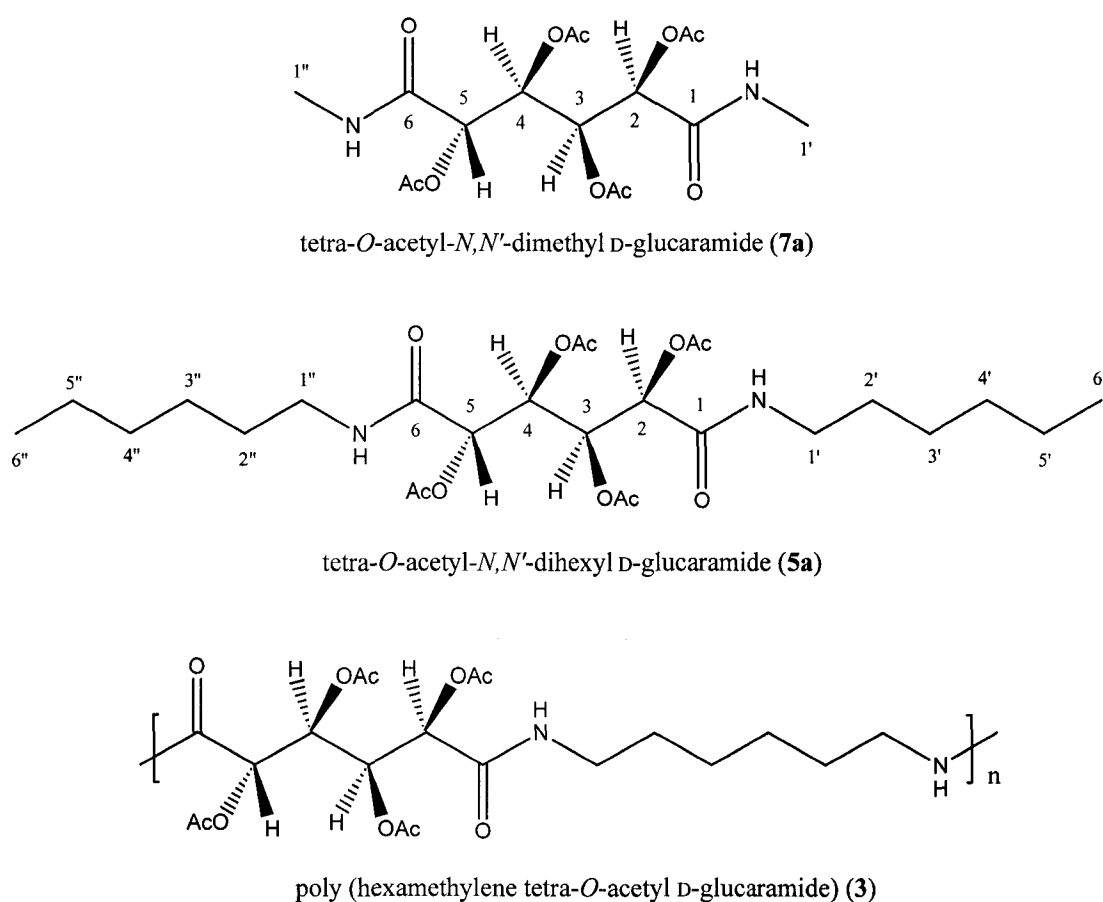


**Figure 3.** 1,3-Interactions between the acetoxy groups on C2 and C4 on diamides **5a** and **7a** and polyamide **3**.

To this point, the only conformational reports on these polyhydroxypolyamides (PHPAs) were molecular mechanics (MM3)/<sup>1</sup>H NMR studies on D-glucaramide<sup>[17]</sup> and polymers therefrom.<sup>[12]</sup> We are interested in the conformational changes that occur on the repeating D-glucaryl unit when the pendant hydroxyl functions are acylated with different acyl groups. This chapter is concerned with the preparations of ten different *N,N'*-dialkyl-tetra-*O*-acyl-D-glucaramides, and the use of <sup>1</sup>H NMR spectra and molecular mechanics (MM3) to evaluate the conformational preferences of these D-glucaramides which might

impact the tertiary structures of the corresponding polyamides.

In the studies described here, a Varian VXR-Unity instrument of 400 MHz was used to record  $^1\text{H}$  NMR spectra and the MM3 program contained in the Tripos Alchemy 2000 package was employed for molecular mechanics calculations of the model diamides.

## Results and Discussion

The conformational studies of 2,3,4,5-tetra-*O*-acyl-*N,N'*-dialkyl-D-glucaramides (**5a** - **5e**, **7a** - **7e**) as model compounds to postulate the conformations of the corresponding poly(alkylene tetra-*O*-acyl-D-glucaramides) are based on the coupling information from  $^1\text{H}$  NMR. A “model building” approach<sup>[26]</sup> was applied in these studies. The conformations of smaller “building blocks” or “molecular fragments” were studied first, and the conformational preferences of these units were applied in building and modeling the larger molecules.

### I. $^1\text{H}$ NMR study of *N,N'*-dialkyl-D-glucaramide and the corresponding esters

Table 1 lists the chemical shifts of H15, H16, H17 and H18 and the vicinal coupling constants for *N,N'*-dihexyl-D-glucaramide (**4**), esters of *N,N'*-dihexyl-D-glucaramide [2,3,4,5-tetra-*O*-acetyl-*N,N'*-dihexyl-D-glucaramide (**5a**), 2,3,4,5-tetra-*O*-propanyl-*N,N'*-dihexyl-D-glucaramide (**5b**), 2,3,4,5-tetra-*O*-methylpropanyl-*N,N'*-dihexyl-D-glucaramide (**5c**), 2,3,4,5-tetra-*O*-dimethylpropanyl-*N,N'*-dihexyl-D-glucaramide (**5d**), and 2,3,4,5-



tetra-*O*-benzoyl-*N,N'*-dihexyl-D-glucaramide (**5e**), *N,N'*-dimethyl-D-glucaramide (**6**), esters of *N,N'*-dimethyl-D-glucaramide [2,3,4,5-tetra-*O*-acetyl-*N,N'*-dimethyl-D-glucaramide (**7a**), 2,3,4,5-tetra-*O*-propanyl-*N,N'*-dimethyl-D-glucaramide (**7b**), 2,3,4,5-tetra-*O*-methylpropanyl-*N,N'*-dimethyl-D-glucaramide (**7c**), 2,3,4,5-tetra-*O*-dimethylpropanyl-*N,N'*-dimethyl-D-glucaramide (**7d**), and 2,3,4,5-tetra-*O*-benzoyl-*N,N'*-dimethyl-D-glucaramide (**7e**)], poly(hexamethylene D-glucaramide) (**2**), and poly(hexamethylene 2,3,4,5-tetra-*O*-acetyl-D-glucaramide) (**3**). Except for the benzoate esters (**5e** and **7e**), all the aliphatic esters (**5a - 5d** and **7a - 7d**) have large coupling constants (7.12 - 8.41 Hz) between H16-H17, implying large dihedral angles (ca. 180°).<sup>[25]</sup> Coupling constants between H15-H16 and H17-H18 are considerably smaller (1.90 - 3.89 Hz), suggesting a *gauche* arrangement of vicinal protons (ca. 60°).<sup>[25]</sup> In general, as the acyl groups become bulkier,  $J_{16,17}$  becomes larger, indicating a sterically more restricted conformation with the H16 and H17 dihedral angle approaching 180°. In contrast, the corresponding couplings for unprotected **4** and **6** are 3.24 Hz and 3.89 Hz, respectively, values in keeping with an average *gauche* arrangement of H16-H17. However, H17-H18 of **4** and **6** have a larger dihedral angle than that observed with the *O*-acylated diamides based upon  $J_{17,18}$  values of 6.47 Hz and 5.82 Hz, respectively.

**Table 1.** Chemical shifts ( $\delta$ , ppm) and coupling constants (J, Hz) for compounds **2** ~ **7e**

Compound	$\delta$ [H (16) <sup>a</sup> ]	$\delta$ [H (15) <sup>a</sup> ]	$\delta$ [H (17) <sup>a</sup> ]	$\delta$ [H (18) <sup>a</sup> ]	J <sub>15,16</sub>	J <sub>16,17</sub>	J <sub>17,18</sub>
<b>4</b> <sup>b, d</sup>	3.85 (m)	3.96 (t)	3.67 (m)	3.90 (t)	3.88	3.24	6.47
<b>6</b> <sup>b, d</sup>	3.86 (m)	3.97 (t)	3.69 (m)	3.91 (t)	3.24	3.89	5.82
<b>5a</b> <sup>c</sup>	5.86 (d of d)	5.54 (d)	5.50 (d of d)	5.23 (d)	3.23	7.12	3.88
<b>7a</b> <sup>c</sup>	5.85 (d of d)	5.55 (d)	5.53 (d of d)	5.28 (d)	3.24	7.11	3.89
<b>5b</b> <sup>c</sup>	5.87(d of d)	5.56 (d)	5.52 (d of d)	5.26 (d)	3.24	7.12	3.88
<b>7b</b> <sup>c</sup>	5.85 (d of d)	5.55 (d)	5.54 (d of d)	5.29 (d)	3.23	7.76	3.88
<b>5c</b> <sup>c</sup>	5.89 (d of d)	5.57 (d)	5.53 (d of d)	5.29 (d)	2.59	7.77	3.24
<b>7c</b> <sup>c</sup>	5.87 (d of d)	5.55 (d)	5.53 (d of d)	5.31 (d)	2.59	8.41	3.24
<b>5d</b> <sup>c</sup>	5.88 (d of d)	5.57 (d)	5.50 (d of d)	5.34 (d)	1.90	8.25	2.54
<b>5e</b> <sup>c</sup>	6.46 (d of d)	5.88 (d)	6.23 (d of d)	5.86 (d)	4.53	5.82	3.89
<b>7e</b> <sup>c</sup>	6.43 (d of d)	5.92 (d)	6.26 (d of d)	5.87 (d)	3.88	5.82	4.53
<b>2</b> <sup>b, d</sup>	3.86 (m)	3.98 (t)	3.67 (m)	3.91 (t)	3.23	3.88	5.82
<b>3</b> <sup>c</sup>	5.83 (b)	5.50 (b)	5.50 (b)	5.21 (b)			

- Numbers in parentheses are the atom numbers assigned in the molecular mechanics studies.
- DMSO-d<sub>6</sub> as solvent.
- CDCl<sub>3</sub> as solvent.
- The coupling constants were obtained after adding 6 drops of D<sub>2</sub>O to the DMSO-d<sub>6</sub> solution.

## II. Conformational study of 2,3,4,5-tetra-*O*-acetyl-*N,N'*-dimethyl-*D*-glucaramide (7a)

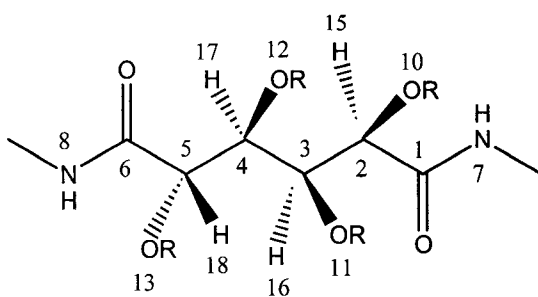
### 1. Starting rotamers of 2,3,4,5-tetra-*O*-acetyl-*N,N'*-dimethyl-*D*-glucaramide (7a)

In keeping with the <sup>1</sup>H NMR results for the *O*-acylated diamides, and beginning with the extended conformation of 7a (Table 2), four different rotamers were considered, all with H16-H17 at 180°, and H15-H16 and H17-H18 with a dihedral angle of ±60°. The four rotamers were built from the extended conformation (P), by a 120° counterclockwise rotation about the C3-C4 bond, and 120° clockwise or counterclockwise rotation about the C2-C3 and C4-C5 bonds (Figure 4). Table 2 shows the dihedral angle set for the starting four rotamers of 7a.

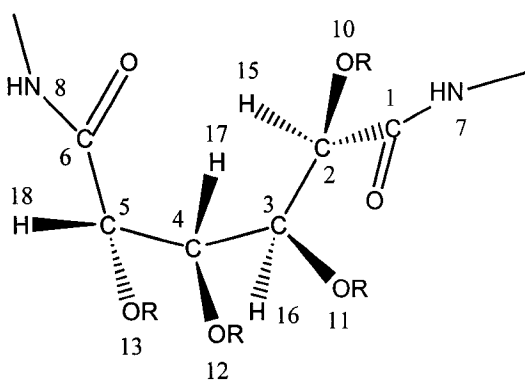
**Table 2.** Dihedral angle ( $\omega$ , °) set for 2,3,4,5-tetra-*O*-acetyl-*N,N'*-dimethyl-*D*-glucaramide (7a)

	$\omega$ (H15 - H16) (°)	$\omega$ (H16 - H17) (°)	$\omega$ (H17 - H18) (°)	Conformation*
Extended	60	-60	180	P
Rotamer 1	60	180	-60	<sub>3</sub> G <sup>+</sup> <sub>4</sub> G <sup>-</sup>
Rotamer 2	60	180	60	<sub>3</sub> G <sup>+</sup> <sub>4</sub> G <sup>+</sup>
Rotamer 2	-60	180	-60	<sub>2</sub> G <sup>+</sup> <sub>3</sub> G <sup>+</sup> <sub>4</sub> G <sup>-</sup>
Rotamer 4	-60	180	60	<sub>2</sub> G <sup>+</sup> <sub>3</sub> G <sup>+</sup> <sub>4</sub> G <sup>+</sup>

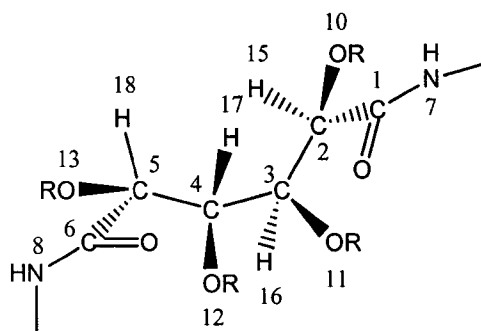
\* <sub>2</sub>G<sup>+</sup> Denotes the sickle conformation obtained by 120° counterclockwise rotation of the remote atom (C3) along the C2-C3 bond; <sub>3</sub>G<sup>+</sup> denotes the sickle obtained by 120° counterclockwise rotation of the remote atom (C4) along the C3-C4 bond; <sub>4</sub>G<sup>+</sup> denotes the sickle obtained by 120° counterclockwise rotation of the remote atom (C5) along the C4-C5 bond; <sub>4</sub>G<sup>-</sup> denotes the sickle obtained by 120° clockwise rotation of the remote atom (C5) along the C4-C5 bond.<sup>[22]</sup>



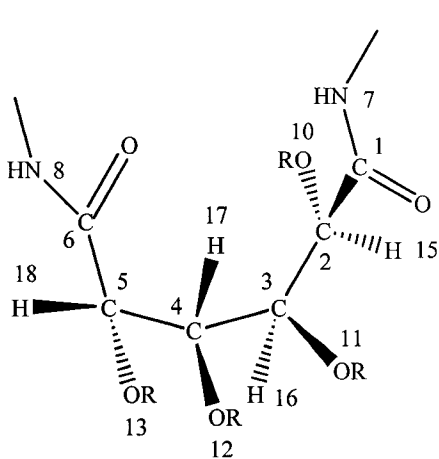
7a, extended conformation (P)



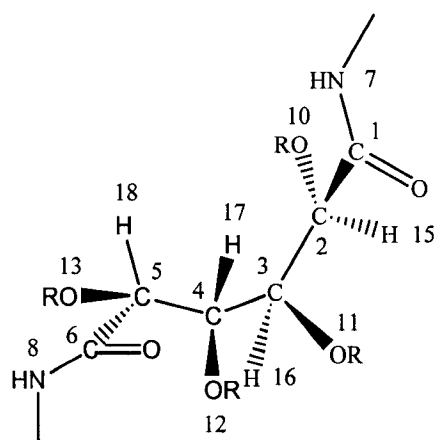
7a, rotamer 1 ( $3G^+4G^-$ )



7a, Rotamer 2 ( $3G^+4G^+$ )



7a, Rotamer 3 ( $2G^+3G^+4G^-$ )



7a, Rotamer 4 ( $2G^+3G^+4G^+$ )

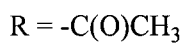


Figure 4. The extended conformation and four starting rotamers of 7a.

## 2. Exhaustive study of 2,3,4,5-tetra-*O*-acetyl-*N,N'*-dimethyl-*D*-glucaramide (7a)

Systematic searching for a global minimum by 120° rotations about single bonds of 2,3,4,5-tetra-*O*-acetyl-*N,N'*-dimethyl-*D*-glucaramide (7a) requires 14,348,907 (3<sup>15</sup>) starting conformations, based upon fifteen separate torsion angles in the molecule (Table 3) and typically three staggered conformations of atoms or groups attached to each of the non-terminal atoms. The staggered orientation for each angle is the prerequisite requirement for a stable conformation. Among the fifteen torsion angles, seven are derived from backbone carbons of 7a, while the other eight originate from the acyloxy groups (Figure 5).

**Table 3.** Torsion angles varied in MM3 studies of 2,3,4,5-tetra-*O*-acetyl-*N,N'*-dimethyl-*D*-glucaramide (7a)

Backbone	Acyloxy moieties
H15-C2-C3-H16	C2-O10-C44-O92
H16-C3-C4-H17	C3-O11-C53-O93
H17-C4-C5-H18	C4-O12-C62-O94
O9-C1-N7-H19	C5-O13-C71-O95
O14-C6-N8-H22	H15-C2-O10-C44
O9-C1-C2-O10	H16-C3-O11-C53
O13-C5-C6-O14	H17-C4-O12-C62
	H18-C5-O13-C71

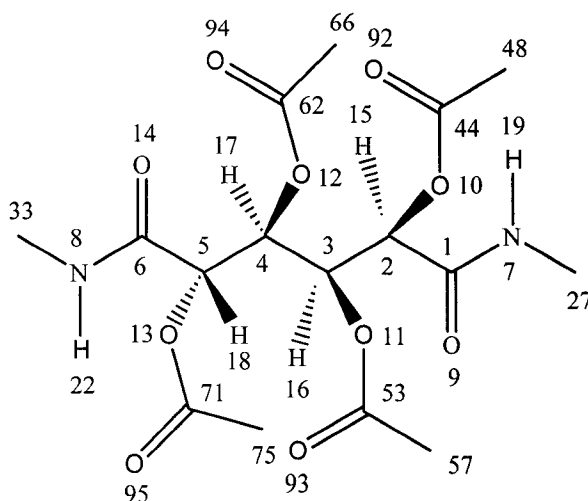


**Figure 5.** Numbering system for compound **7a**.

For more complex tetra-*O*-acyl-*N,N'*-dimethyl-D-glucaramides (**7b – 7e**), additional torsion angles have to be varied, resulting in even more starting conformations.

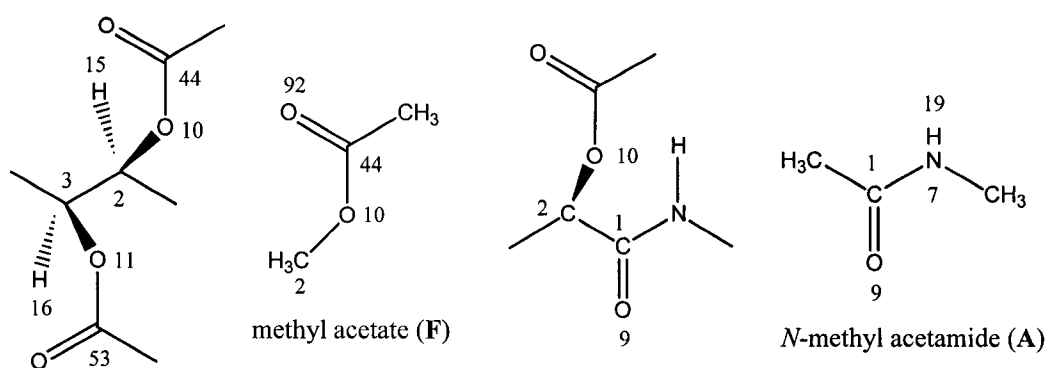
Obviously, for such large and flexible molecules, too many conformations are generated to be optimized in a reasonable length of time (Table 4) using a full conformational search routine. The alternatives to the full-space systematic search are methods based on random variation of coordinates such as molecular dynamics or Monte Carlo (MC) searching in Cartesian space<sup>[26,27]</sup> and MC searching in dihedral space.<sup>[27]</sup> Neither of these modeling approaches was readily available to us, so a simplified conformational study approach, “model building approach”, was carried out, wherein some of the torsion angles were manually defined (fixed) utilizing some small model compounds (“building blocks” or “molecular fragments”).

**Table 4.** Variable dihedral angles and starting conformations for systematic conformational study

	<b>8</b>	<b>6</b>	<b>7a</b>	<b>7b</b>	<b>7c</b>
Variable torsion angles	9	11	15	19	19
Starting conformations	19,683	177,147	14,348,907	1,162,261,467	1,162,261,467
	<b>7d</b>	<b>7e</b>	<b>4</b>	<b>5a</b>	
Variable torsion angles	15	15	13	17	
Starting conformations	14,348,907	14,348,907	1,594,323	129,140,163	

### 3. “Building blocks” studies

Four molecules, *N*-methylacetamide **A**, *N*-methyl-acetoxipropanamide **B** and **D**, methyl acetate **F**, and 2,3-diacetoxybutanes **G**, **J**, **K**, **L** and **M** were studied as “building blocks” (Figure 6) for the conformational study of **7a**. Calculations were carried out using MM3 (92) / Alchemy 2000 at a dielectric constant of 1.0.



2,3-diacetoxybutane (G - M)

*N*-methyl 2-acetoxypropanamide (B and D)

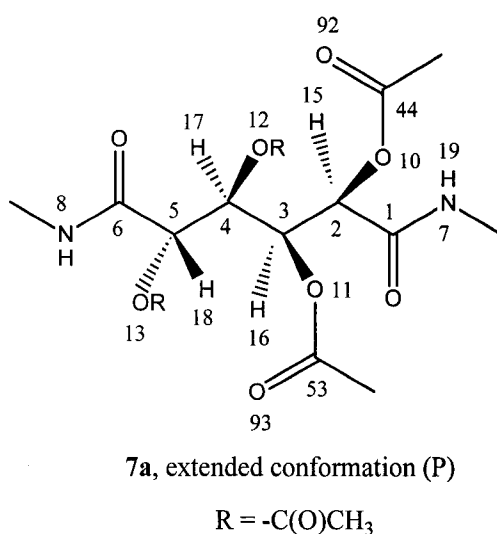


**Figure 6.** “Building blocks” (A - M) for conformational study of tetra-*O*-acetyl-*N,N'*-dimethyl-*D*-glucaramide (7a).

### Model 1: End C Model ----- *N*-methylacetamide

*N*-methylacetamide was selected as the model to search the low energy conformation of the C1-N7 and C2-N8 ends of 7a (Figure 7). The dihedral angle of O9-C1-N7-H19 was increased from 0.0° to 60.0°, 120.0°, 180.0°, 240.0° and 300.0°, and the individual conformations were minimized using MM3 Tripos Alchemy 2000 software (Table 5).



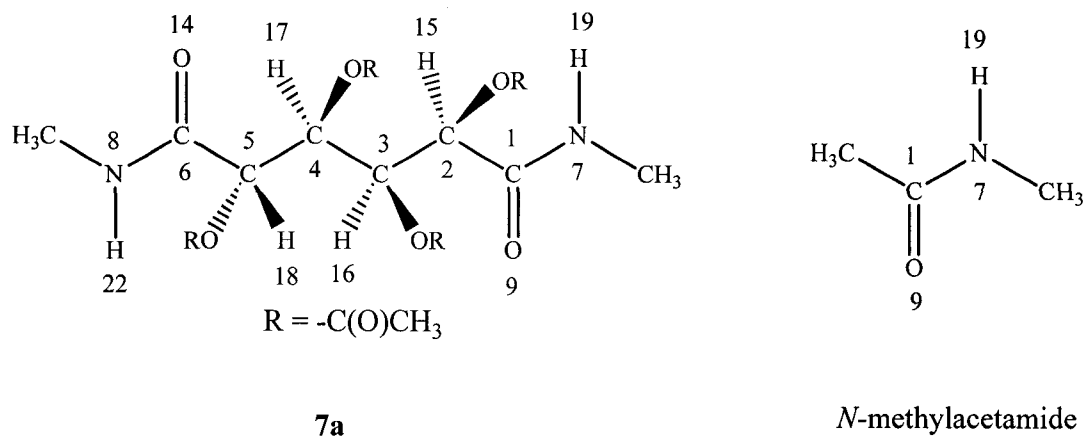


**Figure 7.** End C Model of **7a**: *N*-methylacetamide.

**Table 5.** Minimized conformations **A** of *N*-methylacetamide used to establish a conformational model for O9-C1-N7-H19 and O14-C6-N8-H22 dihedral angle ( $\omega$ , °) of **7a**

	$\omega$ Before MM3 (°)	$\omega$ After MM3 (°)	Total energy (kcal/mol)	Steric relationship	Pverall conformation
<b>A1</b>	0.0	0.0	-0.3065	<i>E</i>	Bent
<b>A2</b>	60.0	0.0	-0.3065	<i>E</i>	Bent
<b>A3</b>	<b>120.0</b>	<b>180.0</b>	<b>-2.9246</b>	<b><i>Z</i></b>	<b>Extended</b>
<b>A4</b>	<b>180.0</b>	<b>180.0</b>	<b>-2.9246</b>	<b><i>Z</i></b>	<b>Extended</b>
<b>A5</b>	<b>240.0</b>	<b>180.0</b>	<b>-2.9246</b>	<b><i>Z</i></b>	<b>Extended</b>
<b>A6</b>	300.0	0.0	-0.3065	<i>E</i>	Bent

Varying the dihedral angle of O9-C1-N7-H19 of *N*-methylacetamide, two conformations were obtained, the lower energy *Z* conformation **A3** and the higher energy *E* conformation **A1**. The energy of the overall extended conformation **A3** is 2.6181

kcal/mol lower than the bent conformation **A1** at dielectric constant 1.0. Introducing nonbonded repulsion between the two methyl groups is the major cause of the destabilization in **A1** (Figure 8). Allinger and coworkers<sup>[28]</sup> studied a range of amides, polypeptides and proteins using the MM3 force field and concluded that *Z*-*N*-methylacetamide (**A3**) is more stable than the *E* form (**A1**) by 2.94 kcal/mol, calculated at dielectric constant 1.5. We obtained a similar value at dielectric constant 1.5 using the Tripos software. The conformational preference was explained by Eliel and Wilen<sup>[29]</sup> as well.

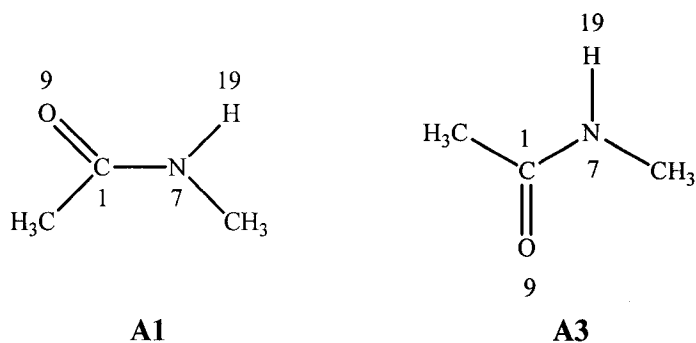


**Figure 8.** Lower energy (**A3**) and higher energy (**A1**) conformations of *N*-methylacetamide.

Based upon the model study, we set the dihedral angle of O9-C1-N7-H19 and O14-C6-N8-H22 on the four tetra-*O*-acetyl-*N,N'*-dimethyl-D-glucaramide (**7a**) rotamers to 180.0°.

**Model 2: C1-C2 & C5-C6 Model ----- *N*-methyl-2-acetoxypropanamide**

(*2R*) and (*2S*)-*N*-Methyl-2-acetoxypropanamide (**B** and **D**, Figure 9) were chosen as models to determine the preferred conformational relationship between each terminal acyloxy group on a chiral carbon, and the amide carbonyl group, i.e., the optimized O9-C1-C2-O10 and O13-C5-C6-O14 dihedral angles. (*2R*)-*N*-methyl-2-acetoxypropanamide (**B**) was used to model the C1-C2 dihedral preference and (*2S*)-*N*-methyl-2-acetoxypropanamide (**D**) was a model for the C5-C6 end. As the low energy conformation of *N*-methylacetamide (**A3**, Model 1) suggested, the H19-N7-C1-O9 dihedral angle was set to 180.0° and the C2-O10-C44-O92 dihedral angle was set to 0.0°, according to the next model study, the Acyloxy Rotamer Model (methyl acetate **F1**, Model 3).

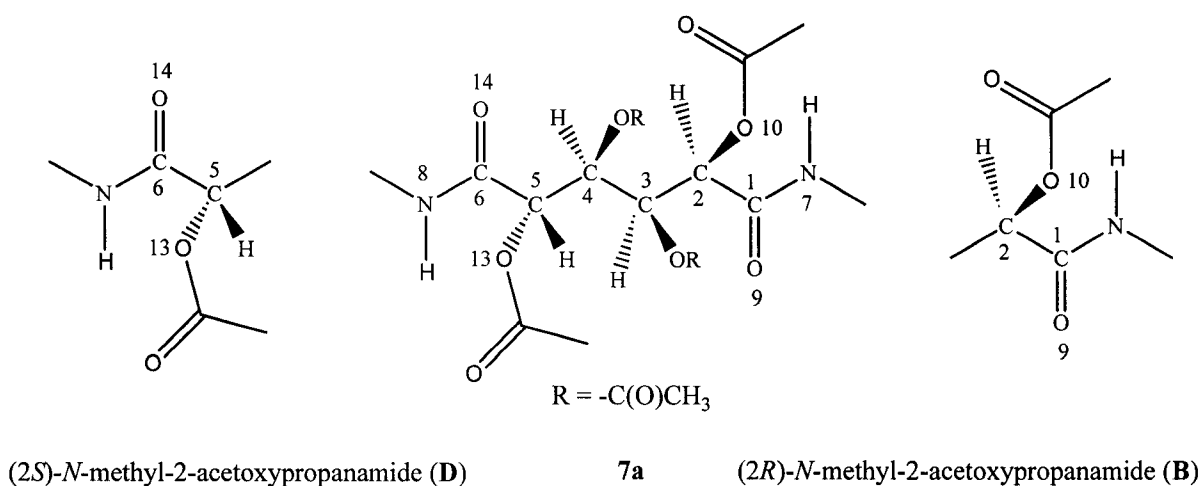


**Figure 9.** C1-C2 Model of **7a**: (*2R*)-*N*-methyl-2-acetoxypropanamide (**B**) and C5-C6 Model of **7a**: (*2S*)-*N*-methyl-2-acetoxypropanamide (**D**).

Rotation about the C1-C2 bond in 60.0° increments from 0.0° to 300.0° generated six original conformations of (2*R*)-*N*-methyl-2-acetoxypropanamide (**B**). After the MM3 minimization, conformation **B1** (equivalent to **B2**, **B4** and **B5**) was determined to have lower energy and conformation **B2** (equivalent to **B6**) was found to have higher energy (Table 6).

**Table 6.** O9-C1-C2-O10 Dihedral angles of C1-C2 Model: (2*R*)-*N*-methyl-2-acetoxypropanamide (**B**)

	$\omega$ Before MM3 (°)	$\omega$ Bfter MM3 (°)	Total energy (kcal/mol)
<b>B1</b>	<b>0</b>	<b>125.8</b>	<b>-9.0980</b>
<b>B2</b>	<b>60</b>	<b>125.8</b>	<b>-9.0981</b>
<b>B3</b>	120	-139.4	-7.3033
<b>B4</b>	<b>180</b>	<b>125.8</b>	<b>-9.0981</b>
<b>B5</b>	<b>240</b>	<b>125.8</b>	<b>-9.0980</b>
<b>B6</b>	300	-139.4	-7.3033

The same process was applied to (2*S*)-*N*-methyl-2-acetoxypropanamide (**D**) to probe the dihedral preference of the C5-C6 bond. The results are listed in Table 7.

**Table 7.** O13-C5-C6-O14 Dihedral angles of C5-C6 Model: (2*S*)-*N*-methyl-2-acetoxypropanamide (**D**)

	$\omega$ Before MM3 (°)	$\omega$ After MM3 (°)	Total energy (kcal/mol)
<b>D1</b>	<b>0</b>	<b>-125.8</b>	<b>-9.0980</b>
<b>D2</b>	60	139.4	-7.3033
<b>D3</b>	<b>120</b>	<b>-125.8</b>	<b>-9.0981</b>
<b>D4</b>	<b>180</b>	<b>-125.8</b>	<b>-9.0981</b>
<b>D5</b>	240	139.4	-7.3033
<b>D6</b>	<b>300</b>	<b>-125.8</b>	<b>-9.0981</b>

The Newman projection formulas (Figure 10, Table 8) of **B1**, **B3**, **D1** and **D2** were drawn looking down the C1-C2 or C6-C5 bond, respectively. Interestingly, the low energy conformations **B1** and **D1** are enantiomers, consequently, **B3** and **D2**, the two higher energy conformations are enantiomers as well.

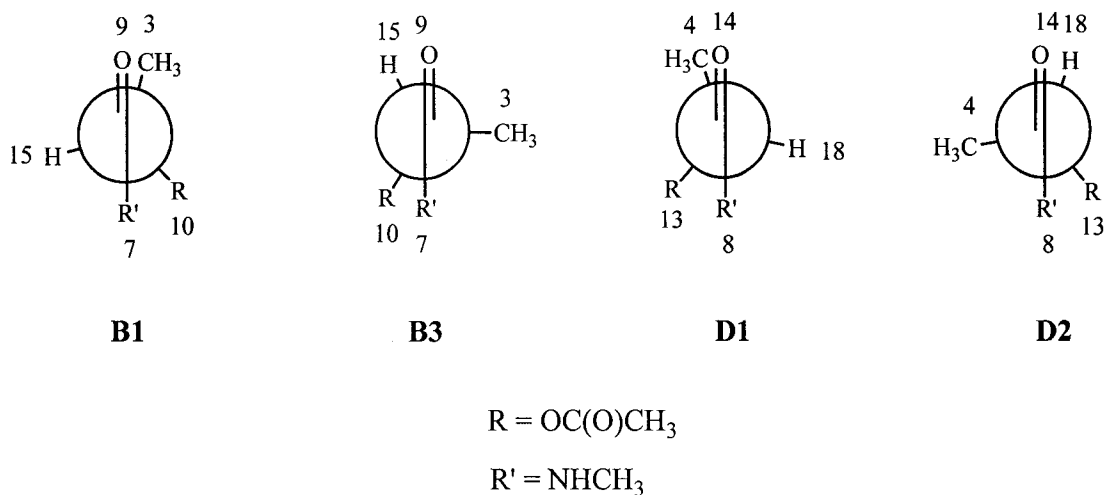


**Figure 10.** Newman projections of **B1** and **B3** of (2*R*)-*N*-methyl-2-acetoxypropanamide looking down the C1-C2 bond, and **D1** and **D2** of (2*S*)-*N*-methyl-2-acetoxypropanamide looking down the C6-C5 bond.

**Table 8.** Dihedral angles ( $\omega$ , °) of atoms attached to C1 and C2 in the **B1** and **B3** conformations of (2*R*)-*N*-methyl-2-acetoxypropanamide after MM3 minimization and **D1** and **D2** of (2*S*)-*N*-methyl-2-acetoxypropanamide

	<b>B1</b>	<b>B3</b>		<b>D1</b>	<b>D2</b>
$\omega$ (O9-C1-C2-C3) (°)	<b>7.4</b>	92.1	$\omega$ (O14-C6-C5-C4) (°)	<b>-7.4</b>	-92.1
$\omega$ (O9-C1-C2-H15) (°)	<b>-111.6</b>	-23.1	$\omega$ (O14-C6-C5-H18) (°)	<b>111.6</b>	23.1
$\omega$ (O9-C1-C2-O10) (°)	<b>125.8</b>	-139.4	$\omega$ (O14-C6-C5-O13) (°)	<b>-125.8</b>	139.4
$\omega$ (N7-C1-C2-C3) (°)	<b>-175.3</b>	-85.1	$\omega$ (N8-C6-C5-C4) (°)	<b>175.3</b>	85.1
$\omega$ (N7-C1-C2-H15) (°)	<b>65.7</b>	159.7	$\omega$ (N8-C6-C5-H18) (°)	<b>-65.7</b>	-159.7
$\omega$ (N7-C1-C2-O10) (°)	<b>-56.9</b>	43.4	$\omega$ (N8-C6-C5-O13) (°)	<b>56.9</b>	-43.4
Total energy (kcal/mol)	<b>-9.0980</b>	-7.3033	Total energy (kcal/mol)	<b>-9.0980</b>	-7.3033

According to the above model studies, the value of O10-C2-C1-O9 dihedral angle was set to +125.8° and the O13-C5-C6-O14 dihedral angle was set to -125.8°, respectively, in the conformational study of tetra-*O*-acetyl-*N,N'*-dimethyl-D-glucaramide (**7a**).

### Model 3: Acyloxy Rotamer Model ----- methyl acetate

Methyl acetate (Figure 11) was chosen as a model compound to help determine the orientation of the carbonyl oxygen on each acetoxy group relative to the *O*-alkyl carbon, i.e., the dihedral angle defined by C2-O10-C44-O92 and similarly the three other acyloxy groups on diamide **7a**. Changing the C2-O10-C44-O92 dihedral angle of methyl acetate from 0.0° to 60.0°, 120.0°, 180.0°, 240.0° and 300.0° followed by MM3 calculation gave two very different conformations, the low energy *syn* or extended conformation (**F1**)<sup>[30]</sup> and the significantly higher energy *anti* conformation (**F3**) (Table 9).

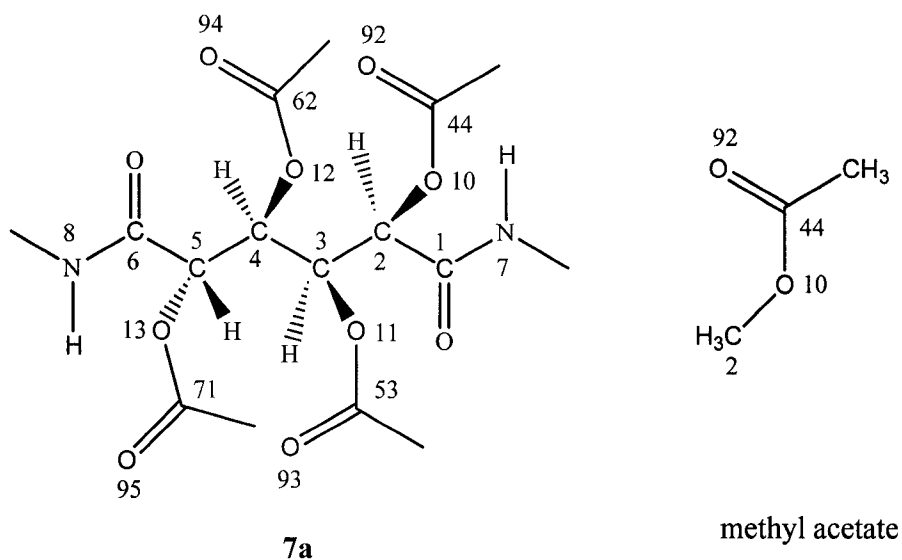


**Figure 11.** Acyloxy Rotamer Model of **7a**: methyl acetate.

**Table 9.** Minimized conformations (**F**) of methyl acetate used to establish a conformational model for the C2-O10-C44-O92, C3-O11-C53-O93, C4-O12-C62-O94, and C5-O13-C71-O95 dihedral angles ( $\omega$ , °) of **7a**

	$\omega$ Before MM3 (°)	$\omega$ After MM3 (°)	Total energy (kcal/mol)	Steric relationship	Overall conformation
<b>F1</b>	<b>0.0</b>	<b>0.0</b>	<b>-2.5551</b>	<i>syn</i>	<b>Extended</b>
<b>F2</b>	<b>60.0</b>	<b>0.0</b>	<b>-2.5551</b>	<i>syn</i>	<b>Extended</b>
<b>F3</b>	120.0	180.0	7.4974	<i>anti</i>	Bent
<b>F4</b>	180.0	180.0	7.4974	<i>anti</i>	Bent
<b>F5</b>	240.0	180.0	7.4974	<i>anti</i>	Bent
<b>F6</b>	<b>300.0</b>	<b>0.0</b>	<b>-2.5551</b>	<i>syn</i>	<b>Extended</b>

The equivalent low energy **F1/F2/F6** conformer is an extended conformer while the equivalent **F3/F4/F5** represents a much higher energy (energy difference 10.05 kcal/mol)

bent and sterically encumbered structure due to the non-bonded repulsions between the end methyl groups (C2 and C48, Figure 12).

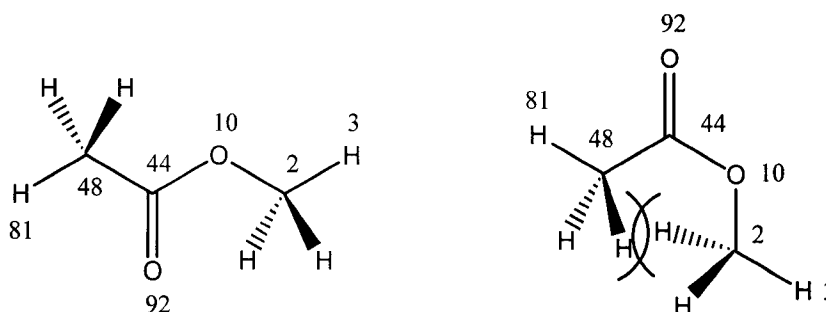


**Figure 12.** The lower energy (F1, left) and higher energy (F3, right) conformations of methyl acetate – Acyloxy Rotamer Model.

Based upon this model study, we set the C2-O10-C44-O92, C3-O11-C53-O93, C4-O12-C62-O94 and C5-O13-C71-O95 dihedral angles to  $0.0^\circ$  for each of the tetra-*O*-acetyl-*N,N'*-dimethyl-D-glucaramide rotamers before MM3 calculation.

#### Model 4: Five Vicinal Acyloxy Models – 2,3-diacetoxybutanes

The remaining models address the rotameric disposition of the four *O*-acetyl groups on carbons 2 - 5 of *N,N'*-dimethyl and -dihexyl 2,3,4,5-tetra-*O*-acetyl-D-glucaramides (**7a** and **5a**) resulting from rotation around the C2-O10, C3-O11, C4-O12 and C5-O13 bonds. By the use of conformationally and configurationally different 2,3-diacetoxybutanes as models, we wished to gain insight into the rotameric preferences of an acetoxy group on a chiral carbon, and more specifically, the rotameric preferences of two acetoxy groups on vicinal carbon atoms of different chirality and carbon chain conformations. (2*S*,3*S*)-2,3-diacetoxybutane conformer (**G**) was used as the model to mimic diamide rotamers 3



and 4 of **7a** with a *gauche* arrangement of H15-H16 (dihedral angle ca.  $-60^\circ$ ) as shown in Figure 13. In similar fashion, (2*S*,3*S*)-2,3-diacetoxybutane conformation (**J**) was employed to mimic diamide rotamers 1 and 2 with the second *gauche* arrangement of H15-H16 (dihedral angle ca.  $+60^\circ$ ) (Figure 15). Two different (2*S*,3*R*)-2,3-diacetoxybutane conformers (**K** and **L**) were used to model the two *gauche* arrangements of H17-H18 (ca.  $-60^\circ$  on **K** for rotamer 1 and rotamer 3; ca  $+60^\circ$  on **L** for rotamer 2 and 4) (Figure 16 and Figure 17). The (2*R*,3*R*)-2,3-diacetoxybutane conformer **M** mimicked the *anti* relationship (H16-H17) present in all rotamers 1 – 4 (Figure 18).

**Vicinal Acyloxy Model I ----- (2*S*3*S*)-2,3-diacetoxybutane G (H15-H16:  $-60.0^\circ$ )**

This model (Figure 13) positions the vicinal H15-H16 in a *gauche* relationship (ca.  $-60^\circ$ ) in accord with the observed *gauche* range coupling in the model diamides, **7a** and **5a**. Rotations around the C2-O10 and C3-O11 bonds in  $120^\circ$  increments from  $60^\circ$  to  $180^\circ$  and  $300^\circ$  gave 9 ( $3^2$ ) original conformations, **G1** - **G9** (Table 10).

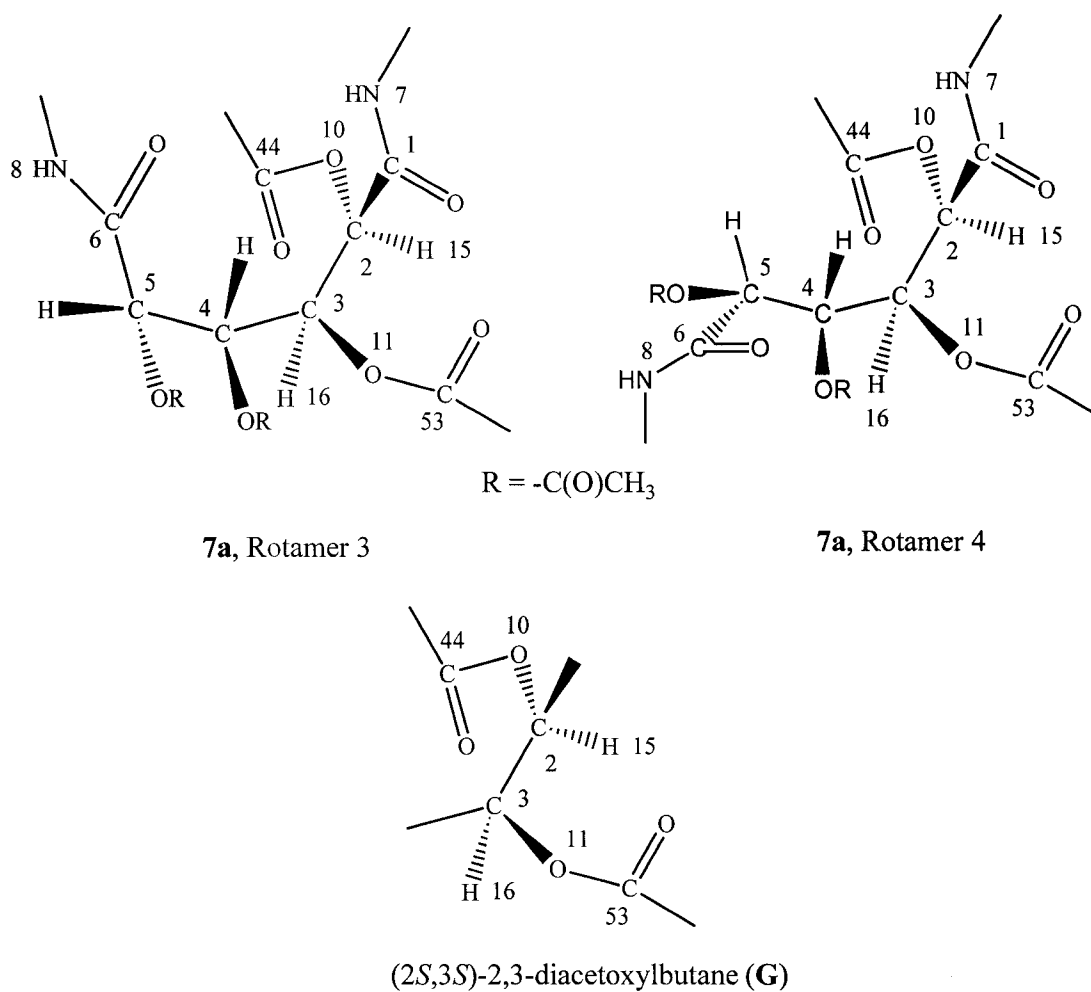


**Figure 13.** Vicinal Acyloxy Model I for C2, C3 vicinal acetyl groups of **7a**, rotamers 3 and 4: [(2*S*,3*S*)-2,3-diacetoxybutane **G** (H15-H16: -60.0°)].

**Table 10.** Torsion angles ( $\omega$ , °) before and after MM3 calculation and final energies (kcal/mol) of (2*S*,3*S*)-2,3-diacetoxybutane to determine the orientation of two adjacent acetoxy groups on C2, C3 with a dihedral angle of 60.0° between H15 and H16

	<b>G1</b>		<b>G2</b>		<b>G3</b>	
	Before MM3	After MM3	Before MM3	After MM3	<b>Before MM3</b>	<b>After MM3</b>
$\omega$ (H15-C2-O10-C44) (°)	60.0	47.3	60.0	41.9	<b>60.0</b>	<b>42.6</b>
$\omega$ (H16-C3-O11-C53) (°)	60.0	47.3	180.0	-154.0	<b>-60.0</b>	<b>-43.7</b>
Total energy (kcal/mol)	3.9532		6.9589		<b>3.8233</b>	
	<b>G4</b>		<b>G5</b>		<b>G6</b>	
	Before MM3	After MM3	Before MM3	After MM3	Before MM3	After MM3
$\omega$ (H15-C2-O10-C44) (°)	180.0	-154.0	180.0	-159.8	180.0	-155.1
$\omega$ (H16-C3-O11-C53) (°)	60.0	41.9	180.0	-159.8	-60.0	-39.3
Total energy (kcal/mol)	6.9589		11.0318		7.5216	
	<b>G7</b>		<b>G8</b>		<b>G9</b>	
	Before MM3	After MM3	Before MM3	After MM3	Before MM3	After MM3
$\omega$ (H15-C2-O10-C44) (°)	-60.0	-43.7	-60.0	-39.3	-60.0	-42.4
$\omega$ (H16-C3-O11-C53) (°)	<b>60.0</b>	<b>42.6</b>	180.0	-155.1	-60.0	-42.4
Total energy (kcal/mol)	<b>3.8233</b>		7.5215		3.9972	

Of the nine different starting conformations of (2*S*,3*S*)-2,3-diacetoxybutane **G**, only six unique conformations were generated, **G1**, **G2**, **G3**, **G5**, **G6** and **G9** (Table 11). The three remaining conformers **G4**, **G7** and **G8** are identical to **G2**, **G3** and **G6**, respectively. The low energy conformations **G3**, **G1** and **G9** are similar in that H15-C2-O10-C44 and H16-

C3-O11-C53 dihedral angles are ca. + or - 43° and +47°. That is, the hydrogen (H15 or H16) beta to the carbonyl carbon (C44 or C53) has preferred dihedral angles of ca. ±43°/+47°, all of which correspond to equally probable (same energy) conformers (Figure 14).

**Table 11.** Conformations (minima) of (2*S*,3*S*)-2,3-diacetoxybutane **G** (H15-C2-C3-H16 ca. -60.0°)

	<b>G3</b>	<b>G1</b>	<b>G9</b>	<b>G2</b>	<b>G6</b>	<b>G5</b>
$\omega$ (H15-C2-O10-C44) (°)	<b>42.6</b>	47.3	-42.4	41.9	-155.1	-159.8
$\omega$ (H16-C3-O11-C53) (°)	<b>-43.7</b>	47.3	-42.4	-154.0	-39.3	-159.8
Total energy (kcal/mol)	<b>3.8233</b>	3.9532	3.9972	6.9589	7.5216	11.0318

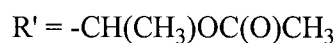
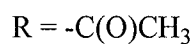
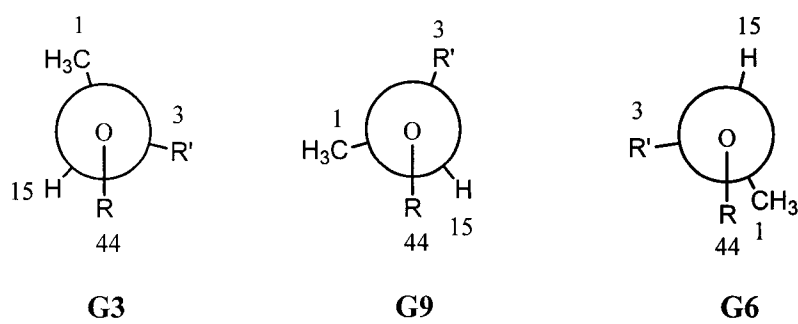


**Figure 14.** Newman projection formula of **G3**, **G9** and **G6** of (2*S*,3*S*)-2,3-diacetoxybutane (H15-C2-C3-H16 -60.0°) looking down the O10-C2 bond (R = -C(O)CH<sub>3</sub>, R' = -CH(CH<sub>3</sub>)OC(O)CH<sub>3</sub>).

Conformations **G3**, **G9** and **G6** have similar H16-C3-O11-C53 torsion angles (-43.7° for **G3**, -42.4° for **G9** and -39.3° for **G6**), but different H15-C2-O10-C44 torsion angles (+42.6° for **G3**, -42.4° for **G9** and -155.1° for **G6**). In the Newman projections (Figure 14) of **G3**, **G9** and **G6** along the O10-C2 bond, for both **G3** and **G9**, the bulky R44 (=C(O)CH<sub>3</sub>) groups are located either between smaller H15-C3 in **G3** or between H15-C1 in **G9**, while in **G6**, R44 is found to be between bulkier C1 and C3, giving **G6** a much higher steric energy (3.6983 kcal/mol) than **G3** (Table 12).

**Table 12.** Dihedral angles (°) of atoms attached to O10 and C2 of conformations **G3**, **G9** and **G6** of (2*S*,3*S*)-2,3-diacetoxybutane (H15-C2-C3-H16 -60.0°)

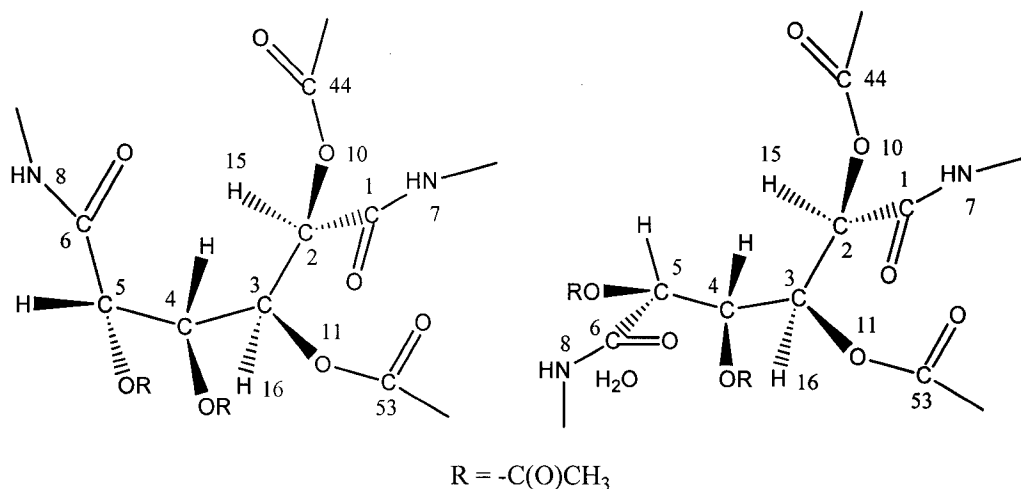
	<b>G3</b>	<b>G9</b>	<b>G6</b>
$\omega$ (C44-O10-C2-C3) (°)	<b>-77.8</b>	-159.5	90.7
$\omega$ (C44-O10-C2-H15) (°)	<b>42.6</b>	-42.4	-155.1
$\omega$ (C44-O10-C2-C1) (°)	<b>159.4</b>	77.8	-39.1
Total energy (kcal/mol)	<b>3.8233</b>	3.9972	7.5216

#### **Vicinal Acyloxy Model II ----- 2*S*3*S*-Butanediol Diacetate J (H15-H16: +60.0°)**

Vicinal Acyloxy Model II (Figure 15) was also derived from (2*S*,3*S*)-2,3-diacetoxybutane but with H15-H16 at a *gauche* angle of +60.0°, compared to -60.0° for Vicinal Acyloxy Model I. Rotation about C2-O10 and C3-O11 bonds clockwise from 60.0° to 300.0° in 120.0° increments give 9 (2<sup>3</sup>) starting conformations **J1** - **J9** (Table 13).

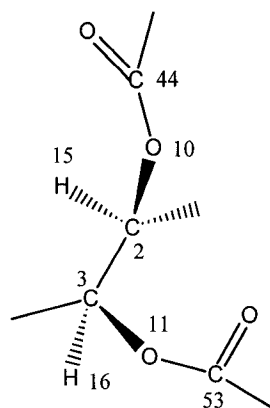
There are six unique conformers **J9**, **J3**, **J1**, **J6**, **J2** and **J5**, and three duplicate conformers, **J7** = **J3**, **J8** = **J6** and **J4** = **J2**, (Table 14). Like the low energy conformers in

Vicinal Acyloxy Model I, a single low energy conformer (**J9**, 2.56 kcal/mol) of Model II has a beta hydrogen (H15 or H16) – ester carbonyl carbon (C44 or C45) dihedral angle of about  $-42^\circ$ . The next low energy conformer (**J3** or **J7**) has one small dihedral angle (ca.  $16.1^\circ$ ) and a typical larger angle ( $-41.3^\circ$ ).



**7a**, Rotamer 1

**7a**, Rotamer 2



(2*S*,3*S*)-2,3-diacetoxybutane (**J**)

**Figure 15.** Vicinal Acyloxy Model II [(2*S*,3*S*)-2,3-diacetoxybutane (H15-H16:  $60.0^\circ$ )] for C2, C3 vicinal acetoxy groups of **7a**: rotamers 1 and 2.

**Table 13.** Torsion angles ( $\omega$ , °) before and after MM3 calculation and final energies (kcal/mol) of (2*S*,3*S*)-2,3-diacetoxybutane to determine the orientation of two adjacent acetoxy groups on C2, C3 with a dihedral angle of 60.0° between H15 and H16

	<b>J1</b>		<b>J2</b>		<b>J3</b>	
	Before MM3	After MM3	Before MM3	After MM3	Before MM3	After MM3
$\omega$ (H15-C2-O10-C44) (°)	60.0	16.1	60.0	22.2	60.0	16.1
$\omega$ (H16-C3-O11-C53) (°)	60.0	16.1	180.0	-163.6	-60.0	-41.3
Total energy (kcal/mol)	4.1369		6.4594		3.3986	
	<b>J4</b>		<b>J5</b>		<b>J6</b>	
	Before MM3	After MM3	Before MM3	After MM3	Before MM3	After MM3
$\omega$ (H15-C2-O10-C44) (°)	180.0	-163.6	180.0	-153.2	180.0	-161.1
$\omega$ (H16-C3-O11-C53) (°)	60.0	22.2	180.0	-153.2	-60.0	-41.1
Total energy (kcal/mol)	6.4593		9.2460		5.9688	
	<b>J7</b>		<b>J8</b>		<b>J9</b>	
	Before MM3	After MM3	Before MM3	After MM3	Before MM3	After MM3
$\omega$ (H15-C2-O10-C44) (°)	-60.0	-41.3	-60.0	-41.1	<b>-60.0</b>	<b>-42.1</b>
$\omega$ (H16-C3-O11-C53) (°)	60.0	16.1	180.0	-161.1	<b>-60.0</b>	<b>-42.1</b>
Total energy (kcal/mol)	3.3986		5.9688		<b>2.5648</b>	

**Table 14.** Conformations (minima) of (2*S*,3*S*)-2,3-diacetoxybutane **J** (H15-C2-C3-H16 ca. +60.0°)

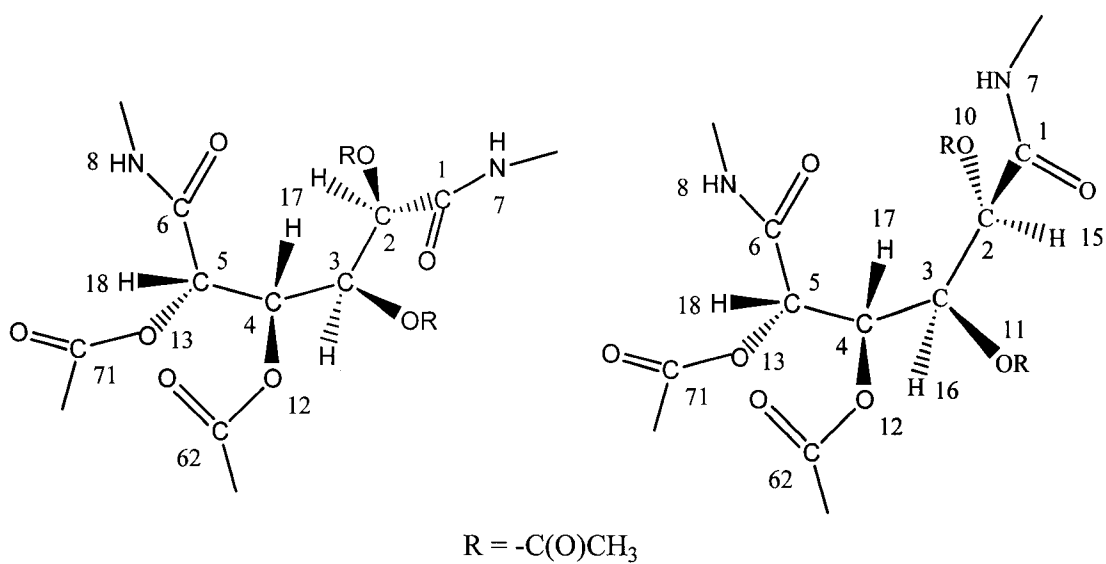
	<b>J9</b>	<b>J3</b>	<b>J1</b>	<b>J6</b>	<b>J2</b>	<b>J5</b>
$\omega$ (H15-C2-O10-C44) (°)	<b>-42.1</b>	16.1	16.1	-161.1	22.2	-153.2
$\omega$ (H16-C3-O11-C53) (°)	<b>-42.1</b>	-41.3	16.1	-41.1	-163.6	-153.2
Total energy (kcal/mol)	<b>2.5648</b>	3.3986	4.1369	5.9688	6.4594	9.2460

**Vicinal Acyloxy Models III and IV ----- (2*S*,3*R*)-2,3-Diacetoxybutane **K** (H17-H18: -60.0°) and (2*S*,3*R*)-2,3-Diacetoxybutane **L** (H17-H18: 60.0°)**

As with H15-H16, the vicinal coupling constant for H17-H18 (3.88 Hz) signifies an average *gauche* relationship of these protons with dihedral angles on the order of +60° or -60°, but with *S*(C4)*S*(C5) chirality. Vicinal Acyloxy Models III and IV represent two *gauche* conformers of (2*S*,3*R*)-2,3-diacetoxybutane.

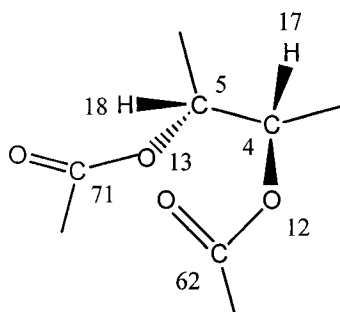
A (2*S*,3*R*)-2,3-diacetoxybutane **K** model with H17-H18 at *gauche* (ca. -60.0°) relationship was constructed (Figure 16). Rotation about C4-O12 and C5-O13 bonds from 60.0° to 300.0° in 120.0° increments generates 9 (2<sup>3</sup>) conformations (Table 15, Table 16).





7a, Rotamer 1

7a, Rotamer 3



(2*S*,3*R*)-2,3-diacetoxybutane (**K**)

**Figure 16.** Vicinal Acyloxy Model III: [(2*S*,3*R*)-2,3-diacetoxybutane **K** (H17-H18: -60.0°)] for C4, C5 vicinal acetoxy groups of 7a, rotamers 1 and 3.

**Table 15.** Torsion angles ( $\omega$ , °) before and after MM3 calculation and final energies (kcal/mol) of (2*S*,3*R*)-2,3-diacetoxybutane to determine the orientation of two adjacent acetoxy groups on C4, C5 with a dihedral angle of -60.0° between H17 and H18

	<b>K1</b>		<b>K2</b>		<b>K3</b>	
	Before MM3	After MM3	Before MM3	After MM3	Before MM3	After MM3
$\omega$ (H17-C4-O12-C62) (°)	60.0	41.7	60.0	41.1	60.0	42.4
$\omega$ (H18-C5-O13-C71) (°)	60.0	41.9	180.0	153.1	-60.0	-26.2
Total energy (kcal/mol)	2.7902		6.0307		3.2950	
	<b>K4</b>		<b>K5</b>		<b>K6</b>	
	Before MM3	After MM3	Before MM3	After MM3	Before MM3	After MM3
$\omega$ (H17-C4-O12-C62) (°)	180.0	-162.6	180.0	-166.9	180.0	-157.9
$\omega$ (H18-C5-O13-C71) (°)	60.0	38.7	180.0	157.8	-60.0	-16.8
Total energy (kcal/mol)	6.2290		9.5385		6.7811	
	<b>K7</b>		<b>K8</b>		<b>K9</b>	
	Before MM3	After MM3	Before MM3	After MM3	Before MM3	After MM3
$\omega$ (H17-C4-O12-C62) (°)	-60.0	41.4	-60.0	-40.3	-60.0	-40.6
$\omega$ (H18-C5-O13-C71) (°)	60.0	41.8	180.0	150.0	-60.0	-23.1
Total energy (kcal/mol)	3.1179		6.6204		4.0440	

**Table 16.** Conformations (minima) of (2*S*,3*R*)-2,3-diacetoxybutane **K** (H17-C4-C5-H18 ca. -60.0°)

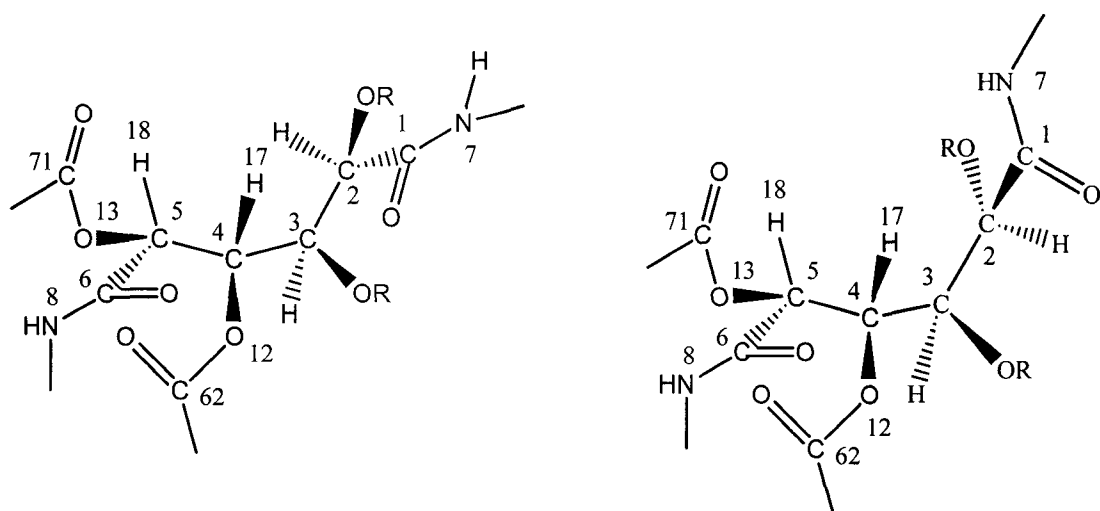
	<b>K1</b>	<b>K7</b>	<b>K3</b>	<b>K9</b>	<b>K2</b>	<b>K8</b>	<b>K4</b>	<b>K6</b>	<b>K5</b>
$\omega$ (H15-C2-O10-C44) (°)	<b>41.7</b>	41.4	42.4	-40.6	41.1	-40.3	-162.6	-157.9	-166.9
$\omega$ (H16-C3-O11-C53) (°)	<b>41.9</b>	41.8	-26.2	-23.1	153.1	150.0	38.7	-16.8	157.8
Total energy (kcal/mol)	<b>2.7902</b>	3.1179	3.2950	4.0440	6.0307	6.6204	6.2290	6.7811	9.5385

Table 17 illustrates the results of Vicinal Acyloxy Model IV - (2*S*,3*R*)-2,3-diacetoxybutane model L (H17-C4-C5-H18 ca. +60.0°) studies (Figure 17) through rotation about the C4-O12 and C5-O13 bonds from 60.0° to 300.0° with 120.0° increment each. Nine (2<sup>3</sup>) individual conformations were generated after MM3 minimization.

Low energy conformers from Vicinal Acyloxy Model III **K1** (+41.7°, +41.9°, 2.79 kcal/mol), **K7** (+41.4°, +41.8°, 3.12 kcal/mol) and **K3** (+42.4°, -26.2°, 3.30 kcal/mol) (Table 16) have similar preferred beta hydrogen-carbonyl carbon dihedral angles (ca. 42° and 26°) to those from Vicinal Acyloxy Model II, as do the corresponding low energy conformers of Model IV **L9** (-41.9°, -41.7°, 2.79 kcal/mol), **L7** (-41.8°, +41.4°, 3.12 kcal/mol) and **L3** (+26.2°, -42.4°, 3.29 kcal/mol) (Table 18).

**Table 17.** Torsion angles ( $\omega$ , °) before and after MM3 calculation and final energies (kcal/mol) of (2*S*,3*R*)-2,3-diacetoxybutane model **L** to determine the orientation of two adjacent acetoxy groups on C4, C5 with a dihedral angle +60.0° between H17 and H18

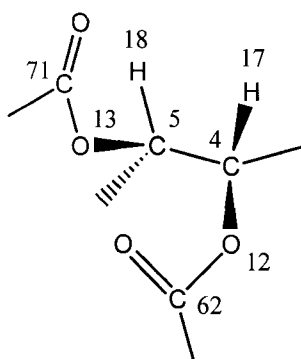
	<b>L1</b>		<b>L2</b>		<b>L3</b>	
	Before MM3	After MM3	Before MM3	After MM3	Before MM3	After MM3
$\omega$ (H17-C4-O12-C62) (°)	60.0	23.1	60.0	16.8	60.0	26.2
$\omega$ (H18-C5-O13-C71) (°)	60.0	40.6	180.0	157.9	-60.0	-42.4
Total energy (kcal/mol)	4.0440		6.7810		3.2940	
	<b>L4</b>		<b>L5</b>		<b>L6</b>	
	Before MM3	After MM3	Before MM3	After MM3	Before MM3	After MM3
$\omega$ (H17-C4-O12-C62) (°)	180.0	-154.0	180.0	-157.8	180.0	-153.1
$\omega$ (H18-C5-O13-C71) (°)	60.0	40.3	180.0	166.9	-60.0	-41.1
Total energy (kcal/mol)	6.6204		9.5385		6.0307	
	<b>L7</b>		<b>L8</b>		<b>L9</b>	
	Before MM3	After MM3	Before MM3	After MM3	Before MM3	After MM3
$\omega$ (H17-C4-O12-C62) (°)	-60.0	-41.8	-60.0	-38.7	<b>-60.0</b>	<b>-41.9</b>
$\omega$ (H18-C5-O13-C71) (°)	60.0	41.4	180.0	162.6	<b>-60.0</b>	<b>-41.7</b>
Total energy (kcal/mol)	3.1179		6.2290		<b>2.7902</b>	



7a, Rotamer 2

R = -C(O)CH<sub>3</sub>

7a, Rotamer 4



(2*S*,3*R*)-2,3-diacetoxybutane (L)

**Figure 17.** Vicinal Acyloxy Model IV: [(2*S*,3*R*)-2,3-diacetoxybutane L (H17-C4-C5-H18 ca. +60.0°)] for vicinal C3, C4 acetoxy groups of 7a, rotamers 1 - 4.

**Table 18.** Conformations (minima) of (2*S*,3*R*)-2,3-diacetoxybutane **L** (H17-C4-C5-H18 ca. +60.0°)

	<b>L9</b>	<b>L7</b>	<b>L3</b>	<b>L1</b>	<b>L6</b>	<b>L8</b>	<b>L4</b>	<b>L2</b>	<b>L5</b>
$\omega$ (H15-C2-O10-C44) (°)	<b>-41.9</b>	-41.8	26.2	23.1	-153.1	-38.7	-154.0	16.8	-157.8
$\omega$ (H16-C3-O11-C53) (°)	<b>-41.7</b>	41.4	-42.4	40.6	-41.1	162.6	40.3	157.9	166.9
Total energy (kcal/mol)	<b>2.7902</b>	3.1179	3.2940	4.0440	6.0307	6.2290	6.6204	6.7810	9.5385

**Vicinal Acyloxy Model V ----- (2R,3R)-2,3-Diacetoxybutane M (H16-H17: 180.0°)**

The last of the Vicinal Acyloxy Models is concerned with the conformational preference of the *anti* H16, H17 protons relative to the corresponding beta-carbonyl carbons C53 and C62 on the chiral 3*S*, 4*S* carbons of the model diamide **7a**. Unlike Acyloxy Models I – IV, the two protons of interests, H16 and H17, are considered to be *anti* rather than *gauche*. This fixed *anti* relationship of H16-H17 is found in all four sickle rotamers of **7a**. A suitable model to mimic this part of **7a** is (2*R*,3*R*)-2,3-diacetoxybutane (Figure 18).

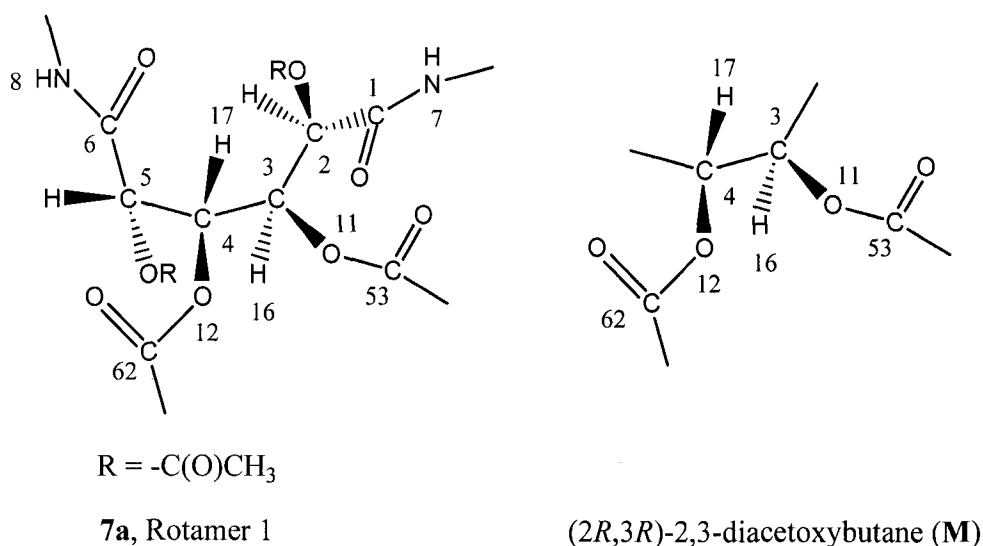


**Figure 18.** Vicinal Acyloxy Model V of **7a**: (2*R*,3*R*)-2,3-acetoxybutane **M** (H16-H17: 180.0°).

Rotation of the dihedral angles formed by H17-C3-O11-C53 and H18-C4-O12-C62 in 120.0° increments (Table 19) generated 9 (2<sup>3</sup>) original conformers. Four unique conformers **M1**, **M3**, **M2**, **M6** (Table 20) were obtained after MM3 minimization, with



one significantly low energy conformer **M1** (2.82 kcal/mol) having both dihedral angles at 39.6°.

**Table 19.** Torsion angles ( $\omega$ , °) before and after MM3 calculation and final energies (kcal/mol) of (2*R*,3*R*)-2,3-acetoxybutane **M** to determine the orientation of two adjacent acetoxy groups on C3, C4 with a dihedral angle of 180.0° between H16 and H17

	<b>M1</b>		<b>M2</b>		<b>M3</b>	
	<b>Before MM3</b>	<b>After MM3</b>	Before MM3	After MM3	Before MM3	After MM3
$\omega$ (H16-C3-O11-C53) (°)	<b>60.0</b>	<b>39.6</b>	60.0	40.2	60.0	38.4
$\omega$ (H17-C4-O12-C62) (°)	<b>60.0</b>	<b>39.6</b>	180.0	177.2	-60.0	-20.9
Total energy (kcal/mol)	<b>2.8220</b>		3.9903		3.6439	
	<b>M4</b>		<b>M5</b>		<b>M6</b>	
	<b>Before MM3</b>	<b>After MM3</b>	Before MM3	After MM3	Before MM3	After MM3
$\omega$ (H16-C3-O11-C53) (°)	180.0	177.2	180.0	177.2	180.0	174.8
$\omega$ (H17-C4-O12-C62) (°)	60.0	40.2	180.0	40.2	-60.0	-21.3
Total energy (kcal/mol)	3.9902		3.9903		4.8466	
	<b>M7</b>		<b>M8</b>		<b>M9</b>	
	<b>Before MM3</b>	<b>After MM3</b>	Before MM3	After MM3	Before MM3	After MM3
$\omega$ (H16-C3-O11-C53) (°)	<b>-60.0</b>	<b>39.6</b>	-60.0	40.2	-60.0	38.4
$\omega$ (H17-C4-O12-C62) (°)	<b>60.0</b>	<b>39.6</b>	180.0	177.2	-60.0	-20.9
Total energy (kcal/mol)	<b>2.8220</b>		3.9903		3.6439	

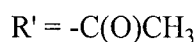
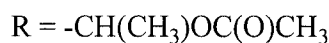
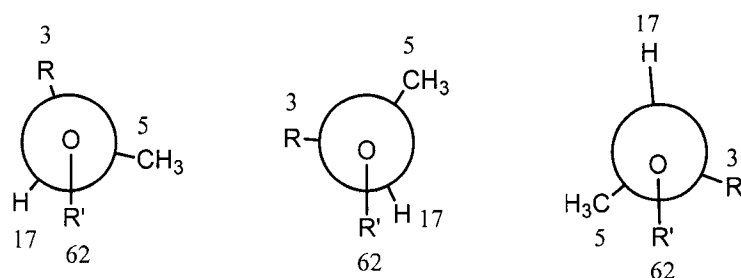
**Table 20.** Minima of (2*R*,3*R*)-2,3-acetoxybutane **M** (H16-C3-C4-H17 ca. 180.0°)

	<b>M1</b>	<b>M3</b>	<b>M2</b>	<b>M6</b>
$\omega$ (H16-C3-O11-C53) (°)	<b>39.6</b>	38.4	40.2	174.8
$\omega$ (H17-C4-O12-C62) (°)	<b>39.6</b>	-20.9	177.2	-21.3
Total energy (kcal/mol)	<b>2.8220</b>	3.6439	3.9903	4.8466

The energy difference between conformations **M1** (global minimum) and **M3** is 0.8219 kcal/mol, but the two conformations look very similar. However, the H17 and C62 dihedral angle in **M3** is  $-20.9^\circ$ , while this angle is  $+39.6^\circ$  in **M1** (Table 21). In **M2** (Figure 19), R'62 (-C(O)CH<sub>3</sub>) is located between bulkier R (R = -CH(CH<sub>3</sub>)OC(O)CH<sub>3</sub>) and the C5 methyl groups, resulting in increased steric strain.

**Table 21.** Dihedral angles (°) of some minima of (2*R*,3*R*)-2,3-acetoxybutane **M** (H16-C3-C4-H17 ca. 180.0°)

	<b>M1</b>	<b>M3</b>	<b>M2</b>
$\omega$ (H17-C4-O12-C62) (°)	<b>39.6</b>	-20.9	177.2
$\omega$ (C3-C4-O12-C62) (°)	<b>158.3</b>	100.7	-65.4
$\omega$ (C5-C4-O12-C62) (°)	<b>-81.1</b>	-139.1	60.9
Total energy (kcal/mol)	<b>2.8220</b>	3.6440	3.9903



**M1**

**M3**

**M2**

**Figure 19.** Newman projections of (2*R*,3*R*)-2,3-acetoxybutane **M** (H16-C3-C4-H17 180.0°) to compare conformations **M1**, **M3** and **M2** with O12 in the front and C4 in the back.

Interestingly, the conformation of the highest energy minimum **M6** (174.8°, -21.3°, 4.8466 kcal/mol) combines the steric strain of both **M3** and **M2**, which is 2.0246 kcal/mol higher in energy than **M1**, just about the sum (1.9902 kcal/mol) of energy difference of **M3** - **M1** (0.8219 kcal/mol) and **M2** - **M1** (1.1683 kcal/mol).

The dihedral angle of 39.6° of conformer **M1** is the value applied to all four starting sickle rotamers of **7a**.

2,3-Diacetoxybutanes (**G**, **J**, **K**, **L** and **M**) employed in the Vicinal Acyloxy Models illustrate that for an acetoxy group, the dihedral angle of H-C-O-C is in the range of ca. -40° to +40° degree. French et al.<sup>[30]</sup> have recently modeled the conformation of acetate groups, as found on isopropyl acetate and 3,4,5-triacetoxytetrahydropyran, using MM3 molecular mechanics and several quantum mechanics protocols. They found that in

general the H-C-O-C (carbonyl) conformations ranged from *eclipsed-to-gauche*, as we have concluded from the studies reported here using the Vicinal Acyloxy Model 4. In addition, X-ray crystal structure data from penta-*O*-acetyl- $\beta$ -D-galactopyranose<sup>[30]</sup> and 164 additional examples in the literature strongly supported the above conformational preference of acetate groups in the crystal state.

Consequently, all combinations of +40° and -40° were applied in the conformational study of **7a**, i.e., for each of the 4 acetoxy groups in **7a**, 16 ( $2^4$ ) conformations can be generated from each of the original rotamers that were refined using Models 1-3 (Table 22).

**Table 22.** Sixteen possible conformations of every rotamer of 2,3,4,5-tetra-*O*-acetyl *N,N'*-dimethyl-D-glucaramide (**7a**)

	$\omega$ (H15-C2-O10-C44) ( $^{\circ}$ )	$\omega$ (H16-C3-O11-C53) ( $^{\circ}$ )	$\omega$ (H17-C4-O12-C62) ( $^{\circ}$ )	$\omega$ (H18-C5-O13-C71) ( $^{\circ}$ )
1	+40	+40	+40	+40
2	+40	+40	+40	-40
3	+40	+40	-40	-40
4	+40	-40	-40	-40
5	+40	+40	-40	+40
6	+40	-40	+40	+40
7	+40	-40	+40	+40
8	+40	-40	+40	-40
9	-40	+40	+40	+40
10	-40	-40	+40	+40
11	-40	-40	-40	+40
12	-40	-40	-40	-40
13	-40	+40	-40	+40
14	-40	+40	-40	-40
15	-40	+40	+40	-40
16	-40	-40	+40	-40

### Summary of Models I - V

Based upon the  $^1\text{H}$  NMR data from **7a**, four rotamers (1 - 4, Figure 4) established the general conformational preferences of this molecule, i.e. with H15, H16 and H17, H18 in *gauche* (ca.  $\pm 60^{\circ}$ ) relationships and H16, H17 in an *anti* (ca.  $180^{\circ}$ ) relationship. Model 1 (End C Model, *N*-methylacetamide) established a starting dihedral angle of  $180^{\circ}$  for dihedral angles O9-C1-N7-H19 and O14-C6-N8-H22 at the ends of the molecule, while

Model 2 (C1-C2 & C5-C6 Model, (2*R*) and (2*S*)-*N*-methyl-2-acetoxypropanamide) set the angular relationship between the end acetoxy groups alkyl oxygens and the amide carbonyl oxygens (O9-C1-C2-O10 dihedral angle +125.8° from (2*R*)-*N*-methyl-2-acetoxypropanamide and O13-C5-C6-O14 dihedral angle -125.8° from (2*S*)-*N*-methyl-2-acetoxypropanamide). Model 3 (Acyloxy Rotamer Model, methyl acetate) was employed to set the acetoxy carbonyl oxygen – backbone carbon dihedral angle [C2-O10-C44-O92 and other similar angles (Table 10)] to 0°. The five different forms of Model 4 (Vicinal Acyloxy Model) led to the conclusion that the four acetoxy carbonyl carbons – beta hydrogen atom dihedral angles are in the range of ca. +40° to -40°. Each of the four starting rotamers (1 – 4) can have 16 (2<sup>4</sup>) different conformations based upon the two conformational possibilities from Model 4 as applied to the four chiral carbons of **7a**, or a total of 64 conformers derived from the original four rotamers. The torsion angles suggested by the model studies for **7a** are given in Table 22.

### **5. Molecular Mechanics Study of 2,3,4,5-tetra-*O*-acetyl-*N,N'*-dimethyl-D-glucaramide (**7a**)**

Molecular Mechanics, the “Block diagonal then full matrix minimization” method at dielectric constant 1.0, was applied to the calculation of the 64 conformations of tetra-*O*-acetyl-*N,N'*-dimethyl-D-glucaramide (**7a**, Table 23). For every rotamer, the lowest energy is bold.

**Table 23.** MM3 calculated energies (kcal/mol) of different 2,3,4,5-tetra-*O*-acetyl-*N,N'*-dimethyl-*D*-glucaramide (**7a**) rotamers

<b>7a</b>	<b>1m</b>	<b>2m</b>	<b>3m</b>	<b>4m</b>
1	<b>-2.6575</b>	0.0288	<b>-4.6424</b>	3.4155
2	8.2420	<b>-0.9764</b>	<b>-4.6423</b>	<b>-3.0162</b>
3	-1.9055	<b>-0.9764</b>	<b>-4.6424</b>	-0.5719
4	8.1910	-0.6953	-3.8013	0.0647
5	0.3752	0.1771	<b>-4.6424</b>	3.4156
6	0.3752	0.0289	<b>-4.6424</b>	3.9032
7	<b>-2.6575</b>	0.0288	-3.8013	3.9032
8	8.2083	<b>-0.9764</b>	-3.8013	0.0648
9	<b>-2.6575</b>	0.0288	-0.4876	-1.6496
10	<b>-2.6575</b>	0.0288	-0.4877	-0.0119
11	-1.5047	0.0779	1.0361	-0.0636
12	1.8594	-0.8410	1.5339	2.0246
13	-1.9054	0.5302	-0.4876	-1.6496
14	1.8595	<b>-0.9764</b>	-0.4876	1.0032
15	0.9998	<b>-0.9764</b>	-0.4877	1.0032
16	0.9998	<b>-0.9764</b>	0.7796	2.0245

The torsion angles suggested by model studies in the above section and all the low energy conformations of rotamers **1m** to **4m** are listed in Table 24. The O9-C1-C2-O10 and O13-C5-C6-O14 dihedral angles from rotamers **1m** – **4m** suggested that they can adopt either *ca.* + or - 130° to 160°. The data in Table 25 also indicate that there is free rotation around the terminal C1-C2 and C5-C6. For example, in rotamer 3, the O9-C1-C2-O10 dihedral angle was set to +125.8° and the O13-C5-C6-O14 dihedral angle was set to -125.8°. However, in minimized **3m**, the first “+” angle went to a large “-” angle, -155.7°, whereas the minimized second angle (-132.8°) was close to the assigned angle of -125.8°. In rotamer **4m**, these same two angles underwent rotation from assigned +125.8° to minimized -163.4°, and -125.8° to +154.5°. The consistency of dihedral angles of target compound (**7a**) and the model compounds validated the “model building” approach employed in this study.



**Table 24.** Calculated torsion angles ( $\omega$ , °) of the final four low energy rotamers of **7a** as compared to the torsion angles suggested by the model studies

Torsion angle ( $\omega$ , °)	1m	2m	3m	4m	Suggested	Model
O9-C1-N7-H19	172.3	174.1	-175.2	-177.2	180.0	End C Model
O14-C6-N8-H22	-169.1	172.4	-172.9	168.4	180.0	End C Model
O9-C1-C2-O10	139.2	132.5	-155.7	-163.4	+125.8	C1-C2 & C5-C6 Model
O13-C5-C6-O14	-141.6	146.6	-132.8	154.5	-125.8	C1-C2 & C5-C6 Model
C2-O10-C44-O92	-7.0	-5.0	4.4	-1.3	0.0	Acyloxy Rotamer Model
C3-O11-C53-O93	-1.1	-1.5	-2.8	-2.2	0.0	Acyloxy Rotamer Model
C4-O12-C62-O94	1.3	3.5	1.8	7.6	0.0	Acyloxy Rotamer Model
C5-O13-C71-O95	7.8	2.5	5.7	0.5	0.0	Acyloxy Rotamer Model
H15-C2-O10-C44	-35.4	-32.7	37.5	-41.0	$\sim \pm 40.0$	Vicinal Acyloxy Model
H16-C3-O11-C53	-23.6	-26.6	39.9	40.7	$\sim \pm 40.0$	Vicinal Acyloxy Model
H17-C4-O12-C62	39.9	12.1	38.4	51.4	$\sim \pm 40.0$	Vicinal Acyloxy Model
H18-C5-O13-C71	33.9	-40.6	30.4	-22.7	$\sim \pm 40.0$	Vicinal Acyloxy Model

## 6. Predominant Conformation of 2,3,4,5-tetra-*O*-acetyl-*N,N'*-dimethyl-*D*-glucaramide (**7a**)

Figure 20 shows the low energy conformations derived from each of the four starting rotamers of **7a**. To make them comparable, they are aligned with same sequence of numbering, from right to left.

The MM3 calculation results for the low energy conformations of rotamers **1m** to **4m** (**7a**) are listed in Table 25. Rotamer **3m** is the lowest energy conformation, 1.5869 kcal/mol lower in energy than the next stable conformer (rotamer **4m**). The following equations<sup>[15-17]</sup> were utilized for percentage population calculation:

$$Na/No = \exp(-\Delta E/RT) \quad 1.1$$

$$Pa = [(Na/No) / \Sigma(Ni/No)] \times 100 \quad 1.2$$

$Na/No$  is the molar ratio of some rotamer  $a$  to the most stable rotamer  $o$ , and the energy difference between the two rotamers is  $\Delta E$  (J, the energy was calculated according to the equation 1 cal = 4.2 J). The constant  $R$  is 8.314 J/(mol·K), and  $T$  is 298 K.  $Pa$  is the population (in percent) of any rotamer  $a$  among a total of  $i$  rotamers.<sup>[15]</sup>

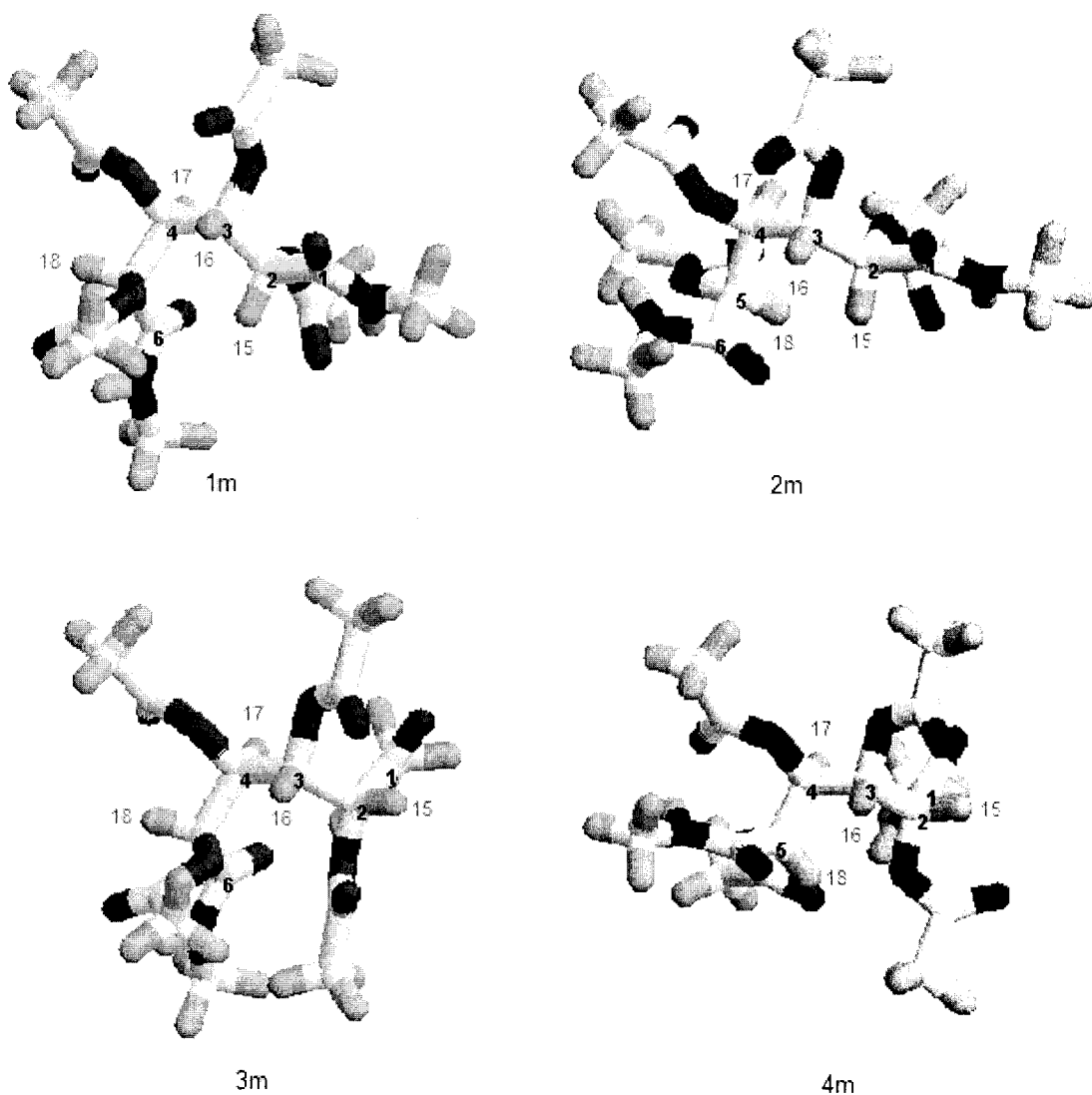


**Figure 20.** Low-energy conformations **1m** – **4m\*** derived from starting rotamers 1 - 4 (**7a**).

\*The “m” indicates a minimized conformation.

**Table 25.** Energy distribution for low-energy conformations **1m** - **4m** of 2,3,4,5-tetra-*O*-acetyl-*N,N'*-dimethyl-*D*-glucaramide (**7a**) using MM3 at dielectric constant 1.0

<b>7a</b>	<b>1m</b>	<b>2m</b>	<b>3m</b>	<b>4m</b>
Total energy (kcal/mol)	-2.6575	-0.9764	<b>-4.6425</b>	-3.0162
Compression (kcal/mol)	3.9323	3.3561	4.3324	4.4306
Bending (kcal/mol)	5.8716	4.6713	6.5251	5.6488
Stretch-bend (kcal/mol)	0.4487	0.3668	0.5770	0.5225
Bend-bend (kcal/mol)	-0.0237	-0.0573	0.0324	-0.0164
Van der waals 1,4 energy (kcal/mol)	20.3510	20.5402	21.0514	20.6140
Other (kcal/mol)	-9.1719	-8.3642	-12.1421	-12.0338
Torsional (kcal/mol)	-4.7361	-5.5050	-3.1280	-3.6718
Torsion-stretch (kcal/mol)	-0.2952	-0.2161	-0.4065	-0.4946
Dipole-dipole (kcal/mol)	-19.0343	-15.7682	-21.4842	-18.0155
Charge-dipole (kcal/mol)	0.0000	0.0000	0.0000	0.0000
Charge-charge (kcal/mol)	0.0000	0.0000	0.0000	0.0000
Na/No	0.034562	0.002000	1	0.063487
Percent population (%)	3.14	0.18	<b>90.91</b>	5.77

Applying equations 1.1 and 1.2, rotamer **3m** is the predominant average conformation of **7a**,  ${}_2G^+{}_3G^+{}_4G^-$ , with a 90.54% population (Figure 21).

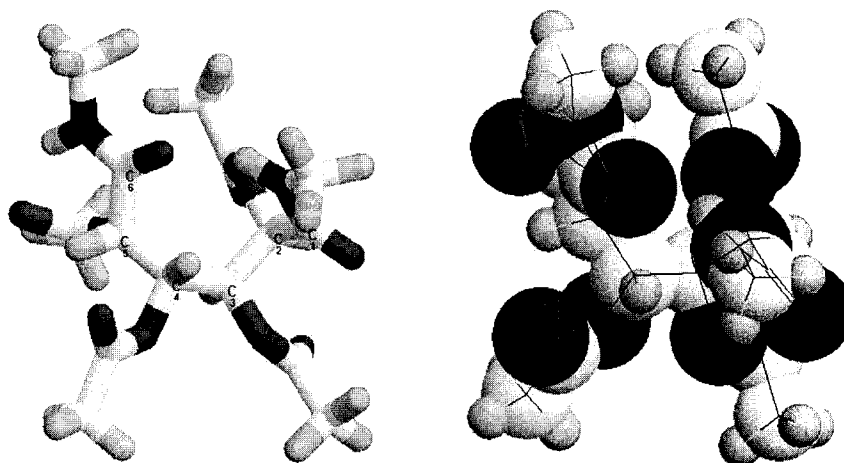


**Figure 21.** Minimum energy (MM3) rotamer **3m** (**7a**) (Tubes and Spheres-and-Sticks rendering).

MM3 calculated vicinal hydrogen dihedral angles in the glucaryl unit of **7a** are listed in Table 26. For rotamer **3m**, the H16, H17 dihedral angle is  $-176.6^\circ$  (close to  $180^\circ$ ), while that between H15-H16 is  $-50.5^\circ$  (close to  $60^\circ$ ). However, the H17-H18 dihedral angle ( $-84.2^\circ$ ) is significantly biased from  $60^\circ$ .

**Table 26.** MM3 calculated dihedral angles ( $\omega$ ,  $^\circ$ ) of 2,3,4,5-tetra-*O*-acetyl-*N,N'*-dimethyl-D-glucaramide (**7a**)

	<b>1m</b>	<b>2m</b>	<b>3m</b>	<b>4m</b>
$\omega$ (H15-C2-C3-H16) ( $^\circ$ )	63.5	55.7	<b>-50.5</b>	-61.1
$\omega$ (H16-C3-C4-H17) ( $^\circ$ )	174.8	172.7	<b>-176.6</b>	-175.3
$\omega$ (H17-C4-C5-H18) ( $^\circ$ )	-81.3	58.9	<b>-84.2</b>	92.9

Vicinal coupling constants for rotamers **1m** – **4m** were calculated according to the Karplus/Altona equation<sup>[25]</sup> and compared to <sup>1</sup>H NMR results (Table 27). For the low energy conformation, rotamer **3m**, the coupling constant between H17 and H18 (0.23 Hz) is much lower than the observed experimental value.

**Table 27.** Vicinal coupling constants (J, Hz) of 2,3,4,5-tetra-*O*-acetyl-*N,N'*-dimethyl-D-glucaramide (**7a**) (Karplus/Altona calculated and <sup>1</sup>H NMR)

	<b>1m</b>	<b>2m</b>	<b>3m</b>	<b>4m</b>	<b>Observed (<sup>1</sup>H NMR)</b>
J <sub>15,16</sub> (Hz)	2.33	3.69	<b>4.49</b>	2.54	<b>3.17</b>
J <sub>16,17</sub> (Hz)	13.15	13.06	<b>13.17</b>	13.12	<b>7.62</b>
J <sub>17,18</sub> (Hz)	0.34	3.01	<b>0.23</b>	0.28	<b>3.81</b>

Careful examinations of rotamer **3m** revealed two intramolecular hydrogen bonds, both including the amide N-H hydrogens and carbonyl oxygens (Figure 22). The first, C71=O95...H22-N8 (1.954 Å) forms a 7-membered ring between an amide N-H and an acetoxy carbonyl oxygen atom. The second hydrogen bond, C6=O14...H19-N7 (1.921 Å), is between an amide N-H at one end (head of the molecule) and an amide carbonyl oxygen at the other end (tail of the molecule). The intra-molecular hydrogen bonding across the structure between terminal amides appears to open the dihedral angle between H17-H18 and fix the final conformation, perhaps contributing to the discrepancy between the theoretical and experimental coupling constants for H17, H18.

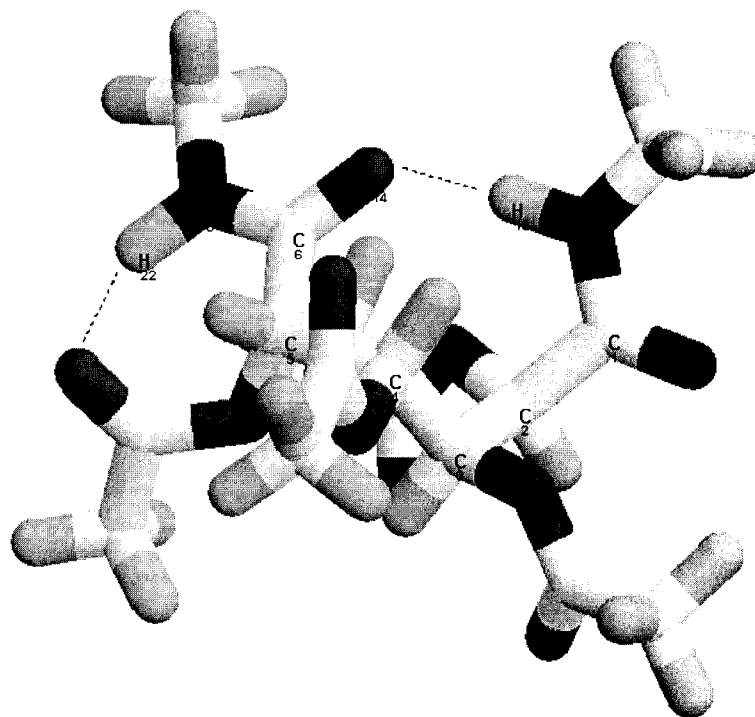


**Figure 22.** Intramolecular hydrogen bonding of rotamer **3m** (**7a**, the distance of C71=O95...H22-N8 is 1.954 Å and the distance of C6=O14...H19-N7 calculated to be 1.921 Å).

A list of all amide N-H and ester oxygens as a measure of potential hydrogen bonding in conformations **1m** – **4m** is given in Table 28. Hydrogen bonds were only considered at an interatomic distance of 2.10 Å or less.<sup>[31-34]</sup> Conformations **1m**, **3m** and **4m** show two intramolecular hydrogen bonds, whereas rotamer **2m** has only one hydrogen bond.

**Table 28.** Distances (Å) of amide hydrogens and oxygen atoms (either carbonyl O or ester O) of low energy minima (**1m – 4m**) of **7a**

		<b>1m</b>	<b>2m</b>	<b>3m</b>	<b>4m</b>	
C=O	H19(N7)-O9(C1)	3.176	3.182	3.191	3.199	
	H19(N7)-O92(C2)	<b>1.955</b>	<b>1.963</b>	4.579	3.420	
	H19(N7)-O93(C3)	6.162	6.304	5.622	5.695	
	H19(N7)-O94(C4)	7.563	7.310	4.837	5.084	
	H19(N7)-O95(C5)	7.395	5.860	6.023	<b>1.937</b>	
	H19(N7)-O14(C6)	4.839	5.222	<b>1.921</b>	5.448	
	H22(N8)-O9(C1)	6.366	6.552	7.296	6.962	
	H22(N8)-O92(C2)	5.008	6.771	4.967	7.795	
	H22(N8)-O93(C3)	6.826	4.658	7.246	6.880	
	H22(N8)-O94(C4)	5.249	3.957	5.029	<b>2.050</b>	
	H22(N8)-O95(C5)	<b>1.972</b>	4.579	<b>1.954</b>	4.515	
	H22(N8)-O14(C6)	3.173	3.176	3.176	3.177	
	C-O-C	H19(N7)-O10(C2)	2.567	2.610	2.325	2.319
		H19(N7)-O11(C3)	4.439	4.517	4.175	4.396
H19(N7)-O12(C4)		6.373	6.351	4.643	4.719	
H19(N7)-O13(C5)		5.497	6.537	4.418	3.421	
H22(N8)-O10(C2)		5.200	5.737	4.263	5.541	
H22(N8)-O11(C3)		6.136	5.072	6.273	5.397	
H22(N8)-O12(C4)		4.912	2.479	4.819	2.951	
H22(N8)-O13(C5)		2.543	2.369	2.616	2.289	



### III. Comparison of 2,3,4,5-tetra-*O*-acetyl-*N,N'*-dimethyl-*D*-glucaramide (7a) and *D*-glucaramide (8) - molecular modeling methods and results

A “systematic search” / “grid search” method<sup>[26]</sup> was applied to conformational studies of *D*-glucaramide (8) at dielectric constant 3.5 generating 19,683 ( $3^9$ ) starting conformations,<sup>[17]</sup> in which 2,085 distinct conformations were obtained after MM3 minimization (“block diagonal then full matrix minimization method”). Among the ten lowest energy conformations (energy difference within 1 kcal/mol), nine adopt a sickle conformation. A single extended conformation (8-9a) accounts for only 4.7% of the ten low energy forms. Conformation 8-1a, with a  ${}_3G^+{}_4G^-$  conformation, is the global minimum and accounts for 24.0% of the population. An almost identical conformation (8-3a) accounts for an additional 16.2%.

Superimposed images of the global minima of both tetra-*O*-acetyl-*N,N'*-dimethyl-*D*-glucaramide (7a, rotamer 3m, numbered carbons) and *D*-glucaramide (conformation 8-1a) are shown in Figure 23. The striking superimposition of the backbone carbons (except for the C1 carbons) and pendant oxygens supports the credibility of the “model building approach” method that has been applied in this study. The terminal carbon locations, for both molecules, using two modeling approaches, are difficult to define accurately since intramolecular hydrogen bonding between amide NH groups as H donors biases all of the structures generated.

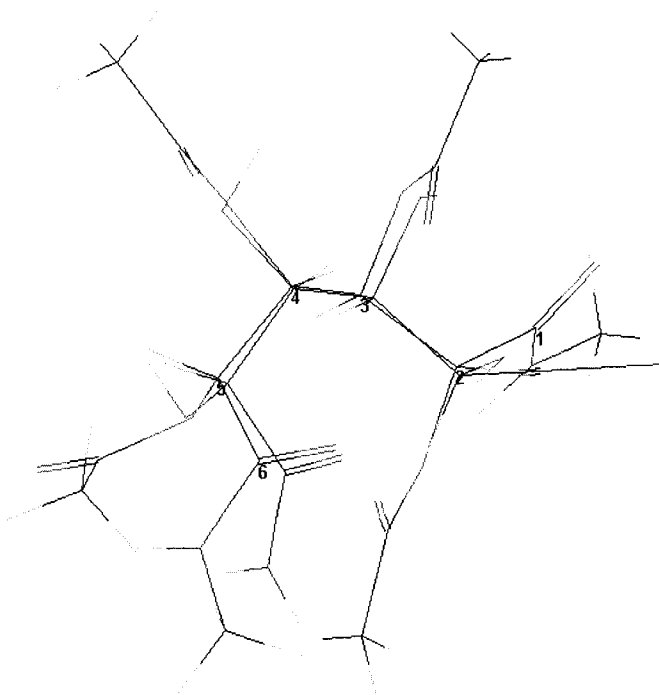


**Figure 23.** Superimposed conformations of global minima of both tetra-*O*-acetyl *N,N'*-dimethyl-*D*-glucaramide (**7a**, rotamer **3m**, numbered carbons) and *D*-glucaramide (conformation **8-1a**). The numbers the figure are for tetra-*O*-acetyl-*N,N'*-dimethyl-*D*-glucaramide (**7a**, rotamer **3m**).

A “model building” approach was applied to evaluate the conformational preference of tetra-*O*-acetyl-*N,N'*-dimethyl-*D*-glucaramide (**7a**). This approach was employed to significantly reduce the total number of conformations ( $3^{15}$ ) or 14,348,907, possible for **7a**, to a valuable 64 conformers. Four different basic model structures were used to conformationally mimic various parts of **7a**, including stereochemistry of the four chiral carbons, and the calculated and predicted angles compared (Table 25). The calculated and predicted angles compared well, indicating that the “model building” approach can be

applied to molecules of the type studied. In addition, the consistency between reported results on the conformation of pendant acetate groups on carbohydrates<sup>[30]</sup> and amide bond angles results<sup>[28]</sup> is very satisfying to the author.

#### IV. X-ray crystallography study of tetra-*O*-acetyl-*N,N'*-dimethyl-*D*-glucaramide (**7a**) and *D*-Glucaramide (**8**)

The X-ray crystal structure of *N,N'*-dimethyl 2,3,4,5-tetra-*O*-acetyl-*D*-glucaramide (**7a**) was determined by Dr. Kenneth I. Hardcastle, Director, Emory University Crystallography Laboratory, Department of Chemistry, Emory University, 1515 Pierce Drive, Atlanta, GA 30322-2210. The numbering of C1 – C6 in Figures 24 and 25 (molecular modeling studies) but the other atoms have different numbers. The solid state structure of **7a** (Figure 24) clearly shows that **7a** has a fully extended conformation and exhibits hydrogen bonding (Figure 25) between the amide hydrogens on one molecule and the amide carbonyl oxygens on another molecule. Similar extended X-ray crystal structures were recently reported by Styron et al. for the unacetylated parent molecule, *N,N'*-dimethyl-*D*-glucaramide<sup>[17]</sup> (Figure 26) and a disalt of precursor glucaric acid, i.e., dipotassium *D*-glucarate. The solid state structure of **7a** does not correspond to a sickle conformation of rotamer **3m** as was shown by the <sup>1</sup>H NMR results described in this chapter, a finding that parallels the results from the molecular modeling / X-ray study of *N,N'*-dimethyl-*D*-glucaramide. However, the solid state low energy sickle conformer of **7a** (rotamer **3m**) is very similar to the monopotassium monosodium *D*-glucarate,<sup>[17]</sup> (Figure 27) a structure that like rotamer **3m**, has two *gauche* arrangements between the

two sets of terminal hydrogens (H15,H16 and H17,H18) and an *anti* arrangement between the central hydrogens (H16, H17).

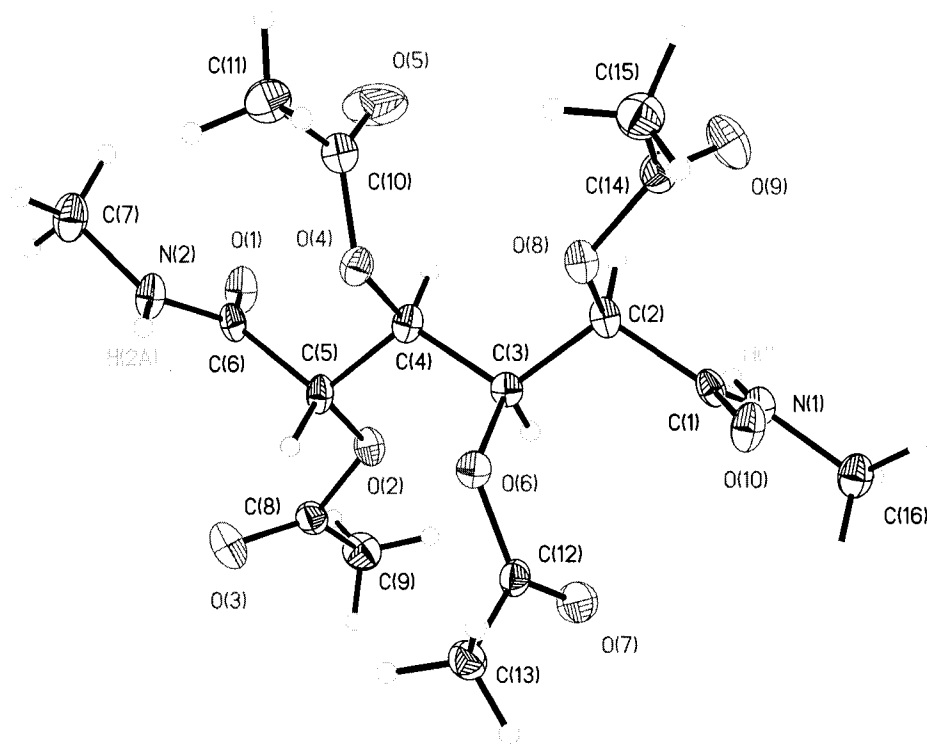


**Figure 24.** X-ray crystal structure of 2,3,4,5-tetra-*O*-acetyl-*N,N'*-dimethyl-*D*-glucaramide (7a).

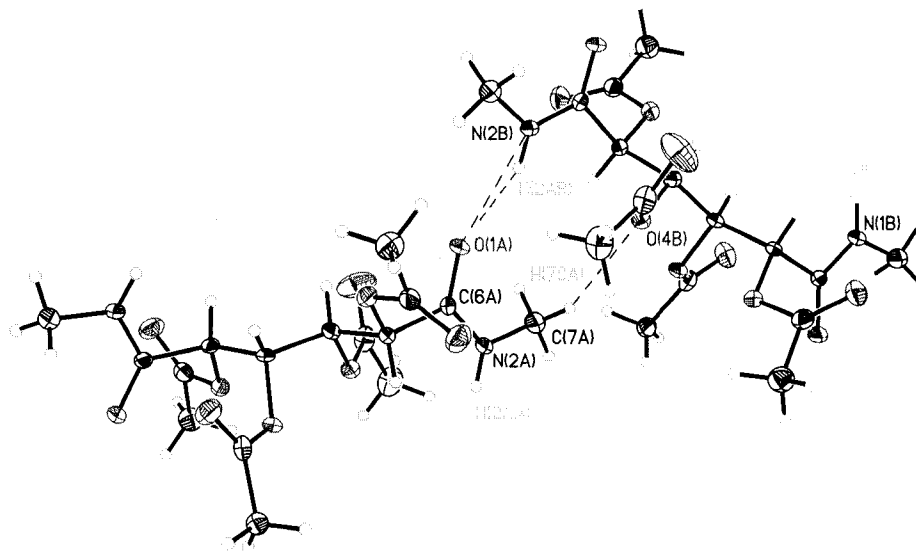


**Figure 25.** Intermolecular hydrogen bonding between pairs of **7a** in the solid state.

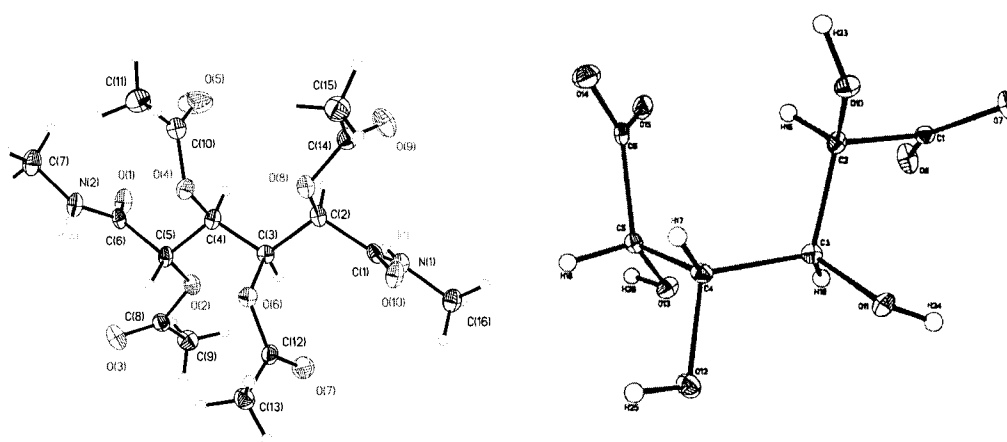


**Figure 26.** A comparison of the crystal structures of 2,3,4,5-tetra-*O*-acetyl-*N,N'*-dimethyl-*D*-glucaramide (**7a**) and *N,N'*-dimethyl-*D*-glucaramide.<sup>[17]</sup>

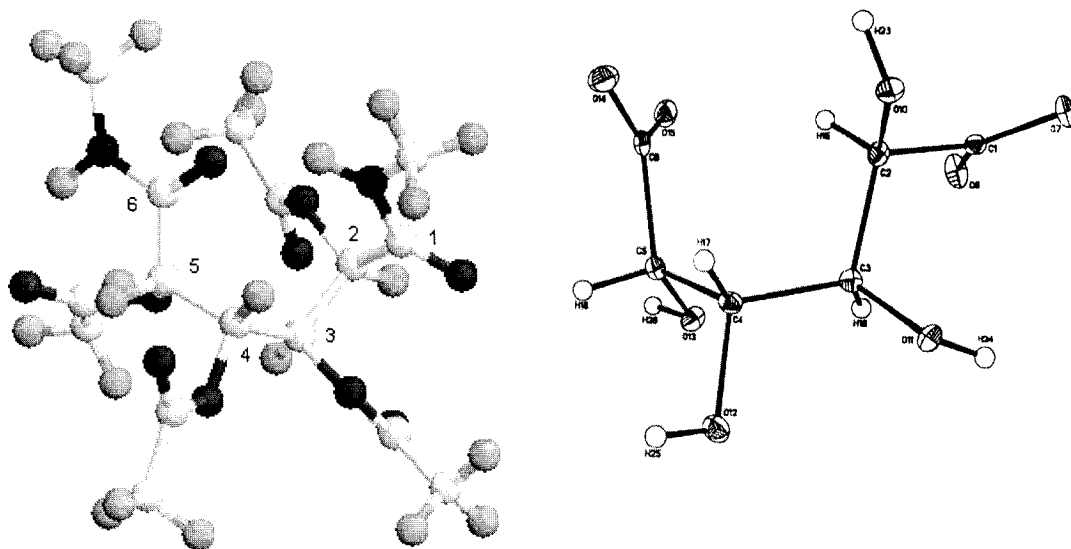


**Figure 27.** Low energy conformations (dielectric constant 1.0) of 2,3,4,5-tetra-*O*-acetyl-*N,N'*-dimethyl-D-glucaramide (**7a**, rotamer **3m**) and the X-ray crystal structure of sodium potassium D-glucarate.<sup>[17]</sup>

## Conclusions

1. Calculated  $^1\text{H}$  NMR vicinal coupling constants are in reasonable agreement with experimental results. However, intramolecular H-bonding influences the conformations of calculated rotamers of 2,3,4,5-tetra-*O*-acetyl-*N,N'*-dimethyl-D-glucaramide (**7a**).
2. For low energy conformers of 2,3,4,5-tetra-*O*-acetyl-*N,N'*-dimethyl-D-glucaramide (**7a**), H15-H16 are *gauche*, H16-H17 are *anti*, and H17-H18 are close-to-*gauche*.
3. For **7a**, the predominant calculated conformation of the acetylated glucaryl unit is a sickle ( ${}_2\text{G}^+{}_3\text{G}^+{}_4\text{G}^-$ ) close to that of the calculated global minimum for D-glucaramide (**8**) cyclic conformation  ${}_3\text{G}^+{}_4\text{G}^-$ .
4. Molecules containing a glucaryl unit (glucaric acid salts and diamides) have two extreme conformations, extended and bent (primarily sickle).
5. Molecular mechanics proved to be a valid method for conformational analysis of both acyclic D-glucaramide and *O*-acylated D-glucaramide.
6. The “model building” approach offers a relatively simple method for the conformational space search of **7a** and, potentially, related structures.



## Experimental Section

**General Methods.** All  $^1\text{H}$  and  $^{13}\text{C}$  NMR were recorded using a Varian Unity of 400 MHz and 100 MHz, respectively. Samples for  $^1\text{H}$  NMR (ca. 5 mg) were dissolved in 0.7 mL of  $\text{CDCl}_3$  or  $\text{DMSO-d}_6$ . Chemical shifts are reported as ppm ( $\delta$ ). Melting points were measured with a Fisher-Johns Melting Point Apparatus and reported uncorrected. High resolution mass spectra (HRMS) were obtained using electrospray ionization (ESI) with a Micromass LCT instrument. Solvent evaporations were carried out at reduced pressure. All solvents used were reagent grade unless stated otherwise. Methanol/diamine solutions were standardized by diluting an aliquot of the solution with water and titrating with standardized hydrochloric acid. A pH meter was employed to determine the titration end points.

**Methyl D-glucarate 1,4-lactone (1).**<sup>[1]</sup> The acid form of a cation-exchange resin (60 mL, DOWEX 50WX8-100, Aldrich) was washed with methanol until the washings were colorless. Monopotassium D-glucarate (16.3 g, 64.4 mmol, 98 %, D-saccharic acid monopotassium salt, Sigma) was mixed well with methanol (80 mL) in a 2000-mL Erlenmeyer flask. The above treated resin was added to the suspension of monopotassium D-glucarate and methanol mixture. The flask was sealed and placed on a radial shaker for 12 h. until the white saccharic acid salt was completely dissolved. The resin was removed by filtration, washed with methanol ( $2 \times 15$  mL), and retained for regeneration to its acid form. The combined filtrate was concentrated to a thick syrup, seeded with pure methyl D-glucarate 1,4-lactone, and solidified at room temperature for 3-7 days. The solid cake

was dried under vacuum at room temperature for 2 d to give a crude, light-yellow solid that could be used without further purification. The crude solid was triturated with absolute ethanol (25 mL) at room temperature, followed by filtration, and dried under vacuum at room temperature for 22 h to give purified methyl D-glucarate 1,4-lactone (7.1664 g, 34.7883 mmol, 54.36%) (JZ01036).

**Poly(hexamethylene D-glucaramide) (2).** A methanol solution of 1.2837 M hexamethylenediamine (3.9690 mL, 5.09 mmol, 1.05:1 molar ratio of diamine to lactone, Aldrich) was added to methyl D-glucarate 1,4-lactone (**1**; 1 g, 4.851 mmol) dissolved in methanol (10 mL). A white precipitate was obtained within 5 min, but the reaction mixture was continuously stirred for an additional 48 h. The white solid was removed by filtration, washed with methanol (2 x 15 mL) and acetone (2 x 15 mL) respectively, and then dried under reduced pressure at 75 °C to give poly(hexamethylene D-glucaramide) (**2**, 1.26 g, 4.35 mmol, 89.65%); mp: 179.5 - 182.5 °C (literature<sup>[1]</sup> 192 - 194 °C).

**Poly(hexamethylene 2,3,4,5-tetra-O-acetyl-D-glucaramide) (3).** Acetic anhydride (3 mL, 31.8 mmol) was added dropwise to a stirred solution of poly(hexamethylene D-glucaramide) (**2**; 200 mg, 0.69 mmol) dissolved in cold (ice bath) anhydrous pyridine (8 mL). The reaction mixture was stirred for 24 h at room temperature. Deionized water (35 mL) was added to the reaction mixture, which was stirred for another 2 h. The aqueous phase was extracted with dichloromethane (3 x 35 mL), and the organic phases were collected and extracted with deionized water (20 mL). The dichloromethane phase was

then dried with sodium sulfate and concentrated to a syrup. Toluene (4 x 10 mL) was added to dissolve the syrup and the solution was concentrated under reduced pressure to remove residual water. The white solid was dried under vacuum at room temperature to give crude poly(hexamethylene 2,3,4,5-tetra-*O*-D-glucaramide) (**3**; 146.6 mg, 0.32 mmol, 46.38 %).

***N,N'*-Dihexyl-D-glucaramide (4)**.<sup>[35]</sup> *n*-Hexylamine (10 mL, 75.10 mmol) was added at room temperature to methyl D-glucarate 1,4-lactone (**1**; 5.40 g, 26.21 mmol) dissolved in methanol (200 mL). A white precipitate was obtained within 5 min, but the reaction mixture was stirred for an additional 1 h. The white solid was removed by filtration, washed with methanol (2 x 15 mL) and then dried under reduced pressure at room temperature for 1.5 h to give *N,N'*-dihexyl-D-glucaramide (**4**; 10.66 g, 28.35 mmol, 108.17%): mp 177.0-177.5 °C.

**2,3,4,5-Tetra-*O*-acetyl-*N,N'*-dihexyl-D-glucaramide (5a)**. Acetic anhydride (3 mL, 31.8 mmol) was added dropwise to a stirred solution of *N,N'*-dihexyl-D-glucaramide (**4**; 325.1 mg, 0.865 mmol) dissolved in cold (ice bath) anhydrous pyridine (9 mL). The reaction mixture was kept cold and stirred for 30 min, and then stirred at room temperature overnight. Ice-cold water (30 - 35 mL) was poured into the reaction mixture and the mixture was stirred for 2 h. The aqueous solution was then extracted with dichloromethane (5 x 20 mL), and the dichloromethane phases were combined and then extracted with deionized water (30 mL). The dichloromethane solution was dried over

sodium sulfate and concentrated to a syrup. Toluene (4 x 10 mL) was added to the syrup and the solution was evaporated under reduced pressure to remove residual pyridine and water. The crude product (white powder) was dried under vacuum overnight and recrystallized from ethyl acetate/hexane to give 2,3,4,5-tetra-*O*-acetyl-*N,N'*-dihexyl-D-glucaramide (**5a**; 277.5 mg, 0.5097 mmol, yield 58.93%): mp 107.5 - 110.5 °C; HRMS: Calcd for C<sub>26</sub>H<sub>45</sub>N<sub>2</sub>O<sub>10</sub> (M+H<sup>+</sup>) m/z 545.3074. Found 545.3085 (JZ01006).

**2,3,4,5-Tetra-*O*-propanyl-*N,N'*-dihexyl-D-glucaramide (5b).** Propanyl chloride (0.60 mL, 6.876 mmol) was added dropwise to a stirred solution of *N,N'*-dihexyl-D-glucaramide (**4**; 320.8 mg, 0.8531 mmol) dissolved in cold (ice bath) anhydrous pyridine (2 mL). The reaction mixture was kept cold and stirred for 3.5 h, and then stirred at room temperature for 30 min. The reaction mixture was dissolved in dichloromethane (35 mL) and the organic phase was extracted with saturated aqueous sodium bicarbonate solution (3 x 6 mL). The dichloromethane solution was dried over sodium sulfate and concentrated to a syrup. Toluene (2 x 10 mL) was added to the syrup and the solution was concentrated under reduced pressure to remove residual pyridine and water. The crude product (amber syrup) was dried under vacuum overnight and purified by chromatography on a column of silica gel with ethyl acetate/hexane (4:6 v/v) to give pure syrupy solid, 2,3,4,5-tetra-*O*-propanyl-*N,N'*-dihexyl-D-glucaramide (**5b**; 380.3 mg, 0.6323 mmol, 74.12 %): HRMS: Calcd for C<sub>30</sub>H<sub>53</sub>N<sub>2</sub>O<sub>10</sub> (M+H<sup>+</sup>) m/z 601.3700. Found 601.3683.

**2,3,4,5-Tetra-*O*-(2-methylpropanyl)-*N,N'*-dihexyl-D-glucaramide (5c).** Isobutyryl chloride (0.63 mL, 6.55 mmol) was added dropwise to a stirred solution of *N,N'*-dihexyl-D-glucaramide (**4**; 305.5 mg, 0.8125 mmol) dissolved in cold (ice bath) anhydrous pyridine (1.6 mL). The reaction mixture was kept cold and stirred for 4 h, and then stirred at room temperature for 3 h. The reaction mixture was dissolved in dichloromethane (35 mL) and the organic phase was extracted with saturated aqueous sodium bicarbonate solution (2 x 6 mL). The dichloromethane solution was dried over sodium sulfate and concentrated to syrup. Toluene (2 x 15 mL) was added to the syrup and the solution was concentrated under reduced pressure to remove residual pyridine and water. The crude product (amber syrup) was dried under vacuum overnight and purified by column chromatography with ethyl acetate/hexane (4:6 v/v) to give a pure syrupy solid, 2,3,4,5-tetra-*O*-(2-methylpropanyl)-*N,N'*-dihexyl-D-glucaramide (**5c**; 250.1 mg, 0.3810 mmol, 46.89 %): HRMS: Calcd for C<sub>34</sub>H<sub>61</sub>N<sub>2</sub>O<sub>10</sub> (M+H<sup>+</sup>) m/z 657.4326. Found 657.4353.

**2,3,4,5-Tetra-*O*-(2,2-dimethylpropanyl)-*N,N'*-dihexyl-D-glucaramide (5d).** Pivavoyl chloride (1.2 mL, 9.74 mmol) was added dropwise to a stirred solution of *N,N'*-dihexyl-D-glucaramide (**4**; 310.4 mg, 0.8255 mmol) dissolved in cold (ice bath) anhydrous pyridine (1.6 mL). The reaction mixture was kept cold and stirred for 4 h, and then stirred at 60 °C for 5.5 h. A 10% pyridine solution of 4-dimethylaminopyridine (5 drops) was added to the reaction mixture, which was then stirred at room temperature for 13 h. The reaction mixture was dissolved in dichloromethane (35 mL) and the organic phase was extracted with saturated aqueous sodium bicarbonate solution (2 x 6 mL). The dichloromethane

solution was dried over sodium sulfate and concentrated to syrup. Toluene (2 x 10 mL) was added to the syrup and the solution was concentrated under reduced pressure to remove residual pyridine and water. The crude product (amber syrup) was dried under vacuum overnight and purified by column chromatography with ethyl acetate/hexane (4:6 v/v) to give a pure syrupy solid, 2,3,4,5-tetra-*O*-(2,2-dimethyl)propanyl-*N,N'*-dihexyl-D-glucaramide (**5d**; 224.0 mg, 0.3144 mmol, yield 39.09%); HRMS: Calcd for C<sub>38</sub>H<sub>69</sub>N<sub>2</sub>O<sub>10</sub> (M+H<sup>+</sup>) m/z 713.4952. Found 713.4982.

**2,3,4,5-Tetra-*O*-benzoyl-*N,N'*-dihexyl-D-glucaramide (5e).** Benzoyl chloride (0.59 mL, 5.08 mmol) was added dropwise to the stirred solution of *N,N'*-dihexyl-D-glucaramide (**4**; 308.0 mg, 0.8191 mmol) dissolved in cold (ice bath) anhydrous pyridine (1.3 mL). The reaction mixture was kept cold and stirred for 22 h, and then stirred at room temperature for 13 h. Deionized water (5 mL) was added to the reaction mixture and the reaction mixture was extracted with dichloromethane (2 x 10 mL). The combined organic phase was then extracted with saturated aqueous sodium bicarbonate solution (6 mL), dried over sodium sulfate and concentrated to a syrup. Toluene (2 x 10 mL) was added to the syrup and the solution was concentrated under reduced pressure to remove residual pyridine and water. The crude product (amber syrup) was dried under vacuum overnight and purified by column chromatography with ethyl acetate/hexane (1:3 v/v) to give a pure syrupy solid, 2,3,4,5-tetra-*O*-benzoyl-*N,N'*-dihexyl-D-glucaramide (**5e**; 302.5 mg, 0.3817 mmol, 46.60 %); HRMS: Calcd for C<sub>46</sub>H<sub>53</sub>N<sub>2</sub>O<sub>10</sub> (M+H<sup>+</sup>) m/z 793.3700. Found 793.3702.

***N,N'*-Dimethyl-D-glucaramide (6).** Methylamine (30 mL, 60 mmol) was added at room temperature to a stirred solution of methyl D-glucarate 1,4-lactone (**1**; 5 g, 24.3 mmol) dissolved in methanol (150 mL). A white precipitate was obtained within 5 min, but the reaction mixture was stirred for an additional 1 h. The white solid was removed by filtration, washed with methanol (2 x 20 mL), and then dried under reduced pressure at room temperature for 2 days to give *N,N'*-dimethyl-D-glucaramide (**6**; 4.98g, 21.1 mmol, 86.77%): mp 165.0-174.0 °C (literature<sup>[9]</sup> 188-190 °C).

**2,3,4,5-Tetra-*O*-acetyl-*N,N'*-dimethyl-D-glucaramide (7a).** The procedure employed was that used to prepare **5a**; acetic anhydride (3 mL, 31.7 mmol), *N,N'*-dimethyl-D-glucaramide (**6**; 307.1 mg, 1.301 mmol) and anhydrous pyridine (9 mL). The reaction was worked up as for **5a** and the crude product (white powder) was dried under vacuum overnight and recrystallized from ethanol to give 2,3,4,5-tetra-*O*-acetyl-*N,N'*-dimethyl-D-glucaramide (**7a**; 264.5 mg, 0.95 mmol, yield 50.07%): HRMS: Calcd for C<sub>16</sub>H<sub>24</sub>N<sub>2</sub>O<sub>10</sub> (M+H<sup>+</sup>) m/z 405.1509. Found 405.2123.

**2,3,4,5-Tetra-*O*-propanyl-*N,N'*-dimethyl-D-glucaramide (7b).** The synthesis procedure of **5b** was followed. Propanyl chloride (0.60 mL, 10.6 mmol) was added dropwise to a stirred solution of *N,N'*-dimethyl-D-glucaramide (**6**; 310.6 mg, 1.32 mmol) dissolved in cold anhydrous pyridine (2.5 mL) (ice bath). The reaction mixture was kept cold and stirred for 3.7 h, and then stirred at room temperature for 30 min. The reaction mixture

was dissolved in dichloromethane (35 mL) and the organic phase was extracted with saturated aqueous sodium bicarbonate solution (3 x 6 mL). The dichloromethane solution was dried over sodium sulfate and concentrated to a syrup. Toluene (2 x 15 mL) was added to the syrup and the solution was concentrated under reduced pressure to remove residual pyridine and water. The crude product (light yellow solid) was dried under vacuum to give 2,3,4,5-tetra-*O*-propanyl-*N,N'*-dimethyl-D-glucaramide (**7b**; 656.4 mg, 1.43 mmol, 108.10%): HRMS: Calcd for C<sub>20</sub>H<sub>32</sub>N<sub>2</sub>O<sub>10</sub> (M+H<sup>+</sup>) m/z 461.2135. Found 461.4291.

**2,3,4,5-Tetra-*O*-(2-methylpropanyl)-*N,N'*-dimethyl-D-glucaramide (7c).** The procedure employed was that used to prepare **5c**; isobutyryl chloride (0.94 mL, 8.98 mmol), *N,N'*-dimethyl-D-glucaramide (**6**; 263.0 mg, 1.11 mmol) and anhydrous pyridine (1.6 mL). The reaction was worked up as for **5c** and the crude product (amber syrup) was dried under vacuum overnight to give 2,3,4,5-tetra-*O*-(2-methylpropanoyl)-*N,N'*-dimethyl-D-glucaramide (**7c**; 692.3 mg, 1.34 mmol, 120.86 %).

**2,3,4,5-Tetra-*O*-benzoyl-*N,N'*-dimethyl-D-glucaramide (7e).** The procedure employed was that used to prepare **5e**; benzoyl chloride (1.24 mL, 10.62 mmol), *N,N'*-dimethyl-D-glucaramide (**6**; 311.0 mg, 1.318 mmol) and anhydrous pyridine (2.5 mL). The reaction was worked up as for **5e** and the crude product (amber syrup) was dried under vacuum to give 2,3,4,5-tetra-*O*-benzoyl-*N,N'*-dimethyl-D-glucaramide (**7d**; 684.9 mg, 1.0504 mmol, 79.70 %): HRMS: Calcd for C<sub>36</sub>H<sub>32</sub>N<sub>2</sub>O<sub>10</sub> (M+H<sup>+</sup>) m/z 653.2135. Found 653.2370.



## References

1. Kiely, D. E., Chen, L. and Lin, T. Hydroxylated Nylons Based on Unprotected Esterified D-Glucaric Acid by Simple Condensation Reactions. *J. Am. Chem. Soc.* **1994**,116(2): 571-8.
2. Kiely, D. E., Chen, L. and Lin, T-H. Simple Preparation of Hydroxylated Nylons - Polyamides Derived From Aldaric Acids. ACS Symposium Series 575, **1994** Washington.
3. Kiely, Donald E.; Chen, Liang; Morton, David W. Process for making activated aldarate esters, ester/lactones and lactones. US. **1994**, Patent 5329044, July 12.
4. Kiely, D. E. L., Tsu Hsing Aldaric acid-based polyhydroxypolyamides and their manufacture. U.S. **1989**, Patent 4833230, May 23.
5. Kiely, D. E. Carbohydrate diacids: Potential as commercial chemicals and hydrophilic polyamide precursors. 218th ACS National Meeting, **1999** New Orleans, American Chemical Society, Washington, D. C.
6. Kiely, D. E., Chen, Liang and Lin, Tsu-Hsing Synthetic Polyhydroxypolyamides from Galactaric, Xylaric, D-Glucaric and D-Mannaric Acid and Alkylenediamine Monomers - Some Comparisons. *J. Polym. Sci.; Polym Chem. Ed*, **2000** 38: 598.
7. Kiely, D. E. Carbohydrate Diacids: Potential as Commercial Chemicals and Hydrophobic Polyamide Precursors. ACS Symposium Series 784, Chemicals and Materials from Renewable Resources, **2001**, 64-81.
8. Kiely, D. E. C., Liang; Morton, David W. polyaldaramide polymers useful for films and adhesives. **1995**. US Patent 5434233, July 18
9. Chen, L. K., Donald E. D-Glucaric acid esters/lactones used in condensation polymerization to produce hydroxylated nylons - a qualitative equilibrium study in acidic and basic alcohol solutions. *Journal of Carbohydrate Chemistry* **1994**.13(4): 585-601.
10. Chen, L. a. K. D. E. Synthesis of Stereoregular Head,Tail - Hydroxylated Nylons Derived from D-Glucose. *J. Org. Chem.* **1996**. 61(17): 3847-51.
11. Carter, A., Morton, D. W., and Kiely, D. E. Synthesis of Some Poly(4-alkyl-4-azaheptamethylene- D-glucaramides). *J. Polym. Sci.; Polym. Chem. Ed.* **2000**. 38: 3892-9.

12. Styron, S. D. K., Donald E.; Ponder, Glenn Alternating stereoregular head, tail-tail, head-poly(alkylene D-glucaramides) derived from a homologous series of symmetrical diamido-di-D-glucaric acid monomers. *Journal of Carbohydrate Chemistry* **2003**, 22(2): 123-142.
13. Morton, D. W., and Kiely, Donald E. Evaluation of the Film and Adhesive Properties of Some Block Copolymer Polyhydroxypolyamides from Esterified Aldaric Acids and Diamines. *J. Applied Polym. Sci.* **2000**, 77: 3085-92.
14. Morton, D. W., and Kiely, Donald E. Synthesis of Poly(azaalkylene aldaramides) and Poly(oxaalkylenealdaramides) Derived from D-Glucaric and D-Galactaric Acids. *J. Polym. Sci.; Polym. Chem. Ed.* **2000**, 38: 404.
15. Chen, L. H., B.; Kane, R. W.; Kiely, D. E.; Rowland, R. S. Molecular modeling of acyclic carbohydrate derivatives N,N'-dimethyl- and N,N'-dihexylxylaramide. Model compounds for synthetic poly(hexamethylenexylaramide). *ACS Symposium Series* (1990), 430 (Computer Modeling of Carbohydrate Molecules), **1990**.
16. Chen, L. Kiely, D. E. Computer aided structural studies of poly(alkylene D-glucaramides). *Polymer Preprints* **1993**, 34(2): 550-1.
17. Styron, Susan D.; French, Alfred D.; Friedrich, Joyce D.; Lake, Charles H.; Kiely, Donald E. MM3(96) conformational analysis of D-glucaramide and x-ray crystal structures of three D-glucaric acid derivatives-models for synthetic poly(alkylene D-glucaramides). *Journal of Carbohydrate Chemistry* **2002**, 21(1 & 2): 27-51.
18. Sweeting, Linda M., Coxon, Bruce, and Varma, Rajendra Conformational analysis of peracetylated hexononitriles. *Carbohydrate Research* **1979**, 72: 43-55.
19. Angyal, S. J., Fur, R. Le, and Gagnaire, D. Conformations of acyclic sugar derivatives part II. Determination of the conformation of alditol acetates in solution by the use of 250-MHz NMR spectra. *Carbohydrate Research* **1972**, 23: 121-134.
20. Angyal, S. J., Fur, R. Le, and Gagnaire, D. Conformations of acyclic sugar derivatives part III. 3,4,5,6,7-penta-acetoxy-trans-1-nitro-1-heptenes. *Carbohydrate Research* **1972**, 23: 135-138.
21. Blanc-Muesser, Michele, Defaye, Jacques, and Horton, Derek Conformations in solution of the stereoisomeric, peracetylated aldohexose dimethyl acetals and diethyl dithioacetals. *Carbohydrate Research* **1980**, 87: 71-86.

22. Horton, Derek, and Wander, Joseph D. Conformation of acyclic derivatives of sugars. XI. Conformations of the D-aldopentose diehtyl and diphenyl dithioacetals in solution. *Journal of Organic Chemistry* **1974**, 39(13): 1859 - 1863.
23. Jeffrey, G. A., and Kim, H. S. Conformations of the alditols. *Carbohydrate Research* **1970**, 14: 207-216.
24. Ferrier, Frederic, Avezou, Arnaud, Terzian, Georges, and Benlian, David Synthesis and crystal structure of copper(II) D-glucarate, tetra-hydrate. *Journal of Molecular Structure THEOCHEM* **1998**, 442: 281-4.
25. Haasnoot, C.A.G., De Leeuw, F.A.A.M., and Altona C. The Relationship between Proton-Rroton NMR Coupling constants and Substituent Electronegativities-I An empirical generalization of the Karplus equation. *Tetrahedron* **1980**, 36: 2783-2792.
26. Leach, Andrew R. *Molecular Modeling Principles and Applications*. **2001**, Prentice Hall.
27. Dosen-Micovic, Ljiljana Searching conformational space with molecular mechanics method. Dihedral angle random increment search. *Tetrahedron* **1995**, 51(24): 6789-96.
28. Lii, Jenn Huei; Allinger, Norman L.. The MM3 force field for amides, polypeptides, and proteins. *Journal of Computational Chemistry* **1991**, 12(2): 186-99.
29. Eliel, E. L.; Wilen, S. H. *Stereochemistry of Organic Compounds*. **1994**, New York, John Wiley and Sons.
30. Thibodeaux, Devron P., Johnson, Glenn P., Stevens, Edwin D., and French, Alfred D. Crystal structure of penta-*O*-acetyl-beta-D-galactopyranose with modeling of the conformation of the acetate groups. *Carbohydrate Research* **2002**, 337: 2301-10.
31. Jeffrey, G. A. *An Introduction to Hydrogen Bonding*. **1997**, New York, Oxford.
32. March, J. *Advanced Organic Chemistry*. **1985**, New York, John Wiley & Sons.
33. Lopez De La Paz, Manuela; Penades, Soledad and Vicent, Cristina Conformational Restriction by Intramolecular Hydrogen Bonding. *Carbohydrate-Carbohydrate Self-Assembly. Tetrahedron Letters* **1997**, 38(9): 1659-1662.

34. Allinger, Norman L.; Kok, Randall A.; Imam, Mita R. Hydrogen bonding in MM2. *Journal of Computational Chemistry* **1988**, 9(6): 591-5.
35. M.S. Thesis, A. Carter, Department of Chemistry, The University of Alabama at Birmingham, 1998.
36. Itoh, Takashi; Yamagata, Tetsuya; Hasegawa, Yuka; Hashimoto, Masato and Konishi, Takashi. Energetically stable conformations of Nylon 66 and Nylon 6 molecules in Crystals. *Japanese Journal of Applied Physics*, **1996**, 35: 4474-4475.

## Chapter 2. Application of A Model Building Approach to Molecular Mechanics (MM3) for Calculating Low Energy Conformations of Tetra-*O*-Acyl-*N,N'*-Dialkyl-D-Glucaramides to Predict Corresponding Polyamide Secondary Structures

### Introduction

In the previous chapter, a “model building” approach<sup>[1-3]</sup> was taken to calculate low energy conformations of 2,3,4,5-tetra-*O*-acetyl-*N,N'*-dimethyl-D-glucaramide (**1**, Figure 1) using the molecular mechanics program MM3 in the Tripos Alchemy 2000 computational package. Use of this approach was driven by the large number of starting conformations (at least 14,348,907,  $3^{15}$ ) possible from the fifteen variable torsion angles of **1**. “Building blocks” or “molecular fragments” can serve as model components to mimic parts of a relatively complex molecule. <sup>1</sup>H NMR results from **1** showed a large coupling (7.11 Hz) for vicinal H16-H17, indicative of an *anti* relationship and a dihedral angle of ca. 180°.<sup>[4]</sup> However, the terminal vicinal couplings from H15-H16 (3.24 Hz) and H17-H18 (3.89 Hz) were clearly in the range of a *gauche* arrangement for these protons (dihedral angle of ca. ±60°<sup>[4]</sup>). Consequently, in the initial models, the H16-H17 angle was set at 180° with the terminal H-H dihedral angles set to ±60°.

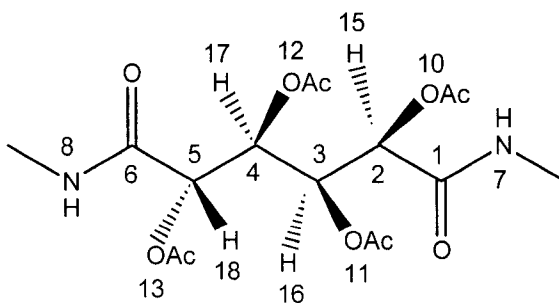


**Figure 1.** 2,3,4,5-Tetra-*O*-acetyl-*N,N'*-dimethyl-D-glucaramide (**1**).

Based upon these angular restrictions, initial starting rotamers 1 - 4 (Figure 2) were generated. Four different “building blocks” models were then developed to establish the conformational preferences of different parts of **1**: the End C Model that employed *N*-methylacetamide to define the low energy O9-C1-N7-H19 and O14-C6-N8-H22 dihedral angle; the C1-C2 & C5-C6 Model utilizing *2R* and *2S* *N*-methyl-2-acetoxypropanamide to determine the preferred conformational relationship between the terminal acetoxy group on a chiral carbon and the amide carbonyl functions, *i.e.*, the O9-C1-C3-O10 and O13-C5-C6-O14 dihedral angles; the Acyloxy Rotamer Model based on methyl acetate to determine the orientation of the carbonyl oxygen of each acetoxy group to the corresponding *O*-alkyl carbon, *i.e.*, the dihedral angles C-O-C=O (carbonyl) formed by each of the four acetoxy groups; and five Vicinal Acyloxy Models, based upon (*2S,3S*), (*2S,3R*) and (*2R,3R*)-2,3-diacetoxybutanes. These last models were used to mimic the rotameric preferences for two vicinal acetoxy groups on carbons of different chirality and conformational (*gauche* or *anti*) disposition, specifically to set the dihedral angle range of H-C-O-C (carbonyl) before minimization. The results from this “building blocks” modeling approach allowed us to set the following angles (Table 1) in **1** prior to minimization.

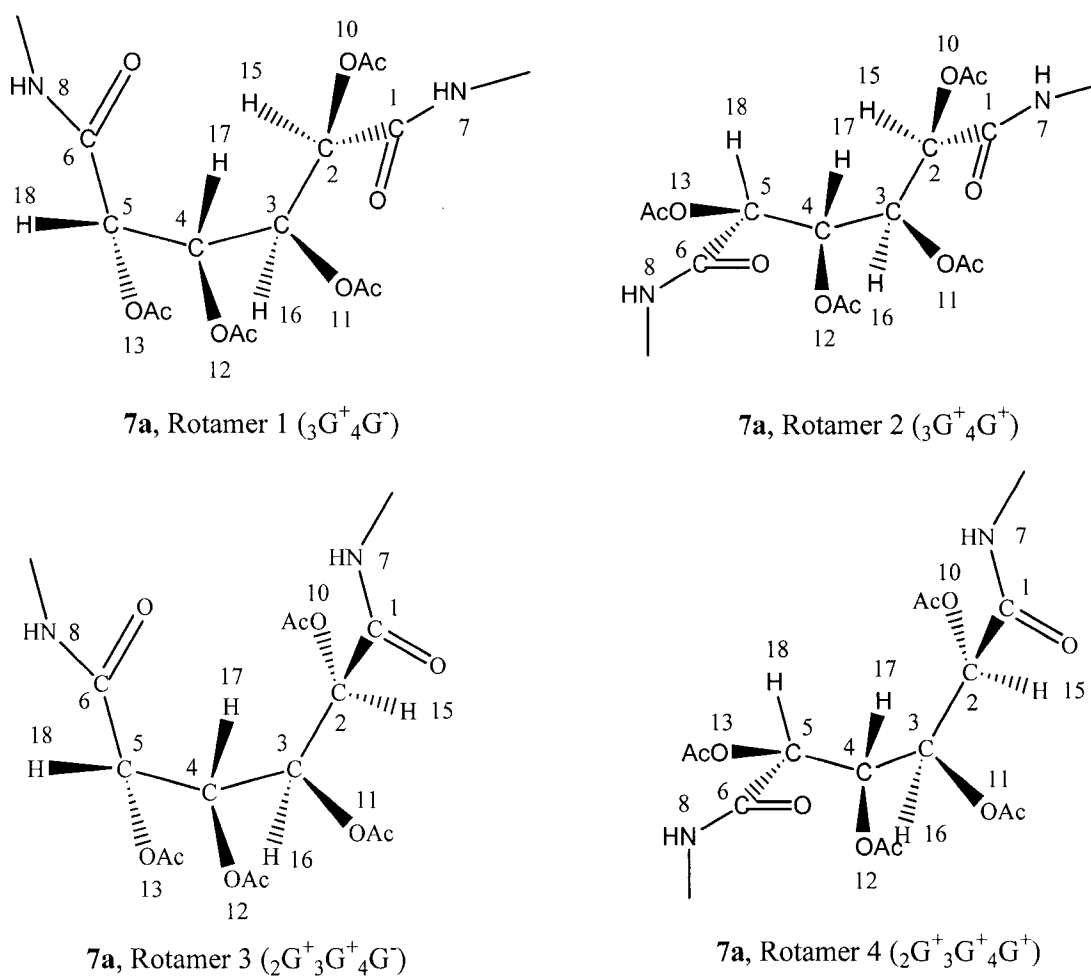


**Figure 2.** Four starting rotamers of **1**, generated according to vicinal H15, H16, H17 and H18  $^1\text{H}$  NMR coupling constants information.

**Table 1.** Calculated torsion angles ( $\omega$ ,  $^\circ$ ) of building blocks for **1**

	Model	Torsion angle	$\omega$ ( $^\circ$ )	Building blocks
Model 1	End C Model	O=C-N-H	<b>180.0</b>	<i>N</i> -methylacetamide
Model 2	C1-C2 & C5-C6 Model	O-C-C=O	<b>+125.8/ -125.8</b>	<i>N</i> -methyl-2-acetoxypropanamide
Model 3	Acyloxy Rotamer Model	C-O-C=O	<b>0.0</b>	methyl acetate
Model 4	Vicinal Acyloxy Model	H-C-O-C	<b><math>\sim \pm 40.0</math></b>	2,3-diacetoxybutane

From each of the four starting rotamers, 16 ( $2^4$ ) conformations were generated from the two starting conformations (two dihedral angle  $\pm 43^\circ$ ) from each of the four acetate bearing carbons. Each of the resulting 64 conformations of **1** was then minimized using the MM3 program and applying the “block diagonal then full matrix minimization” protocol at a dielectric constant of 1.0. Of the four low energy “sickle” conformations generated, one was dominant and accounted for *ca.* 90% of the conformation population.

In the present study, the “model building” approach has been applied to model more complex acyloxy derivatives of D-glucaramide, *i.e.*, propanyl, methylpropanyl and dimethylpropanyl esters of *N,N'*-dimethyl-D-glucaramide (**2**, **3**, and **4**), plus the tetraacetate of *N,N'*-dihexyl-D-glucaramide (**5**).

### Results and Discussion

From  $^1\text{H}$  NMR data reported in the previous chapter, it is clear that as the pendant acyl group becomes bulkier, *i.e.*, acetyl  $\rightarrow$  propanyl  $\rightarrow$  methylpropanyl  $\rightarrow$  dimethylpropanyl, a general increase in H16-H17 coupling is observed, corresponding to a likely increase in the dihedral angle between these two protons and a decrease in conformational flexibilities in the middle of these molecules (Figure 3).



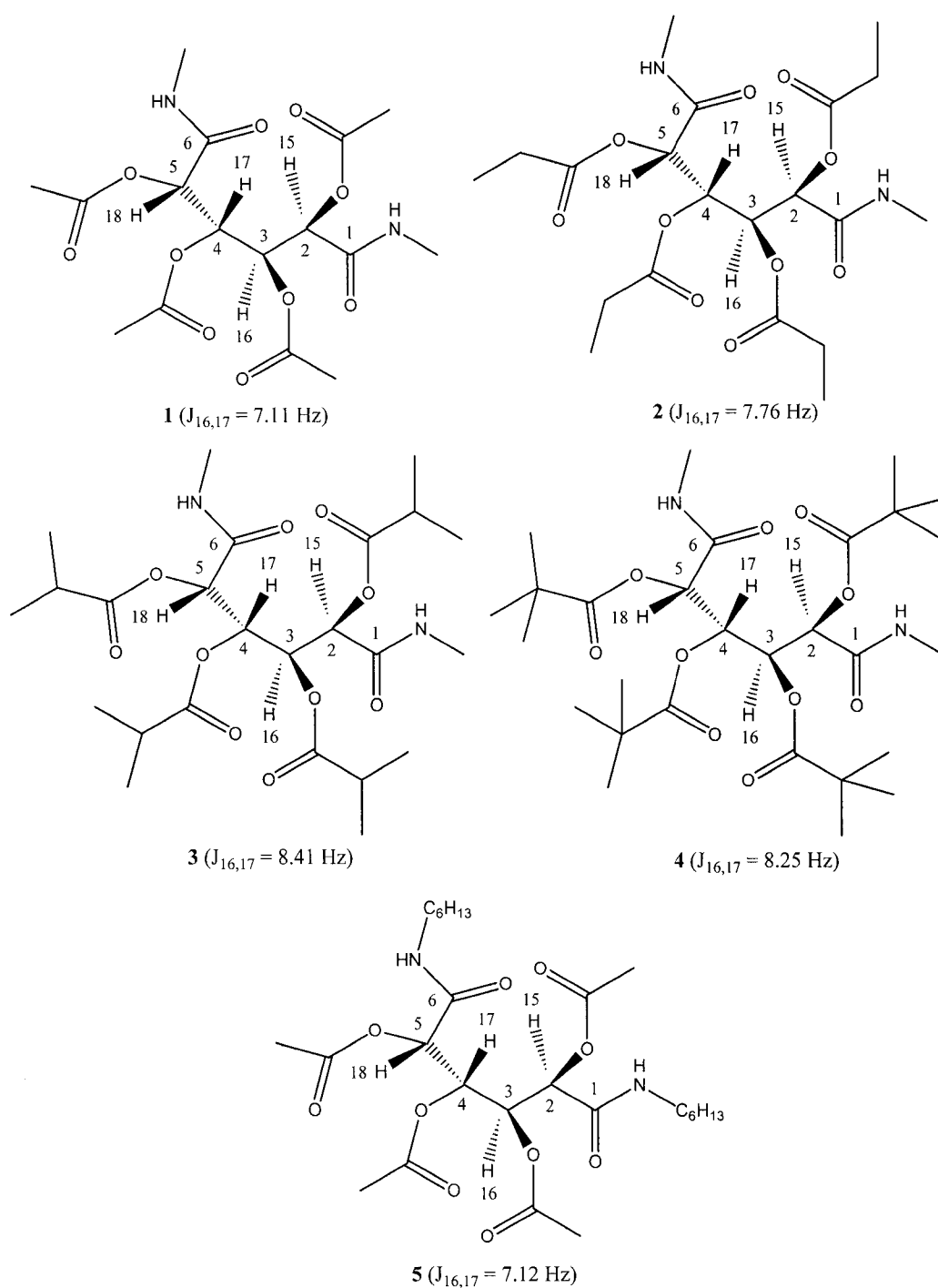


**Figure 3.** The compounds modeled in the previous chapter (1) and this study (2 - 5) and their H16-H17 couplings (in parentheses).

The “model building” approach has now been applied to compounds **2** - **5**, whose preparation and characterization are described in the previous chapter, but with some modifications to account for the added complexity of the *O*-acyl functions and the amide hexyl groups of **5**.

### I. Building blocks for conformational studies of **2** - **5**

#### 1. Propanate Model for **2** ----- methyl propanate (A)

One additional “building block” model was required for 2,3,4,5-tetra-*O*-propanyl-*N,N'*-dimethyl-*D*-glucaramide (**2**), a model to help define the location of the CH<sub>3</sub> unit of the ethyl group relative to the ester carbonyl oxygen, the C-C-C=O dihedral angle. A suitable model compound chosen for this determination was methyl propanate (A, Figure 4).

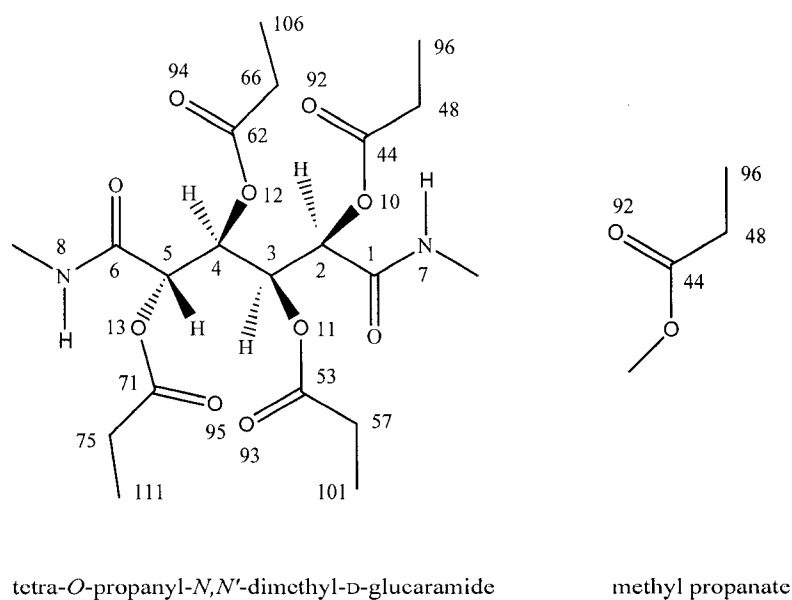


**Figure 4.** Propanate Model ----- methyl propanate (A).

Starting with an extended conformation of methyl propanate, rotation around the C44-C48 bond from 0° to 300° in 60° increments followed by MM3 minimization, generated three different conformations (**A1**, **A3**, **A4**). The results from the conformational study of methyl propanate are present in Table 2 and indicate a clear preference for a conformation in which the methyl group and the carbonyl oxygen are *eclipsed*, as in conformation **A1**.

**Table 2.** Conformational study of methyl propanate (**A**) to determine the O92=C44-C48-C96, O93=C53-C57-C101, O94=C62-C66-C106 and O95=C71-C75-C111 dihedral angle ( $\omega$ , °)

	$\omega$ Before MM3 (°)	$\omega$ After MM3 (°)	Total energy (kcal/mol)	Steric relationship	Overall conformation
<b>A1</b>	<b>0.0</b>	<b>0.0</b>	<b>-1.2534</b>	<i>eclipsed</i>	<b>extended</b>
<b>A2</b>	<b>60.0</b>	<b>0.0</b>	<b>-1.2534</b>	<i>eclipsed</i>	<b>extended</b>
<b>A3</b>	120.0	143.5	0.2610	<i>36.5° to anti</i>	sickle
<b>A4</b>	180.0	180.0	0.3355	<i>anti</i>	bent
<b>A5</b>	240.0	-143.5	0.2610	<i>-36.5° to anti</i>	sickle
<b>A6</b>	<b>300.0</b>	<b>0.0</b>	<b>-1.2534</b>	<i>eclipsed</i>	<b>extended</b>

The Newman projection formulas for conformer **A1** and two higher energy conformers **A3** and **A4** are shown in Figure 5. Additional relevant dihedral angles are presented in Table 3.

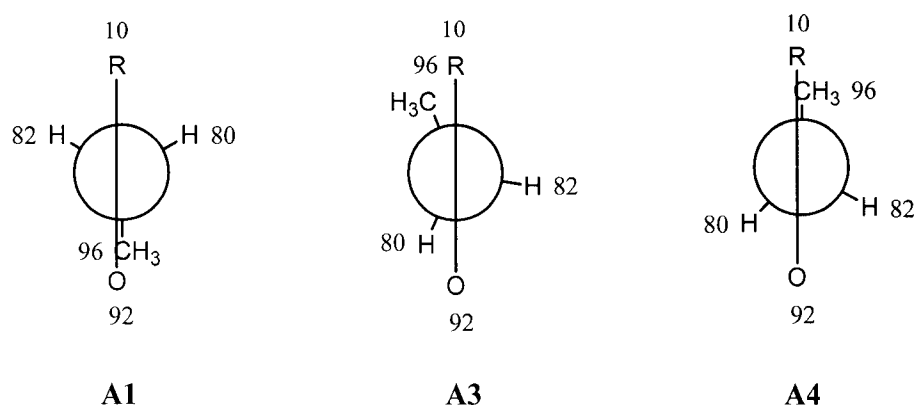


**Figure 5.** Newman projections along C44-C48 bond of methyl propanate (**A**) minima (R = -OCH<sub>3</sub>).

**Table 3.** Relevant dihedral angles ( $\omega$ , °) along C44-C48 bond of methyl propanate (**A**) minima

Dihedral Angles	<b>A1</b>	<b>A3</b>	<b>A4</b>
$\omega$ (O92-C44-C48-C96) (°)	<b>0.0</b>	143.5	0.0
$\omega$ (O92-C44-C48- H80) (°)	<b>-121.9</b>	21.0	57.3
$\omega$ (O92-C44- C48-H82) (°)	<b>121.9</b>	-94.5	-57.4
$\omega$ (O10-C44-C48-C96) (°)	<b>180.0</b>	-37.5	0.0
$\omega$ (O10-C44-C48-H80) (°)	<b>58.1</b>	-159.9	-122.7
$\omega$ (O10-C44-C48-H82) (°)	<b>-58.1</b>	84.5	122.6
Total energy (kcal/mol)	<b>-1.2534</b>	0.2610	0.3355

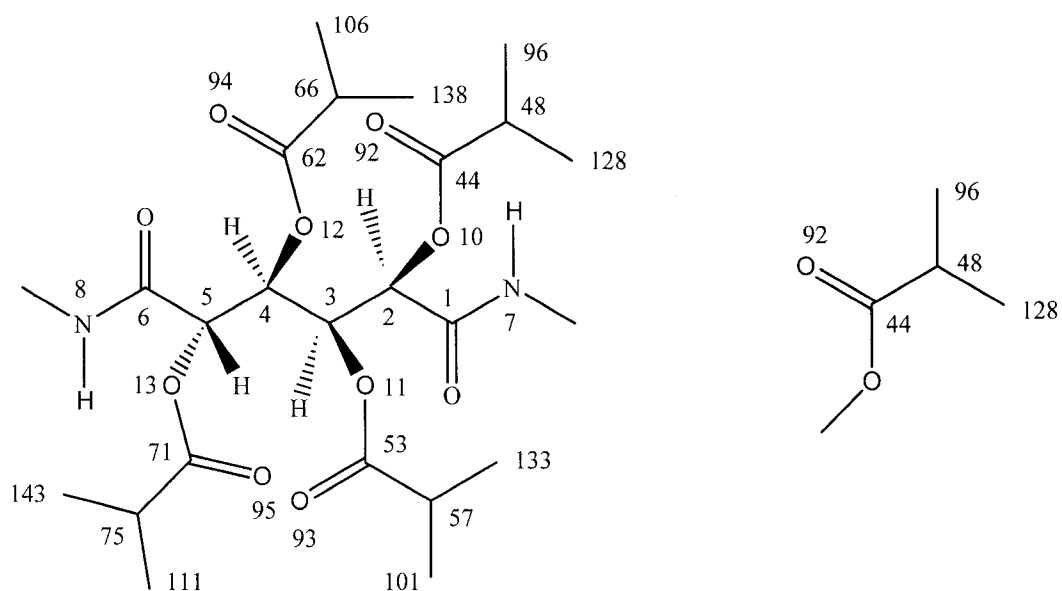
Applying the Propanate Model, the O92=C44-C48-C96, O93=C53-C57-C101, O94=C62-C66-C106 and O95=C71-C75-C111 dihedral angles of **2** were set to 0.0°.

Klimkowski et al.<sup>[6]</sup> carried out *ab initio* calculations of methyl propanate and determined that the conformational energy minimum is at a torsional angle of 0° for C-C-C=O. Moravie et al.<sup>[7,8]</sup> also reported IR and Raman spectra of methyl propanate in both

liquid and crystal states and suggested that the *cis* conformation of C-C-C=O is  $1.1 \pm 0.3$  kcal/mol lower in energy than the *gauche* conformation, which is quite comparable to 1.51 kcal/mol from this study.

## 2. Isobutanate Model for 3 -- methyl 2-methylpropanate (**B**)

Methyl 2-methylpropanate (**B**, Figure 6) was employed to model the pendant *O*-2-methylpropanyl groups of 2,3,4,5-tetra-*O*-methylpropanyl-*N,N'*-dimethyl-*D*-glucaramide (**3**) in order to probe the rotation about the C44-C48, C53-C57, C62-C66 and C71-C75 bonds. The ester was minimized by rotating the carbonyl carbon (44) –  $\alpha$  carbon (48) bond in  $60^\circ$  increments (Table 4). Two enantiomeric conformers of low energy, **B1** (equivalent to **B2** and **B6**) and **B3** (equivalent to **B4**), were generated with a  $+2.0^\circ$  and  $-2.0^\circ$  dihedral angle for the O=C-C-C linkage (O92=C44-C48-C128 for **B1** and O92=C44-C48-C96 for **B3**).



tetra-*O*-methylpropanyl-*N,N'*-dimethyl-*D*-glucaramide

methyl 2-methylpropanoate

**Figure 6.** Isobutanate Model – methyl 2-methylpropanoate (**B**).

**Table 4.** Conformational study of methyl 2-methylpropanoate (**B**) to determine the O92=C44-C48-C128, O93=C53-C57-C133, O94=C62-C66-C138, and O95=C71-C75-C143 dihedral angles ( $\omega_1$ , °) and the O92=C44-C48-C96, O93=C53-C57-C101, O94=C62-C66-C116, and O95=C71-C75-C111 dihedral angles ( $\omega_2$ , °)

	$\omega_1$ Before MM3 (°)	$\omega_1$ After MM3 (°)	$\omega_2$ After MM3 (°)	Total energy (kcal/mol)	Steric relationship
<b>B1</b>	<b>0.0</b>	<b>-2.0</b>	<b>125.5</b>	<b>1.8192</b>	<b>O92=C44-C48-C128 elipsed</b>
<b>B2</b>	<b>60.0</b>	<b>-2.0</b>	<b>125.5</b>	<b>1.8192</b>	<b>O92=C44-C48-C128 elipsed</b>
<b>B3</b>	<b>120.0</b>	<b>125.5</b>	<b>-2.0</b>	<b>1.8192</b>	<b>O92=C44-C48-C96 elipsed</b>
<b>B4</b>	<b>180.0</b>	<b>125.5</b>	<b>-2.0</b>	<b>1.8192</b>	<b>O92=C44-C48-C96 elipsed</b>
<b>B5</b>	240.0	-118.5	118.5	3.2548	
<b>B6</b>	<b>300.0</b>	<b>-2.0</b>	<b>125.5</b>	<b>1.8192</b>	<b>O92=C44-C48-C128 elipsed</b>

The two low energy conformers **B1** and **B3** are so close to being *eclipsed* (Figure 7) that we employed a single *eclipsed* conformer as the low energy model. However, when the OCH<sub>3</sub> is *gauche* to both vicinal methyl groups, the energy of the resulting conformer (**B5**, Figure 7) is considerably raised due to steric strain (Table 5).

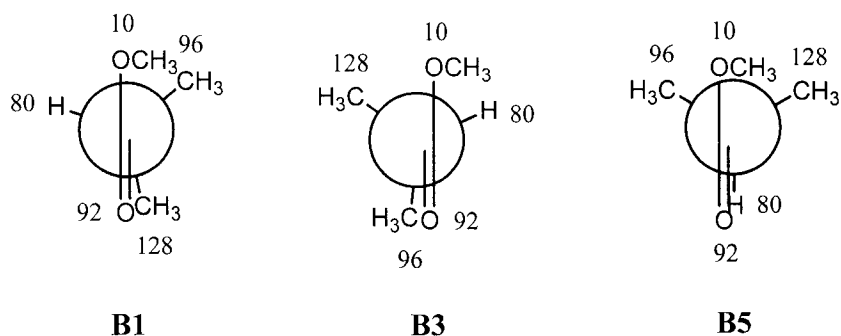


**Figure 7.** Newman projection of methyl 2-methylpropanate (**B**) minima: along C44-C48 bond.

**Table 5.** Relevant dihedral angles ( $\omega$ , °) along C44-C48 bond of methyl 2-methylpropanate (**B**) minima

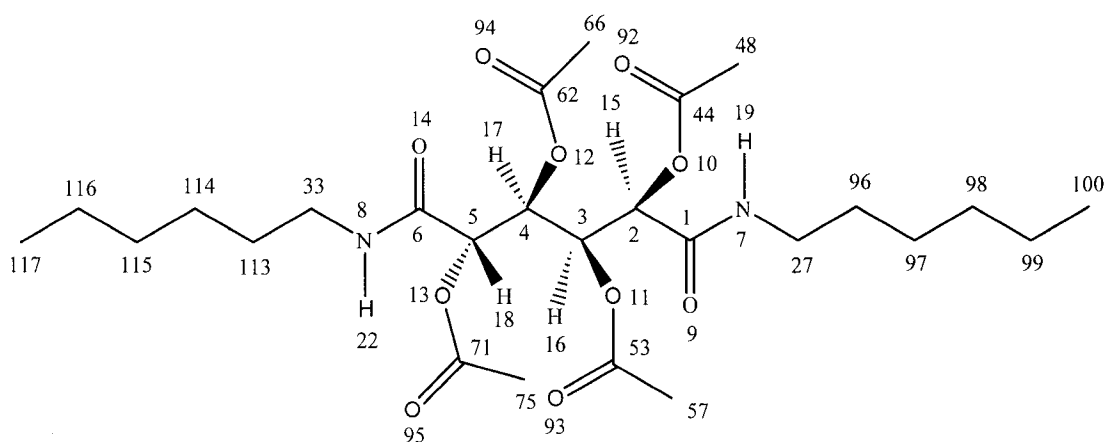
Dihedral Angles	<b>B1</b>	<b>B3</b>	<b>B5</b>
$\omega$ (O92-C44-C48-C96) (°)	<b>-125.5</b>	<b>2.0</b>	118.5
$\omega$ (O92-C44-C48- H80) (°)	<b>116.3</b>	<b>-116.3</b>	0.0
$\omega$ (O92-C44- C48-C128) (°)	<b>-2.0</b>	<b>125.5</b>	-118.5
$\omega$ (O10-C44-C48-C96) (°)	<b>55.4</b>	<b>-178.9</b>	-61.5
$\omega$ (O10-C44-C48-H80) (°)	<b>-62.8</b>	<b>62.8</b>	180.0
$\omega$ (O10-C44-C48-C128) (°)	<b>178.9</b>	<b>-55.4</b>	61.5
Total energy (kcal/mol)	<b>1.8192</b>	<b>1.8192</b>	3.2548

Because the low energy conformers **B1** and **B3** are enantiomers and the two methyl groups (C128 and C96) on C48 (the carbon  $\alpha$  to carbonyl carbon C44) are equivalent, the O92=C44-C48-C128/C96, O93=C53-C57-C133/C101, O94=C62-C66-C138/C106, and O95=C71-C75-C143/C111 dihedral angles were set at 0.0° in the conformational study of 2,3,4,5-tetra-*O*-methylpropanyl-*N,N'*-dimethyl-*D*-glucaramide (**3**).

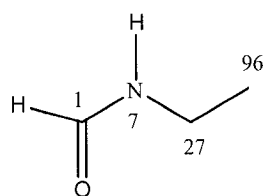
### 3. *N*-ethylformamide (**D**) / *N*-ethylacetamide (**E**) Models for **5**

For compound 2,3,4,5-tetra-*O*-acetyl-*N,N'*-dihexyl-*D*-glucaramide (**5**), a model was required to establish the rotameric preference of the *n*-hexyl group on the amide nitrogens. *N*-Ethylformamide (**D**, Figure 8) was selected as the simplest model for the *n*-hexylamido group in order to evaluate the carbonyl C-N-C-C dihedral angle, *i.e.*, that between the amide carbonyl and the  $\beta$ -alkyl carbon of any unbranched alkyl chain bound to the amide nitrogen. Rotation around the above bond (C1-N7-C27-C96) in 120.0° increments gave three essentially energetically comparable conformers, **D1**, **D2** and **D4** (Table 6). Two have the  $\beta$ -carbon in an almost *gauche* relationship ( $\pm 80.4^\circ$ ) to the amide carbonyl carbon (**D1** and **D2**), and one has the  $\beta$ -carbon *anti* (180.0°) to the carbonyl carbon (Table 9, Figure 9).

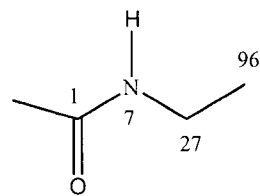




tetra-*O*-acetyl-*N,N'*-dihexyl-D-glucaramide



*N*-ethyl formamide



*N*-ethyl acetamide

**Figure 8.** 2,3,4,5-tetra-*O*-Acetyl-*N,N'*-dihexyl-D-glucaramide (**5**), *N*-ethylformamide (**D**) and *N*-ethylacetamide (**E**).

**Table 6.** Conformational study of *N*-ethyl formamide (**D**) to determine the C1-N7-C27-C96 and C6-N8-C33-C112 dihedral angle ( $\omega$ , °)

	$\omega$ Before MM3 (°)	$\omega$ After MM3 (°)	Total energy (kcal/mol)	Conformation
<b>D1</b>	<b>0.0</b>	<b>-80.4</b>	<b>-4.1038</b>	<b>Close-to-gauche</b>
<b>D2</b>	<b>60.0</b>	<b>80.4</b>	<b>-4.1038</b>	<b>Close-to-gauche</b>
<b>D3</b>	<b>120.0</b>	<b>80.4</b>	<b>-4.1038</b>	<b>Close-to-gauche</b>
<b>D4</b>	180.0	180.0	-3.8960	<i>Anti</i>
<b>D5</b>	<b>240.0</b>	<b>-80.4</b>	<b>-4.1038</b>	<b>Close-to-gauche</b>
<b>D6</b>	<b>300.0</b>	<b>-80.4</b>	<b>-4.1038</b>	<b>Close-to- gauche</b>

**Table 7.** Relevant dihedral angles ( $\omega$ , °) along C27-N7 bond of *N*-ethyl formamide (**D**) minima

Dihedral angles	<b>D1</b>	<b>D2</b>	<b>D4</b>
$\omega$ (C1-N7-C27-C96) (°)	<b>-80.4</b>	<b>80.4</b>	180.0
$\omega$ (C1-N7- C27-H39) (°)	<b>42.0</b>	<b>-158.4</b>	-58.7
$\omega$ (C1-N7- C27-H40) (°)	<b>158.4</b>	<b>-42.0</b>	58.7
$\omega$ (H19-N7- C27-C96) (°)	<b>97.8</b>	<b>-97.8</b>	0.0
$\omega$ (H19-N7-C27-H39) (°)	<b>-139.8</b>	<b>23.3</b>	121.3
$\omega$ (H19-N7--C27-H40) (°)	<b>-23.3</b>	<b>139.8</b>	-121.3
Total energy (kcal/mol)	<b>-4.1038</b>	<b>-4.1038</b>	-3.8960

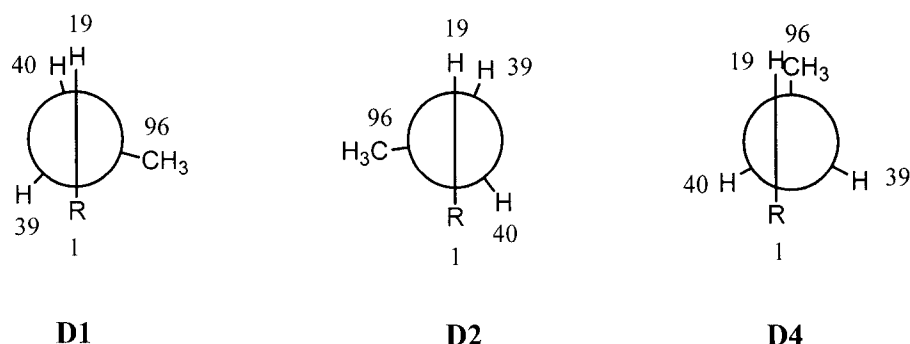


**Figure 9.** Newman projections along the N7-C27 bond of the *N*-ethylformamide (**D**) minima [R = C(O)H].

A second model compound, *N*-ethylacetamide (**E**) that has a carbon atom directly attached to the carbonyl carbon (Figure 8), was also studied for comparison. Rotation around the N7-C27 bond in 60.0° increments, generated 6 starting conformations. Three unique conformers, **E1**, **E3** and **E5**, were obtained, with the C1-N7-C27-C96 dihedral angles +80.5°, 180.0° and -80.5°, respectively (Table 8), results that are essentially identical with those derived from model compound **D**.

**Table 8.** Conformational study of *N*-ethyl acetamide (**E**) to determine the C1-N7-C27-C96 and C6-N8-C33-C112 dihedral angle ( $\omega$ , °)

	$\omega$ Before MM3 (°)	$\omega$ After MM3 (°)	Total energy (kcal/mol)	Conformation
<b>E1</b>	<b>0.0</b>	<b>80.5</b>	<b>-1.7159</b>	<b>Close-to-gauche</b>
<b>E2</b>	<b>60.0</b>	<b>80.5</b>	<b>-1.7159</b>	<b>Close-to-gauche</b>
<b>E3</b>	180.0	180.0	-1.5270	<i>Anti</i>
<b>E4</b>	180.0	180.0	-1.5270	<i>Anti</i>
<b>E5</b>	<b>240.0</b>	<b>-80.5</b>	<b>-1.7159</b>	<b>Close-to-gauche</b>
<b>E6</b>	<b>300.0</b>	<b>-80.5</b>	<b>-1.7159</b>	<b>Close-to-gauche</b>

These models simply imply that there is no obvious angular preference between the amide carbonyl carbon and the alkyl chain beginning with the  $\beta$ -carbon.

## II. Molecular mechanics study of compounds 2 - 5

### 1. Computational protocols

Using MM3 in the Alchemy 2000 computing software by Tripos, compounds **2 - 5** were minimized using the same protocol as described for **1** in Chapter 1 employing molecular mechanics, block diagonal then full matrix minimization at a dielectric constant of 1.0. However, results from the methyl propanate (**A**) model were applied to the pendant ester groups of **2** and those from the methyl 2-methylpropanate (**B**) to the ester groups of **3**. The 2,2-dimethylpropanyl groups of **4** with three equivalent methyl groups attached to the  $\alpha$ -carbon of the ester function, were treated in the same way as the acetyl groups in **1**.

The identical models employed to calculate low energy conformers of **1**, were applied to 2,3,4,5-tetra-*O*-acetyl-*N,N'*-dihexyl-D-glucaramide (**5**) but with consideration given to the last model employing *N*-ethyl formamide (**D**).

## 2. Computational results

### Diamides **2 – 4** (2,3,4,5-tetra-*O*-alkyl-*N,N'*-dimethyl-D-glucaramide)

Table 9 contains the calculated energies (kcal/mol) of the 64 rotamers generated for **2**.

Rotamer 3 (Figure 10,  ${}_2G^+{}_3G^+{}_4G^-$ ), and as with compound **1**, is the dominant low energy conformation and accounts for 95.62% of the population (Table 10).

**Table 9.** MM3 calculated energies (kcal/mol) of different 2,3,4,5-tetra-*O*-propanyl-*N,N'*-dimethyl-*D*-glucaramide (**2**) rotamers

<b>2</b>	Rotamer 1	Rotamer 2	Rotamer 3	Rotamer 4
1	<b>1.7942</b>	13.3647	<b>-0.1081</b>	7.8965
2	7.7207	6.9796	-0.1080	3.8974
3	7.9373	6.7489	-0.1080	3.6706
4	5.9701	3.3391	1.6363	4.3217
5	4.5316	7.7676	-0.1080	7.8965
6	2.2509	9.7474	1.6391	8.3723
7	1.7943	5.9355	0.6365	8.3230
8	5.3522	<b>3.3021</b>	0.6366	4.3217
9	1.7942	5.9379	0.8899	6.1136
10	1.7942	5.9366	1.9817	7.1147
11	2.2508	5.8050	2.9491	7.0060
12	5.9701	3.3391	2.9600	6.7306
13	2.2509	5.8050	0.8899	<b>3.3205</b>
14	5.9700	3.3391	0.8900	5.5768
15	5.3522	3.3021	6.0938	5.5768
16	5.3523	3.3021	7.0485	6.4622

**Table 10.** Energy distribution for low-energy conformations 1 – 4 of 2,3,4,5-tetra-*O*-propanyl-*N,N'*-dimethyl-*D*-glucaramide (**2**) using MM3 at dielectric constant 1.0

<b>2</b>	Rotamer 1	Rotamer 2	<b>Rotamer 3</b>	Rotamer 4
Total energy (kcal/mol)	1.7942	3.3021	<b>-0.1080</b>	3.3205
Compression (kcal/mol)	4.1515	3.5705	4.5349	3.8930
Bending (kcal/mol)	6.1523	4.9256	6.8276	6.6243
Stretch-bend (kcal/mol)	0.5325	0.4467	0.6591	0.6741
Bend-bend (kcal/mol)	0.0144	-0.0198	0.0743	0.0378
Van der waals 1,4 energy (kcal/mol)	25.8514	26.0687	26.5255	25.5078
Other (kcal/mol)	-9.7420	-9.1019	-12.6869	-8.9134
Torsional (kcal/mol)	-5.7915	-6.5467	-4.1029	-4.2707
Torsion-stretch (kcal/mol)	-0.2985	-0.2147	-0.3995	-0.2170
Dipole-dipole (kcal/mol)	-19.0759	-15.8264	-21.5401	-20.0154
Charge-dipole (kcal/mol)	0.0000	0.0000	0.0000	0.0000
Charge-charge (kcal/mol)	0.0000	0.0000	0.0000	0.0000
Na/No	0.039771	0.003086	1	0.002991
Percent population (%)	3.80	0.30	<b>95.62</b>	0.29

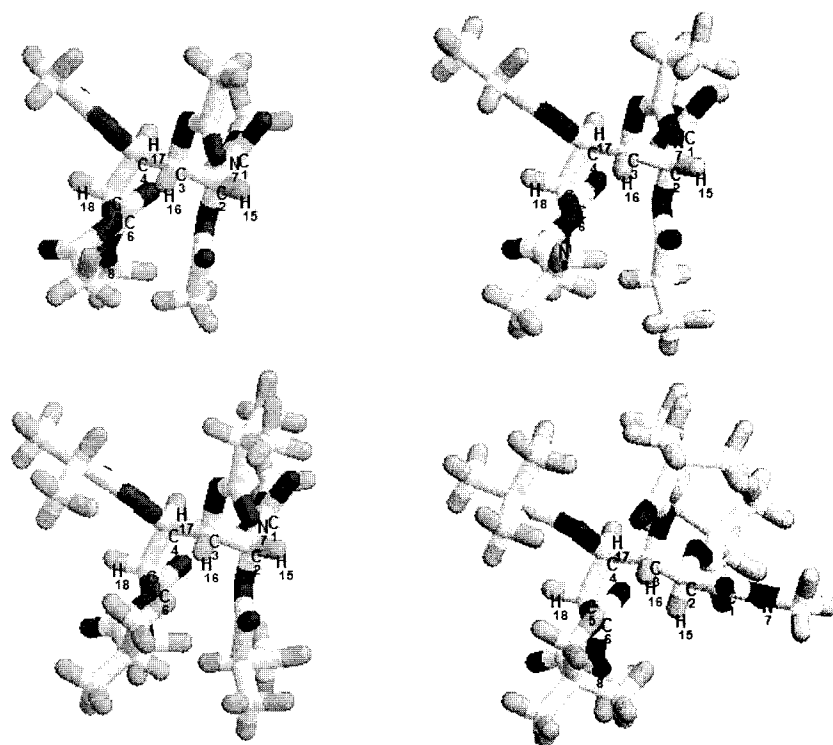


**Figure 10.** Lowest energy conformations for the minimized conformations of the 2,3,4,5-tetra-*O*-acyl-*N,N'*-dimethyl-*D*-glucaramides **1** – **4** (the upper row, from left to right are **1** and **2**; the bottom row, from left to right are **3** and **4**, respectively).

Calculation of relative percentages of each rotamer type (1 - 4) was carried out as described in Chapter 1, employing the following equations:<sup>[5]</sup>

$$N_a/N_o = \exp(-\Delta E/RT) \quad 2.1$$

$$P_a = [(N_a/N_o) / \Sigma(N_i/N_o)] \times 100 \quad 2.2$$

The calculated low energy conformation of the methyl propanate (**A**), Propanate Model, was very consistent with the final minima of tetra-*O*-propanyl-*N,N'*-dimethyl-*D*-

glucaramide (**2**) (Table 11).

**Table 11.** Torsion angles ( $\omega$ , °) suggested by Propanate Model (methyl propanate (**A**)) and the low energy conformations of rotamer 1 to 4 of **2**

Dihedral Angles	Rotamer 1	Rotamer 2	Rotamer 3	Rotamer 4	Suggested
$\omega$ (O92=C44-C48-C96) (°)	6.0	5.3	<b>-8.4</b>	-0.7	<b>0.0</b>
$\omega$ (O93=C53-C57-C101) (°)	-1.2	-2.1	<b>0.6</b>	0.0	<b>0.0</b>
$\omega$ (O94=C62-C66-C106) (°)	0.0	0.5	<b>0.0</b>	-1.1	<b>0.0</b>
$\omega$ (O95=C71-C75-C111) (°)	-0.7	-2.3	<b>0.0</b>	-0.5	<b>0.0</b>

The calculated energies of the 64 rotamers generated for **3** and **4** are presented in Tables 12 and 15, respectively. For the diamide **3** with *O*-methylpropanyl groups, rotamer 3 is again dominant with a 97.50% population among the four low energy conformers derived from the original four rotamers (Table 13). However, for diamide **4**, with *O*-dimethylpropanyl ester functions, rotamer 1 is the low energy conformation accounting for 81.37% of the lowest energy members of rotamers 1 - 4 (Table 16). It may be that the very bulky dimethylpropanyl group in some way sterically impacts the overall conformation beyond what was calculated for the smaller acetyl, propanyl and methylpropanyl groups of **1** - **3**, respectively.



**Table 12.** MM3 calculated energies (kcal/mol) of different 2,3,4,5-tetra-*O*-(2-methylpropanyl)-*N,N'*-dimethyl-D-glucaramide (**3**) rotamers

<b>3</b>	Rotamer 1	Rotamer 2	Rotamer 3	Rotamer 4
1	<b>12.3043</b>	18.3507	12.1405	19.1217
2	16.1510	17.9210	<b>10.0376</b>	15.1388
3	18.8759	17.5798	10.0376	15.1343
4	16.7650	17.9693	13.4654	16.6595
5	12.9222	18.0353	13.5978	19.1217
6	12.9222	18.0381	14.8578	19.8019
7	12.3046	18.3324	13.4654	19.4478
8	16.1476	14.5298	10.4389	15.5739
9	12.3044	<b>14.1704</b>	11.6944	<b>13.4148</b>
10	12.3044	15.7497	12.3059	15.1181
11	12.9222	14.3332	12.3060	15.1115
12	16.7636	14.4721	12.3060	18.4935
13	12.9222	13.3329	11.6945	14.0053
14	16.7654	14.4720	11.6945	16.8347
15	16.1293	14.6448	11.6945	17.1143
16	16.1516	14.6463	12.3060	18.5304

**Table 13.** Energy distribution for low-energy conformations 1 – 4 of 2,3,4,5-tetra-*O*-(2-methylpropanyl)-*N,N'*-dimethyl-D-glucaramide (**2**) using MM3 at dielectric constant 1.0

<b>3</b>	Rotamer 1	Rotamer 2	<b>Rotamer 3</b>	Rotamer 4
Total energy (kcal/mol)	12.3042	14.1704	<b>10.0376</b>	13.4148
Compression (kcal/mol)	4.7550	4.4044	5.1131	4.6149
Bending (kcal/mol)	6.8166	6.9653	7.6298	6.8329
Stretch-bend (kcal/mol)	0.5234	0.5891	0.6811	0.6591
Bend-bend (kcal/mol)	-0.0431	-0.0285	0.0296	-0.0322
Van der waals 1,4 energy (kcal/mol)	30.6906	30.4140	31.2777	30.1926
Other (kcal/mol)	-10.9554	-11.6697	-14.2154	-10.1728
Torsional (kcal/mol)	-0.2734	-0.3719	1.3396	1.6835
Torsion-stretch (kcal/mol)	-0.2924	-0.2486	-0.3953	-0.2177
Dipole-dipole (kcal/mol)	-18.9171	-15.8838	-21.4224	-20.1454
Charge-dipole (kcal/mol)	0.0000	0.0000	0.0000	0.0000
Charge-charge (kcal/mol)	0.0000	0.0000	0.0000	0.0000
Na/No	0.021443	0.000907	1	0.003263
Percent population (%)	2.09	0.09	<b>97.50</b>	0.32

As shown in Table 14, the conformational preference of the methylpropanyl group based on the methyl 2-methylpropanate (**B**), Isobutanate Model, was dominant in minimized rotamers 1 - 4 of **3**.

**Table 14.** Torsion angles ( $\omega$ , °) suggested by Isobutanate Model (methyl 2-methylpropanate (**B**)) and the low energy conformations of rotamer 1 to 4 of **3**

Dihedral angles	Rotamer 1	Rotamer 2	Rotamer 3	Rotamer 4	Suggested
$\omega$ (O92=C44-C48-C96/C128) (°)	20.8	5.3	<b>34.3</b>	-16.3	<b>0.0</b>
$\omega$ (O93=C53-C57-C101/C133) (°)	2.3	1.9	<b>5.4</b>	3.5	<b>0.0</b>
$\omega$ (O94=C62-C66-C106/C138) (°)	3.6	5.8	<b>3.4</b>	3.2	<b>0.0</b>
$\omega$ (O95=C71-C75-C111/143) (°)	4.1	4.9	<b>-2.0</b>	3.5	<b>0.0</b>

**Table 15.** MM3 calculated energies (kcal/mol) of different rotamers of 2,3,4,5-tetra-*O*-(2,2-dimethylpropanyl)-*N,N'*-dimethyl-*D*-glucaramide (**4**)

<b>4</b>	Rotamer 1	Rotamer 2	Rotamer 3	Rotamer 4
1	22.7505	29.8710	24.8454	29.8986
2	22.7043	30.6925	24.8454	27.1996
3	27.7598	29.9676	24.9847	26.9768
4	27.9832	29.4155	25.4648	27.7769
5	23.9476	29.8792	24.9847	30.1228
6	23.9649	29.1323	25.0228	30.2202
7	22.7269	28.8568	24.7164	30.2178
8	22.7139	26.2827	24.7163	27.8561
9	23.8276	25.7415	24.3890	<b>23.9298</b>
10	<b>22.7010</b>	<b>24.7566</b>	<b>24.2390</b>	25.3875
11	23.9503	24.8576	25.0516	24.7883
12	27.6795	26.2448	24.8613	30.3580
13	23.9601	24.8594	24.5265	24.1465
14	27.7146	26.4827	24.5336	28.7254
15	22.7047	27.3181	24.8493	28.5791
16	23.1353	26.5258	24.2390	30.1569

**Table 16.** Energy distribution for low-energy conformations 1 – 4 of 2,3,4,5-tetra-*O*-(2,2-dimethylpropanoyl)-*N,N'*-dimethyl-D-glucaramide (**2**) using MM3 at dielectric constant 1.0

<b>4</b>	<b>Rotamer 1</b>	Rotamer 2	Rotamer 3	Rotamer 4
Total energy (kcal/mol)	<b>22.7010</b>	24.7566	24.2390	23.9298
Compression (kcal/mol)	5.7416	5.4145	6.1536	5.5829
Bending (kcal/mol)	6.7252	6.8489	7.7154	6.8019
Stretch-bend (kcal/mol)	0.4494	0.5240	0.6042	0.6238
Bend-bend (kcal/mol)	-0.0830	-0.0662	0.0118	-0.0650
Van der waals 1,4 energy (kcal/mol)	35.0786	34.8535	36.2164	34.7386
Other (kcal/mol)	-12.8060	-13.5271	-14.8590	-11.3298
Torsional (kcal/mol)	6.7773	6.6413	9.1277	7.8263
Torsion-stretch (kcal/mol)	-0.2776	-0.2637	-0.4967	-0.2270
Dipole-dipole (kcal/mol)	-18.9044	-15.6686	-20.2345	-20.0218
Charge-dipole (kcal/mol)	0.0000	0.0000	0.0000	0.0000
Charge-charge (kcal/mol)	0.0000	0.0000	0.0000	0.0000
Na/No	<b>1</b>	0.030664	0.073739	0.124547
Percent population (%)	<b>81.37</b>	2.50	6.00	10.13

The dihedral angles between the hydrogens on the chiral carbons of the glucaryl units of tetra-*O*-acyl-*N,N'*-dimethyl-D-glucaramides (**1 - 4**) minima were calculated using the Alchemy MM3 program (Table 17). The corresponding coupling constants were calculated with a modified Altona equation<sup>[4]</sup> (Table 18) as described in chapter 1.

**Table 17.** MM3 calculated dihedral angles ( $\omega$ , °) for 2,3,4,5-tetra-*O*-acyl-*N,N'*-dimethyl-*D*-glucaramide (**1** - **4**)

	<b>1</b>	<b>2</b>	<b>3</b>	<b>4</b>
$\omega$ (H15-C2-C3-H16) (°)	-50.5	-51.1	-51.8	66.4
$\omega$ (H16-C3-C4-H17) (°)	-176.6	-176.5	-176.5	177.8
$\omega$ (H17-C4-C5-H18) (°)	-84.2	-84.8	-83.5	-78.6

**Table 18.** Calculated and experimental ( $^1\text{H}$  NMR) coupling constants (J, Hz) from global minima of 2,3,4,5-tetra-*O*-acyl-*N,N'*-dimethyl-*D*-glucaramides (**1** - **4**)

	<b>1</b>		<b>2</b>		<b>3</b>		<b>4</b>
	MM3	$^1\text{H}$ NMR	MM3	$^1\text{H}$ NMR	MM3	$^1\text{H}$ NMR	MM3
$J_{15,16}$ (Hz)	4.49	3.17	4.38	3.23	4.23	2.59	1.89
$J_{16,17}$ (Hz)	13.17	7.62	13.16	7.76	13.16	8.41	13.22
$J_{17,18}$ (Hz)	0.23	3.81	0.22	3.88	0.25	3.24	0.49

### 2,3,4,5-tetra-*O*-Acetyl-*N,N'*-dihexyl-*D*-glucaramide (**5**)

The models applied to dimethyl diamide **1** were applied to the dihexyl analog **5**. Results from the remaining models, *N*-ethyl formamide (**D**) and *N*-ethyl acetamide (**E**), implied that the various staggered conformations of the  $\beta$ -methylene group (analogous to the  $\beta$ -methyl group of *N*-ethyl acetamide) are of equal energy, are equally probable and would have similar energies. Applying three different conformations of the methylene group of the hexyl group at both ends of the molecule would increase our typical set of 64 conformers per diamide to 576 conformers per diamide. Since the three rotameric forms of the *n*-hexyl groups are essentially equivalent, they will be equally populate all of the different conformations of the tetra-*O*-acetyl-*D*-glucaryl unit and contribute to the energy

total of all the conformers of **5** by the same amount. Consequently, to simplify the computational process, only the energy for one rotameric form of the terminal hexyl groups was calculated, the conformation in which each hexyl group is fully extended. The C1-N7-C27-C96 and C6-N8-C33-C112 dihedral angles were both set to 180.0°, and 64 original conformations were generated. The MM3 minimization results from the 64 conformations are listed in Table 19. The lowest energy of every rotamer is in bold.

**Table 19.** MM3 calculated energies (kcal/mol) of different rotamers of 2,3,4,5-tetra-*O*-acetyl-*N,N'*-dihexyl-*D*-glucaramide (**5**)

<b>5</b>	Rotamer 1	Rotamer 2	Rotamer 3	Rotamer 4
1	<b>7.8030</b>	12.1995	<b>6.1038</b>	18.0509
2	11.3554	<b>9.7733</b>	11.1699	15.1714
3	12.2310	9.7747	11.1644	14.1458
4	12.2130	10.1382	20.2491	14.3225
5	8.5847	16.5768	6.1135	18.0571
6	8.5847	12.2237	6.9730	17.9213
7	7.8031	12.2123	6.9407	17.9339
8	11.3556	9.9803	11.1945	15.3190
9	7.8033	12.6439	9.6941	12.3897
10	8.3329	12.2477	11.0156	13.3486
11	8.5850	12.2539	10.3959	13.4312
12	12.2858	9.7980	10.5944	12.7292
13	8.5847	12.6500	11.0689	12.3270
14	12.6277	9.9803	11.0156	<b>11.8343</b>
15	11.3932	10.2059	10.5944	11.8588
16	11.3703	9.8205	10.9912	12.7510

Out of the four rotamers, rotamer 3 (Table 20) is again the lowest energy conformation, i.e., predominant conformation of 2,3,4,5-tetra-*O*-acetyl-*N,N'*-dihexyl-*D*-glucaramide (**5**), out of the four rotamers, accounting for 94.50% of the population. All four rotamers adopt a sickle conformation (Figure 11).

**Table 20.** Energy distribution for low-energy conformations 1 – 4 of 2,3,4,5-tetra-*O*-acetyl-*N,N'*-dihexyl-*D*-glucaramide (**5**) using MM3 at dielectric constant 1.0

<b>5</b>	Rotamer 1	Rotamer 2	<b>Rotamer 3</b>	Rotamer 4
Total energy (kcal/mol)	7.8030	9.7733	<b>6.1038</b>	11.8343
Compression (kcal/mol)	4.5866	3.9088	4.8907	4.2394
Bending (kcal/mol)	6.4966	5.0956	7.4229	5.6483
Stretch-bend (kcal/mol)	0.5406	0.4626	0.6967	0.5714
Bend-bend (kcal/mol)	-0.0368	-0.0747	0.0469	-0.0517
Van der waals 1,4 energy (kcal/mol)	30.3659	30.8444	31.12.49	30.6569
Other (kcal/mol)	-10.9516	-9.2159	-13.1926	-7.2944
Torsional (kcal/mol)	-4.1671	-5.3682	-3.1119	-4.2742
Torsion-stretch (kcal/mol)	-0.2471	-0.2088	-0.4165	-0.1786
Dipole-dipole (kcal/mol)	-18.7841	-16.6705	-21.3573	-17.4828
Charge-dipole (kcal/mol)	0.0000	0.0000	0.0000	0.0000
Charge-charge (kcal/mol)	0.0000	0.0000	0.0000	0.0000
Na/No	0.056107	0.001988	1	0.000060
Percent population (%)	5.30	0.19	<b>94.50</b>	0.01



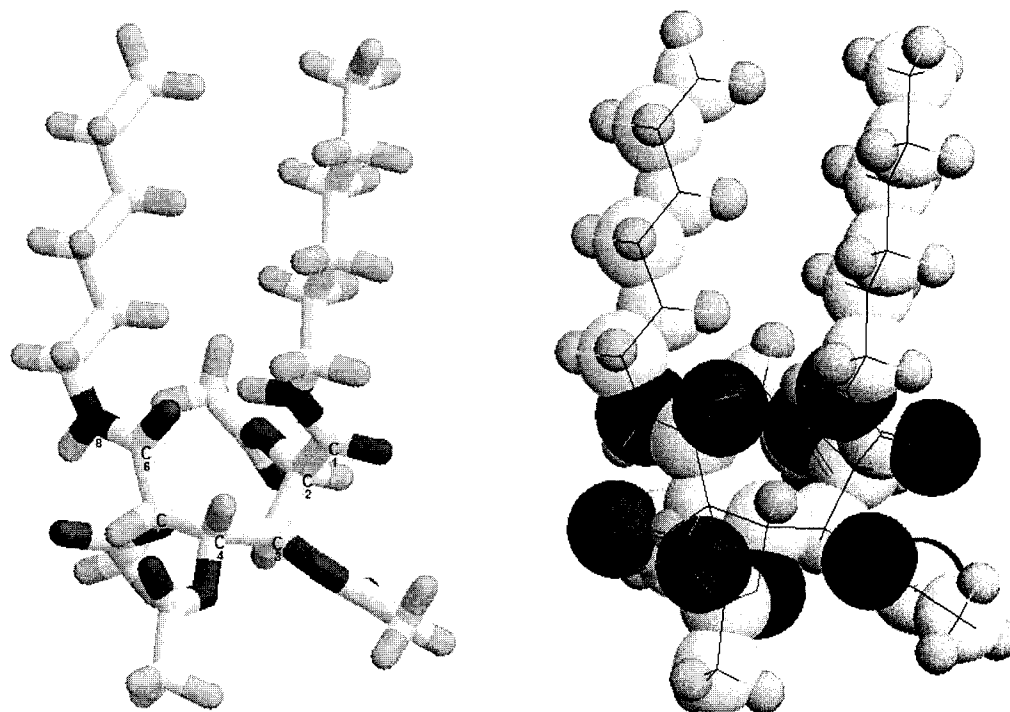


**Figure 11.** 2,3,4,5-Tetra-*O*-acetyl-*N,N'*-dihexyl-*D*-glucaramide (**5**) low energy rotamer 3 (Tubes and Spheres-and-Sticks rendering).

The calculated dihedral angles of vicinal hydrogens attached to chiral carbons of the glucaryl unit of rotamer 1 to 4 are listed in Table 21. The corresponding coupling constants were calculated with a modified Altona equation,<sup>[4]</sup> compared with <sup>1</sup>H NMR results and presented in Table 22.

**Table 21.** MM3 calculated dihedral angles ( $\omega$ , °) of 2,3,4,5-tetra-*O*-acetyl-*N,N'*-dihexyl-D-glucaramide (**5**)

Dihedral angles	Rotamer 1	Rotamer 2	<b>Rotamer 3</b>	Rotamer 4
$\omega$ (H15-C2-C3-H16) (°)	65.77	55.89	<b>-50.98</b>	-61.80
$\omega$ (H16-C3-C4-H17) (°)	-179.04	172.97	<b>-179.45</b>	177.93
$\omega$ (H17-C4-C5-H18) (°)	-75.63	57.93	<b>-86.23</b>	63.96

**Table 22.** Vicinal coupling constants (J, Hz) for 2,3,4,5-tetra-*O*-acetyl-*N,N'*-dihexyl-D-glucaramide (**5**) (Karplus/Altona<sup>[4]</sup> calculated and <sup>1</sup>H NMR results)

	Rotamer 1	Rotamer 2	<b>Rotamer 3</b>	Rotamer 4	<b>Observed (<sup>1</sup>H NMR)</b>
J <sub>15,16</sub> (Hz)	1.98	3.66	<b>4.40</b>	2.43	<b>3.17</b>
J <sub>16,17</sub> (Hz)	13.22	13.22	<b>13.23</b>	13.22	<b>7.62</b>
J <sub>17,18</sub> (Hz)	0.72	3.22	<b>0.19</b>	2.20	<b>3.81</b>

The rotamer populations are very similar to those calculated for tetra-*O*-acetyl-*N,N'*-dimethyl-D-glucaramide (**1**), in which rotamer 3 has a 90.91% population compare to 94.50% of **5** described above.

A list of all amide N-H and ester oxygens as a measure of potential hydrogen bonding in lowest energy conformations of **1** – **5** is given in Table 23. Hydrogen bonds were only considered at an interatomic distance of 2.10 Å or less.<sup>[9-12]</sup> For each of the lowest energy esters **1** – **5**, two intramolecular hydrogen bonds were shown.

**Table 23.** Hydrogen bonding of global minima **1** to **5** indicated by distances (Å) between amide hydrogen and ester oxygen atoms

Distance (Å)	<b>1</b>	<b>2</b>	<b>3</b>	<b>4</b>	<b>5</b>
H22(N8)-O95(C5)	1.954	1.952	1.954	1.971	1.955
H19(N7)-O14(C6)	1.921	1.921	1.918		1.922
H19(N7)-O92(C2)				1.951	

For all of the lowest energy esters **1** – **5**, C71=O95...H22-N8 forms a 7-membered ring between an amide N-H and an acetoxy carbonyl oxygen atom (Figure 12). Except compound **4**, all of the other molecules have a hydrogen bond, C6=O14...H19-N7, between an amide N-H at one end (head of the molecule) and an amide carbonyl oxygen at the other end (tail of the molecule). The intra-molecular hydrogen bonding across the structure between terminal amides appears to open the dihedral angle between H17-H18 and fix the final conformation, perhaps contributing to the discrepancy between the theoretical and experimental coupling constants for H17, H18.

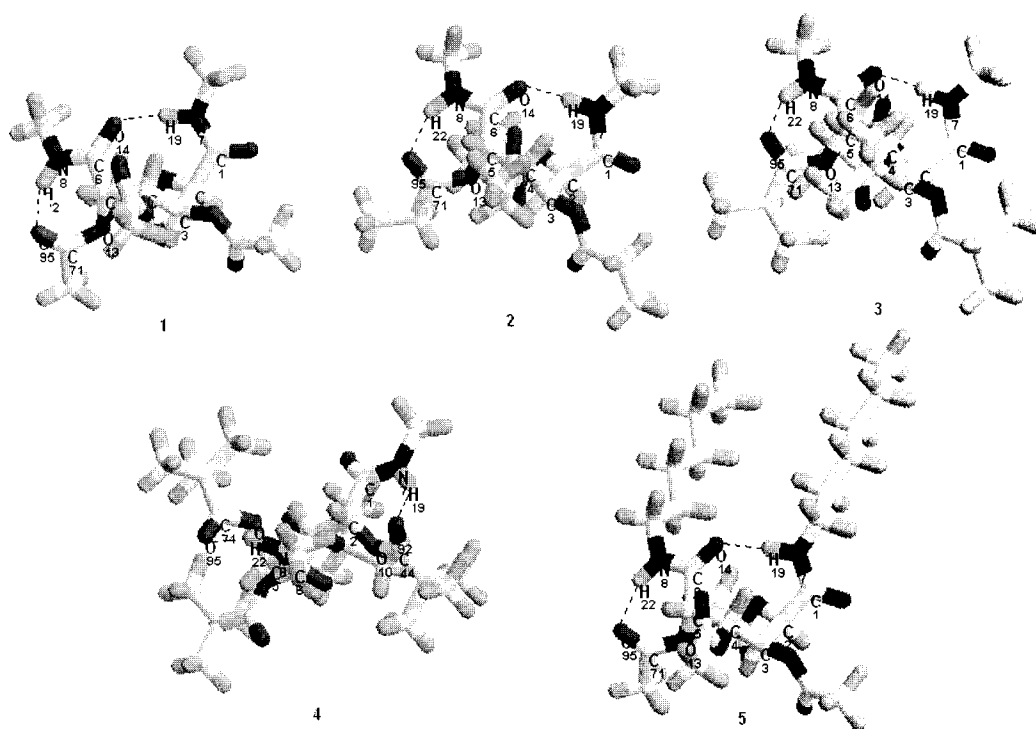


**Figure 12.** Hydrogen bonds of global minima of **1 – 5**.

### III. Conformation of poly(hexamethylene 2,3,4,5-tetra-*O*-acetyl-*D*-glucaramides) – some possibilities

Repeating *head, tail* - poly(hexamethylene 2,3,4,5-tetra-*O*-acetyl-*D*-glucaramide) (Figure 13 and Figure 14) and alternating *head, tail* - *tail, head* - poly(hexamethylene 2,3,4,5-tetra-*O*-acetyl-*D*-glucaramide) (Figure 14) were built according to the structure of low energy conformation, rotamer 3 of 2,3,4,5-tetra-*O*-acetyl-*N,N'*-dihexyl-*D*-glucaramide (**5**). Repeating oligomer 3G6G6G6G3 (composed of four acetylated glucaryl units, with two *N*-propyl terminals to simplify the end structures, and three repeating hexamethylene units between the acetylated glucaryl units) represent a segment of a stereoregular, repeating *head, tail* - poly(hexamethylene 2,3,4,5-tetra-*O*-acetyl-

D-glucaramide). Alternating oligomer 3G'6G'6G'6G'3 represents a segment of the other stereoregular form of the polymer, alternating *head, tail - tail, head -* poly(hexamethylene 2,3,4,5-tetra-*O*-acetyl-D-glucaramide). The overall structure has a somewhat helical shape constituted with the hydrophobic alkylene backbone, which is surrounded with scattered hydrophilic group (heteroatoms, e.g., oxygen and nitrogens) outside of the loop.

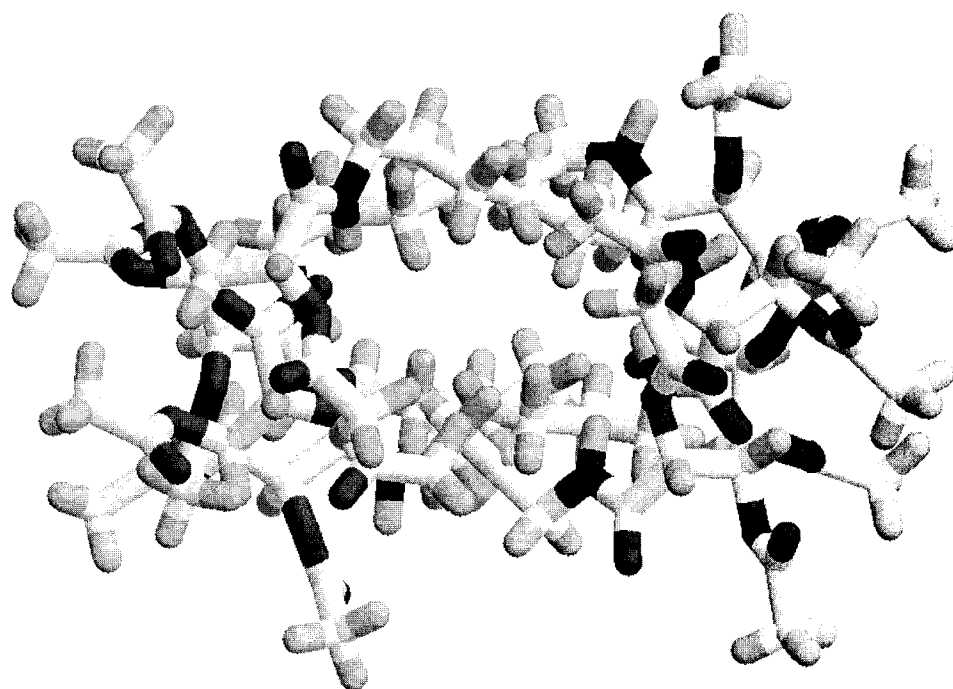


**Figure 13.** Repeating oligomer 3G6G6G6G3 (composed of four acetylated glucaryl units, with two *N*-propyl terminals, and three repeating hexamethylene units between the acetylated glucaryl units), as a segment of a stereoregular, repeating *head, tail -* poly(hexamethylene 2,3,4,5-tetra-*O*-acetyl-D-glucaramide).

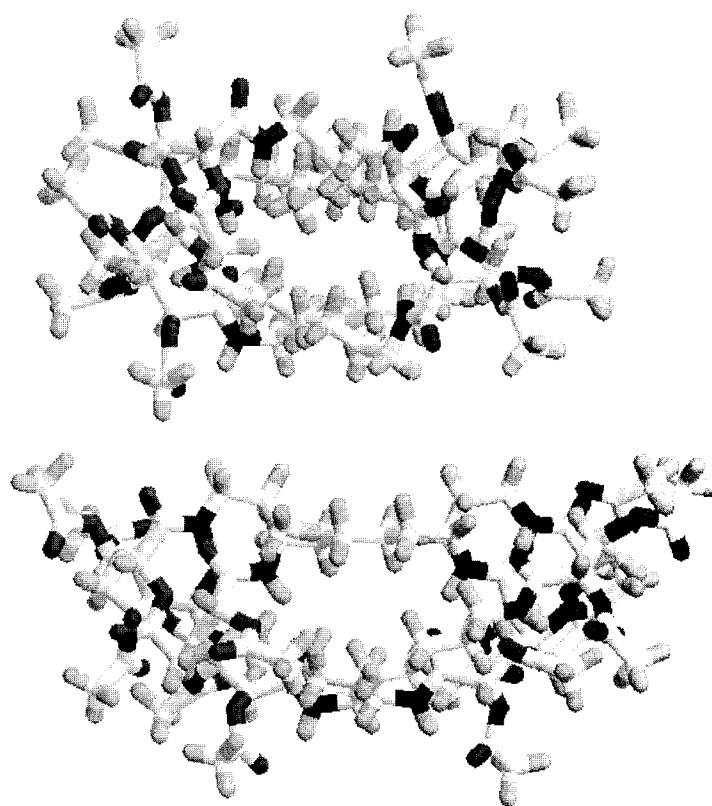


**Figure 14.** Repeating oligomer 3G6G6G6G3 (top, represent repeating *head, tail* - poly(hexamethylene 2,3,4,5-tetra-*O*-acetyl-D-glucaramide)) and alternating oligomer 3G'6G'6G'6G'3 (bottom, composed of four acetylated glucaryl units, with two *N*-propyl terminals, and three repeating hexamethylene units between the acetylated glucaryl units), as a segment of a alternating *head, tail – tail, head* - poly(hexamethylene 2,3,4,5-tetra-*O*-acetyl-D-glucaramide).

## Conclusions

1. Calculated  $^1\text{H}$  NMR vicinal coupling constants are in reasonable agreement with experimental results, but as with **1** described in chapter 1, intramolecular H-bonding influences the conformations of calculated rotamers **2**, **3**, **4**, **5**.
2. For low energy conformers, H15-H16 is conformational *gauche*, H16-H17 is *anti*, and H17-H18 is close-to-*gauche*.
3. For most of the esterified dialkyl-D-glucaramides, **1**, **2**, **3** and **5**, the predominant conformation of acylated glucaryl unit is sickle,  ${}_2\text{G}^+{}_3\text{G}^+{}_4\text{G}^-$ . The only exception is 2,3,4,5-tetra-*O*-(2,2-dimethylpropanyl)-*N,N'*-dimethyl-D-glucaramide (**4**), which adopts a different sickle conformation,  ${}_3\text{G}^+{}_4\text{G}^-$ .
4. A predicted overall conformation of the polymer in a nonpolar solvent appears to be coiled.
5. A “model building” approach has proved to be an efficient method for conformational analysis of medium size, somewhat complex molecules, and has been applied in both chapters 1 and 2.
6. Molecular mechanics (MM3) has proved to be a valid method for conformational analysis of both acyclic D-glucaramide and acylated D-glucaramides.

## References

1. Leach, Andrew R. *Molecular Modeling Principles and Applications*. **2001**, Prentice Hall.
2. Gibson, K. D. And Scheraga, H. A. Revised Algorithms for the Build-Up Procedure for Predicting Protein Conformations by Energy Minimization. *Journal of Computational Chemistry* **1987**, 8(6): 826-834.
3. Leach, Andrew R., Rrout, Keith and Dolata, Daniel P. An Investigation into the Construction of Molecular Models by the Template Joining Method. *Journal of Computer-Aided Molecular Design* **1988**, 2: 107-123.
4. Haasnoot, C.A.G., De Leeuw, F.A.A.M., and Altona C. The Relationship between Proton-Rroton NMR Coupling constants and Substituent Electronegativities-I An empirical generalization of the Karplus equation. *Tetrahedron* **1980**, 36: 2783-2792.
5. Chen, L. H., B.; Kane, R. W.; Kiely, D. E.; Rowland, R. S. Molecular modeling of acyclic carbohydrate derivatives N,N'-dimethyl- and N,N'-dihexylxylaramide. Model compounds for synthetic poly(hexamethylenexylaramide). *ACS Symposium Series* (1990), 430 (Computer Modeling of Carbohydrate Molecules), **1990**.
6. Klimkowski, V. J.; Scarsdale, J. N. And Schaefer, L Ab initio studies of structural features not easily amenable to experiment. 25. Conformational analysis of methyl propanoate and comparison with the methyl ester of glycin. *Journal of Computational Chemistry* **1983**, 4(4): 194-198.
7. Moravie, R. M. And Coreset, J. Conformational behavior and vibrational spectra of methyl propionate. *Chemical physics letters* **1974**, 26(2): 210-214.
8. Moravie, R. M. And Coreset, J. Vibration spectra and conformation of methyl propionate and isobutyrate. *Journal of Molecular Structure THEOCHEM* **1975**, 24(1): 91-108.
9. Jeffrey, G. A. *An Introduction to Hydrogen Bonding*. **1997**, New York, Oxford.
10. March, J. *Advanced Organic Chemistry*. **1985**, New York, John Wiley & Sons.
11. Lopez De La Paz, Manuela; Penades, Soledad and Vicent, Cristina Conformational Restriction by Intramolecular Hydrogen Bonding. Carbohydrate-Carbohydrate Self-Assembly. *Tetrahedron Letters* **1997**, 38(9): 1659-1662.



12. Allinger, Norman L.; Kok, Randall A.; Imam, Mita R. Hydrogen bonding in MM2. *Journal of Computational Chemistry* **1988**, 9(6): 591-5.

### **Chapter 3. Preparation of salts of selected D-aldaric acids and a new procedure for stereochemically random hydroxylated nylons preparation**

#### **Introduction**

The history of using polymers is as long as the length of human existence. Primitive man used animal furs for clothing and as a covering for the floor in his cave. Both animal (wool and silk) and vegetable (cotton, flax and ramie) fibers were used at least 5,000 years ago. Cotton was used for making cloth in the Indus Valley and in Mexico before 2,500 B.C.. Cotton bolls found in Mexico are believed to be 7,500 years old. Silk cloth was used in China over 5,000 years ago, and linen (flax) was the preferred wrapping material for mummies in ancient Egypt.

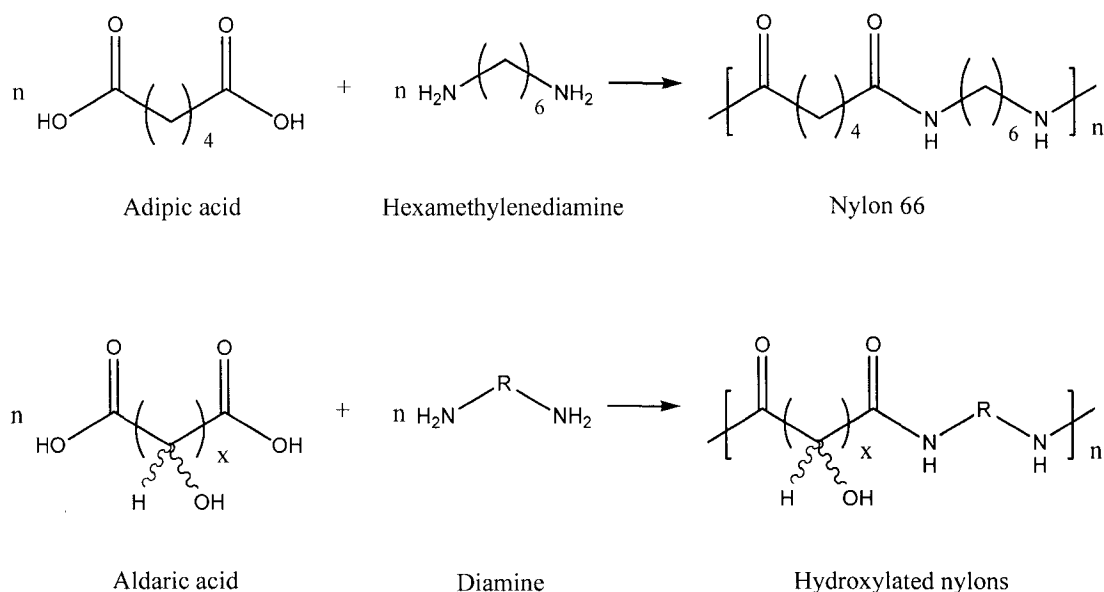
However, not until the twentieth century did people realize that both natural rubber and cellulose are polymers. The patent of Hyatt's Celluloid (1868)<sup>[1]</sup> was considered the beginning of plastic industry.

The 1920s witnessed a "plastic craze" after the development of cellophane. Wallace Hume Carothers accidentally discovered the method of producing polyamides, and most notably nylon66, poly(hexamethylene adipamide), when he was doing some research on polymerization mechanisms. The discovery made Carothers a pioneer in the plastics industry and head of fundamental research in organic chemistry at DuPont in the 1930s. Nylon replaced animal hair in toothbrush and silk stockings as well.

Nylon 66 was the first successful synthetic polyamide. Even till today, it is still an important commercial polyamide, notable for its high strength, elasticity, toughness and abrasion resistance, and it has been applied to a variety of applications. As a textile fiber, it is widely employed for apparel fabrics and tire cords, as well as for ropes, cords, belting and filter cloth. As a molded plastic, it has been utilized as an engineering material in bearings, gears, cams, rollers, slides, door latches and other objects. It is also employed as an outer jacket covering for the primary insulation of electrical wires because of its abrasion resistance.<sup>[1]</sup>

Nylon 66, poly(hexamethylene adipamide) is obtained by the condensation polymerization of adipic acid (1,6-hexanedioic acid) with hexamethylenediamine (1,6-hexanediamine)<sup>[2,3]</sup> (Scheme 1). However, high molecular weight polymer is almost impossible to obtain if the diacid and diamine are simply condensed. One of Carother's important contributions to polymer chemistry is that he divided the condensation reaction into two steps: salt formation and then polymerization. Diacids and diamines can form 1:1 salts (e.g., hexamethylenediammonium adipate or nylon 66 salt). The salt is easily isolated, recrystallized and then subjected to melt polymerization at high temperature (280 °C). This process solved the major problem of nylon 66 preparation (the stoichiometry problem), which is always a big concern related to condensation polymerizations. A 1:1 ratio of diacid : diamine monomers is the prerequisite condition to get high molecular weight polymers (>10,000). Since the solubility of nylon 66 salt in

methanol is very low, the disalt formation is usually carried in methanol solution and the disalt is easily isolated.

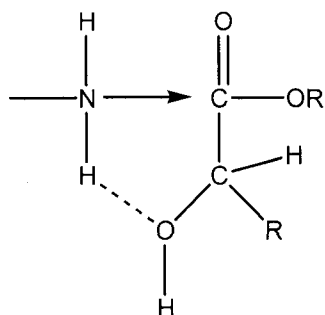


**Scheme 1.** Nylon 66 and hydroxylated nylons.

A related group of polyamides, polyhydroxypolyamides (PHPAs), was first reported by Ogata's group in the mid 1970s and early 1980's.<sup>[4-15]</sup> Condensation of an esterified polyhydroxyladipic acid (aldaric acid) and alkylenediamine can produce a class of polymers, called "hydroxylated nylons" or "polyhydroxypolyamides" (Scheme 1). In recent years, the Kiely labs have been a major contributor in the preparation of hydroxylated nylons based on D-glucose, D-mannose, D-galactose and D-xylose.<sup>[16-29]</sup> Glucaric acid based polymers are potentially the most important, being derived from inexpensive and readily available D-glucose. Oxidation of a starting monosaccharide can

produce the starting carbohydrate diacids, *i.e.*, aldaric acid. Biodegradability is another important characteristic of this group of environmentally friendly polyamides. The use of different diamines leads to polyamides of different melt and solubility characteristics, suggesting a range of different hydrophilicity and hydrophobicity properties, and thus different potential applications.

Ogata and co-workers were the first to prepare PHPAs, starting with the aldaric acid diesters diethyl mucate (diethyl galactarate) or diethyl tartarate, and several diamines. They found that diesters having hetero atoms such as oxygen or sulfur at the  $\alpha$  or  $\beta$  positions underwent easy polycondensation. According to their hypothesis, ester aminolysis is enhanced due to formation of a transition state 5 or 6 membered ring involving amine N-H hydrogen bonding to the pendant heteroatom on the ester (*e.g.*, Scheme 2). However, Hoagland<sup>[30]</sup> established that the diester of the aldaric acids, mucic acid<sup>[30]</sup> and xylaric acid,<sup>[31]</sup> first undergo rapid ring closure to a five membered lactone which then is opened by aminolysis to yield the amide. Consequently, the polycondensation of aldaric acids with diamines does not require high temperature condition as does the preparation of nylon 66.



**Scheme 2.** Aminolysis of an ester with a hetero atom at the  $\alpha$  position (Rate enhancement according to Ogata et al<sup>[15]</sup>).

Kiely and co-workers have successfully synthesized a variety of poly(alkylene D-aldaramides).<sup>[16,17,19,20,22-25,27-29]</sup> Taking the synthesis of poly(alkylene D-glucaramide) as an example, monopotassium D-glucarate was acidified with either an acid form ion-exchange resin or HCl in methanol to form the activated D-glucarate, a mixture of methyl D-glucarate 1,4-lactone, methyl D-glucarate 6,3-lactone and acyclic dimethyl D-glucarate. The activated D-glucarate undergoes polymerization with diamines in the presence of some weak bases, particularly triethylamine, to keep the reaction basic and promote lactonization. The reaction is simple and efficient and the product is very conveniently isolated by precipitation.

The work reported here is an effort to pursue another approach to the above polycondensation reaction. Taking preparation of a poly(alkylene D-glucarate) as an example, instead of reacting esterified D-glucaric acid (lactone acids and acyclic forms mixture) with a diamine, the mixture of acyclic D-glucaric acid, D-glucaro 1,4-lactone and D-glucaro 6,3-lactone can be reacted with an alkylendiamine (e.g.

hexamethylenediamine) in aqueous solution to form hexamethylenediammonium D-glucarate disalt. The disalt can then be esterified with methanolic/HCl solution to form a 1:1 esterified D-glucaric acid / hexamethylenediammonium dichloride disalt. Starting with the correct stoichiometry (1:1 ratio) of diacid and diamine, higher molecular weight polymers are more likely to be obtained. Given that D-glucaric acid is actually a mixture of cyclic D-glucaro 1,4-lactone and D-glucaro 6,3-lactone, and acyclic D-glucaric acid, the pure 100% diammonium glucarate could be difficult to obtain, *i.e.*, a mixture of hexamethylenediammonium D-glucarate (disalt) and *N*-(6-aminohexyl)-D-glucar-6-amic acid salt (amic acid salt) is more likely to be obtained, particularly in the initial stages of the reaction. However, this mixture still has the essentially desired diacid : diamine 1 : 1 stoichiometric ratio and could eventually lead to high molecular weight polyamide.

The objectives of the research to be described in this chapter are the following:

1. Synthesis of alkylendiammonium D-alдарates, including D-glucarate, D-galactarate and D-xylarate;
2. Development of a new method of polycondensation between aldraric acids and diamines;
3. Synthesis of higher molecular weight polyhydroxypolyamides.

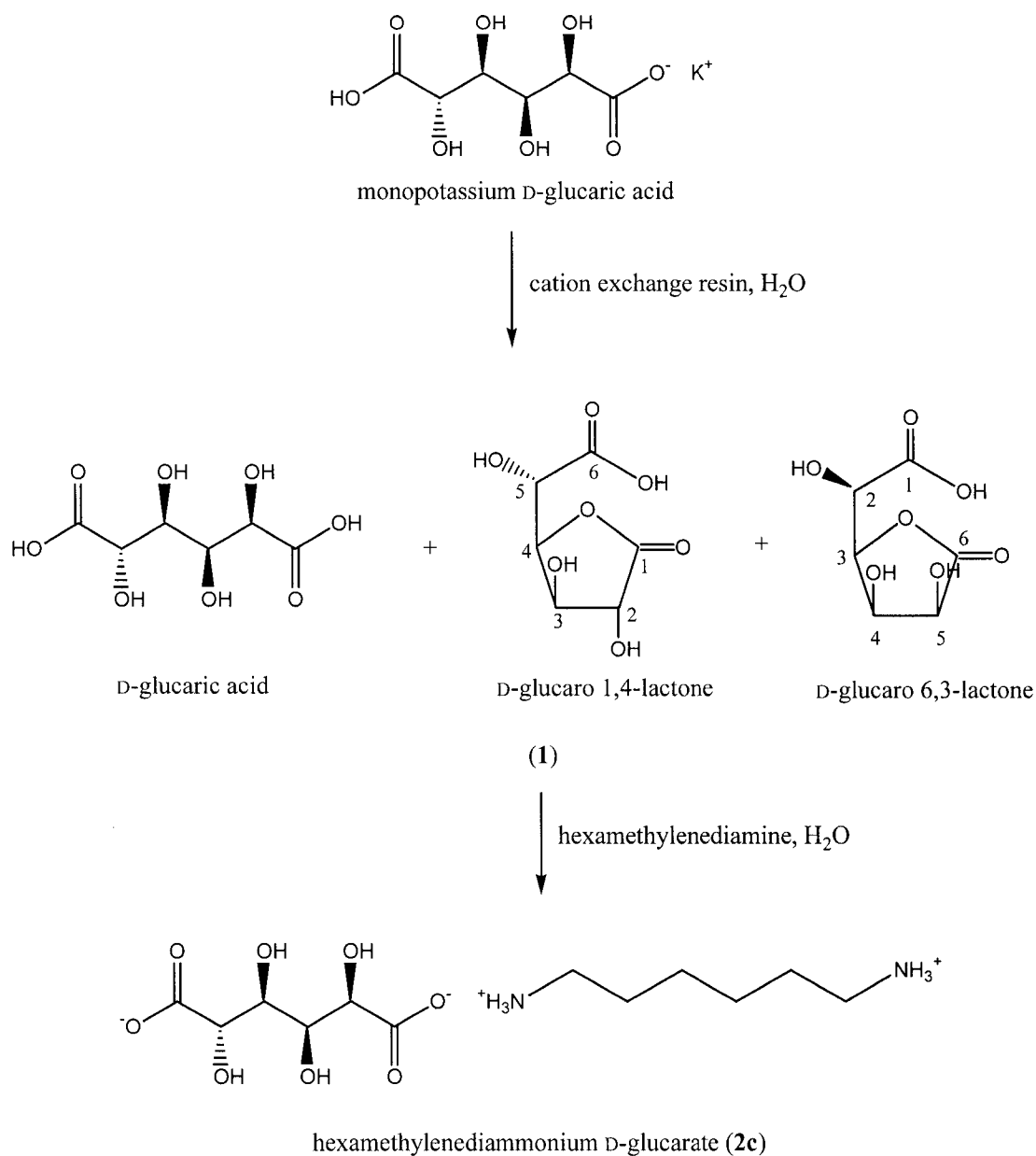
## Results and Discussion

### I. Methods for preparation of hexamethylenediammonium D-glucarate (**2c**)

Starting with monopotassium D-glucarate, an acid form cation exchange resin was utilized to acidify the monopotassium salt to a mixture (**1**) of acyclic D-glucaric acid, D-glucaro 1,4-lactone and D-glucaro 6,3-lactone in aqueous solution. The aqueous solution of **1** was concentrated and dried under vacuum. The mixture (**1**) was redissolved in deionized water to form a 1 M solution and reacted with hexamethylenediamine aqueous solution (1 M) at 80 °C to form hexamethylenediammonium D-glucarate (**2c**) disalt (Scheme 3). The disalt (**2c**) will next be activated by esterification and polymerized to form poly(hexamethylene D-glucaramide) (**7c**).

During the reaction of the acyclic D-glucaric acid / D-glucaro 1,4-lactone / D-glucaro 6,3-lactone mixture (**1**) with hexamethylenediamine, the chance of getting 100% hexamethylenediammonium D-glucarate (**2c**) disalt is not as likely as getting a mixture of **2c** (disalt), *N*-(6-aminohexyl)-D-glucar-6-amic acid salt (**3c** amic acid salt), and *N*-(1-aminohexyl)-D-glucar-1-amic acid salt (**4c**, amic acid salt). Reaction conditions for obtaining either pure disalt (**2c**) or a mixture of **2c**, **3c** and **4c** were studied.





**Scheme 3.** Preparation of hexamethylenediammonium D-glucarate (**2c**).

The reaction conditions for the preparation of the diammonium salt, hexamethylenediammonium D-glucarate (**2c**) or the amic acid salts **3c** and **4c**, depends on two factors, the method of preparation of the starting D-glucaric acid aqueous solution,

and the reaction temperature. It was determined by  $^1\text{H}$  NMR monitoring that when the lactone-acid / diacid aqueous solution was prepared from dissolving the product directly after acidification of monopotassium D-glucarate with ion exchange resin, a higher disalt (**2c**) / amic acid salts (**3c** and **4c**) ratio product was formed. On the other hand, when the D-glucaric acid (**1**) aqueous solution was prepared by dissolving crystalline / solid D-glucaric acid mixture, a lower disalt / amic acid ratio product was formed (Table 1). It is also reasonable that starting from D-glucaro-6,3-lactone, the dominant (if not only) amic acid salt formed is *N*-(6-aminohexyl)-D-glucar-6-amic acid salt (**3c**). Different reaction temperatures also affect this ratio. Higher temperature (70.0 – 80.0 °C) helps the formation of pure diammonium salt (**2c**) and raises the diammonium salt (**2c**) to amic acid salts (**3c** and **4c**) ratio. Lower temperature (*e.g.* room temperature) favors amic acid salts formation, i.e. the ratio of diammonium salt (**2c**) to amic acid salts (**3c** and **4c**) in the mixture is lower (Table 1). Formation of only amic acid salt (**3c** or **4c**) was not observed during the study.

**Table 1.** Formation of hexamethylenediammonium D-glucarate (**2c**) and amic acid salts **3c** and **4c** under different reaction conditions

Lactone* <sup>1</sup>	T (°C)* <sup>2</sup>	<b>2c</b> :( <b>3c</b> / <b>4c</b> )	Precipitation	mp (°C)* <sup>3</sup>	Product	Yield (%)	Note
JZ02006	r.t.	0.65:1	Easy	87.5-170.0	White	85.66	JZ02015
JZ02006	r.t.	0.80:1	Easy		White	90.40	JZ02029
JZ02012	r.t.	1.94:1	Hard		Light yellow, sticky	25.23	JZ02013
JZ02012	80.0	100:0	Hard		White	62.74	JZ03005
JZ02012	73.5	100:0	Hard	152.0-165.0	White	78.89	JZ02023
JZ03065	80.0	100:0	Easy		White	66.77	JZ03092

\*<sup>1</sup> JZ02006, JZ02012 and JZ03065 are all D-glucaric acid mixtures (**1**), for the formation of **2c** and/or **3c** and **4c**. JZ02006 represents the D-glucaric acid mixture (**1**) aqueous solution obtained from crystalline/solid D-glucaro-6,3-lactone; JZ02012 and JZ03065 represent the D-glucaric acid mixture aqueous solution obtained directly from syrupy D-glucaric acid without crystallization

\*<sup>2</sup> T: temperature; r.t: room temperature

\*<sup>3</sup>mp: melting point

A second effort was directed to applying milder conditions for the acid-base reaction. The reaction started with D-glucaric acid (**1**) aqueous solution, which was obtained directly from syrupy D-glucaric acid without crystallization, and hexamethylenediamine in an aqueous solution at room temperature. The temperature was kept at 40 °C in the reaction flask during the whole reaction period. Five drops of the reaction mixture were collected during certain time intervals. The reaction mixture was worked up according to the same

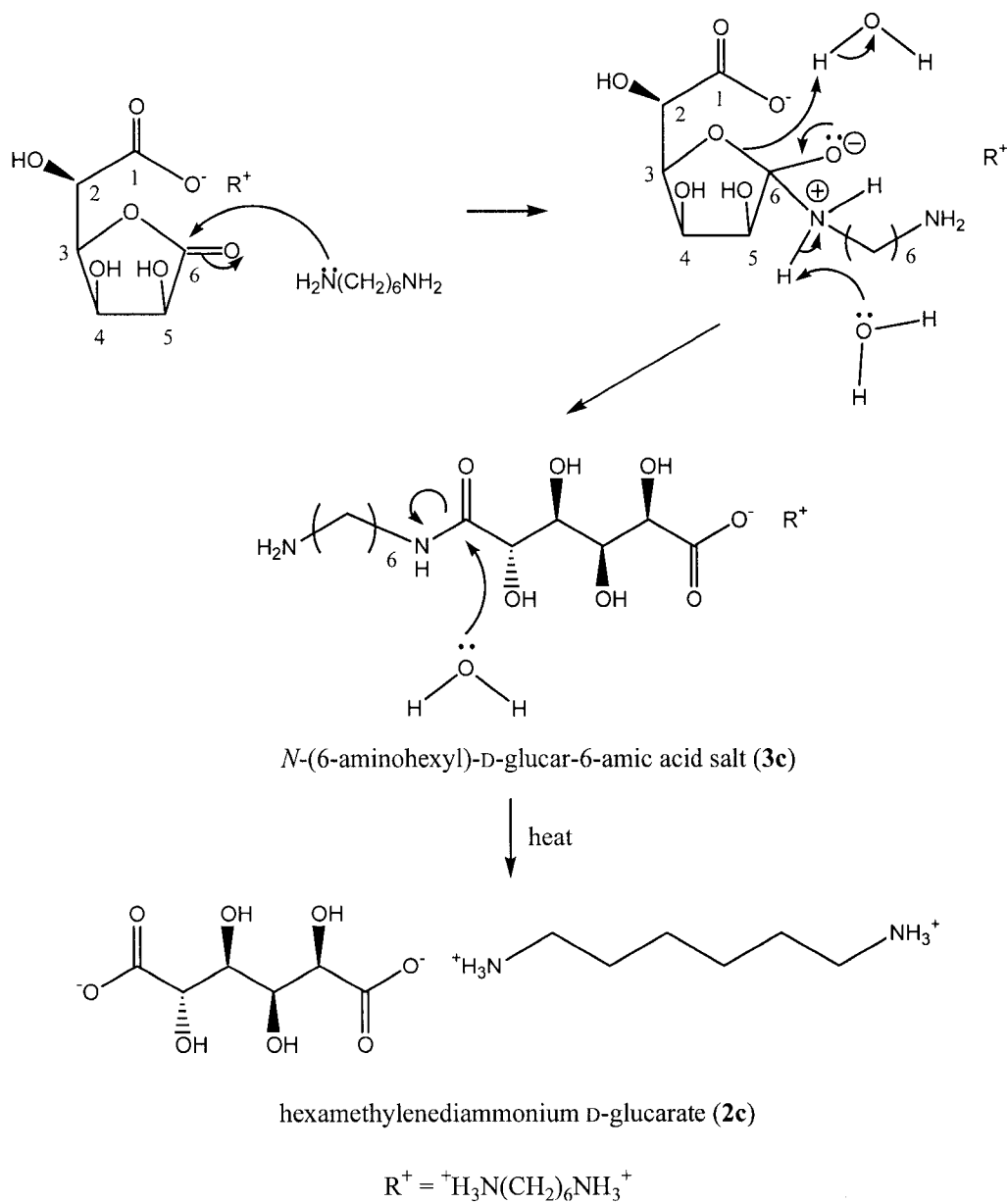
procedure as for the preparation of hexamethylenediammonium D-glucarate (**2c**) and monitored by  $^1\text{H}$  NMR ( $\text{D}_2\text{O}$ ) to determine the ratio of diammonium salt (**2c**) to amic acid salts (**3c** and **4c**). Table 2 summarizes the results of the study.

**Table 2.** Formation of **2c**, **3c** and **4c** over a temperature range at different time intervals

Sample	Reaction time (h)	<b>2c</b> : <b>3c/4c</b>	<b>2c</b> (%)	<b>3c/4c</b> (%)	Vacuum dry (h)
1	6	2.02:1	66.91	33.09	2.75
2	26	2.56:1	71.93	28.07	22
3	46	3.49:1	77.73	22.27	1.75
4	53	4.13:1	80.52	19.48	14.5
5	53 h, sonicate 1 h	4.24:1	80.93	19.07	14.5
6	55	4.22:1	80.84	19.16	13.5
7	55 h, 60 °C 2 h	5.53:1	84.69	15.31	5.5
8	78 h, 70 °C 2 h work-up immediately	3.76:1	79.00	21.00	16
9	78 h, 70 °C 2 h cool over night before work-up	5.56:1	84.76	15.24	3
10	91 h, 80 °C 2 h	5.83:1	85.37	14.63	165.5
11	91 h, 80 °C 2 h, sonicate 1 h	5.85:1	85.40	14.60	164.5

These results showed several trends. First of all, with stirring for a longer time, the ratio of diammonium salt (**2c**) to amic acid salt (**3c** and **4c**) increased, *i.e.*, hydrolysis of amides is slower compared to direct salt formation. Secondly, sonication has some influence on increasing the aminolysis but this effect is not significant (sample 5/6 and sample 10/11). Thirdly, increasing temperature also promotes aminolysis. Sample 7 was taken from the reaction mixture at 55 h, and then heated to 60 °C for 2 h. The ratio of

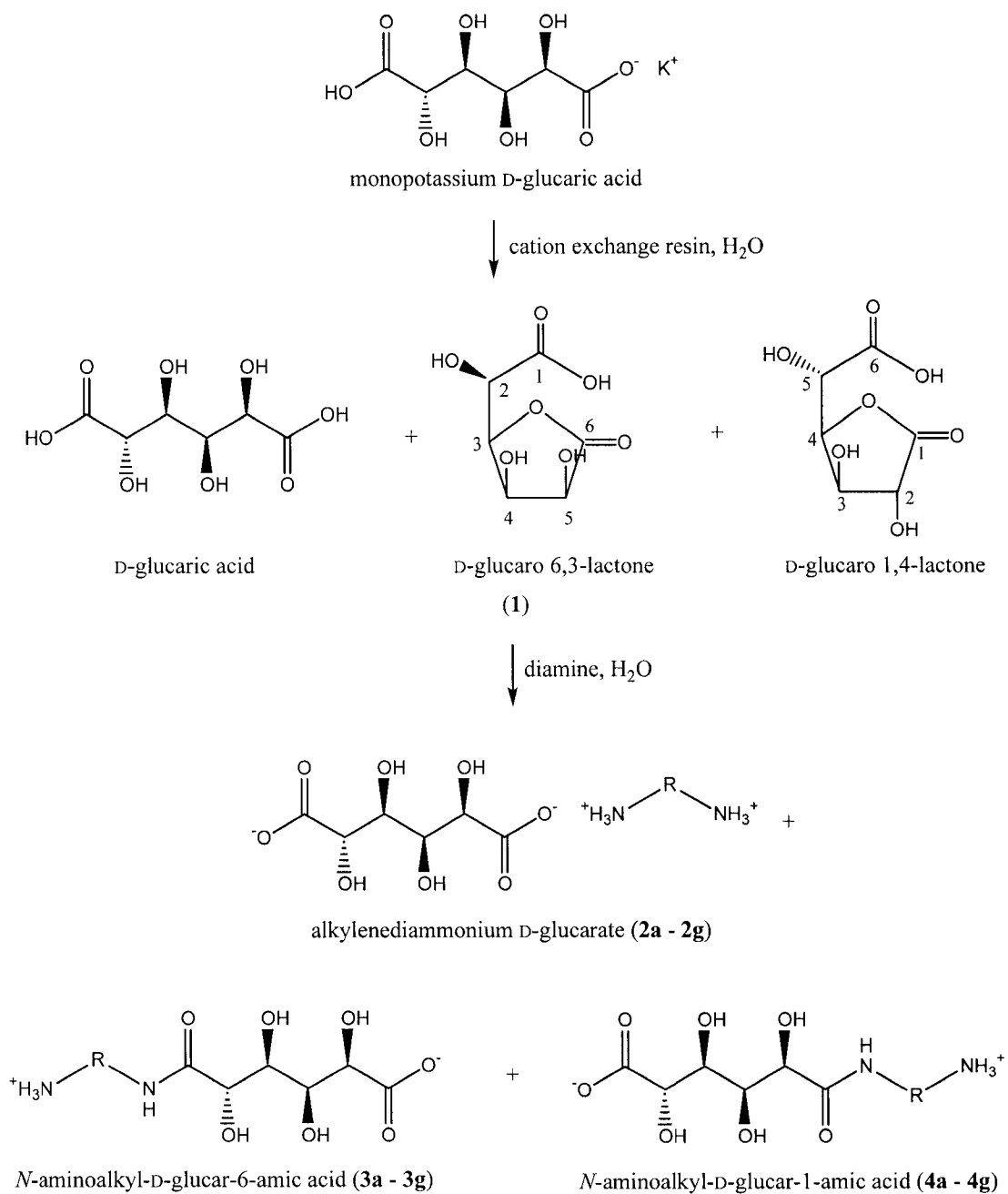
diammonium salt (**2c**) to amic acid salt (**3c** / **4c**) (5.53:1) increased compared to sample 6 (4.22:1).



**Scheme 4.** Disalt (**2c**) and *N*-(6-aminohexyl)-D-glucar-6-amic acid salt (**3c**) formation in the reaction of a diamine (hexamethylenediamine) with an acid/lactone form of D-glucuronic acid.

## **II. Preparation of other alkylenediammonium D-glucarates (2a – 2g) and the corresponding amic acid salts (3a – 3g and 4a – 4g)**

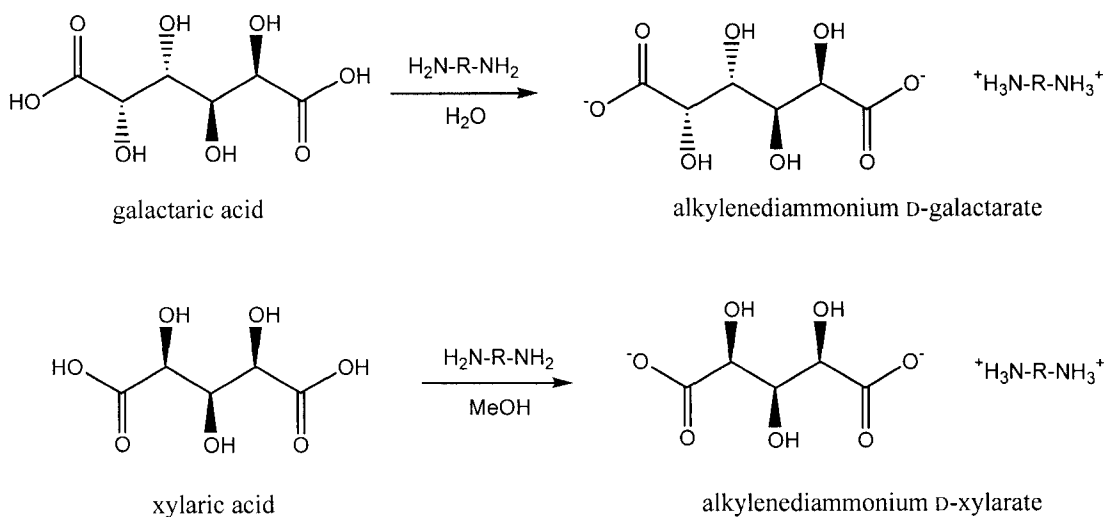
The preparation of other alkylenediammonium D-glucarates was carried out (Scheme 5). The products are mostly mixtures of disalts (**2a – 2g**) and the corresponding amic acid salts (**3a – 3g** and **4a – 4g**). Most of the reaction conditions reported use aqueous D-glucaric acid mixture (**1**) solutions obtained directly from the dried syrupy D-glucaric acid mixture without recrystallization, and salt formation was carried out at a temperature of ~75 °C. Polymerizations of most of the salt / amic acid salt mixtures were carried out and are reported here.



**Scheme 5.** Preparation of alkylendiammonium D-glucarate (**2a – 2g**) and the corresponding amic acid salt (**3a – 3g** and **4a – 4g**).

### III. Preparation of alkylenediammonium D-galactarate (5a – 5c, 5e – 5h) and alkylenediammonium D-xylarate (6c)

The preparation of alkylenediammonium D-galactarates (5a – 5c, 5e – 5h) was also carried out (Scheme 6). The reactions were generally carried out using a D-galactaric acid (mucic acid) aqueous suspension and an alkylenediamine aqueous solution. Even though galactaric acid does not dissolve in water, the product diammonium salts do. Often the suspension gradually dissolved after adding diamine to the mucic acid suspension. The reactions are more like typical inorganic acid-base reaction, fast, clean, easy to work up, and of high yield.



**Scheme 6.** Preparation of alkylenediammonium D-galactarate (5a – 5c, 5e – 5h) and D-xylarate (6c).

The preparation of alkylenediammonium D-xylarate (6c) was carried out in methanol solution (Scheme 6) because both reactants, D-xylaric acid and hexamethylenediamine, dissolve in methanol, while the product, hexamethylenediammonium D-xylarate (6c) does



not. The reaction again is very easy to carry out at room temperature and gives a good yield.

All of the above alkylenediammonium D-aldarate salts (**2a – 2g**, **3a – 3g**, **4a – 4g**, **5a – 5c**, **5e – 5h** and **6c**) synthesized have not been reported before. Many of them have gone through polymerization reactions and will be reported here.

#### **IV. Use of alkylenediammonium D-glucarate (2a – 2g) and the corresponding amic acid salts (3a – 3g and 4a – 4g) to prepare poly(alkylene D-glucaramides) (7a – 7g) (prepolymers)**

For the preparation of poly(hexamethylene D-glucaramide), hexamethylenediammonium D-glucarate (**2c**, diammonium salt) was the first candidate proposed to be a starting material (Table 3) for polyamide synthesis. The experimental results suggest that hexamethylenediammonium D-glucarate (**2c**) is a very promising starting material.

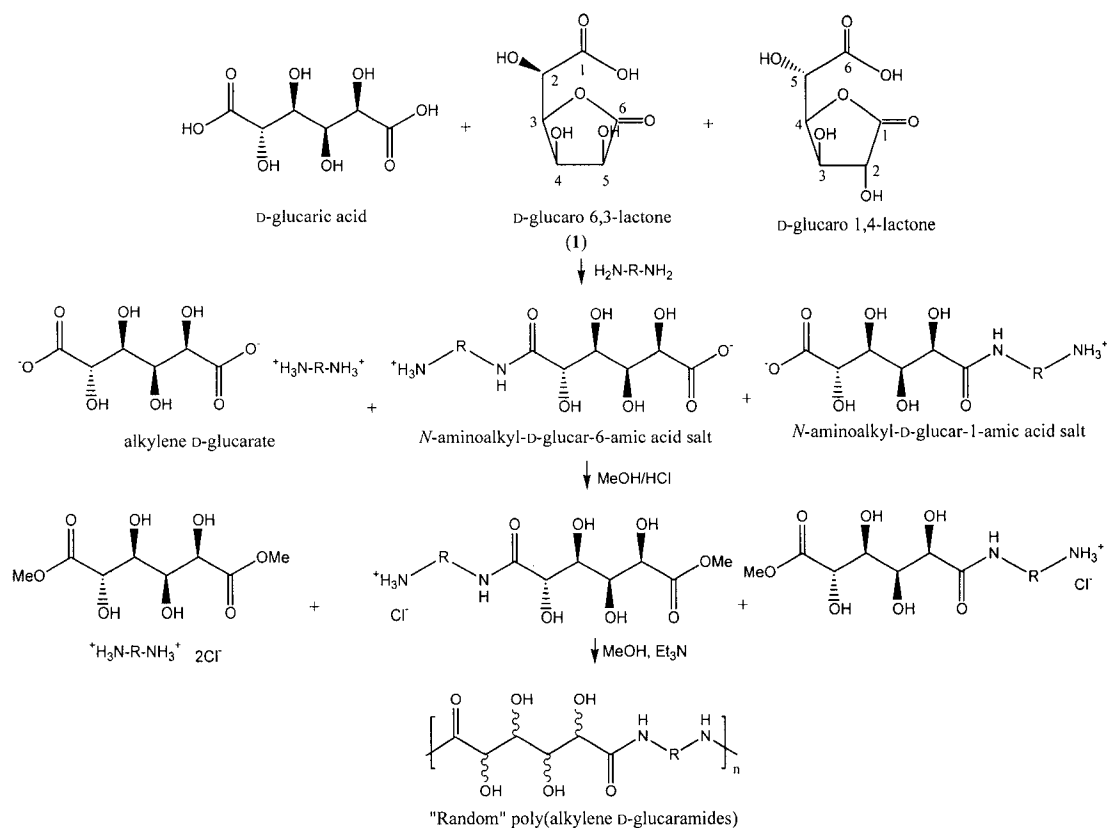
However, because natural D-glucaric acid (**1**) in aqueous solution exists as a mixture of D-glucaric acid 1,4-lactone, D-glucaric acid 6,3-lactone and acyclic D-glucaric acid, the formation of 100% diammonium salt requires very strict reaction conditions. The hexamethylenediammonium D-glucarate (**2c**, 100% diammonium salt) was the first diammonium salt of D-glucaric acid to be prepared successfully. During efforts to prepare other salts of D-glucaric acid, a mixture of diammonium salt (**2a – 2g**) and amic acids (**3a**

– **3g** and **4a – 4g**) were often obtained. Use of mixtures of diammonium salts and amic acid salts for polymerizations to polyamides therefore is an important issue to be considered.

**Table 3.** Preparation of poly(alkylene D-glucaramide) from alkylenediammonium D-glucarate and the corresponding amic acid salts

Monomer	Polymer	d.p.	Yield (%)	Note
Hexamethylenediammonium D-glucarate ( <b>2c</b> )	Poly(hexamethylene D-glucaramide) ( <b>7c</b> )	4.80	77.67	JZ04009
Hexamethylenediammonium D-glucarate ( <b>2c</b> )	Poly(hexamethylene D-glucaramide) ( <b>7c</b> )	7.98	60.35	JZ03091
Hexamethylenediammonium D-glucarate ( <b>2c</b> , 44.30%) and amic acid salts ( <b>3c</b> and <b>4c</b> , 55.70%) mixture	Poly(hexamethylene D-glucaramide) ( <b>7c</b> )	8.58	50.06	JZ02034
Hexamethylenediammonium D-glucarate ( <b>2c</b> , 44.30%) and amic acid salts ( <b>3c</b> and <b>4c</b> , 55.70%) mixture	Poly(hexamethylene D-glucaramide) ( <b>7c</b> )	2.62	27.52	JZ02039
Hexamethylenediammonium D-glucarate ( <b>2c</b> , 68.14%) and amic acid salts ( <b>3c</b> and <b>4c</b> , 30.86%) mixture	Poly(hexamethylene D-glucaramide) ( <b>7c</b> )	6.35	71.63	JZ04018
Tetramethylenediammonium D-glucarate ( <b>2b</b> , 86.84%) and amic acid salts ( <b>3b</b> and <b>4b</b> , 13.16%) mixture	Poly(tetramethylene D-glucaramide) ( <b>7b</b> )	4.75	45.97	JZ04040
3,6-Dioxa-1,8-octanediammonium D-glucarate ( <b>2f</b> , 86.84%) and amic acid salts ( <b>3f</b> and <b>4f</b> , 13.16%) mixture	Poly(3,6-dioxa-1,8-octamethylene D-glucaramide) ( <b>7f</b> )	12.25	26.96	JZ04069_2
<i>m</i> -Xylylenediammonium D-glucarate ( <b>2g</b> ) and amic acid salts ( <b>3g</b> and <b>4g</b> ) mixture	Poly( <i>m</i> -xylylene D-glucaramide) ( <b>7g</b> )	*	92.10	JZ04070

\* Degree of polymerization of **7g** is not available from end-group analysis of <sup>1</sup>H NMR due to frequency overlapping of solvent and end-group proton



**Scheme 7.** Preparation of poly(alkylene D-glucaramide).

Some results on preparation of poly(hexamethylene D-glucaramide) (**7c**) from mixtures of hexamethylenediammonium D-glucarate (**2c**) and amic acid salts (**3c** and **4c**) are recorded in Table 3. Efforts to prepare other poly(alkylene D-glucaramides) (Table 3) suggests that both 100% diammonium salt and diammonium salt / amic acid salt mixture are able to serve as starting materials. Since the 1:1 ratio of acid and amine part exists, the stoichiometric requirement for polymerization is met.

**V. Reaction solvents for preparation of poly(alkylene D-glucaramide) (prepolymer)**

**1. Dimethyl sulfoxide (DMSO) or methanol (MeOH)**

Dimethyl sulfoxide is a good solvent for the monomers mixture of esterified D-glucarate and hexamethylenediammonium dichloride and product polymer poly(hexamethylene D-glucaramide) (**7c**). Methanol is a good solvent for the esterified D-glucarate / hexamethylenediammonium dichloride mixture but not a good solvent for the corresponding polymer. Therefore, the ratio of DMSO:MeOH in the polymerization procedure is of significant importance.

The results from using different ratios of DMSO and MeOH as solvent for the polymerization are summarized in Table 4.

**Table 4.** Different ratios of DMSO to MeOH as solvent used to prepare poly(hexamethylene D-glucaramide) (**7c**)

DMSO:MeOH	MeOH (%)	d.p. of Polymer	Yield (%)	Note
3 : 1	25	2.6	27.52	JZ02039*
1 : 1	50	2.7	19.66	JZ02043_2**
1 : 4	20	3.4	56.78	JZ02043_3**
0 : 1	100	3.8	64.88	JZ02044**

\* JZ02039 was prepared from JZ02029 (44.30% diammonium salt)

\*\* All other prepolymers were prepared with JZ02023 (100% disalt)

DMSO is a good solvent for both reactants and product, which theoretically maximizes the possibility of generating large polymers. However, the drawback is that the polymer is quite soluble in this solvent. Even though the d.p. of the polymers do not vary dramatically in Table 4, the yield is lower for the higher percentages of DMSO as solvent. Although methanol is not a good solvent for the growing polymer, reaction proceeds rapidly in this solvent and higher yields of insoluble polymer are attained. Based upon these results, methanol was selected as the solvent for the polymerization. Obviously, the polymer is not large enough after this first polymerization (pre-polymerization), so a second or “post-polymerization” was applied and will be described later in this chapter.

## **2. Ethylene glycol (EG) or methanol (MeOH)**

Ethylene glycol was also tested as a solvent for polymerization. Since the dielectric constant of ethylene glycol is 41.4 (293.2K) and greater than that of methanol (33.0), ethylene glycol was considered as a potentially better solvent for growing polyamides than methanol. Several trials using ethylene glycol or ethylene glycol / methanol mixture as polymerization solvent were carried out and the results were compared with the reaction taking place in methanol only (Table 5).

**Table 5.** Ethylene glycol and methanol as solvent for pre-polymerization of **7c**

disalt ( <b>2c</b> )	EG:MeOH	temperature (°C)	d.p.	yield (%)	polymer ( <b>7c</b> )
JZ03005	1:0	r.t	4.36	15.05	JZ03020_2
JZ03005	1:0	50	3.48	34.98	JZ03020_3
JZ03005	1:1	r.t	6.47	56.44	JZ03020_6
JZ03005	0:1	r.t	4.90	71.05	JZ03020_4
JZ03005	0:1	50	4.17	69.09	JZ03020_5
JZ02023	2:1	r.t	6.28	22.79	JZ03023_2
JZ02023	1:1	r.t	7.14	55.99	JZ03023_3
JZ02023	1:1	44	5.50	45.37	JZ03023_4
JZ02023	1:2	r.t	7.33	78.11	JZ03023_5
JZ03012_1	1:1	r.t	4.29	41.29	JZ03039_2
JZ03044	1:1	r.t	4.74	43.27	JZ03045_2
JZ03066_7	1:1	r.t.	8.10	50.29	JZ03095_1
JZ03066_7	0:1	r.t	8.63	64.53	JZ03095_2
JZ03066_7	0:1	r.t.	7.98	60.35	JZ03091

The first group studied (JZ03005) employed hexamethylenediammonium D-glucarate (**2c**) as monomer. The monomer was first esterified in a methanolic/HCl solution, dried and then redissolved in ethylene glycol and/or methanol for polymerization. The results suggest that when ethylene glycol and methanol are used in a 1:1 (v : v) ratio, the isolated yield is significantly reduced. The less ethylene glycol used in the reaction, the higher the

isolated yield. Furthermore, increasing the temperature of the reaction, as shown in the first trial, does not appear to improve the degree of polymerization.

The second trial was carried out with JZ02023 (hexamethylenediammonium D-glucarate, **2c**) as starting material. Again, the results suggest that use of a higher ratio of methanol as solvent gives higher yield of polymer. The results with JZ03066 disalt (hexamethylenediammonium D-glucarate, **2c**) also suggest that methanol itself can be used to give high d.p. and yield of polyhydroxypolyamide.

All of the above efforts suggest that both ethylene glycol and methanol are good solvents for the polymerization. However although the polymer is less soluble in methanol, in general methanol as solvent gives a higher yield and d.p. of polyamides.

#### **VI. Effect of triethylamine on polymerization (prepolymer)**

The first step of the polymerization procedure is activation of the diammonium salt with or without the amic acid salt by esterification in a methanolic / HCl solution. The ester / alkylenediammonium dichloride is dried before being redissolved in fresh methanol for the polymerization. Neutralization of the alkylenediammonium dichloride is then necessary, and a choice of bases is available. The best candidate is one that has appropriate basicity and is easy to work-up with. Some bases were tested including NABCO (1,4-diazabicyclo[2.2.2]octane) and DBN (1,5-diazabicyclo[4.3.0]non-5-ene) but none performed better than triethylamine.<sup>[18]</sup>

To determine the appropriate amount of triethylamine, several polymerizations were compared (Table 6). With 0.1250 g of hexamethylenediammonium D-glucarate (**2c**) as starting material and methanol as solvent (2 mL), following esterification, different amounts of triethylamine (TEA) were added to neutralize the acid and to keep the reaction solution basic. Table 6 summarizes some of these results.

**Table 6.** Effect of triethylamine on polymerization (prepolymer) of poly(hexamethylene D-glucaramide) (**7c**)

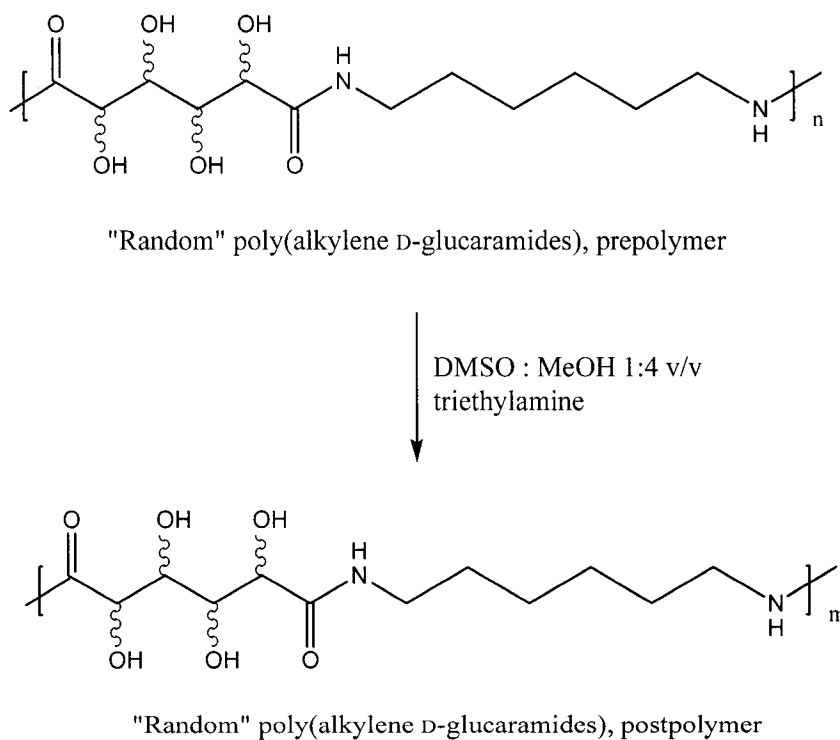
trial	disalt ( <b>2c</b> )	TEA (mL)	d.p.	yield (%)	polymer ( <b>7c</b> )
1	JZ03005	0.1	2.25	19.53	JZ03014_2
2	JZ02015	0.15	4.51	46.01	JZ03009_2
3	JZ03017_2	0.2	5.17	63.04	JZ03047_4
4	JZ03049	0.2	6.21	63.23	JZ03050_2
5	JZ03049	0.4	7.44	74.35	JZ03050_3
6	JZ03049	0.6	6.76	73.91	JZ03050_4
7	JZ03049	0.8	6.64	68.22	JZ03050_5
8	JZ03017_2	1.2	5.20	60.28	JZ03047_5

To determine the appropriate amount of triethylamine to be used in polymerization, two criteria were considered; the size of polymer obtained (i.e. degree of polymerization) and the polymer yield. From the top of the table to the bottom, both the d.p. and yield increase to a certain point (Trial 5). The amount of triethylamine used in the polymerization (prepolymer) was according to Trial 5.



## VII. Optimized reaction condition for polymerization (post-polymer)

Since pre-polymerization takes place in methanol solution, polymers precipitate out before growing big. Another polymerization, post-polymerization (Scheme 8), was required in order to get higher molecular weight polymer. Dimethyl sulfoxide has proved to be a very important solvent for polymerization since polymer has higher solubility in DMSO. However, methanol as a solvent is important in precipitation of the polymer. The ratio of DMSO and methanol is thus one of the critical reaction conditions to be considered.



**Scheme 8.** Post-polymerization for random poly(alkylene D-glucaramide).

Table 7 summarizes several trials of post-polymerization with different DMSO : MeOH ratios. It is clear from these trials that both d.p. and isolated yield of polymer are dependent up the DMSO:MeOH ratio. In general, as this ratio was changed from 3:1 to 1:4, both polymer d.p. and isolated yield increased. In addition, both d.p. and yield improved with heating and when the reaction was carried out in the presence of triethylamine.

**Table 7.** Reaction conditions and the corresponding polymers (**7c**) after postpolymerization

	Prepolymer	d.p. (pre)	DMSO: MeOH	Et <sub>3</sub> N (mL)	Temp	d.p. (post)	Yield	Post /pre	Postpolymer
1	JZ02043_2	2.74	3:1	N/A	r.t.	3.54	64.34	1.30	JZ02045_1
2	JZ02043_3	3.39	3:1	N/A	r.t.	4.36	69.53	1.29	JZ02045_2
3	JZ02044	3.81	3:1	N/A	r.t.	5.06	64.48	1.33	JZ02045_3
4	JZ04009	4.80	2:1	N/A	Reflux	8.27	26.84	1.72	JZ04011_3
5	JZ03091	7.98	2:1	N/A	r.t.	12.78	60.20	1.60	JZ03094
6	JZ02043_3	3.39	3:2	N/A	r.t.	4.54	74.40	1.34	JZ02047_1
7	JZ02044	3.81	3:2	N/A	r.t.	4.96	72.46	1.30	JZ02047_2
8	JZ04009	4.80	2:3	0.100	Reflux	10.95	96.87	2.28	JZ04017
9	JZ04009	4.80	1:4	0.100	Reflux	8.40	96.57	1.75	JZ04020
10	JZ04009	4.80	1:4	N/A	Reflux	9.30	67.42	1.94	JZ04016_1
11	JZ04009	4.80	1:4	0.100	Reflux	14.98	90.55	3.12	JZ04016_2
12	JZ04009	4.80	1:4	0.100	Reflux	12.66	105.26	2.64	JZ04019
13	JZ04009	4.80	0:1	N/A	Reflux	7.80	89.18	1.63	JZ04011_1
14	JZ04009	4.80	0:1	0.100	Reflux	10.35	89.89	2.16	JZ04011_2

## Conclusions

The synthetic work described here demonstrated the synthesis of novel alkylenediammonium D-aldarate salts. These salts can undergo a two step polycondensation sequence to afford poly(alkylene D-aldaramides). A postpolymerization step greatly improves d.p. of the product polymers. This improved new method to prepare polyhydroxypolyamides is a valuable contribution to the exciting blend of carbohydrate and polymer chemistry.

## Experimental Section

**General Methods.** All  $^1\text{H}$  and  $^{13}\text{C}$  NMR spectra were recorded on Varian Unity 400 MHz and 100 MHz, respectively. Samples for  $^1\text{H}$  NMR (ca. 5 mg) were dissolved in 0.7 mL DMSO- $d_6$ ,  $\text{D}_2\text{O}$  or TFA- $d_1$ . Chemical shifts are reported as ppm ( $\delta$ ) downfield. IR spectra were recorded with a Nicolet FTIR spectrometer as KBr pellets. Melting points were measured with a Fisher-Johns Melting Point Apparatus and reported uncorrected. Solvent evaporations were carried out at reduced pressure. All solvents used were reagent grade unless stated otherwise. Methanol/diamine solutions were standardized by diluting an aliquot of the solution with water and titrated with standardized hydrochloric acid. A pH meter was employed to determine the titration end points.

**D-Glucaric Acid Aqueous Solution (1).** Monopotassium D-glucarate (30.0 g, 120.87 mmol) was spooned into a 2 L Erlenmeyer flask containing deionized water (300.0 mL) and mixed well. Dowex 50WX8 ion-exchange resin ( $\text{H}^+$ , 72.0 mL, 2.1 meq/mL) was

washed with deionized water until the aqueous wash was colorless. The resin was added to the Erlenmeyer flask, and the mixture was stirred for 4 h. The resin was removed by filtration, washed with deionized water and stored for regeneration. The filtrate was concentrated to a syrup using a freeze dryer (20.8 g, 108.28 mmol, 89.55%, calculated as 100% D-glucaric acid) and without further purification, redissolved into deionized water to give D-glucaric acid aqueous solution (**1**, 1 M, 108.28 mL) for the preparation of alkylenediammonium D-glucarate salt (**2a** – **2g** and **3a** – **3g**). (JZ03065)

**Ethylenediammonium D-Glucarate (2a), N-(2-Aminoethyl)-D-Glucar-6-amic Acid Salt (3a) and N-(2-Aminoethyl)-D-Glucar-1-amic Acid Salt (4a) Mixture.** D-Glucaric acid aqueous solution (**1**, ~1 M, 4.62 mL) and ethylenediamine aqueous solution (1 M, 6.01 mL) were mixed in a round bottom flask, stirred at room temperature for 10 h and concentrated to less than 25% of the total volume. Methanol (~10 mL) was added dropwise and the reaction mixture was stirred for 8 h. The top methanol liquid layer was decanted and the light amber syrup was dried under vacuum at room temperature for 24 h to give a mixture of ethylenediammonium D-glucarate (**2a**) and N-(2-aminoethyl)-D-glucar-6-amic acid salt (**3a**) and N-(2-aminoethyl)-D-glucar-1-amic acid salt (**4a**) ( 1.13 g, 4.55 mmol, 98.41%). (JZ04032)

**Tetramethylenediammonium D-Glucarate (2b).** D-Glucaric acid aqueous solution (**1**, ~1 M, 5.96 mL) and tetramethylenediamine (putrescine) aqueous solution (1 M, 8.42 mL) were mixed in a round bottom flask, and stirred at room temperature for 10 min. The

reaction mixture was then stirred at 60 °C for 15 h and concentrated to less than 25% of the total volume. Methanol (~5 mL) was added drop-wise to the concentrated solution to precipitate out a large quantity of white solid. The white solid was removed by filtration, washed with methanol (2×5 mL), and then dried under vacuum at room temperature for 24 h to give tetramethylenediammonium D-glucarate salt (**2b**, 1.13 g, 3.81 mmol, 63.91%): Anal. Calcd for C<sub>10</sub>H<sub>22</sub>N<sub>2</sub>O<sub>8</sub> (298.29): C, 40.27; H, 7.43; N, 9.39. Found: C, 40.33; H, 7.35; N, 9.38. (JZ04036)

**Tetramethylenediammonium D-Glucarate (2b), N-(4-Aminobutanyl)-D-Glucar-6-amic Acid Salt (3b) and N-(4-Aminobutanyl)-D-Glucar-1-amic Acid Salt (4b)**

**Mixture.** D-Glucaric acid aqueous solution (**1**, ~1 M, 4.95 mL) and tetramethylenediamine (putrescine) aqueous solution (1 M, 5.15 mL) were mixed in a round bottom flask, and stirred at room temperature for 10 min. The reaction mixture was then stirred at 60 °C for 15 h and concentrated to less than 25% of the total volume. Methanol (~5 mL) was added drop-wise to the concentrated solution to precipitate out a large quantity of white syrupy solid. The top methanol phase was removed and the white solid was washed with methanol (2×5 mL), and then dried under vacuum at room temperature for 24 h to give a mixture of tetramethylenediammonium D-glucarate salt (**2b**), N-(4-aminobutanyl)-D-glucar-6-amic acid salt (**3b**) and ), N-(4-aminobutanyl)-D-glucar-1-amic acid salt (**4b**) (0.69 g, 2.21 mmol, 46.74%). (JZ02019)

**Hexamethylenediammonium D-Glucarate (2c).** D-Glucaric acid aqueous solution (**1**, ~1 M, 5.0 mL) and hexamethylenediamine aqueous solution (1 M, 5.25 mL) were mixed in a round bottom flask, and stirred at room temperature for 10 min. The reaction mixture was then stirred at 78 °C for 16 h and concentrated to less than 25% of the total volume. Methanol (6~8 mL) was added drop-wise to the concentrated solution to precipitate out a large quantity of white solid. The white solid was removed by filtration, washed with methanol (2×5 mL), and then dried under vacuum at room temperature for 24 h to give hexamethylenediammonium D-glucarate salt (**2c**, 1.04 g, 3.19 mmol, 63.71%): Anal. Calcd for C<sub>12</sub>H<sub>26</sub>N<sub>2</sub>O<sub>8</sub> (326.34): C, 44.16; H, 8.03; N, 8.58. Found: C, 44.11; H, 8.10; N, 8.59. (JZ03089)

**Octamethylenediammonium D-Glucarate (2d) / N-(8-Aminooctyl)-D-Glucar-6-amic Acid Salt (3d) Mixture and N-(8-Aminooctyl)-D-Glucar-1-amic Acid Salt (4d)**

**Mixture.** D-Glucaric acid aqueous solution (**1**, ~1 M, 4.51 mL) and octamethylenediamine aqueous solution (1 M, 5.94 mL) were mixed in a round bottom flask, and stirred at room temperature for 10 min. The reaction mixture was then stirred at 60 °C for 26 h and concentrated to less than 25% of the total volume. Methanol (6~8 mL) was added drop-wise to the concentrated solution and the reaction mixture was stirred for 12 h. The top methanol phase was removed and the light amber syrup was washed with methanol (2×5 mL), and then dried under vacuum at room temperature for 24 h to give octamethylenediammonium D-glucarate (**2d**) / N-(8-aminooctyl)-D-glucar-6-amic acid

salt (**3d**) / *N*-(8-aminooctyl)-D-glucar-1-amic acid salt (**4d**) mixture (1.54 g, 4.35 mmol, 96.43%). (JZ04074)

**3,6-Dioxa-1,8-Octanediammonium D-Glucarate (2f) / N-(8-Amino-3,6-Dioxa-Octyl)-D-Glucar-6-amic Acid Salt / N-(8-Amino-3,6-Dioxa-Octyl)-D-Glucar-1-amic Acid Salt (4f) Mixture.** D-Glucaric acid aqueous solution (**1**, 0.9719 M, 6.5 mL) and Jeffamine EDR-148 (3,6-dioxa-1,8-octanediamine) aqueous solution (0.9826 g, 6.6392 mmol, 6 mL, 1.1065 M) were mixed in a round bottom flask, and the reaction mixture was stirred at room temperature for 10 min. The reaction mixture was then stirred at 80 °C for 17.5 h and concentrated to less than 25% of the total volume. Methanol (~ 15 mL) was added dropwise to the concentrated solution to try to precipitate out the product. The reaction mixture was placed in ice-bath for 2 h, the top liquid was removed and the product was dried under vacuum at room temperature for 23 h to give a mixture of 3,6-dioxa-1,8-octanediammonium D-glucarate (**2f**), *N*-(8-amino-3,6-dioxa-octyl)-D-glucar-6-amic acid salt (**3f**) and *N*-(8-amino-3,6-dioxa-octyl)-D-glucar-1-amic acid salt (**4f**) (1.18 g, diammonium salt 79.20% & amic acid salts 20.79%, ca M.W. 354.22, 3.33 mmol, 52.65%). (JZ03096)

***m*-Xylylenediammonium D-Glucarate Salt (2g) / N-(*m*-Amino-Xylylene)-D-Glucar-6-amic Acid Salt (3g) / N-(*m*-Amino-Xylylene)-D-Glucar-1-amic Acid Salt (4g) Mixture.** D-Glucaric acid aqueous solution (**1**, ~1 M, 5.60 mL) and *m*-xylylenediamine aqueous solution (1 M, 7.27 mL) were mixed in a round bottom flask, and the reaction mixture

was stirred at room temperature for 10 h. The reaction mixture was concentrated to less than 25% of the total volume. Methanol (6~8 mL) was added drop-wise to the concentrated solution to precipitate out a large quantity of a light amber solid. The solid was removed by filtration, washed with methanol (2×5 mL), and then dried under vacuum at room temperature for 18 h to give a mixture of *m*-xylylenediammonium D-glucarate salt (**2g**), *N*-(*m*-amino-xylylene)-D-glucar-6-amic acid salt (**3g**) and *N*-(*m*-amino-xylylene)-D-glucar-1-amic acid salt (**4g**) (0.99 g, 2.86 mmol, 51.05%). (JZ04029)

**Ethylenediammonium Galactarate (5a).** Galactaric acid (mucic acid purified from commercial product, 1.0363 g, 4.9315 mmol) was mixed well with deionized water (5.0 mL). Ethylenediamine aqueous solution (0.31 g, 5.18 mmol, 1.0363 M, 5 mL) was added to galactaric acid aqueous suspension and the reaction mixture was stirred for 1 h. The reaction mixture was stirred at 60 °C for 1 h and stirred at room temperature for 25 h. The amount of white solid decreased and then increased during the stirring period. The white solid was removed by centrifugation, washed with deionized water (2 × 10 mL), and then dried under vacuum at room temperature for 14.5 h to give white solid, ethylenediammonium galactarate (**5a**, 1.25 g, 4.64 mmol, 93.87%): Anal Calcd for C<sub>8</sub>H<sub>18</sub>N<sub>2</sub>O<sub>8</sub> (270.24): C, 35.56; H, 6.71; N, 10.37. Found: C, 33.34; H, 7.07; N, 9.59 (JZ04028\_2)

**Tetramethylenediammonium Galactarate (5b).** Galactaric acid (mucic acid, 1.1755 g, 5.5939 mmol) was mixed well with deionized water (6.0 mL). Tetramethylenediamine



(putrescine) aqueous solution (0.7150 g, 8.1112 mmol, 1.3519 M, 6.0 mL) was added to the galactaric acid aqueous suspension and the reaction mixture was stirred for 10 min until all of the galactaric acid dissolved. The reaction mixture was stirred at 60 °C for 10 min and stirred at room temperature for 5.5 h. A white precipitate appeared within 30 min. The white solid was removed by filtration, washed with 2 × 10 mL deionized water, and then dried under vacuum at room temperature for 18 h to give white solid, tetramethylenediammonium galactarate (**5b**, 0.4587 g, 1.5393 mmol, 27.52%): Anal Calcd for C<sub>10</sub>H<sub>22</sub>N<sub>2</sub>O<sub>8</sub> (298.29): C, 40.27; H, 7.43; N, 9.39. Found: C, 40.32; H, 7.52; N, 9.29. (JZ03093)

**Hexamethylenediammonium Galactarate (5c).** Galactaric acid (mucic acid after trituration, 5.0909 g, 24.23 mmol) was mixed well with deionized water (24.0 mL). Hexamethylenediamine aqueous solution (26.0 mL, 25.61 mmol, 0.985 M) was added to the galactaric acid aqueous suspension and the reaction mixture was stirred for 30 min until all of the galactaric acid dissolved. The reaction mixture was stirred at 70 °C for 10 min and stirred at room temperature for 18 h. A white precipitate appeared within 30 min. The white solid was removed by filtration, washed with 2 × 10 mL MeOH, and then dried under vacuum at room temperature for 24 h to give white solid, hexamethylenediammonium galactarate (**5c**, 1.6080 g, 4.9325 mmol, 20.36%, JZ03071\_1). The filtrate was placed in a refrigerator for 6 days to give a large amount of white precipitate. The white solid was removed by filtration, washed with 2 × 10 mL MeOH, and then dried under vacuum at room temperature for 24 h to give a second crop

of hexamethylenediammonium galactarate (**5c**, 2.0112 g, 6.1963 mmol, 25.46%, JZ03071\_2): Anal Calcd for  $C_{12}H_{26}N_2O_8$  (326.34): C, 44.16; H, 8.03; N, 8.58. Found: C, 43.94; H, 8.19; N, 8.54.

**Dodecamethylenediammonium Galactarate (5e).** Galactaric acid (0.5875 g, 2.7958 mmol) was dissolved in hot DMSO (5 mL, 60 °C). A hot 1,2-Diaminododecane methanol solution (1.1121 g, 5.5502 mmol, 6.0 mL, 0.9250 M, 60 °C) was added to the galactaric acid DMSO solution and the reaction mixture was stirred for 30 min until a large quantity of solid precipitated out. More DMSO (4 mL) and methanol (15 mL) were added to the reaction mixture to dissolve the unreacted reactant. The reaction mixture was stirred at room temperature for 22 h. The white solid was removed by filtration, washed with 2 × 10 mL MeOH, and then dried under vacuum at room temperature for 24 h to give dodecamethylenediammonium galactarate (**5e**, 1.2827 g, 3.1285 mmol, 111.90%): Anal Calcd for  $C_{18}H_{38}N_2O_8$  (410.50): C, 52.67; H, 9.33; N, 6.82. Found: C, 53.21; H, 9.50; N, 7.01. (JZ04035)

**3,6-Dioxa-1,8-Octanediammonium Galactarate (5f).** Galactaric acid (0.9485 g, 4.5137 mmol) was mixed well with deionized water (4.50 mL). After the addition of Jeffamine EDR-148 (3,6-dioxa-1,8-octanediamine) aqueous solution (0.8674 g, 5.8608 mmol, 0.9768 M, 6.0 mL), the galactaric acid dissolved immediately. The reaction mixture was stirred at room temperature for 16 h, concentrated under reduced pressure, and then dried under vacuum at room temperature for 24 h to give white solid, crude 3,6-dioxa-1,8-

octanediammonium galactarate (1.6634 g, 4.6464 mmol, 102.94%). The crude salt was then recrystallized from deionized water by dissolving into hot water (3.0 mL). The product crystallized when water cooled to room temperature, filtered, washed with cold water (4 °C), and dried under vacuum at room temperature for 18 h to give pure 3,6-dioxa-1,8-octanediammonium galactarate salt (**5f**, 0.9594 g, 2.6800 mmol, 57.68%): Anal Calcd for C<sub>12</sub>H<sub>26</sub>N<sub>2</sub>O<sub>10</sub> (358.34): C, 40.22; H, 7.31; N, 7.82. Found: C, 40.29; H, 7.44; N, 8.03. (JZ03089)

***m*-Xylylenediammonium Galactarate (5g).** Galactaric acid (1.0351 g, 4.9258 mmol) was mixed well with deionized water (5.0 mL). After the addition of *m*-xylylene diamine aqueous solution (0.850 mL, 6.4405 mmol, 1.0734 M, 6.0 mL), the galactaric acid dissolved within 2 min. The reaction mixture was stirred at room temperature for 11 h with a large quantity of precipitate appearing after 5 min. The reaction mixture was filtered, washed with cold methanol, and then dried under vacuum at room temperature for 12 h to give white solid, *m*-xylylenediammonium galactarate (**5g**, 1.3755 g, 3.9754 mmol). The filtrate was filtered again, washed with cold methanol, and then dried under vacuum at room temperature for 12 h to give a second crop of *m*-xylylenediammonium galactarate (**5g**, 0.2263 g, 0.6540 mmol). The overall yield of both crops is 93.98%: Anal Calcd for C<sub>14</sub>H<sub>22</sub>N<sub>2</sub>O<sub>8</sub> (346.33): C, 48.55; H, 6.40; N, 8.09. Found: C, 44.38; H, 6.94; N, 7.31. (JZ04030)

**3,3'-Diamino-*N*-Methyl Dipropylammonium Galactarate (5h).** Galactaric acid (mucic acid purified from commercial product, 1.3593 g, 6.4685 mmol) was mixed well with deionized water (6.0 mL). 3,3'-Diamino-*N*-methyl dipropylamine aqueous solution (solute: 1.360 mL, 1.2254 g, 8.4362 mmol, solution 6.0 mL, 1.4063 M) was added to the galactaric acid aqueous suspension and the reaction mixture was stirred for 25 min. The reaction mixture was stirred at 60 °C for 15 min and stirred at room temperature for 24 h. The solvent was removed with a rotary evaporator until dry syrup was left in the flask. Methanol (4 mL) was added into the syrup drop-wise and the mixture was stirred for 4 h. Extra methanol (3 mL) was added into the flask. The white gummy solid was broken with a glass rod and the methanol-solid mixture was stirred for another 5 h until a fine, nice, white solid was appeared. The white solid was removed by filtration, washed with 2 × 10 mL methanol, and then dried under vacuum at room temperature for 16.5 h to give white solid, 3,3'-diamino-*N*-methyl dipropylammonium galactarate (**5h**, 2.0806 g, 5.8608 mmol, 90.61%): Anal Calcd for C<sub>13</sub>H<sub>29</sub>N<sub>3</sub>O<sub>8</sub> (355.38): C, 43.94; H, 8.22; N, 11.82. Found: C, 41.92; H, 8.02; N, 10.65. (JZ04031)

**Hexamethylenediammonium Xylarate (6c).** Hexamethylenediamine methanol solution (5.35 mL, 6.1172 mmol, 1.143 M) was added to xylaric acid methanol solution (0.9831 g, 5.4617 mmol, 6.5 mL, 0.8403 M). A white precipitate appeared within 5 min. The reaction mixture was stirred at room temperature for another 20.5 h. The white solid was removed by filtration, washed with 2 × 10 mL MeOH, and then dried under vacuum at room temperature for 23.5 h to give hexamethylenediammonium xylarate (**6c**, 1.4410 g,

4.8683 mmol, 89.14%): Anal Calcd for C<sub>11</sub>H<sub>24</sub>N<sub>2</sub>O<sub>7</sub> (296.32): C, 44.59; H, 8.16; N, 9.45. Found: C, 43.69; H, 8.16; N, 9.24. (JZ03076\_2 & JZ03076\_3).

**Random Poly(tetramethylene D-glucaramide) (7b) Prepolymer.** Acetyl chloride (0.750 mL, 10.548 mmol) was added drop-wise to cold methanol (5.0 mL) while stirring in an ice bath for 10 min to make methanolic/HCl solution. Tetramethylenediammonium D-glucarate (**2b**, 0.4364 g, 1.4921 mmol) was added to the MeOH/HCl solution. The reaction mixture was stirred at room temperature for 20 min and then sonicated for 20 min. The reaction mixture was concentrated under reduced pressure and then dried under vacuum at room temperature for 4 h to give esterified D-glucarate / tetramethylenediammonium dichloride (i.e., ester/salt). The ester/salt was dissolved in fresh methanol (10 mL) and the solution (pH 1~2, pH paper) was made basic by drop-wise addition of triethylamine (0.800 mL) (pH 8~9). Additional triethylamine (0.400 mL) was added after 10 min to keep the basicity of the reaction mixture at about pH 9. A precipitate appeared within 30 min after the second addition of triethylamine. The reaction mixture was stirred at room temperature for 19.5 h to allow further precipitation. The white solid was removed by centrifugation, washed with methanol (2×5 mL) and dried under vacuum at room temperature for 20 h to give *random* poly(tetramethylene D-glucaramide) (**7b**) prepolymer (0.1797 g, 0.6859 mmol, 45.97%, dp 4.75, estimated Mn 1,300) (JZ04040)

**Random Poly(hexamethylene D-glucaramide) (7c) Prepolymer.** Acetyl chloride (0.750 mL, 10.548 mmol) was added drop-wise to cold methanol (5.0 mL) while stirring in an ice bath for 10 min to make methanolic/HCl solution. Hexamethylenediammonium D-glucarate (**2c**, 0.5000 g, 1.5337 mmol) was added to the MeOH/HCl solution. The reaction mixture was stirred at room temperature for 10 min and then sonicated for 10 min. The reaction mixture was concentrated under reduced pressure and then dried under vacuum at room temperature for 4 h to give esterified D-glucarate / hexamethylenediammonium dichloride (i.e., ester/salt). The ester/salt was dissolved in fresh methanol (10 mL) and the solution (pH 1~2, pH paper) was made basic by drop-wise addition of triethylamine (0.800 mL) (pH 8~9). Additional triethylamine (0.800 mL) was added after 10 min to keep the basicity of the reaction mixture at about pH 9. A precipitate appeared within 30 min after the second addition of triethylamine. The reaction mixture was stirred at room temperature for 6 h to allow further precipitation. The white solid was removed by centrifugation, washed with methanol (2×10 mL), then acetone (2×10 mL), and dried under vacuum at room temperature for 10 h to give *random* poly(hexamethylene D-glucaramide) (**7c**) prepolymer (0.2997 g, 1.0323 mmol, 67.31%, dp 6.42, estimated Mn 1,900): Anal Calcd for (C<sub>12</sub>H<sub>22</sub>N<sub>2</sub>O<sub>6</sub>)<sub>n</sub> (290.31)<sub>n</sub>: C, 49.65; H, 7.64; N, 9.65. Found: C, 47.82; H, 7.63; N, 9.09. (JZ04023)

**Random Poly(hexamethylene D-glucaramide) (7c) Postpolymer.** Methanol (3.0 mL) was added at room temperature to *random* poly(hexamethylene D-glucaramide) (**7c**) prepolymer (100.0 mg, dp 5.72) dissolved in dimethyl sulfoxide (0.750 mL). A white

precipitate appeared within 5 min. The reaction mixture was refluxed for 12 h after drop-wise addition of triethylamine (0.100 mL) to ensure basicity. The white solid was separated from solution by centrifugation and washed with DMSO/methanol (DMSO:methanol 1:4) solution (2×3 mL). The white solid was dried under vacuum for 12 h to give *random* poly(hexamethylene D-glucaramide) postpolymer (**7c**, 90.55 mg, 90.55%, dp 14.62, estimated Mn 4500): Anal Calcd for  $(C_{12}H_{22}N_2O_6)_n$  (290.31)<sub>n</sub>: C, 49.65; H, 7.64; N, 9.65. Found: C, 47.52; H, 7.62; N, 9.10. (JZ04016\_2)

**Random Poly(3,6-dioxa-1,8-octamethylene D-glucaramide) (7f) Prepolymer.** Acetyl chloride (1.500 mL, 21.10 mmol) was added drop-wise to cold methanol (13.0 mL) while stirring in an ice bath for 10 min to make methanolic/HCl solution. The MeOH/HCl solution was added to 3,6-dioxa-1,8-octanediammonium D-glucarate (**2f**) / *N*-(8-amino-3,6-dioxa-octyl)-D-glucar-6-amic acid salt (**3f**) / *N*-(8-amino-3,6-dioxa-octyl)-D-glucar-1-amic acid salt (**4f**) mixture (1.1781 g, 3.3259 mmol) syrup. The reaction mixture was stirred at room temperature for 1.5 h and then sonicated for 15 min. The reaction mixture was concentrated with evaporation under reduced pressure and then dried under vacuum at room temperature for 7 h to give esterified D-glucarate / hexamethylenediammonium dichloride / methyl *N*-(8-ammonium-3,6-dioxa-octyl)-D-glucar-6-amic acid chloride / methyl *N*-(8-ammonium-3,6-dioxa-octyl)-D-glucar-1-amic acid chloride (i.e., ester/salt). The ester/salt was dissolved in fresh methanol (19 mL) and the solution (pH 2~3, pH paper) was made basic by drop-wise addition of triethylamine (1.000 mL) (pH 8~9).

Additional triethylamine (1.000 mL) was added after 10 min to keep the basicity of the reaction mixture at about pH 9. The reaction mixture was then divided into two portions.

- (A) The first portion was stirred at room temperature for 13 h. A precipitate appeared within 30 min after the second addition of triethylamine. The white solid was removed by centrifugation, washed with methanol (2×5 mL) and dried under vacuum at room temperature for 10 h to give *random* poly(3,6-dioxo-1,8-octamethylene D-glucaramide) (**7f**) prepolymer (0.1395 g, 0.4332 mmol, 24.87%, dp 9.5, estimated Mn 3,100 (JZ04069\_1)).
- (B) The second portion was stirred at 60 °C for 13 h. A precipitate appeared within 30 min after the second addition of triethylamine. The white solid was removed by centrifugation, washed with methanol (2×5 mL) and dried under vacuum at room temperature for 10 h to give *random* poly(3,6-dioxo-1,8-octamethylene D-glucaramide) (**7f**) prepolymer (0.1375 g, 0.4270 mmol, 26.96%, dp 12.25, estimated Mn 4,000) (JZ04069\_2).

***Random Poly(m-xylylene D-glucaramide) (7g) Prepolymer.***

Acetyl chloride (0.750 mL, 10.55 mmol) was added drop-wise to cold methanol (5.0 mL) while stirring in an ice bath for 10 min to make methanolic/HCl solution. *m*-Xylylenediammonium D-glucarate salt (**2g**) / *N*-(1,3-diaminoxylylene)-D-glucar-6-amic acid salt (**3g**) / *N*-(1,3-diaminoxylylene)-D-glucar-1-amic acid salt (**4g**) mixture (0.4855 g, 1.4032 mmol) was added to the MeOH/HCl solution. The reaction mixture was stirred at room temperature for 10 min and then sonicated for 15 min. The reaction mixture was



concentrated under reduced pressure and then dried under vacuum at room temperature for 4 h to give esterified D-glucarate / m-xylylenediammonium dichloride / methyl *N*-(1,3-diammoniumxylylene)-D-glucar-6-amic acid ester chloride / methyl *N*-(1,3-diammoniumxylylene)-D-glucar-1-amic acid ester chloride (i.e., ester/salt). The ester/salt was dissolved in fresh methanol (10 mL) and the solution (pH 1~2, pH paper) was made basic by dropwise addition of triethylamine (0.800 mL) (pH 8~9). Additional triethylamine (0.400 mL) was added after 10 min to keep the basicity of the reaction mixture at about pH 9. The reaction mixture was then divided into two portions.

(A) One portion of the reaction mixture was stirred at room temperature for 46 h. A precipitate appeared within 30 min after the second addition of triethylamine. The white solid was removed by centrifugation, washed with methanol (2×5 mL) and dried under vacuum at room temperature for 16.5 h to give *random* poly(*m*-xylylene D-glucaramide) (**7g**) prepolymer (0.1934 g, 0.6239 mmol, 92.10%).  
(JZ04070\_1)

(B) The other portion of the reaction mixture was stirred at 60 °C for 46 h. A precipitate appeared within 30 min after the second addition of triethylamine. The white solid was removed by centrifugation, washed with methanol (2×5 mL) and dried under vacuum at room temperature for 16.5 h to give *random* poly(*m*-xylylene D-glucaramide) (**7g**) prepolymer (0.0747 g, 0.2410 mmol, 33.20%).  
(JZ04070\_2)

**Poly(hexamethylene galactaramide) (8c) Prepolymer.** Acetyl chloride (0.750 mL, 10.5 mmol) was added drop-wise to cold methanol (5.0 mL) while stirring in an ice bath for 10 min to make methanolic/HCl solution. hexamethylenediammonium galactarate (**5c**, 0.4894 g, 1.5012 mmol) was added into the MeOH/HCl solution. The reaction mixture was stirred at room temperature for 1 h 20 min, sonicated for 25 min, stirred at 40 °C for 30 min and 50 °C for 1 h 10 min. The white solid did not dissolve in the MeOH/HCl solution. The reaction mixture was concentrated under reduced pressure and then dried under vacuum at room temperature for 17.5 h to give esterified galactarate / hexamethylenediammonium dichloride (i.e., ester/salt). The ester/salt was dissolved in fresh methanol (10 mL) and the solution (pH ~1, pH paper) was made basic by drop-wise addition of triethylamine (0.800 mL) (pH 8~9). Additional triethylamine (0.800 mL) was added after 10 min to keep the basicity of the reaction mixture at about pH 9. The reaction mixture was refluxed for 25.5 h. The white solid was removed by centrifugation, washed with methanol (2×7.5 mL) and dried under vacuum at room temperature for 9.5 h to give poly(hexamethylene galactaramide) (**8c**) prepolymer (0.4191 g, 1.4436 mmol, 96.17%, dp 3.40, estimated Mn 1,000) (JZ04055)

**Poly(dodecamethylene galactaramide) (8e) prepolymer.** Acetyl chloride (0.750 mL, 10.5 mmol) was added drop-wise to cold methanol (5.0 mL) while stirring in an ice bath for 10 min to make methanolic/HCl solution. Dodecamethylenediammonium galactarate (**5e**, 0.4810 g, 1.1732 mmol) was added into the MeOH/HCl solution. The reaction mixture was stirred at room temperature for 20 min, sonicated for 20 min, concentrated

under reduced pressure and then dried under vacuum at room temperature for 4 h to give esterified galactarate / dodecamethylenediammonium dichloride (i.e., ester/salt). The ester/salt was mixed with fresh methanol (10 mL) and the reaction mixture (pH 1~2, pH paper) was made basic by drop-wise addition of triethylamine (0.800 mL) (pH 8~9). Additional triethylamine (0.400 mL) was added after 10 min to keep the basicity of the reaction mixture at about pH 9. The reaction mixture was refluxed for 19.5 h. The white solid was removed by centrifugation, washed with methanol (2×5 mL) and dried under vacuum at room temperature for 20 h to give poly(dodecamethylene galactaramide) (**8e**, 0.3285 g, 0.8783 mmol, 74.87%, dp 2.79, estimated Mn 1,100) (JZ04041)

**Poly(3,6-dioxa-octamethylene galactaramide) (8f) prepolymer.** Acetyl chloride (0.750 mL, 10.5 mmol) was added drop-wise to cold methanol (5.0 mL) while stirring in an ice bath for 10 min to make methanolic/HCl solution. 3,6-Dioxa-1,8-octanediammonium galactarate (**5f**, 0.5000 g, 1.3966 mmol) was added to the MeOH/HCl solution. The reaction mixture was stirred at room temperature for 10 min, sonicated for 20 min, concentrated under reduced pressure and then dried under vacuum at room temperature for 4 h to give esterified galactarate / 3,6-dioxa-1,8-octanediammonium dichloride (i.e., ester/salt). The ester/salt was dissolved in fresh methanol (10 mL) and the solution (pH 1~2, pH paper) was made basic by drop-wise addition of triethylamine (0.800 mL) (pH 8~9). Additional triethylamine (0.800 mL) was added after 10 min to keep the basicity of the reaction mixture at about pH 9. The reaction mixture was refluxed for 16 h. The white solid was removed by centrifugation, washed with methanol (2×10 mL), then acetone

(2×10 mL), and dried under vacuum at room temperature for 10 h to give poly(3,6-dioxaoctamethylene galactaramide) (**8f**, 0.2064 g, 0.6404 mmol, 45.85%, dp 9.41, estimated Mn 3,100) (JZ04007)

## References

1. Bolker, Henry I. *Natural and Synthetic Polymers An Introduction*. New York, Marcel Dekker. **1974**.
2. Seymour, Raymond B. *Introduction to Polymer Chemistry*. **1971**, McGraw-Hill.
3. Billmeyer, Fred W. Jr. *Textbook of Polymer Science*. **1984**, New York, John Wiley & Sons.
4. Ogata, N. And Hosoda, Y. Synthesis of Hydrophilic Polyamide by Active Polycondensation. *Journal of Polymer Science, Polymer Letters Edition* **1974**, 12: 355-358.
5. Ogata, N. And Hosoda, Y. Synthesis of Hydrophilic Polyamide from L-Tartarate and Diamines by Active Polycondensation. *Journal of Polymer Science, Polymer Chemistry Edition* **1975**, 13: 1793-1801.
6. Ogata, N. New Polycondensation Systems. *Polymer Reprints* **1976**, 17(1): 151-162.
7. Ogata, N. And Hosoda, Y. Active Polycondensation of Methylene Tartarate with Hexamethylenediamine. *Journal of Polymer Science, Polymer Letters Edition* **1976**, 14: 409-412.
8. Ogata, N., Sanui, K. And Kayamo, Y. Copolycondensation of Hydroxyl Diesters and Active Diesters with Hexamethylenediamine. *Journal of Polymer Science, Polymer Chemistry Edition* **1977**, 15: 1523-1526.
9. Ogata, N., Sanui, K., Tanaka, H. And Suzuki, T. Active Polycondensation of alpha, alpha'-Disubstituted Adipate with Hexamethylenediamine. *Journal of Polymer Science, Polymer Chemistry Edition* **1977**, 15: 2531-2534.
10. Ogata, N. Synthesis of Polyamides and Polyesters Having Various Functional Groups. *Journal of Macromolecul Science-Chemistry* **1979**, A13(4): 177-501.

11. Ogata, N., Sanui, K., Nakamura, H. And Kishi H. Polycondensation of Diethyl Mucate with Hexamethylenediamine in the Presence of Poly(Vinyl Pyridine). *Journal of Polymer Science, Polymer Chemistry Edition* **1980**, 18: 933-938.
12. Ogata, N., Sanui, K., Nakamura, H. And Kuwahara, M Polycondensation Reaction of Dimethyl Tartrate with Hexamethylenediamine in the Presence of Various matrices. *Journal of Polymer Science, Polymer Chemistry Edition* **1980**, 18: 939-948.
13. Ogata, N., Sanui, K., Tanaka, H. And Matsuo, H. Molecular Weight Control in Polycondensation of Hydroxyl Diesters with Hexamethylenediamine by Polymer Matrices. *Journal of Polymer Science, Polymer Chemistry Edition* **1981**, 19: 2609-2617.
14. Ogata, N., Sanui, K. And Kato, A. Polycondensation of Diesters with Hetero Atom Groups with Hexamethylenediamine in the Presence of Polyme Matrix. *Journal of Polymer Science, Polymer Chemistry Edition* **1982**, 20: 227-231.
15. Ogata, N., Sanui, K., Iwaki, F. And Nomiyama, A. Matrix Polycondensation through Hydrogen Bonding Interaction. *Journal of Polymer Science, Polymer Chemistry Edition* **1984**, 22: 793-800.
16. Kiely, Donald E.; Lin, Tsu Hsing Aldaric acid-based polyhydroxypolyamides and their manufacture. U.S. **1989**, Patent 4833230, May 23.
17. Chen, Liang; Kiely, Donald E. D-Glucaric acid esters/lactones used in condensation polymerization to produce hydroxylated nylons - a qualitative equilibrium study in acidic and basic alcohol solutions. *Journal of Carbohydrate Chemistry* **1994**, 13(4): 585-601.
18. Kiely, D.E., Chen, L. And Lin, T. Hydroxylated Nylons Based on Unprotected Esterified D-Glucaric Acid by Simple Condensation Reactions. *J. Am. Chem. Soc.* **1994**, 116(2): 571-8.
19. Kiely, D.E., Chen, L. And Lin, T-H. Simple Preparation of Hydroxylated Nylons - Polyamides Derived From Aldaric Acids. *ACS Symposium Series 575*, **1994**, Washington.
20. Kiely, Donald E.; Chen, Liang; Morton, David W. Glucaric acid monoamides and their use to prepare poly(glucaramides). **1994**.

21. Kiely, Donald E.; Chen, Liang; Morton, David W. Process for making activated aldarate esters, ester/lactones and lactones. US. **1994**, Patent 5329044, July 12.
22. Kiely, Donald E.; Chen, Liang; Morton, David W. polyaldaramide polymers useful for films and adhesives. U.S. **1995**. US Patent 5434233, July 18
23. Chen, L. And Kiely D. E. Synthesis of Stereoregular Head,Tail - Hydroxylated Nylons Derived from D-Glucose. *J. Org. Chem.* **1996**, 61(17): 3847-51.
24. Kiely, Donald E. Carbohydrate diacids: Potential as commercial chemicals and hydrophilic polyamide precursors. 218th ACS National Meeting, **1999**, New Orleans, American Chemical Society, Washington, D. C.
25. Kiely, Donald E., Chen, Liang and Lin, Tsu-Hsing Synthetic Polyhydroxypolyamides from Galactaric, Xylaric, D-Glucaric and D-Mannaric Acid and Alkylenediamine Monomers - Some Comparisons. *J. Polym. Sci.; Polym Chem. Ed* **2000**, 38: 598.
26. Morton, David W., and Kiely, Donald E. Evaluation of the Film and Adhesive Properties of Some Block Copolymer Polyhydroxypolyamides from Esterified Aldaric Acids and Diamines. *J. Applied Polym. Sci.* **2000**, 77: 3085-92.
27. Morton, David W., and Kiely, Donald E. Synthesis of Poly(azaalkylene aldaramides) and Poly(oxaalkylenealdaramides) Derived from D-Glucaric and D-Galactaric Acids. *J. Polym. Sci.; Polym. Chem. Ed.* **2000**, 38: 404.
28. Kiely, Donald E. Carbohydrate Diacids: Potential as Commercial Chemicals and Hydrophobic Polyamide Precursors. ACS Symposium Series 784, Chemicals and Materials from Renewable Resources, **2001**.
29. Styron, Susan D.; Kiely, Donald E.; Ponder, Glenn Alternating stereoregular head, tail-tail, head-poly(alkylene D-glucaramides) derived from a homologous series of symmetrical diamido-di-D-glucaric acid monomers. *Journal of Carbohydrate Chemistry* **2003**, 22(2): 123-142.
30. Hoagland, P. D. The Formation of Intermediate Lactones during Aminolysis of Diethyl Galactarate. *Carbohydrate Research* **1981**, 98: 203-208.
31. Hoagland, P. D.; Pessen, H. And Mcdonald, G. G. The Formation of Intermediate Lactones during Aminolysis of Diethyl Xylarate. *journal of Carbohydrate Chemistry* **1987**, 6(3): 495-499.

## Chapter 4. GPC Study to Determine the Molecular Weight and Molecular Weight Distribution of Some Polyhydroxypolyamides

### Introduction

#### Average molecular weight

For most macromolecules, perhaps their most important feature is the existence of a distribution of chain lengths representing varying degrees of polymerization and molecular weights, in the other words, polydispersity. The range of different molecular weights of the molecules in a sample may be narrowed by fractionation but monodisperse systems are seldom encountered in synthetic polymer systems. Hence, the polymer scientist is usually concerned with an average molecular weight. The distribution of molecular weight can be illustrated by plotting the weight of polymer of a given molecular weight against the chain length (Figure 1).

Because of the existence of molecular weight distribution in any polymer, the experimental measurement of molecular weight gives an average value only. Several different averages are important. One of them is the molecular weight measurement according to the number of molecules in a known mass of material, leading to the “number-average molecular weight”,  $M_n (\overline{M}_n)$ . For typical polymers the number average molecular weight lies near the peak of the weight-distribution curve or the most probable molecular weight.

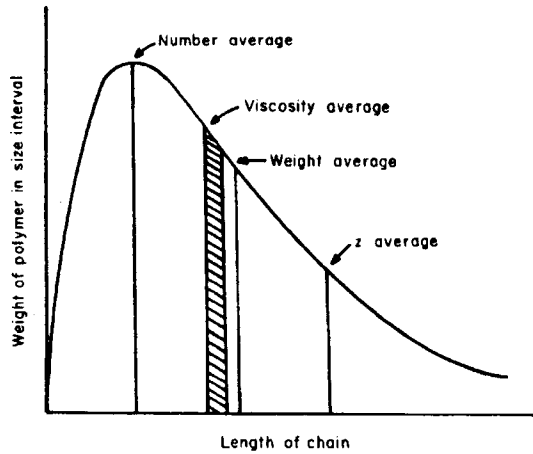


**Figure 1.** Distribution of molecular weight in a typical polymer.<sup>[1]</sup>

If the sample contains  $N_i$  molecules of the  $i$ th kind, for a total number of molecules

$\sum_{i=1}^{\infty} N_i$ , and each of the  $i$ th kind of molecule has a mass  $m_i$ ; then the total mass of all the

molecules is  $\sum_{i=1}^{\infty} m_i N_i$ . The number-average molecular mass (equation 4.1) is:

$$\bar{m}_n = \frac{\sum_{i=1}^{\infty} m_i N_i}{\sum_{i=1}^{\infty} N_i} \quad 4.1$$

Multiplication of  $\bar{m}_n$  by Avogadro's number ( $6.023 \times 10^{23}$ ) gives the number-average molecular weight (mole weight, equation 4.2):



$$\overline{M}_n = \frac{\sum_{i=1}^{\infty} M_i N_i}{\sum_{i=1}^{\infty} N_i} \quad 4.2$$

The number average molecular weight may be calculated by end-group analysis, tagged atoms, or chromophoric groups.<sup>[2,3]</sup> Indirect calculations, i.e., measuring the effect of the molecules on colligative properties, vapor pressure depression, osmometry (osmotic pressure measurement)<sup>[4]</sup>, cryoscopy (freezing point depression) and ebulliometry (boiling point elevation)<sup>[5]</sup>, can also give similar values.

The other average molecular weight that can be measured by an absolute method is the “weight-average molecular weight”,  $M_w$  ( $\overline{M}_w$ ), obtained by dividing the summation of the square of the molecular weight values by the summation of the molecular weights of all the molecules present (equation 4.3):

$$\overline{M}_w = \frac{\sum_{i=1}^{\infty} N_i M_i^2}{\sum_{i=1}^{\infty} N_i M_i} \quad 4.3$$

Light scattering<sup>[6]</sup> and sedimentation equilibrium (ultracentrifugation) techniques<sup>[7]</sup>, which measure molecular size, yield weight average molecular weight data.

Because heavier molecules contribute more to  $M_w$  than light ones,  $M_w$  is always greater than  $M_n$ , except for a hypothetical monodisperse polymer. The value of  $M_w$  is greatly

influenced by the presence of high molecular weight species, just as  $M_n$  is influenced by species at the low end of the molecular weight distribution curve.

Polydispersity, which is the ratio of  $M_w/M_n$ , is a measure of the breadth of the molecular weight distribution. Since  $M_w$  is always larger than  $M_n$ , PDI (polydispersity index) is always  $\geq 1$ . Monodispersity polymers have PDI values of 1.

$M_z$  ( $\overline{M}_z$ ) is called the z-average molecular weight and is defined as follows (equation 4.4):

$$\overline{M}_z = \frac{\sum_{i=1}^{\infty} N_i M_i^3}{\sum_{i=1}^{\infty} N_i M_i^2} \quad 4.4$$

The z-average molecular weight  $M_z$  obtained from measurements of the radial distribution of the refractive-index gradient in sedimentation equilibrium is greater than the weight average  $M_w$ .

$M_v$  ( $\overline{M}_v$ ) is called viscosity average molecular weight, obtained from the intrinsic viscosity (equation 4.5):

$$\overline{M}_v = \left( \frac{\sum_{i=1}^{\infty} N_i M_i^{1+a}}{\sum_{i=1}^{\infty} N_i M_i} \right)^{\frac{1}{a}} \quad 4.5$$

In equation 4.5, “a” is a constant, called the Mark-Houwink exponent,<sup>[1]</sup> obtained from absolute or direct weight average molecular weight measurements of known distributions.  $M_v$  is typically between the number average  $M_n$  and weight average  $M_w$  and closer to the latter.

As shown in Figure 1, the distribution of molecular weights for typical non-homogeneous polydisperse systems is as follows:  $M_z > M_w > M_v > M_n$ .

### **Gel Permeation Chromatography**

Gel permeation chromatography (GPC), also called size exclusion chromatography (SEC), gel filtration chromatography, gel chromatography, steric exclusion chromatography and exclusion chromatography, is a liquid chromatographic separation technique used to separate macromolecules by molecular size.<sup>[8,9]</sup>

The primary purpose and use of GPC is to provide molecular weight distribution information about a particular polymer material. The general role of the column is that when a sample is injected onto a GPC column, the sample polymer molecules pass through the column with the mobile phase. The smaller macromolecules penetrate the pores of the stationary phase (packing material) while the larger molecules are too large to be accommodated and remain in the interstitial space. The small molecules flow down the column after a temporary stay in the pores. The larger molecules come off the column prior to the small molecules resulting in the chromatographic separation of different size

molecules (Figure 2). A real GPC sample chromatogram typically shows a continuum of molecular weight components contained unresolved within a single peak.

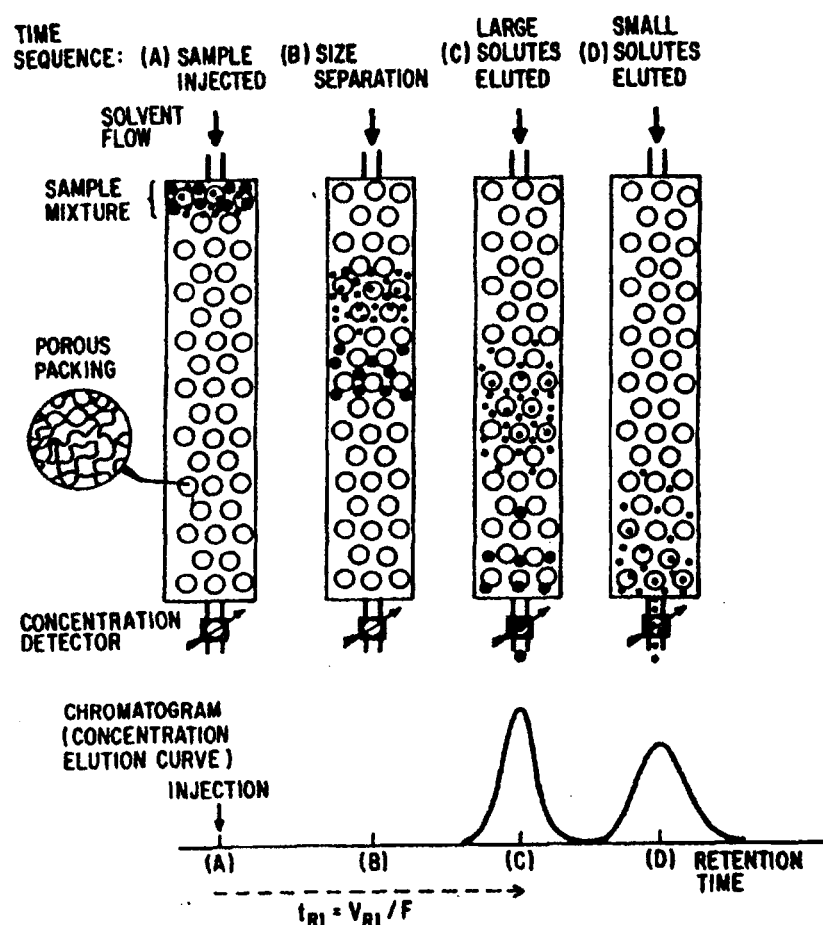


**Figure 2.** Development and detection of size separation by GPC.<sup>[10]</sup>

A typical GPC system is essentially a specialized, isocratic, high-performance liquid chromatography system. It is composed of the following parts; solvent reservoir, pump, injector, column and detector (Figure 3). The mobile phase is stored in the solvent

reservoir, pumped through a degasser to prevent air bubbles from entering the detector downstream, and pumped to the sample injector through a pulse dampener and in-line filter. A dilute polymer solution is introduced through an injector, too, and then sample and mobile phase are carried through the column set, passed through the detector and into a waste container.

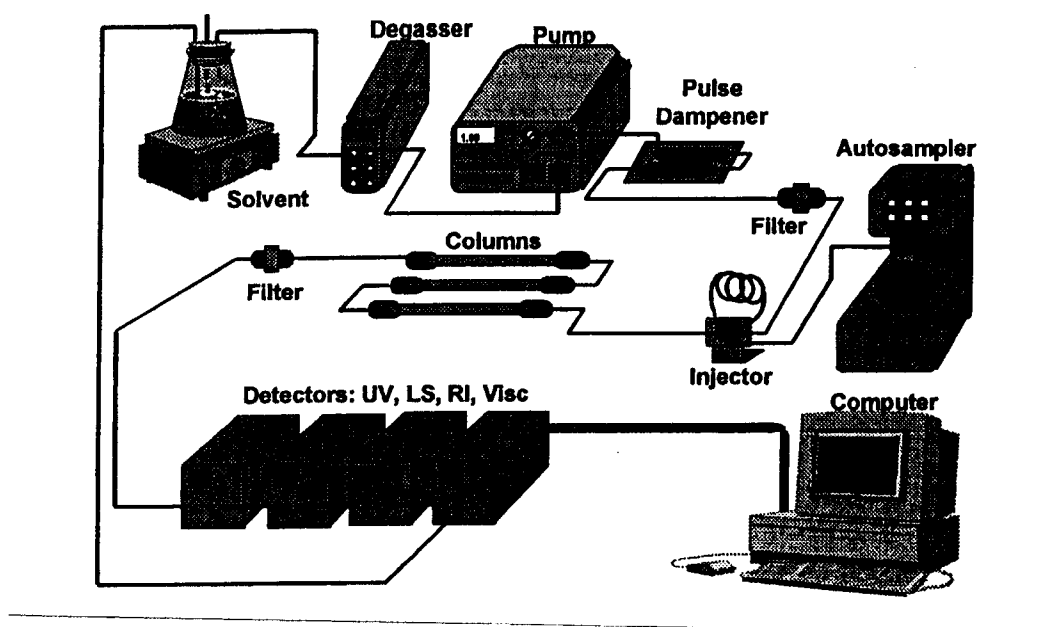


**Figure 3.** Schematic of a GPC system.<sup>[10]</sup>

The most common/standard detectors for GPC are RI detector (Refractive Index or Differential Refractometer) and Ultra Violet Detector, both are universal detectors. RI detectors measure the difference in refractive index between a moving (sample

containing) stream and a static reference of mobile phase using a split optical cell. It responds well to most polymeric samples.

It is possible to add a second or third, molecular weight-sensitive detector to a GPC system. These detectors represent refinements of classic techniques, such as light-scattering photometry, capillary viscometry (for intrinsic viscosity) and membrane osmometry (for on-line molecular weight determination). Both light-scattering photometry and capillary viscometry are commercially available, with RI as part of a triple detector system.

Light scattering photometry is based on the principle that light is scattered by particles, whose size is comparable to the wavelength of the incident light.<sup>[6]</sup> The intensity of the scattered light is directly related to the weight-average molecular weight. The accuracy of the light-scattering measurement depends on prior determinations of the solvent refractive index and of the specific refractive index increment of the sample in the solvent. Right-angle light-scattering detection, multi-angle light-scattering detection and low-angle light-scattering detection have been widely used in determine the weight average molecular weight and molecular weight distribution of polymers.

Viscometry is another molecular weight-sensitive detection method.<sup>[10]</sup> At a constant flow rate, the pressure drop across a capillary tube is proportional to the viscosity of the liquid flowing through the tube. The intrinsic viscosity of an eluting polymer can be

determined from measurements of the specific viscosity and concentration of the eluting polymer solution at each elution volume.

In order to define the relationship between molecular weight (or typically its logarithm) and retention volume in the selective permeation range of the column set used, and to calculate the molecular weight averages of the sample under investigation, calibration is required in modern high performance GPC. Two calibration methods are commonly employed, conventional calibration and universal calibration. The conventional calibration is based on the refractive index measurement. On the other hand, universal calibration correlates the polymer hydrodynamic volume against elution volume, achieved by using narrow molecular weight distribution standards with known molecular weights and known intrinsic viscosities.

### **Results and Discussion**

Aceylated random poly(alkylene D-glucaramide) and poly(alkylene galactaramide) (polyhydroxyl polyamides, PHPAs) were applied to Gel Permeation Chromatography (GPC) analysis.

## **I. Gel Permeation Chromatography**

Two Gel Permeation Chromatography systems were applied.

One is comprised of a Waters Model 515 Pump equipped with a Waters In-line Degasser with chloroform as the mobile phase, Styragel column HR 3, 2 and 1 (Waters Corporation, Milford, MA) in series maintained at 50 °C using a column oven, and a Waters 2414 Refractive Index Detector also maintained at 50 °C. Flow rate was set at 1 mL/min. The calibration were performed using narrow dispersity poly(ethylene oxide) standards (Polymer Laboratories, Amherst, MA) of molecular weights 194, 400, 620, 1080, 1900, 6450, 11840, 22450 and 43520.

The other GPC system is comprised of a Waters Model 515 Pump with a Viscotek In-line Degasser (VE 7510 GPC Degasser), Styragel column HR 3, 2 and 1 (Waters Corporation, Milford, MA) at 50 °C and a Viscotek Triple Detector Array (TDA 302), composed of Refractive Index Detector (temperature maintained at 50 °C), Light-scattering Detector and Viscometer. The mobile phase is chloroform. The same narrow dispersity poly(ethylene oxide) (Polymer Laboratories, Amherst, MA) standards were employed for calibration. Both conventional calibration based on refractive index and universal calibration based on intrinsic viscosity measurement were used to calculate molecular weight and molecular weight distribution.



The Waters Stryragel columns are packed with high-performance, fully porous, highly cross-linked styrene-divinylbenzene copolymer particles.

## II. Acetylation

Acetylation of the polyhydroxypolyamides (PHPAs) was carried out using two different procedures, the pyridine method and the *N*-methylimidazole method.

The pyridine method is a conventional method for hydroxyl group acetylation.

Polyhydroxypolyamide and acetic anhydride (ca. 1:3) were mixed in pyridine (ca. 1:1 ratio of acetic anhydride and pyridine). Here, pyridine functions as both solvent and catalyst. The acetylation reaction mixture was stirred at 60 °C. After the reaction was completed, deionized water was added to decompose excess acetic anhydride. The reaction mixture was extracted with dichloromethane, neutralized with sodium bicarbonate and then solvent evaporated under vacuum. Toluene was added several times to form an azeotrope with residual pyridine, and the azeotrope was removed under vacuum. The product was dried under vacuum to give the acetylated product rendered chloroform soluble in order to be analyzed with the GPC system.

An alternative method is to use excess acetic anhydride to function as both reactant and solvent. A catalytic amount of *N*-methylimidazole (<0.1 mL) was added to facilitate the reaction. The reaction temperature again was 60 °C. After the reaction was complete, deionized water was added to decompose excess acetic anhydride. The reaction mixture

was extracted with dichloromethane. Sodium bicarbonate was added to neutralize residual acid and a small amount of sodium sulfate was applied to remove residual water. The solvent was removed with a nitrogen stream and the product was dried under vacuum. Since this method avoids the use of pyridine and is much easier to work up, it was applied to most of the acetylation reactions.

### **III. GPC analysis of some acetylated PHPAs**

#### **1. GPC analysis of poly(hexamethylene 2,3,4,5-tetra-*O*-acetyl-D-glucaramide) (2)**

Acetylation of poly(hexamethylene D-glucaramide) (1) prepolymer and GPC analysis of the acetate was carried out. The reports described GPC analysis of poly(hexamethylene D-glucaramide) (1) prepolymer acetylated using both pyridine and the *N*-methylimidazole methods. The prepolymers and postpolymers (1) were prepared under different reaction conditions. These studies were employed to demonstrate the applicability of the acetylation methods and the appropriate method of GPC analysis to determine molecular weight and molecular weight distribution.

#### **Acetylation of prepolymer 1 using the pyridine or *N*-methylimidazole method**

Poly(hexamethylene D-glucaramide) (1) prepolymer was acetylated using the pyridine and *N*-methylimidazole methods, respectively. Both of the polymer acetates (2) were injected into the Waters GPC – RI instrument (Table 1, Figure 4). Interestingly the number average molecular weight data, 2395 g/mol and 2872 g/mol from GPC analysis, are consistent with the <sup>1</sup>H NMR end-group analysis of the non-acetylated PHPA

corresponding to a calculated  $M_n$  (2908 g/mol) for the acetylated polymer. The similarity of the results of the two trials also showed that both acetylation methods are applicable.

**Table 1.** GPC analysis results of molecular weight and molecular weight distribution of acetates (**2**) derived from the same poly(hexamethylene D-glucaramide) (**1**) prepolymer acetylated using the pyridine method (JZ040440 and *N*-methylimidazole method (JZ04047) with Waters – conventional calibration

	Acetylation method	$M_n$	$M_w$	MP	$M_z$	Polydispersity	$M_n^*$
JZ04044 ( <b>2</b> )	Pyridine	2395	2946	1746	3857	1.230	2908
JZ04047 ( <b>2</b> )	<i>N</i> -Methylimidazole	2872	3536	2086	4737	1.231	2908

The number average molecular weight was calculated based on the  $M_n$  of the non-acetylated polymer obtained by end-group analysis ( $^1\text{H}$  NMR).

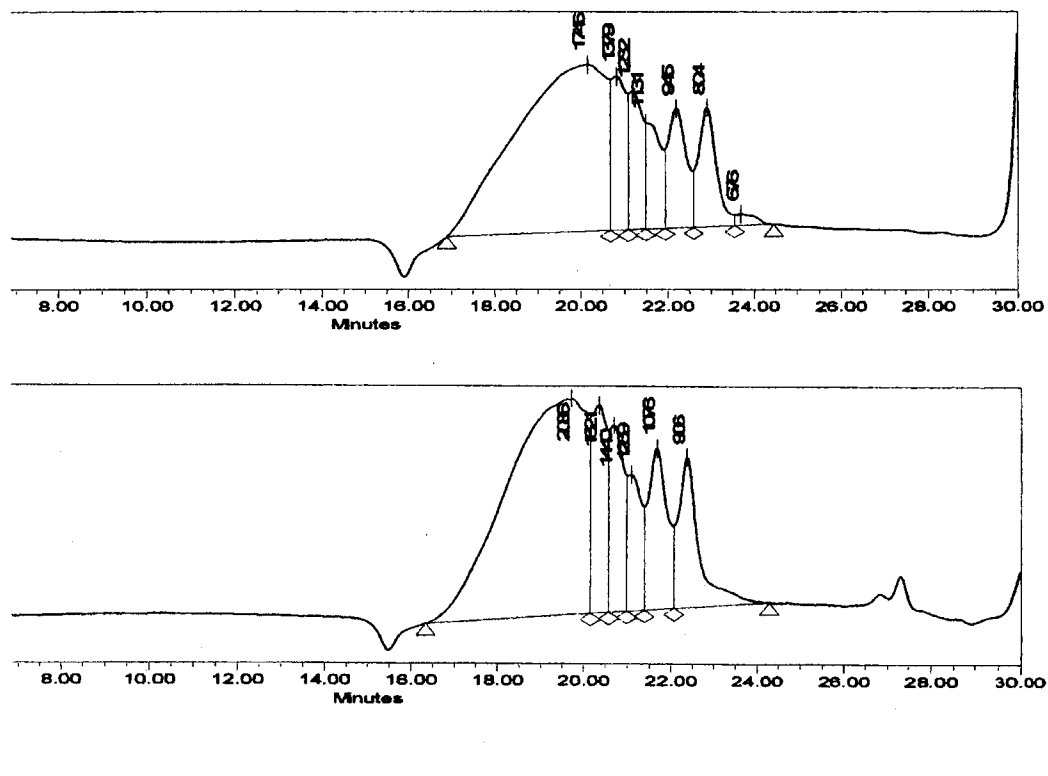


**Figure 4.** Chromatograms of acetates **2** derived from same prepolymer **1** using the pyridine method (top) and *N*-methylimidazole method (bottom).

#### **Prepolymer 1 obtained using different polymerization reaction conditions**

GPC studies were carried out on three poly(hexamethylene tetra-*O*-acetyl-D-glucaramide) (**2**) samples, derived from three poly(hexamethylene D-glucaramide) (**1**) prepolymers that were synthesized under different conditions (*i.e.*, solvent and reaction temperature, Table 2). Under different polymerization conditions, the polymers obtained have different molecular weights.

**Table 2.** Reaction conditions for preparation of poly(hexamethylene D-glucaramide) (**1**) prepolymer samples and the GPC analysis of the corresponding acetates using the Viscotek instrument – universal calibration and conventional calibration methods

<b>2</b>	$M_n^{*1}$	$M_n^{*2}$	EG:MeOH <sup>*3</sup>	Temperature (°C) <sup>*3</sup>	Yield (%) <sup>*3</sup>	$M_n^{*4}$	<b>1</b>
JZ04051_1	1685	798	1:0	50	34.98	1594	JZ03020_3
JZ04051_3	2273	916	1:1	r.t	56.44	2963	JZ03020_6
JZ04051_2	1829	814	0:1	50	69.09	1910	JZ03020_5

\*<sup>1</sup> Number average molecular weight of **2** obtained from Viscotek – universal calibration

\*<sup>2</sup> Number average molecular weight of **2** obtained from Viscotek – conventional calibration

\*<sup>3</sup> Reaction conditions for preparations of obtain poly(hexamethylene D-glucaramide) (**1**) prepolymers; EG = ethylene glycol

\*<sup>4</sup> The number average molecular weight was calculated based on the  $M_n$  of the non-acetylated polymer obtained by end-group analysis (<sup>1</sup>H NMR)

### GPC analysis of acetylated prepolymer and postpolymer of **1** – Waters RI

#### Instrument

A pair of acetylated poly(hexamethylene D-glucaramide) pre and postpolymers were studied using Waters RI instrument (Table 3). The chromatogram of the prepolymer shows multimodal distribution while the chromatogram of the postpolymer appears as a broad peak (Figure 5). The polymerization of prepolymer was carried out in methanol solution in the presence of triethylamine. Since the higher molecular weight polymers have very low solubility in methanol, the polyamide precipitating from methanol has a relatively low molecular weight distribution and thus a low polydispersity (Table 3). On the other hand, the postpolymer was synthesized in methanol/DMSO mixed solvent,

which increases the solubility of polyamide and a higher molecular weight postpolymer of higher polydispersity (Table 3) is formed.

**Table 3.** GPC analysis of the acetates (**2**) of poly(hexamethylene D-glucaramide) (**1**) prepolymer (JZ04050\_1) and postpolymer (JZ04050\_2) pair (Waters – conventional calibration)

<b>2</b>	$M_n$	$M_w$	MP	$M_z$	Polydispersity	$M_n^*$
JZ04050_1	2883	3534	2163	4715	1.226	2198
JZ04050_2	2813	3665	5590	4531	1.303	5015

\* The number average molecular weight was calculated based on the  $M_n$  of the non-acetylated polymer obtained by end-group analysis ( $^1\text{H}$  NMR)

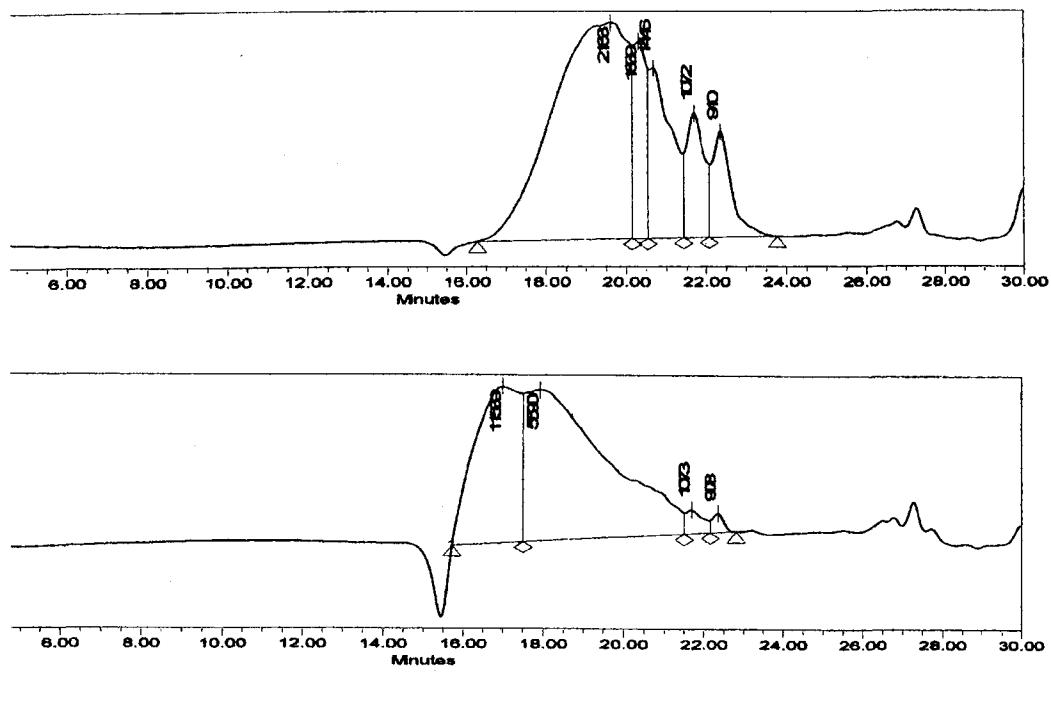


**Figure 5.** Chromatogram of poly(hexamethylene D-glucaramide) prepolymer and postpolymer acetates – Waters RI instrument.

### **GPC analysis of acetylated prepolymer and postpolymer of 1 – Viscotek Triple Detector Instrument**

A second pair of pre and post poly(hexamethylene D-glucaramide) acetates (**2**) were subjected to GPC analysis with Viscotek Triple Detector Instrument (Figure 6 and 7). Universal calibration was applied to determine the molecular weight and molecular weight distribution of these polyamides (Table 4).

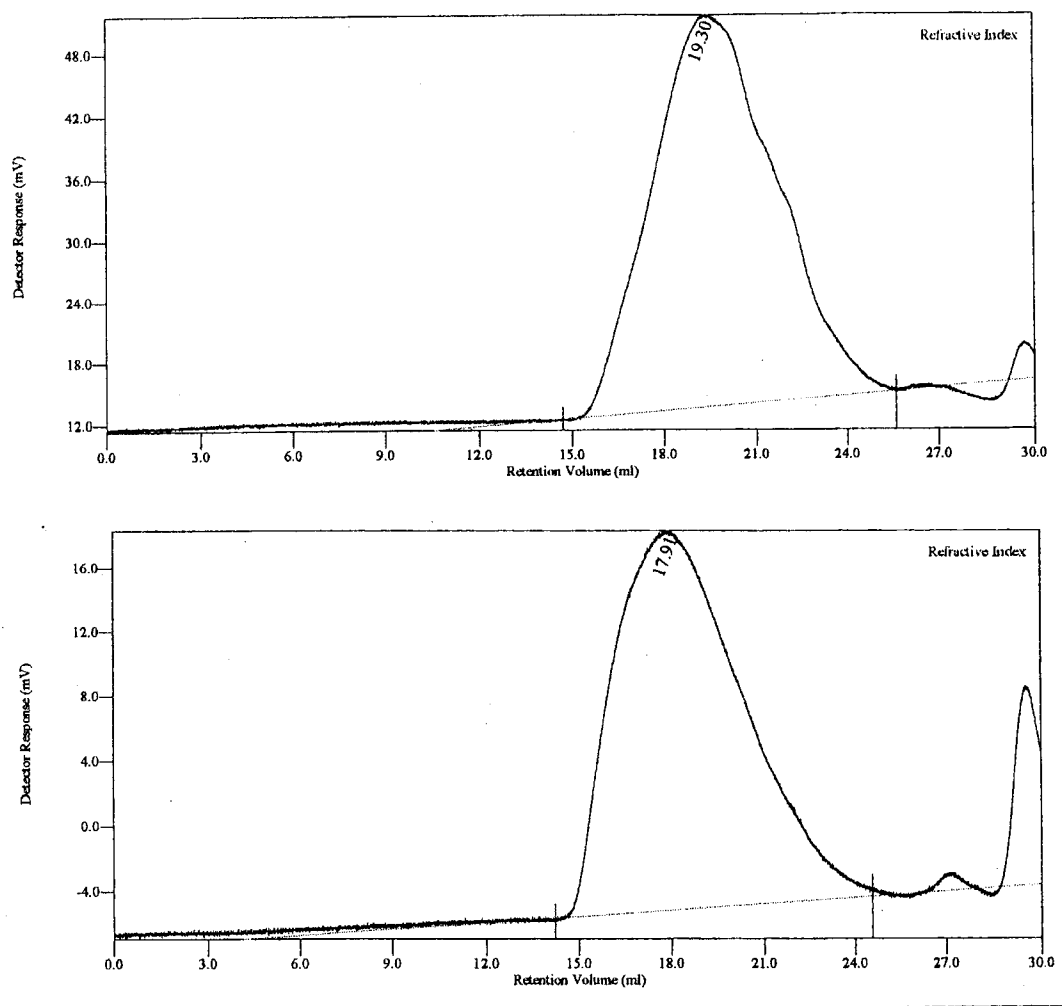


**Figure 6.** Viscotek chromatograms (RI chromatograms) of acetylated poly(hexamethylene D-glucaramide) pre (top) and post (bottom) polymers.



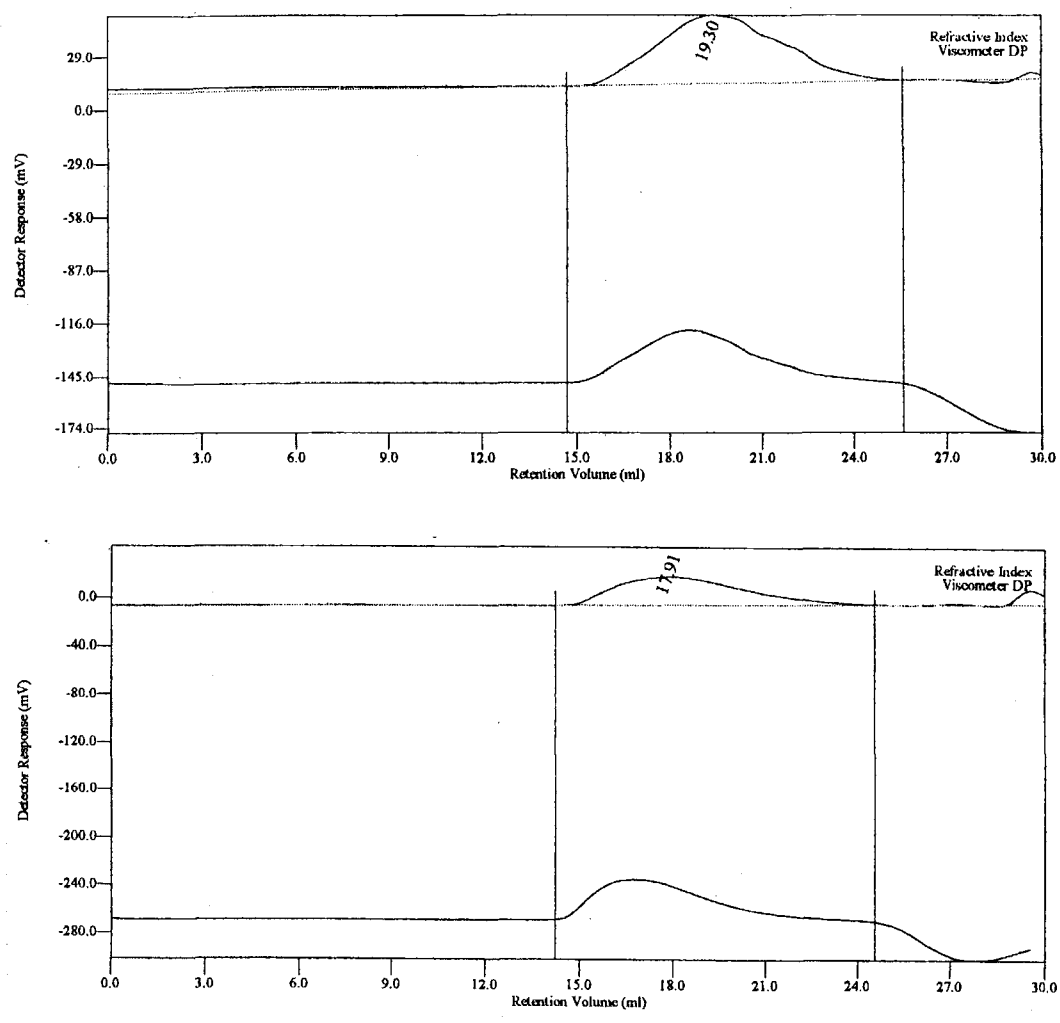


**Figure 7.** Viscotek chromatograms (RI and viscometry) of acetylated poly(hexamethylene D-glucaramide) pre (top) and post (bottom) polymers.

**Table 4.** GPC analysis of the poly(hexamethylene D-glucaramide) prepolymer (JZ04083) and postpolymer (JZ04084) acetates (**2**) (Viscotek – universal calibration)

<b>2</b>	$M_n$	$M_w$	MP	$M_z$	Polydispersity	$M_n^*$
JZ04083	2809	7521	4356	25250	2.677	2176
JZ04084	5107	17738	9173	56268	3.473	6270

\* The number average molecular weight was calculated based on the  $M_n$  of the non-acetylated polymer obtained by end-group analysis ( $^1\text{H}$  NMR)

## **2. GPC analysis of poly(tetramethylene tetra-*O*-acetyl-D-glucaramide) (**4**)**

GPC analysis with the Waters and Viscotek instruments of two different pre poly(tetramethylene tetra-*O*-acetyl-D-glucaramides) (**4**) derived from same poly(tetramethylene D-glucaramide) (**3**) prepolymer were carried out (Table 5). The same acetylation procedures were applied as described. Surprisingly the number average molecular weight ( $M_n$ ) obtained from Waters GPC analysis is closer to what was calculated with  $^1\text{H}$  NMR end group analysis of the non-acetylated polymer.

**Table 5.** GPC analysis of poly(tetramethylene tetra-*O*-acetyl-*D*-glucaramide) (**4**) with Waters – conventional calibration and Viscotek – universal and conventional calibration

	M <sub>n</sub>	M <sub>w</sub>	MP	M <sub>z</sub>	Polydispersity	M <sub>n</sub> <sup>*1</sup>
JZ04049 <sup>*2</sup>	1842	2048	1999	2324	1.112	2043
JZ04062 <sup>*3</sup>	3426	5638	4100	8298	1.646	2043
JZ04062 <sup>*4</sup>	1447	2403	1446	4995	1.661	2043

<sup>\*1</sup> The number average molecular weight was calculated based on the M<sub>n</sub> of the non-acetylated polymer obtained by end-group analysis (<sup>1</sup>H NMR)

<sup>\*2</sup> Waters – conventional calibration

<sup>\*3</sup> Viscotek – universal calibration

<sup>\*4</sup> Viscotek – conventional calibration

A pair of poly(tetramethylene *D*-glucaramide) prepolymer and postpolymer acetates were analyzed with the Viscotek Triple Detector instrument (Table 6). Interestingly, two separate peaks appeared in both the Refractive Index and Viscometer chromatograms. The second peaks are small and represent low molecular weight molecules.

**Table 6.** GPC analysis results of acetates (**4**) from poly(tetramethylene D-glucaramide) prepolymer (JZ04081) and postpolymer (JZ04082) (Viscotek – universal calibration and conventional calibration)

	M <sub>n</sub>	M <sub>w</sub>	MP	M <sub>z</sub>	Polydispersity	M <sub>n</sub> <sup>*1</sup>
JZ04081 <sup>*2</sup>	2654	5961	4696	15196	2.246	2030
JZ04081 <sup>*3</sup>	1108	1483	1386	2079	1.338	2030
JZ04082 <sup>*2</sup>	2799	5538	5601	7481	1.979	2464
JZ04082 <sup>*3</sup>	1239	1588	1496	2065	1.281	2464

<sup>\*1</sup> The number average molecular weight was obtained for the non-acetylated polymer with end-group analysis (<sup>1</sup>H NMR)

<sup>\*2</sup> Viscotek – universal calibration

<sup>\*3</sup> Viscotek – conventional calibration

### 3. GPC of poly(3,6-dioxa-1,8-octamethylene tetra-*O*-acetyl galactaramide) (**6**)

Poly(3,6-dioxa-1,8-octamethylene galactaramide) (**5**) prepolymer was acetylated and the corresponding acetate (**6**) was analyzed with the Viscotek Triple Detector instrument (Table 7). Again, the number average molecular weight (M<sub>n</sub>) obtained from universal calibration is closer to <sup>1</sup>H NMR end-group estimation.

**Table 7.** GPC analysis of poly(3,6-dioxa-1,8-octamethylene tetra-*O*-acetyl galactaramide) (**6**) (Viscotek – universal and conventional calibration)

	calibration	M <sub>n</sub>	M <sub>w</sub>	MP	M <sub>z</sub>	polydispersity	M <sub>n</sub> <sup>*</sup>
JZ04068	universal	1855	2129	1174	2453	1.148	3210
JZ04068	conventional	2386	3831	2329	5584	1.605	3210

<sup>\*</sup> The number average molecular weight was calculated based on the M<sub>n</sub> of the non-acetylated polymer obtained by end-group analysis (<sup>1</sup>H NMR)

#### 4. GPC study of poly(dodecamethylene tetra-*O*-acetyl galactaramide) (8)

Acetylation of poly(dodecamethylene galactaramide) (7) was carried out and the resulting acetate (8) was injected on the Viscotek GPC system (Table 8). Again, universal calibration gave a larger number compared to conventional calibration.

**Table 8.** GPC analysis results of poly(dodecamethylene tetra-*O*-acetyl galactaramide) (8) (Viscotek – universal calibration and conventional calibration)

	calibration	M <sub>n</sub>	M <sub>w</sub>	MP	M <sub>z</sub>	polydispersity	M <sub>n</sub> <sup>*</sup>
JZ04065	universal	2477	2772	2396	3158	1.119	1512
JZ04065	conventional	1450	2220	2175	3434	1.530	1512

\* The number average molecular weight was calculated based on the M<sub>n</sub> of the non-acetylated polymer obtained by end-group analysis (<sup>1</sup>H NMR)

#### Conclusions

1. Acetylation of polyhydroxypolyamides (PHPAs) was effected using the pyridine and *N*-methylimidazole methods to render the polymers chloroform soluble.
2. A Waters GPC system with an RI detector and Viscotek GPC system with a Triple Detector were used to obtain both molecular weight and molecular weight distribution information.
3. <sup>1</sup>H NMR end group analysis proved to be applicable and a convenient method to determine number average molecular weights (M<sub>n</sub>), which generally compare favorably with M<sub>n</sub> values reported using the Viscotek – universal calibration method.

## References

1. Bolker, Henry I. Natural and Synthetic Polymers An Introduction. **1974**, New York, Marcel Dekker.
2. Seymour, Raymond B. Introduction of Polymer Chemistry. **1971**, New York, McGraw-Hill.
3. Billmeyer, Fred W. Jr. Textbook of Polymer Science. **1984**, New York, John Wiley & Sons.
4. Burge, D. E. Molecular Weight Determination by Osmometry. American Laboratory **1977**, 9(b): 41-51.
5. Glover, C. A. Determination of Molecular Weights by Ebulliometry. Advances in Analytical Chemistry and Instrumentation. Reilley, C. N. a. M., Fred W. New York, Wiley-Interscience. **1966**, 5: 1-67.
6. Collins, Edward A., Bares, Jan, and Billmeyer, Fred W. Jr. Experiments in Polymer Science. **1973**, New York, Wiley-Interscience.
7. Bowen, T. J. An Introduction to Ultracentrifugation. **1970**, New York, Wiley-Interscience.
8. Cazes, Jack, Ed. Chromatographic Science Series. Handbook of Size Exclusion Chromatography. **1995** New York, Marcel Dekker.
9. Yau, W. W., Kirkland, J. J. And Bly, D. D. Modern Size-Exclusion Liquid Chromatography: Practice of Gel Permeation and Gel Filtration Chromatorgraphy. **1979**, New York, John Wiley & Sons.
10. Welch, Shawn, Austin, Dan, Murphy, Michael and Wong, Wei Sen Viscotek GPC School Handbook.

## Chapter 5. Monte Carlo Dihedral Angle Search and Molecular Mechanics Study.

### Method and Application

#### Introduction

Molecular modeling has evolved from the use of simple hand held models (such as “stick” models devised by Dreiding or the “space filling” models of Corey, Pauling and Koltun (CPK models), pencil, paper and hand calculators to sophisticated computer hardware and software. Computational chemistry is now widely applied to probing the physical, chemical and biological properties of molecules, employing both quantum mechanics and molecular mechanics protocols.

#### 1. Quantum Mechanics & Molecular Mechanics

Quantum mechanics provides the mathematical framework for describing motions of electrons in molecules. A number of quantum theories have been generated, including molecular orbital theory, *ab initio*, Hückel theory, valence bond theory and more recently, density functional theory.<sup>[1-6]</sup> Starting with the Schrödinger equation (Equation 5.1), quantum mechanics explicitly represents the electrons in a calculation. With quantum mechanics, it is possible to derive properties that depend upon the electronic distribution in atoms and molecules and in particular, to investigate energy changes for chemical reactions in which bonds are broken and formed.

$$\left\{ -\frac{\hbar^2}{2m} \left( \frac{\partial^2}{\partial x^2} + \frac{\partial^2}{\partial y^2} + \frac{\partial^2}{\partial z^2} \right) + \gamma \right\} \Psi(r,t) = i\hbar \frac{\partial \Psi(r,t)}{\partial t} \quad 5.1$$

However, since quantum mechanics deals with the electrons in a system, calculations are complex and very time consuming. Applying some semi-empirical quantum mechanics schemes, some of the electrons are ignored and the calculations become more manageable, but not practical with larger molecules.

Molecular mechanics computations are based upon platforms called force fields that ignore the electronic motions and calculate the energy of a molecule as a function of the nuclear positions only. Molecular mechanics is based on simple models of atomic interactions within a molecule with energy contributions from processes such as the stretching of bonds, opening and closing of bond angles and rotations about single bonds. Many molecular modeling force fields can be viewed in terms of a relatively simple four component picture of the intra- and inter-molecular forces within the system as described in the following equation<sup>[6]</sup>:

$$E(r^N) = \sum_{bonds} \frac{k_l}{2} (l_i - l_{i,0})^2 + \sum_{angles} \frac{k_\theta}{2} (\theta_i - \theta_{i,0})^2 + \sum_{torsions} \frac{V_n}{2} (1 + \cos(n\omega - \gamma)) \\ + \sum_{i=1}^N \sum_{j=i+1}^N \left\{ 4\epsilon_{i,j} \left[ \left( \frac{\sigma_{ij}}{r_{ij}} \right)^{12} - \left( \frac{\sigma_{ij}}{r_{ij}} \right)^6 \right] + \frac{q_i q_j}{4\pi\epsilon_0 r_{ij}} \right\} \quad 5.2$$



$E(r^N)$  denotes the potential energy, which is a function of the position ( $r$ ) of  $N$  particles (usually atoms). The various contributions are described as the energetic penalties associated with deviation of bonds and angles away from their “reference” or “equilibrium” or “ideal” values (Figure 1). The first term in Equation (5.2) models the interaction between pairs of bonded atoms. The harmonic potential is given the increase in energy as the bond length  $l_i$  deviates from the reference value  $l_{i,0}$ . The second term is a summation over all valence angles in the molecule, again modeled using a harmonic potential (a valence angle is the angle formed between three atoms A-B-C in which A and C are both bonded to B). The third term in Equation 5.2 called the torsional potential, models how the energy changes as a bond rotates. The fourth contribution is the non-bonded term. It is calculated between all pairs of atoms ( $i$  and  $j$ ) that are in different molecules or that are in same molecule but separated by at least three bonds (*i.e.* have a 1, $n$  relationship where  $n \geq 4$ ). In a simple force field the non-bonded term is usually modeled using a Coulomb potential term for electrostatic interactions and a Lennard-Jones potential for van der Waals interactions.

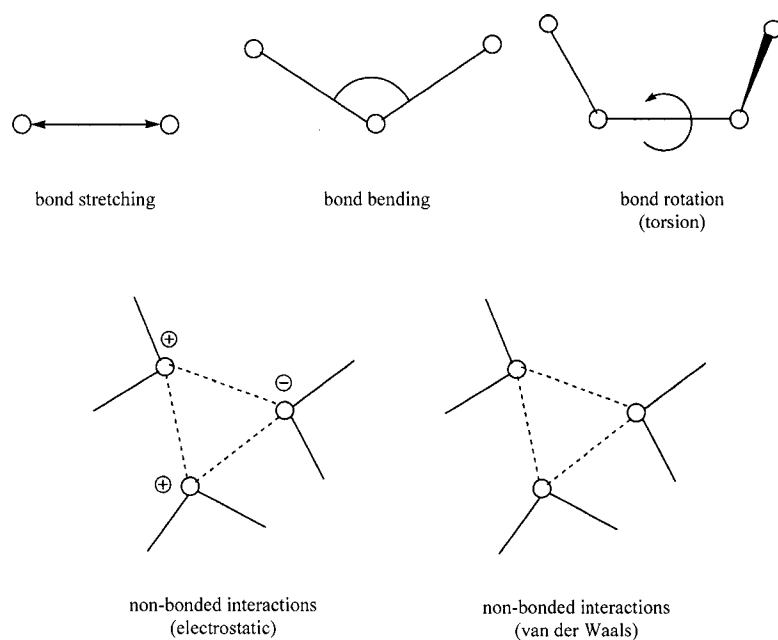


**Figure 1.** Schematic representation of the four key contributions to a molecular mechanics force field: bond stretching, angle bending, torsional terms and non-bonded interactions.

One of the concepts common to most force fields is that of atom type. Each atom in the system is assigned an atom type. The atom type is not only the atomic number of an atom, but also contains information about its hybridization state and sometimes the local environment. For example, in most force fields,  $sp^3$ -hybridized carbon atoms (which adopt a tetrahedral geometry),  $sp^2$ -hybridized carbon atoms (which adopt a trigonal geometry) and  $sp$ -hybridized carbon atoms (which linearly connect to other atoms) are often distinguished. The force field parameters are expressed in terms of these atom types, so that the reference angle  $\theta_0$  for a tetrahedral carbon atom is near  $109.5^\circ$ , and that for a trigonal carbon atom the angle is close to  $120^\circ$ . The neighborhood environment is the other consideration in defining atom types. In MM2/MM3/MM3 force fields, carbon atoms are distinguished as the following types:  $sp^3$ ,  $sp^2$ ,  $sp$ , carbonyl, cyclopropane,

radical, cyclopropene and carbonium ion.<sup>[7-16]</sup> In the AMBER force field, the carbon atom at the junction between a six- and a five-member ring (*e.g.*, in the amino acid tryptophan) is assigned a specific atom type different from the carbon atom in an isolated five-member ring. The AMBER force field even uses different atom types for a histidine amino acid depending upon its protonation state.<sup>[17,18]</sup>

The contemporary force fields in widespread use are MM2/MM3/MM4 force fields of Allinger and co-workers and the AMBER force field of Kollman and co-workers. AMBER is widely used for study of biologically active compound, such as proteins and nucleic acids. On the other hand, MM2/MM3/MM4 force fields are designed for general-purpose use. For carbohydrate and derivatives, MM2/MM3/MM4 force fields have proven to be the preferred force fields.

## 2. MM3 1992 Force Field for UNIX and VAX

In the MM3 force field, which we are utilized in molecular modeling reported in this chapter, the energy equation and parameters can be summarized in Equation 5.3<sup>[19]</sup>:

$$E = \sum E_S + \sum E_B + \sum E_{oop} + \sum E_{SB} + \sum E_{BB} + \sum E_T + \sum E_{TS} + \sum E_V + \sum E_\mu + \sum E_Q + \sum E_{Q\mu} \quad 5.3$$

$E$  denotes the total steric energy of a molecule summarizing all the bonds, bond angles, torsion angles and non-bonded interactions between atoms not bound to each other or to a

common atom (*i.e.*, 1,4-interactions and higher). Here,  $E_S$  (bond stretching energy) stands for the energy of a bond stretched or compressed from its natural bond length.  $E_B$  (bending energy) denotes the energy of bending a bond angle from its natural value;  $E_{OOP}$  (out-of-plane bending energy) is the energy of bending a planar atom out of its neighbor's plane;  $E_{SB}$  (stretch-bend energy) represents the energy of interaction between bond stretching and angle bending, in which stretch-bend is limited to an angle at the end of a bond being stretched;  $E_{BB}$  (bend-bend energy) is a term relating the energy of interaction between two angle bending, in which bend-bend is limited to angles centered to a common atom.  $E_B$ ,  $E_{OOP}$ ,  $E_{SB}$  and  $E_{BB}$  are all bending energy terms. Both  $E_T$  (torsional energy, energy of twisting/torsion about a bond) and  $E_{TS}$  (energy of interaction between angle twisting and bond stretching) are terms of torsional strain.  $E_V$  (van der Waals energy) is the energy due to van der Waals non bonded interactions (also hydrogen bonding). The last three terms are  $E_\mu$  (dipole interaction energy),  $E_Q$  (charge interaction energies for ions) and  $E_{Q\mu}$  (charge-dipole interaction energies).

### 3. Computer Simulation Methods

To predict conformations of molecules, the ideal situation is to be able to carry out energy minimization and to identify all the minimum conformations on an energy surface, followed by calculation according to a partition function using a statistical mechanical formula. However, this approach is only possible with relatively small molecules or small molecules assemblies in the gas phase. With a large number of atoms in a molecule, an

enormous number of minima on the energy surface are possible requiring some type of simulation process.

The two most common simulation methods in molecular modeling are the molecular dynamics and Monte Carlo methods.

The first molecular dynamics simulation of a molecular system was performed by Alder and Wainwright in 1975 using a hard-sphere model.<sup>[2]</sup> The behavior of the particles in the potential is similar to that of billiard or snooker balls: the particles move in straight lines at constant velocity between collisions. The collisions are perfectly elastic and occur when the separation between a pair of spheres equals the sum of their radii. After a collision, the new velocities of the colliding spheres are calculated using the principle of conservation of linear momentum. The hard-sphere model has provided many useful results but is obviously not ideal for simulating atomic or molecular systems. The continuous nature of the more realistic potentials requires the equations of motion to be integrated by breaking the calculation into a series of very short time steps (typically between 1 femtosecond and 10 femtoseconds;  $10^{-15}$  s to  $10^{-14}$  s). At each step, the forces on the atoms are computed and combined with the current positions and velocities to generate new positions and velocities a short time ahead. The force acting on each atom is assumed to be constant during the time interval. The atoms are then moved to the new positions, an updated set of forces is computed, and so on. The set of atomic positions are

derived by applying Newton's law of motion. The dynamic variables change with time can be described as trajectory.

The other common simulation method is the Monte Carlo method. In fact, the first computer simulations of fluids were Monte Carlo simulation method, performed by Metropolis, Rosenbluth, Rosenbluth, Teller and Teller in 1952.<sup>[2]</sup> In contrast to molecular dynamics, which simulates the successive configurations of the system connecting in time, the Monte Carlo simulation generates configurations randomly. Each configuration depends only on its predecessor and not on any other configurations previously visited.

In Monte Carlo simulations, each new conformation of a molecule may be generated by randomly moving a single atom or molecule. The energy of the new conformation is then calculated using the potential energy function. If the energy of the new conformation is lower than the energy of its predecessor then the new conformation is accepted. If the energy of the new conformation is higher than the energy of its predecessor then the Boltzmann factor of the energy difference is calculated. A random number is then generated between 0 and 1 and compared with the Boltzmann factor. If the random number is higher than the Boltzmann factor, the move is rejected and the original conformation is retained for the next iteration. If the random number is lower, the move is accepted and the new conformation becomes the next state. This procedure has the effect of permitting moves to states of higher energy.

The difference between molecular dynamics and Monte Carlo simulation methods can be summarized as following. First of all, molecular dynamics provides information of time dependence of the properties of the system while there is no temporal relationship between successive Monte Carlo configurations. In a Monte Carlo simulation, the outcome of each trial depends on its predecessor while in molecular dynamics it is possible to predict the next trial or, in the other words, know every configuration at any time in the past as well. The second difference is that molecular dynamics has a kinetic energy contribution to the total energy whereas in a Monte Carlo simulation the total energy is determined directly from the potential energy function. Thirdly, they sample different ensembles. Molecular dynamics is performed under conditions of constant number of particles ( $N$ ), volume ( $V$ ) and energy ( $E$ ), *i.e.* the microcanonical or constant NVE ensemble. Monte Carlo simulation samples from canonical ensemble (constant  $N$ ,  $V$  and temperature  $T$ ).

The application of either molecular dynamics or Monte Carlo simulations depends on the properties of the two simulation methods and the purpose of the simulation. Molecular dynamics is required if one wishes to calculate time-dependent quantities such as transport coefficients. On the other hand, Monte Carlo is often the most appropriate method to investigate systems in certain ensembles. For instance, it is much easier to perform simulations at exact temperatures and pressures with Monte Carlo than using molecular dynamics simulation. For isolated molecules, there may be a large number of minimum energy states separated by high barriers. Since molecular dynamics advances

the positions and velocities of all the particles simultaneously, it can be very useful for exploration of the local phase space. Conversely, since the Monte Carlo method does not simulate physical movement, it is more effective for conformational searching by jumping to a completely different area of phase space.

#### **4. Conformational Analysis**

The physical, chemical and biological properties of a molecule often depend critically upon the three-dimensional structures, or conformations, that it adopts. The first conformational analysis was performed by D. H. R. Barton in 1950.<sup>[20]</sup> Barton showed that the reactivity of substituted cyclohexanes was influenced by the equatorial or axial nature of the substituents.

The “conformational search” method for the “global minimum” (the “preferred” conformation at the minimum point on the energy surface) range from systematic search algorithms, model-building methods, random approaches, distance geometry and molecular dynamics.

The systematic search method is also called a “grid search”, and explores conformational space by making regular and predictable changes to the conformation.<sup>[21,22]</sup> By fixing the bond lengths and angles, all rotatable bonds are systematically rotated through 360° using a fixed increment. Every conformation generated is subjected to energy minimization to derive the associated minimum energy conformation. A simplified systematic search is to



define torsion angles to +60, -60 and 180, corresponding to *gauche*(+), *gauche*(-) and *anti* conformations to determine the theoretical minimum energy conformation. For a molecule with 1 rotatable bond, there will be 3 conformations generated. For a molecule containing 2 rotatable bonds, there will be 9 ( $3^2$ ) starting conformations generated and so forth. For a molecule containing 9 rotatable bonds, 19,683 ( $3^9$ ) starting conformations will be generated and minimized with the corresponding force field to obtain the global minimum. This kind of systematic search, can obviously help to find the global minimum, as was illustrated by Styron et al in their study of the acyclic carbohydrate diamide, D-glucaramide.<sup>[22]</sup> However, the compound of interest in this chapter, 2,3,4,5-tetra-*O*-acetyl-*N,N'*-dimethyl-D-glucaramide (**3**), with total 52 atoms and 15 rotatable torsion angles would require 14,348,907 ( $3^{15}$ ) starting conformations, presenting a formidable computational challenge.

A model-building method, employing three-dimensional structures of “molecular fragments” or “building blocks”, was designed for a simplified conformational study.<sup>[23-25]</sup> The conformational study of tetra-*O*-acyloxy-*N,N'*-dialkyl D-glucaramides described in Chapters 1 and 2 was an application of the model-building method.

A random search method represents another approach for conformational searching.<sup>[2,26]</sup> Unlike a systematic search which explores the energy surface of the molecule in a predictable fashion, the random search method searches the energy surface in a “random” mode. By changing either the atomic Cartesian coordinates or the torsion angles of

rotatable bonds, the conformational space can be explored. The Metropolis Monte Carlo scheme is often widely used for carrying out global minimum searches. The conformational analysis method for **3** described in this chapter is based on the Monte Carlo scheme.

The distance geometry method represents another conformational search approach.<sup>[27]</sup> Through changing inter-atomic distance within certain upper and lower inter-atomic “distance bounds”, the energy surface is explored and the low energy conformations are obtained.

The last but not the least conformational search method is called “molecular dynamics”.<sup>[28]</sup> In fact, it is a sum of two simulation methods, “Monte Carlo” and “molecular dynamics”. The method is basically the same as the corresponding simulation methods. The only difference is that the simulation methods do not include energy minimization. The Monte Carlo simulation method introduced here can be interdisciplinary between the random search method and the simulation method. The work report in this chapter is a modified Monte Carlo method with random change of torsion angles.

## **Results and Discussion**

A modified Monte Carlo search routine in dihedral space was developed and applied to help locate the global minimum of the acyclic organic small molecules, butane (**1**), *N*-methylacetamide (**2**) and tetra-*O*-acetyl-*N,N'*-dimethyl-*D*-glucaramide (**3**).

### **1. Monte Carlo method**

The general concept of a Monte Carlo (MC) dihedral space searching method is described. Our method started with a MM3 (Cartesian coordinates) file of the corresponding molecule, generated by Alchemy 2000 (Tripos). The molecule file was created with Alchemy 2000, subjected to a MM3 minimization to obtain a nearest energy minimum. The MM3 file for this low energy conformer represents the starting conformation in the study. The starting conformation was altered one random torsion angle selected randomly with a random increment angle, minimized to its nearest energy minimum, and the total steric energy was calculated. The energy is subject to a comparison with the “energy of the last completed step” to determine if the conformation is getting closer to a minimum value (global or local minimum). If the current energy is lower than the energy of last completed step, the conformation is kept as the starting conformation for the next run. If the energy is higher than the previous energy, the conformation is either discarded or undergoes a “temperature shaking” process. If the current conformation is discarded, the previous conformation will serve as the starting conformation again for the next run. A “temperature shaking” operation may be employed to determine if the conformation can be applied as the starting conformation for the next

run. The “temperature shaking” method will be discussed shortly in this section. After every completed step, the minimized conformation is also compared with all the saved conformations to determine if the conformation is unique from all the others. The MM3 (coordinates) files, total steric energy and variable torsion angles are all saved for future reference. Again, Alchemy 2000 was utilized to visualize the conformation.

In order to determine if a conformation is new or not, all the variable torsion angles of a conformation are subject to a comparison with all the previous conformations. Even if only one torsion angle difference is over the allowed value, the conformation is considered to be new. The criteria are subject to change according to the researcher’s requirements. The torsion angle difference tolerance is  $2.5^\circ$  in this study.

One common question for all random search methods: how can one be sure if the true global minimum is found.

In order to locate the real global minimum, several issues need to be considered. First of all, enough running steps should be performed, which depends on the size and complexity of the molecule being studied. It takes only about 9 steps on average to locate all the minima of butane but that number can be 10,000 – 100,000 or more to find the global minimum of a larger molecule. A fairly number of MC run is required in order to find the global minimum. Secondly, repeat running using the same protocol if necessary. For example, to locate all the minima of butane, five independent MC-MM3 studies with

1,000 steps each were carried out. All of the different runs located the same global minimum. A third and very critical issue is being able to simulate conformations at higher temperatures. The idea is that when the search is performed at low temperature (*e.g.*, room temperature or 0 °C), the conformation search quite often falls into a local minimum “crater” (“well”). By simulating the conformation and energy at a higher temperature, the Boltzmann factor ( $P = \exp(-\Delta E/RT)$ , also called probability) is calculated and compared with EFACT (a number generated randomly between 0 and 1). If the Boltzmann factor ( $P$ ) is larger than EFACT, the conformation is accepted and is utilized as the starting conformation for the next run. In other words, a higher energy conformation is accepted and functions as a starting conformation for the next run. This process simulates jumping out of the previous local minimum well and searching in another conformation region. This is the so called “temperature shaking” method. In this MC simulation study, for every 300 steps, 30 steps of temperature shaking at 100,000 K were applied.

## **2. Molecular mechanics modification**

The molecular mechanics method applied in this study is Allinger’s MM3 (92) program.<sup>[8-11]</sup>

One of the advantages of MM2/MM3/MM4 is that the atom types are defined very carefully according to hybridization and the molecular environment. The atom types applied in MM3 minimizations applied in this chapter are listed in Table 1.

**Table 1.** Atom types in MM3 (92)\*

ATOM TYPE	DESCRIPTION	AT WT	LTG	LT3	LT4	LT5	ITP	MPL	CRD
1	C CSP3	12.000	0	0	0	0	0	0	0
3	C CSP2 CARBONYL	12.000	0	0	0	0	0	3	0
5	H EXCEPT ON N, O, S	1.008	0	0	0	0	0	0	0
9	N NSP2	14.003	0	0	0	0	0	9	0
28	H H-N-C=O (AMIDE)	1.008	0	0	0	0	0	0	0
75	O O-H, O-C (CARBOXYL)	15.995	6	6	6	6	0	0	0
78	O O=C-O-C (ESTER)	15.995	7	0	0	0	7	0	0
79	O O=C-N< (AMIDE)	15.995	7	0	0	0	7	0	0

\* AT WT = ATOMIC WEIGHT  
 LTG = REPLACABLE ATOM TYPE FOR GENERAL LOCALIZED (LTYPEG)  
 LT3 = REPLACABLE ATOM TYPE FOR 3-MEM LOCALIZED (LTYPE3)  
 LT4 = REPLACABLE ATOM TYPE FOR 4-MEM LOCALIZED (LTYPE4)  
 LT5 = REPLACABLE ATOM TYPE FOR 5-MEM LOCALIZED (LTYPE5)  
 LTP = REPLACABLE ATOM TYPE DELOCALIZED (LTYPEP)  
 MPL = ATOM HAVING OUT-OF-PLANE BENDING IF NOT ZERO (KOUTP)  
 CRD = ATOM HAVING 4-COORDINATE BOND IF NOT ZERO (ITCOORD)

Torsion parameters are the other important constants in MM3. For most MM3 studies, bond angle and bond length are considered to be constant / ideal, and the torsion change is very critical to determine a conformation. Most torsion parameters required in this study were included in MM3 (92) (Table 2). However, two parameters were missing, 9-3-1-75 (N-C-C-O) and 3-1-75-3 (C-C-O-C).

The torsion angle of the 9-3-1-75 sequence is associated with an ester group adjacent to the amide moiety O-C-C(=O)-N. A set of constants was generated (ref) as V1=-2.157, V2=-0.592 and V3=-0.466. In this MC-MM3 project, the constants were added to the list of constants for MM3 (file KONST.MM3).

The second torsion angle sequence (3-1-75-3) is associated with an acetylated hydroxyl group adjacent to a carbonyl group. On the commercial program (Alchemy 2000, Tripos), these torsion parameters in MM3 are listed as V1=0.0, V2=0.0 and V3= 0.20. According to the suggestion of Dr. Jenn-Huei Lii at Allinger's lab at the University of Georgia, the torsion parameters of 2-1-75-3, are a fairly reasonable approximation of 3-1-75-3 and can be applied as the torsion constants of 3-1-75-3; V1=0.7246, V2=-0.6033 and V3=0.2583.

**Table 2.** Selected torsion parameters of MM3 (92)\*

W	ANGLE	V1	V2	V3	
0	1001001001	0.1850	0.1700	0.5200	( 1 T1)
0	1001001003	0.0000	0.4000	0.0100	( 11 T1)
0	1001001005	0.0000	0.0000	0.2800	( 42 T1)
0	1001075003	-2.2800	1.0000	0.0000	( 93 T1)
0	1003075001	1.0500	7.5000	-0.2000	( 95 T1)
0	1001003009	0.7000	-1.1000	0.3000	(178 T1)
0	1003009001	1.1000	3.8000	0.0000	(180 T1)
1	1003009028	0.0000	3.8000	0.0000	(468 T1)
1	5001009028	0.0000	0.0000	0.0800	(470 T1)
0	3001001005	0.0000	0.0000	0.1800	( 51 T1)
0	5001001005	0.0000	0.0000	0.2380	( 69 T1)
0	5001003075	0.2500	0.8500	0.0000	(118 T1)
0	5001075003	0.0100	0.0000	0.0000	(120 T1)
0	5001009003	0.0000	0.0000	0.0100	(191 T1)
0	78003075001	-2.6600	7.5000	0.2000	(142 T1)
2	75001003009	-2.1570	-0.5920	-0.4660	5/19/03
2	3001075003	0.7246	-0.6033	0.2583	5/19/03

\*  
W = RELIABILITY  
0 : FINAL  
1 : RELIABLE, BUT NOT FINAL (\*)  
2 : CRUED (TEMPORARY) (\*\*)  
ANGLE = TORSIONAL ANGLE  
V1, V2, V3 = TORSIONAL CONST

Another problem relates to coding of MM3 (92). Since MM3 (92) was the last version of this program to be distributed with a source code, it is by far the best choice for our

generation of a MC-MM3 package. Several modifications of the introductory part of the code have been performed (file naming conventions, etc) to make it easier to run the program in an automated fashion inside UNIX-based scripts. However, the full-matrix optimization routine in this version sometimes inverts the chirality of an atom. In the MC-MM3 package created in this study, the bug was corrected according to Dr. Lii's suggestions, too. The subroutine "fixyz" in mivib31.f was modified and a new subroutine "chkinv" was added to the mvib31.f module.

### **3. Program**

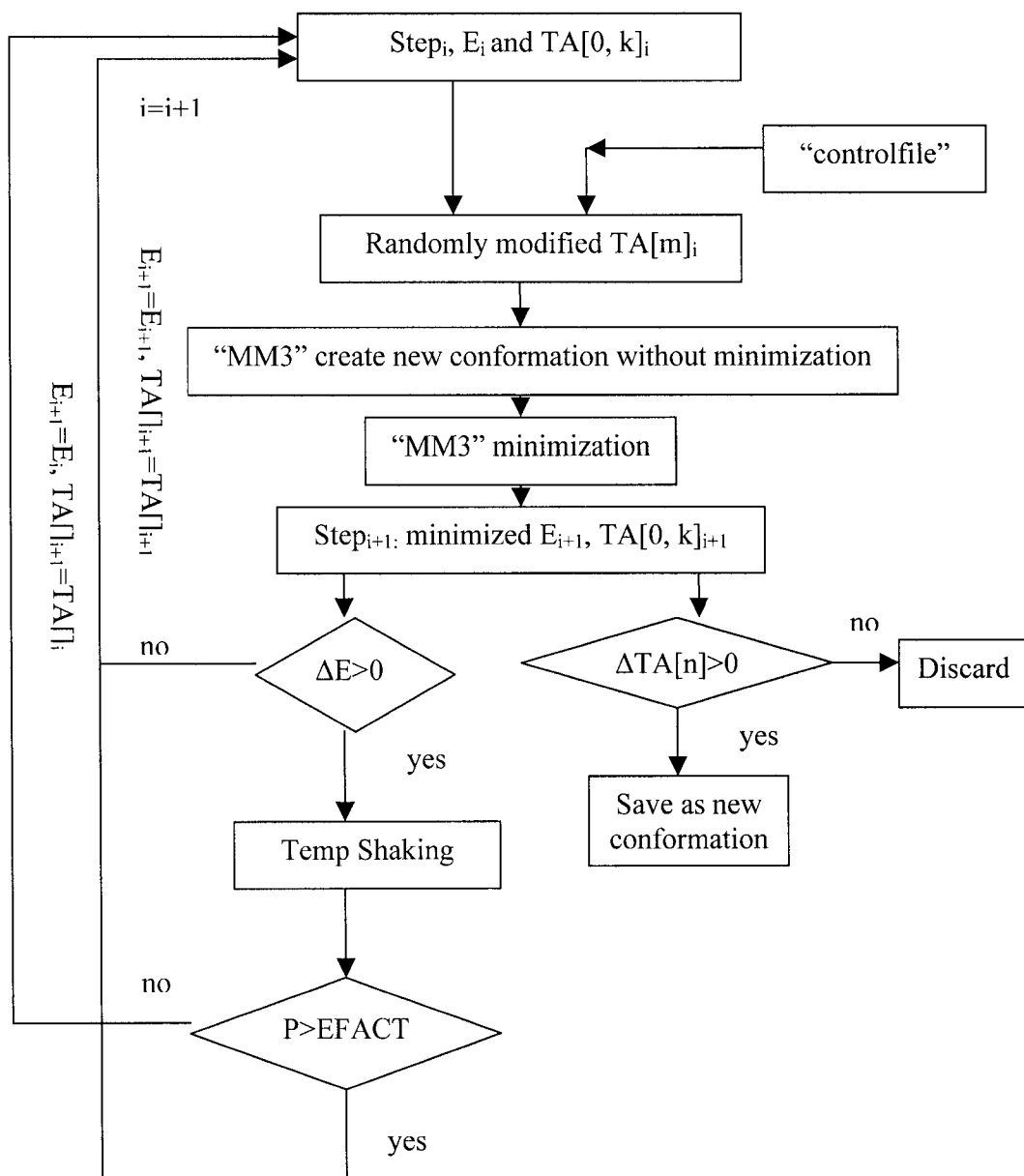
The MC searching program is written in FORTRAN 77. Two FORTRAN programs were written, "driver" and "analysis". A script was written to connect the subroutines and the MM3 (92).

The "driver" subroutine is utilized to generate a starting conformation set for MM3 by modifying a given MM3 coordinates file. A torsion angle is selected randomly from the control file. Then the adjustment of this torsion angle is generated randomly between -120° and +120°. Based on this information, a new "driverline", which forces MM3 to create a new conformation, will be generated. A new MM3 coordinates file is generated by putting the "driverline" into original MM3 coordinates file.

The new MM3 coordinates file is then served as input for the first MM3 run. In the first run, MM3 reads the driveline and forces the selected bond to rotate for selected degrees,



then creates another new MM3 coordinates file. The new MM3 coordinates file represents a new conformation which is consistent with our settings and serves as a new input file for the second MM3 run. The second MM3 run minimizes the conformation to its nearest minimum and calculates the total steric energy of the conformation. The total steric energy is compared with the energy of the last completed step in the following “analysis” subroutine.



**Scheme 1.** Flow diagram of MC-MM3.

The “analysis” subroutine “analyzes” the new conformation. Total steric energy is compared with the previous accepted energy (“energy of last completed step”). If the new

conformation has lower energy than the previous one, the conformation is kept to serve as the starting conformation for the next step of the MC-MM3 study. If the energy is higher than the previous energy, the energy may undergo a probability test. The Boltzmann factor [also called probability,  $P = (-\Delta E/RT)$ ] is calculated simulating very high temperature (100,000 K) and then compared with a random number between 0 and 1, which is called EFACT. If the probability (Boltzmann factor) is larger than EFACT, i.e., the energy is low enough for this certain conformation at high temperature, the energy is accepted and the conformation can serve as the starting conformation for the next step. Since the temperature is very high (100,000 K), the Boltzmann factor (probability) can be close to 1, i.e. the Boltzmann factor is always higher than EFACT and the conformation is always accepted at a reasonable energy level. The probability of locating other energy “craters”/ “wells” is very high and the probability of identifying a global minimum structure is very high, as well. The high temperature in this study is set at 100,000 K. In this study, for every 300 steps, 30 steps are processed to “temperature shaking”. The other task of the “analysis” subroutine is to determine if the accepted conformation is a new / unique conformation or not. Torsion angles of the accepted conformation are compared with all the previous conformations in the database generated in the course of MC searching process. The torsion angle difference allowed is defined by the user. In the study reported here, the torsion angle difference allowance is set to 2.5°. The Cartesian coordinates of every unique conformation are saved as “conformer.\*” (\* represent the number of new conformations generated) and the total steric energy and torsion angles are saved in “torsionsumm” file.

The script (script.mc) is utilized to connect the subroutines (“driver” and “analysis”) and MM3 code. The coordinates file (MM3 file) is copied in the script as the starting conformation for the next step of the MC study after going through the “analysis” subroutine.

#### 4. Demonstration studies

In order to demonstrate and test the MC-MM3 program, global minimum search of several small compounds are reported. The studies were performed on a Silicon Graphics (SGI) workstation. The MM3 minimizations were carried at dielectric constant 1.5 for the demonstration study.

Butane (**1**, Figure 2) was the first compound studied. Five independent runs with 1,000 steps were carried out. Three conformations were found by using the torsion angle criterion, the *anti* and both of the *gauche* forms. Among the five simulations, 4 steps were needed to locate all the three minima for the shortest run, 14 steps were needed to locate all the minima for the longest run, and the average number of steps to locate all the minima is 9. The total steric energy and the corresponding torsion angles are listed in Table 3.

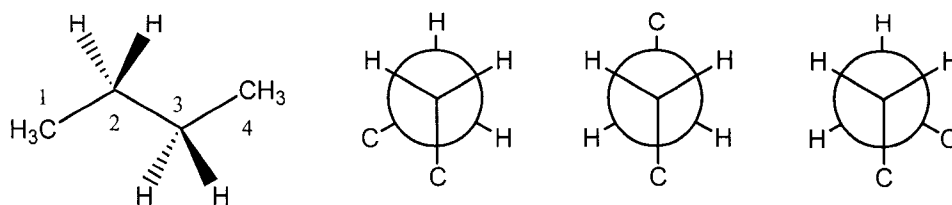


**Figure 2.** Newman projection of three minima of butane (1) along C2-C3 bond, from left to right are **1A** (*gauche*), **1B** (*anti*) and **1C** (*gauche*), respectively.

**Table 3.** Total steric energies (*E*, kcal/mol) and torsion angles ( $\omega$ , °) of butane minima at dielectric constant 1.5

	<i>E</i> (kcal/mol)	$\omega$ (C1-C2-C3-C4) (°)	steric relationship	overall conformation
<b>1A</b>	3.8952	65.1	<i>gauche</i>	bent
<b>1B</b>	<b>3.0862</b>	<b>180.0</b>	<b><i>anti</i></b>	<b>extended</b>
<b>1C</b>	3.8952	-65.1	<i>gauche</i>	bent

The other simple compound subjected to this computational routine was *N*-methylacetamide (**2**) (Figure 3). Three independent runs with 1,000 steps each were performed.

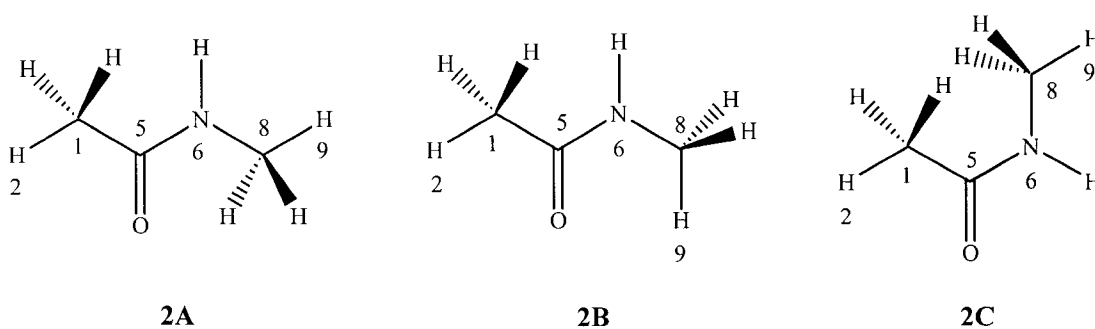


**Figure 3.** Minima of *N*-methylacetamide (**2**).

Interestingly, three minima (**2A**, **2B**, **2C**) of *N*-methylacetamide (**2**) were obtained. Three torsion angles were subject to vary in MC-MM3 simulation, H2-C1-C5-N6, C1-C5-N6-C8 and C5-N6-C8-H9.

The torsion angle of H2-C1-C5-N6 is always 180° or ±60° (*anti* or *gauche*, Table 4).

Since the three hydrogens (H2, H3, H4) are identical, either 180° or ±60° corresponds to the same conformation, *i.e.*, the hydrogen attached to the  $\alpha$ -carbon always adopts a *staggered* steric relationship with the amide nitrogen atom.

**Table 4.** Total steric energy (E, kcal/mol) and torsion angles ( $\omega$ , °) of *N*-methylacetamide (**2**) minima

	E (kcal/mol)	$\omega$ (H2-C1-C5- N6) (°)	$\omega$ (C1-C5- N6-C8) (°)	$\omega$ (C5-N6-C8- H9) (°)	overall conformation
<b>2A</b>	<b>-1.2308</b>	<b>±60.2/180.0</b>	<b>180.0</b>	<b>±60.3/180.0</b>	<b>zig-zag</b>
<b>2B</b>	-0.9146	±60.2/180.0	180.0	±120.4/0.0	zig-zag
<b>2C</b>	1.7045	±60.7/180.0	0.0	±60.7/180.0	bent

The torsion angle of C1-C5-N6-C8 turns out to be either 180° (**2A** and **2B**) or 0° (**2C**) for the minima, in which the energy difference of conformations **2A** and **2C** (identical for the rest part of the molecule) are 2.9353 kcal/mol (Table 4). The results suggest that the steric relationship of the two methyl groups are either *anti* (**2A**) or *eclipsed* (**2C**), in which, the *anti* conformation is more stable than the *eclipsed* conformation, consistent with the model-building method study introduced in chapter 1<sup>[29]</sup> of this dissertation and Allinger's study.<sup>[30]</sup>

The torsion angle of C5-N6-C8-H9 can be  $180^\circ/\pm 60^\circ$  (**2A** and **2C**), denotes an *anti* or *gauche* steric relationship, or  $0^\circ/\pm 120^\circ$  (**2B**), denotes *eclipsed* steric relationship. When H9 adopts an *anti* or *gauche* steric relationship with C5, the steric energy is lower than the *eclipsed* at 0.3162 kcal/mol. Even though the *anti* or *gauche* steric relationship of H9 and C5 leads to an *eclipsed* relationship of H9 and H7, the H9 prefers to be *staggered* with the much bulkier C5 to alleviate steric strain. Interestingly, this steric difference of C5-N6-C8-H9 only appeared on the lower energy conformers (**2A** and **2B**). For **2C**, the corresponding higher energy alignment of C5-N6-C8-H9 was not recognized as a fourth minimum. Consequently, the MC-MM3 ignored the higher energy alignment and generated only three minima for *N*-methylacetamide (**2**).

The longest run of MC-MM3 on *N*-methyl acetamide (**2**) took 12 steps to locate all the three minima. The shortest run located all the three minima in 3 steps and the other run located all the three minima in 5 steps.

##### **5. MC-MM3 study of 2,3,4,5-tetra-*O*-acetyl-*N,N'*-dimethyl-D-glucaramide (**3**)**

A MC-MM3 study of 2,3,4,5-tetra-*O*-acetyl-*N,N'*-dimethyl-D-glucaramide (**3**) was carried out at a dielectric constant 1.0 and was done in the “model building” approach (Chapter1). Here, 100,000 steps were performed with 12,737 unique conformations obtained (Table 5). The calculation was performed in 1,000, 3,000, 10,000, 20,000, 30,000, 40,000, 50,000, 60,000, 70,000, 80,000, 90,000 and 100,000 consecutive steps,

continued from the previous run by utilizing the last accepted conformation as the starting conformation. The last accepted energy is the “energy of the last completed step” for comparison, and the temperature shaking routine is employed.

**Table 5.** Number of new conformations found for MC-MM3 study of **3**

steps	1,000	3,000	10,000	20,000	30,000	40,000
unique conformations	416	882	2,200	3,835	5,093	6,316
steps	50,000	60,000	70,000	80,000	90,000	100,000
unique conformations	7,503	8,695	9,765	10,792	11,784	12,737

The MC-MM3 study of **3** gave four low energy conformations within a 1 kcal/mol range (Table 6). In the glucaryl backbone, the conformations are essentially identical. The differences of the four conformations are located at the acyloxy groups and C5-C6 end alignment. **C264** differs from **C250** in the torsion angle of carbonyl carbon (C29) to the backbone carbone (C1), C29-O10-C2-C1 torsion angle is 137.8° for **C250** but is 91.0° for **C264**. The **C2788** also differs from **C250** and **C264** with the same torsion angle (114.4°). **C5930** differs from the above three lower energy conformers at the C4-C5-C6-N8 torsion angle (109.6° for **C5930** and 102.4°, 102.8° and 102.6° for **C250**, **C264** and **C2788**, respectively).



**Table 6.** Four low energy conformations obtained from MC-MM3 study of **3**, total steric energy (E, kcal/mol) and backbone torsion angles ( $\omega$ , °)

	E (kcal/mole)	$\omega$ (C1-C2-C3-C4) (°)	$\omega$ (C2-C3-C4-C5) (°)	$\omega$ (C3-C4-C5-C6) (°)	Conformation
<b>C250</b>	0.8427	-53.7	-174.3	101.9	${}_2G^-$
<b>C264</b>	0.8857	-55.2	-173.2	101.6	${}_2G^-$
<b>C2788</b>	1.0235	-54.6	-173.5	101.6	${}_2G^-$
<b>C5930</b>	1.4385	-55.2	-172.9	102.7	${}_2G^-$
Extended	7.0895	-164.2	-175.9	-177.4	P

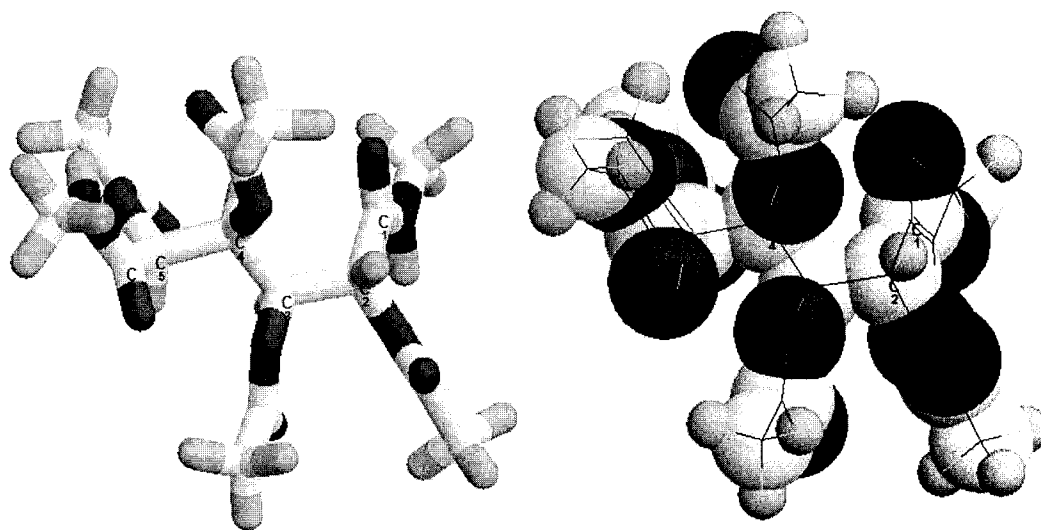


**Figure 4.** C250, the lowest energy conformation of **3**, tubing and spheres-and-sticks rendering ( ${}_2G^-$ ).

Although the conformation **C250** has a sickle conformation, it is not the same conformation as rotamer **3m** from 2,3,4,5-tetra-*O*-acetyl-*N,N'*-dimethyl-*D*-glucaramide in chapter 1 (numbered as compound **7a**, Figure 5), obtained using a “model-building approach”. Conformation C250 has a large dihedral angle (ca. -171.9°) between H15 – H16 and not between H16 – H17 (ca. -67.1) as suggested by the “model building” approach and <sup>1</sup>H NMR in Chapter 1. The lowest energy conformer **C250** was applied to Alchemy 2000 for energy calculation, the total steric energy appeared to be -1.1780 kcal/mol, much higher than the global minimum **3m** obtained from Alchemy MM3 calculation / “model-building approach” (-4.6424 kcal/mol). On the other hand, the global minimum **3m** obtained from the “model-building approach” was subjected to a MM3 minimization with the MM3 (Allinger) program in MC-MM3 system, the energy is 5.0840 kcal/mol, much higher than **C250** (Table 7).

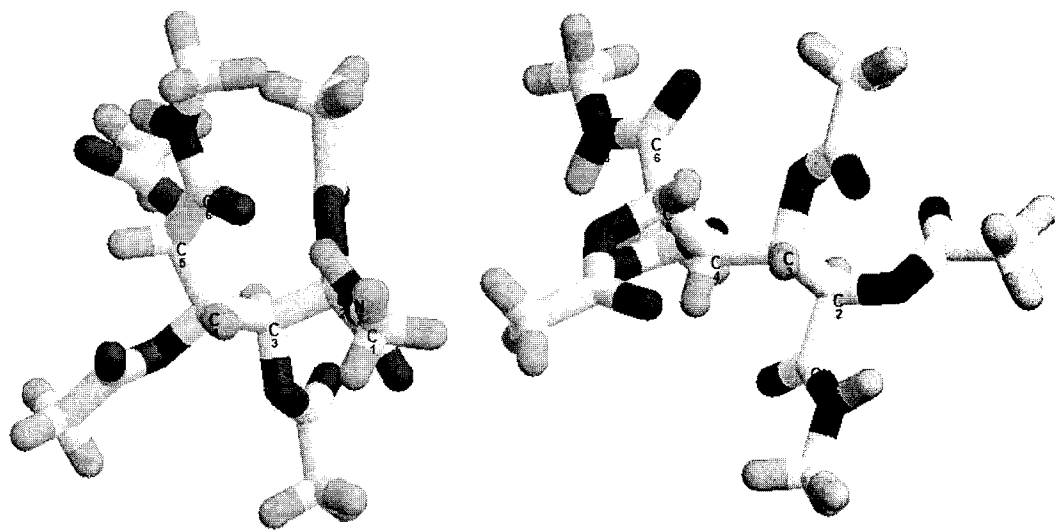


**Figure 5.** Global minimum (**3m**) generated from “model building” approach with the Tripos MM3 force field and **C250** generated from Monte Carlo dihedral angle search with MM3 (92) Allinger force field.

**Table 7.** Comparison of global minimum obtained from two different conformational analysis approaches (“model-building approach” and Monte Carlo dihedral angle search)

	Total steric energy (Alchemy 2000)	Total steric energy (MC-MM3)	Conformation	Force field	Conformational analysis method
<b>C250</b>	-1.1780	<b>0.8427</b>	${}_2G^-$	MM3 (Allinger)	Monte Carlo dihedral angle search
<b>3m</b>	<b>-4.6424</b>	5.0840	${}_2G^+{}_3G^+{}_4G^-$	MM3 (Sybyl)	Model building approach
Extended	0.6012	7.0895	P		

It was anticipated that the application of the different conformational analysis methods would lead to identical or comparable results. However, it appears that since the force fields applied in the two methods are not identical, it is understandable that the results are different. However, the results from this study do not appear to be in line with the  $^1\text{H}$  NMR data analyzed in Chapter 1.

**Conclusions:**

1. Monte Carlo dihedral space search joint with MM3 minimization is a reliable technique for probing conformational space locating global minimum.
2. Temperature shaking represents a valid approach to bypass the energy barrier between different energy regions to facilitate the global minimum search.
3. Again, molecular mechanics proved to be a promising method for conformational study of a somewhat complex carbohydrate related molecule.

## References

1. Wiberg, K. B and Murcko, M.A. Rotational Barriers. 2. Energies of Alkane Rotamers. An Examination of Gauche Interactions. *Journal of American Chemical Society* **1988**, 110: 8029-8038.
2. Leach, Andrew R. *Molecular Modeling Principles and Applications*. **2001**, Prentice Hall.
3. Dewar, M. J. S.; Jie, C. And Yu J. SAM1; The First of a New Series of General Purpose Quantum Mechanical Model Models. *Tetrahedron* **1993**, 49: 5003-5038.
4. Dewar, M. J. S. *The Molecular Orbital Theory of Organic Chemistry*. **1969**, New York, McGraw-Hill.
5. Atkins, P. W. And Friedman, R. S. *Molecular Quantum Mechanics*. **1996**, Oxford, Oxford University Press.
6. Szabo, A. And Oslund, N. S. *Modern Quantum Chemistry. Introduction to Advanced Electronic Structure Theory*. **1982**, New York, McGraw-Hill.
7. Allinger, N. L. Conformational Analysis 130. MM2. A Hydrocarbon Force Field Utilizing V1 and V2 Torsional Terms. *Journal of American Chemical Society* **1977**, 99: 8127-8134.
8. Allinger, N. L., Yuh, Y. H. And Lii, J-J *Molecular Mechanics. The MM3 Force Field for Hydrocarbons I*. *Journal of American Chemical Society* **1989**, 111: 8551-8556.
9. Lii, J-H and Allinger, N. L. *Molecular Mechanics. The MM3 Force Field for Hydrocarbons. 2. Vibrational Frequencies and Thermodynamics*. *Journal of American Chemical Society* **1989**, 111: 8566-8582.
10. Allinger, N. L., Li, F. And Yan, L. *Molecular Mechanics. The MM3 Force Field for Alkenes*. *Journal of Computational Chemistry* **1990**, 11: 848-867.
11. Allinger, N. L., Li, F., Yan, L. And Tai J. C. *Molecular Mechanics (MM3) Calculations on Conjugated Hydrocarbons*. *Journal of Computational Chemistry* **1990**, 11: 868-895.
12. Allinger, N. L., Chen, K. And Lii, J-H *An Improved Force Field (MM4) for Saturated Hydrocarbons*. *Journal of Computational Chemistry* **1996**, 17(642-668).

13. Allinger, N. L., Chen, K., Katzenelenbogen, J. A., Wilson, S. R. And Anstead, G. M. Hyperconjugative Effects on Carbon-Carbon Bond Lengths in Molecular Mechanics (MM4). *Journal of Computational Chemistry* **1996**, 17: 747-755.
14. Nevins, N., Chen, K. And Allinger, N. L. Molecular Mechanics (MM4) Calculations on Alkenes. *Journal of Computational Chemistry* **1996**, 17: 669-694.
15. Nevins, N., Chen, K. And Allinger, N. L. Molecular Mechanics (MM4) Calculations on Conjugated Hydrocarbons. *Journal of Computational Chemistry* **1996**, 17: 695-729.
16. Nevins, N., Chen, K. And Allinger, N. L. Molecular Mechanics (MM4) Vibrational Frequency Calculations for Alkenes and Conjugated Hydrocarbons. *Journal of Computational Chemistry* **1996**, 17: 730-746.
17. Weiner, S. J., Kollman, P. A., Case, D. A., Singh, U. C., Chio, C., Alagona, G., Profeta, S. And Weiner, P. A New Force Field for Molecular Mechanical Simulation of Nucleic Acids and Proteins. *Journal of American Chemical Society* **1984**, 106(765-784).
18. Cornell, W. D., Cieplak, P., Bayly, C. I., Gould, I. R., Merz, K. M. Jr, Ferguson, D. M., Spellmeyer, D. C., Fox, T., Caldwell, J. W. And Kollman, P. A. A Second Generation Force Field for the Simulation of Proteins, Nucleic Acids and Organic Molecules. *Journal of American Chemical Society* **1995**, 117(5179-5197).
19. Allinger, N. L. Operating Instructions for MM3 (92) Force Field for Unix and Vax **1992**.
20. Barton, D. H. R. The Conformation of the Steroid Nucleus. *Experientia* **1950**, 6: 66-69.
21. Ramachadran, G. N., Ramakrishnana, C. And Sasiexharan, V. Stereochemistry of Polypeptide Chain Configurations. *Journal of Molecular Biology* **1963**, 7: 95-99.
22. Styron, Susan D.; French, Alfred D.; Friedrich, Joyce D.; Lake, Charles H.; Kiely, Donald E. MM3(96) conformational analysis of D-glucaramide and x-ray crystal structures of three D-glucaric acid derivatives-models for synthetic poly(alkylene D-glucaramides). *Journal of Carbohydrate Chemistry* **2002**, 21(1 & 2): 27-51.
23. Gibson, K. D. And Scheraga, H. A. Revised Algorithms for the Build-Up Procedure for Predicting Protein Conformations by Energy Minimization. *Journal of Computational Chemistry* **1987**, 8(6): 826-834.

24. Leach, Andrew R., Rrout, Keith and Dolata, Daniel P. An Investigation into the Construction of Molecular Models by the Template Joining Method. *Journal of Computer-Aided Molecular Design* **1988**, 2: 107-123.
25. Leach, A. R., Dolata, D. P. And Prout, K. Automated Conformational Analysis and Structure Generation: Algorithms for Molecular Perception. *Journal of Chemical Information and Computer Science* **1990**, 30: 316-324.
26. Saunders, M. Stochastic Exploration of Molecular Mechanics Energy Surface: Hunting for the Golbal Minimum. *Journal of American Chemical Society* **1987**, 109: 3150-3152.
27. Crippen, G. M. Distance Geometry and Conformational Calculations. *Chemometrics REsearch Studies Series 1*. **1981**, New York, John Wiley & Sons.
28. Dosen-Micovic, Ljiljana Searching conformational space with molecular mechanics method. Dihedral angle random increment search. *Tetrahedron* **1995**, 51(24): 6789-96.
29. Zhang, Jinsong; Styron, Susan D.; Davis, Erin S.; Gerdes, John M.; Kiely, Donald E.. Comparison of molecular mechanics and dynamics studies of D-glucaramide and related derivatives. **2003**, Abstracts of Papers, 225th ACS National Meeting, New Orleans, LA, United States, March 23-27, 2003
30. Lii, Jenn Huei; Allinger, Norman L.. The MM3 force field for amides, polypeptides, and proteins. *Journal of Computational Chemistry* **1991**, 12(2): 186-99.

Appendix 1. Spectra of Compounds in Chapter 1 and Chapter 2

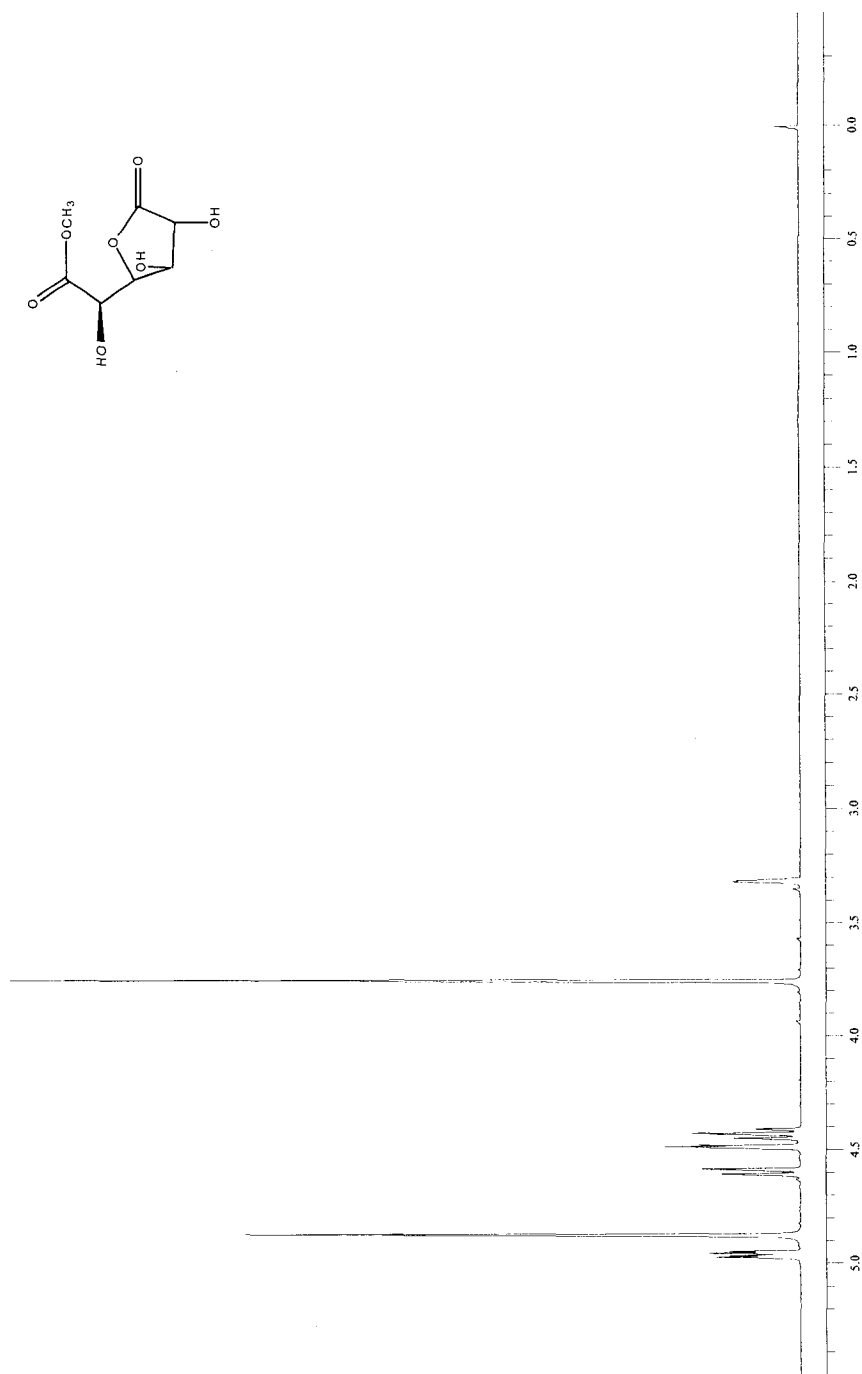
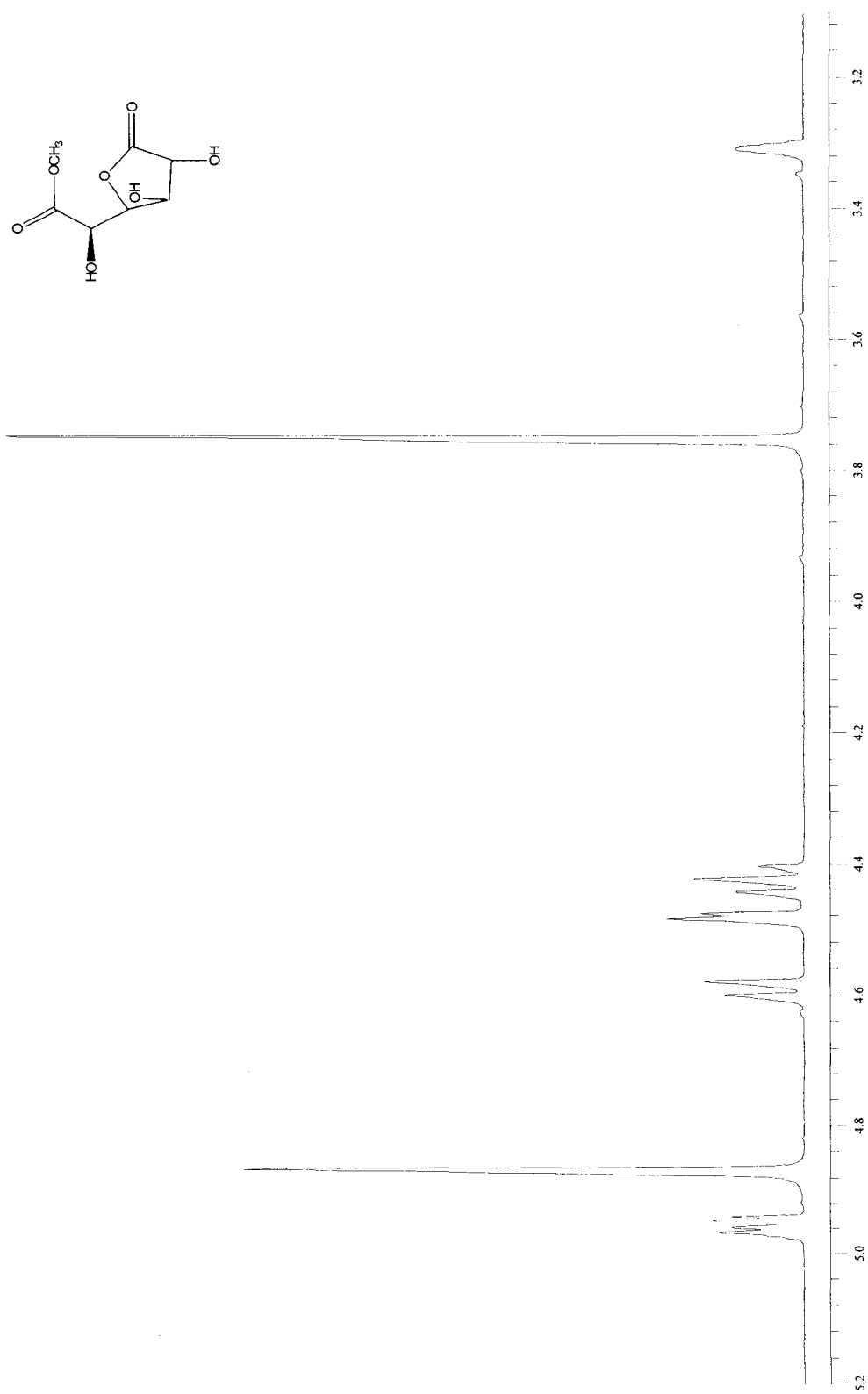
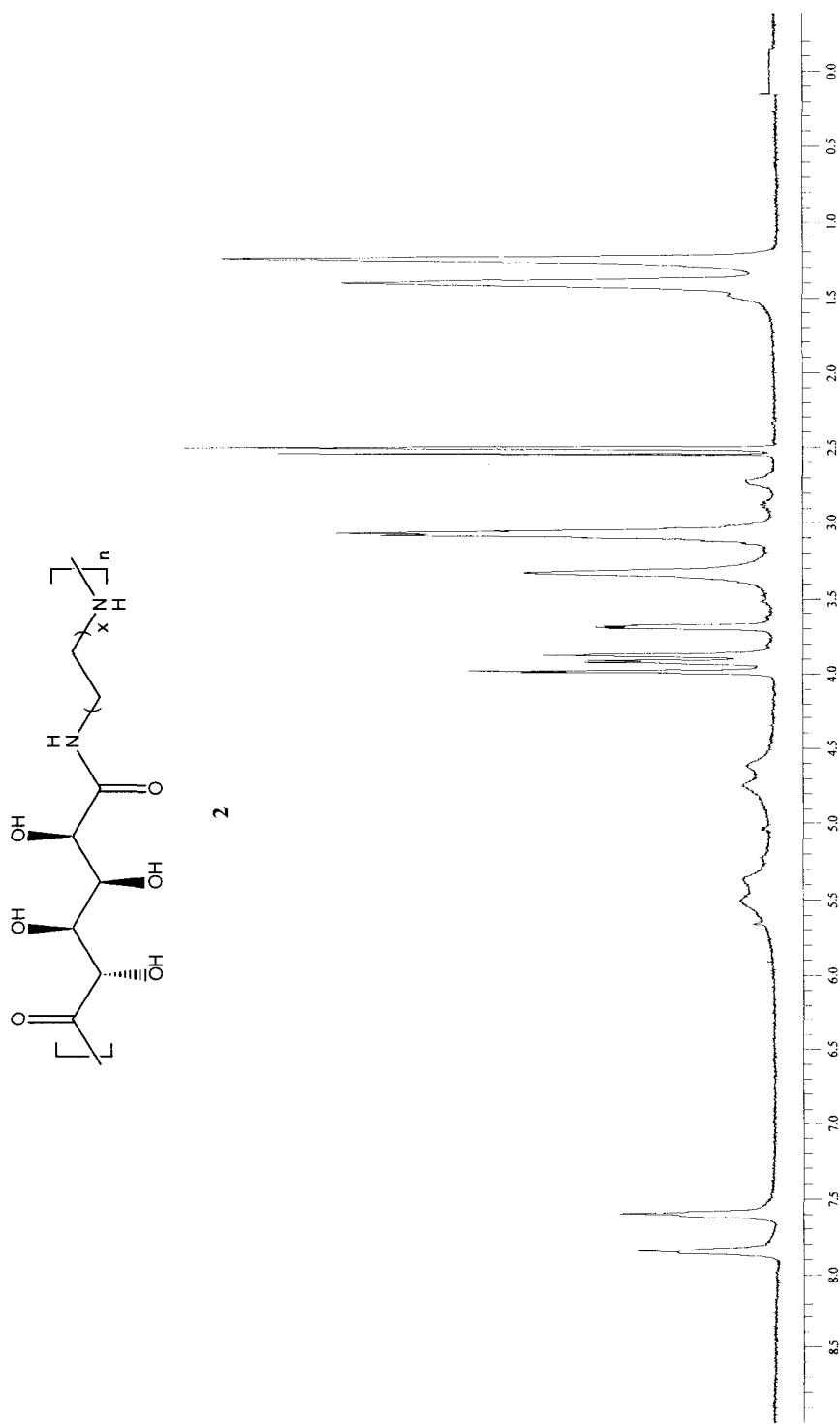


Figure 1. <sup>1</sup>H NMR (DMSO-d<sub>6</sub>) spectrum of methyl D-glucarate 1,4-lactone (I).





**Figure 2.** <sup>1</sup>H NMR (DMSO-d<sub>6</sub>) spectrum of methyl D-glucarate 1,4-lactone (I).



**Figure 3.** <sup>1</sup>H NMR (CDCl<sub>3</sub>) spectrum of poly(hexamethylene D-glucaramide) (2).

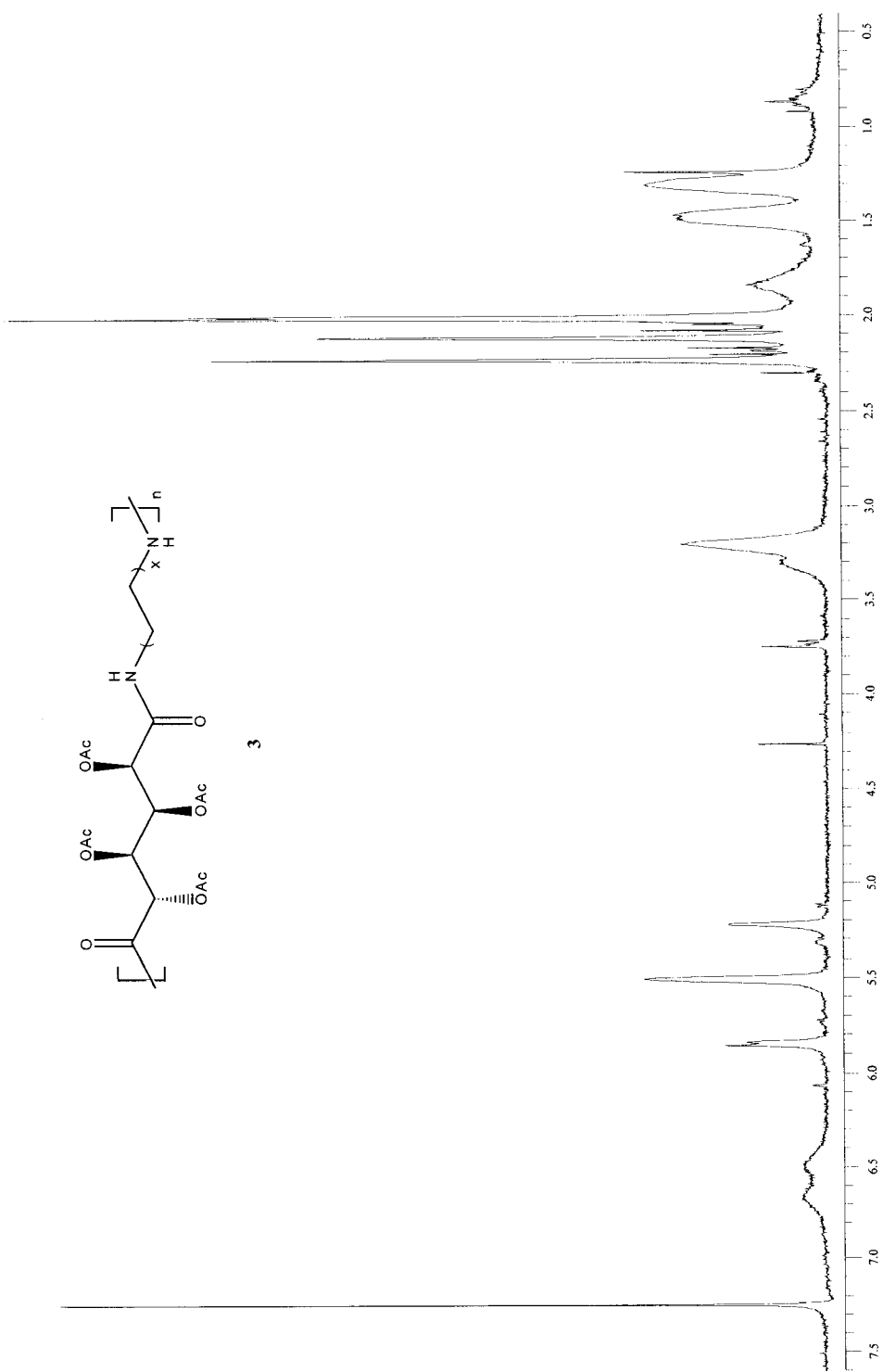


**Figure 4.** <sup>1</sup>H NMR (CDCl<sub>3</sub>) spectrum of poly(hexamethylene tetra-O-acetyl-D-glucaramide) (3).

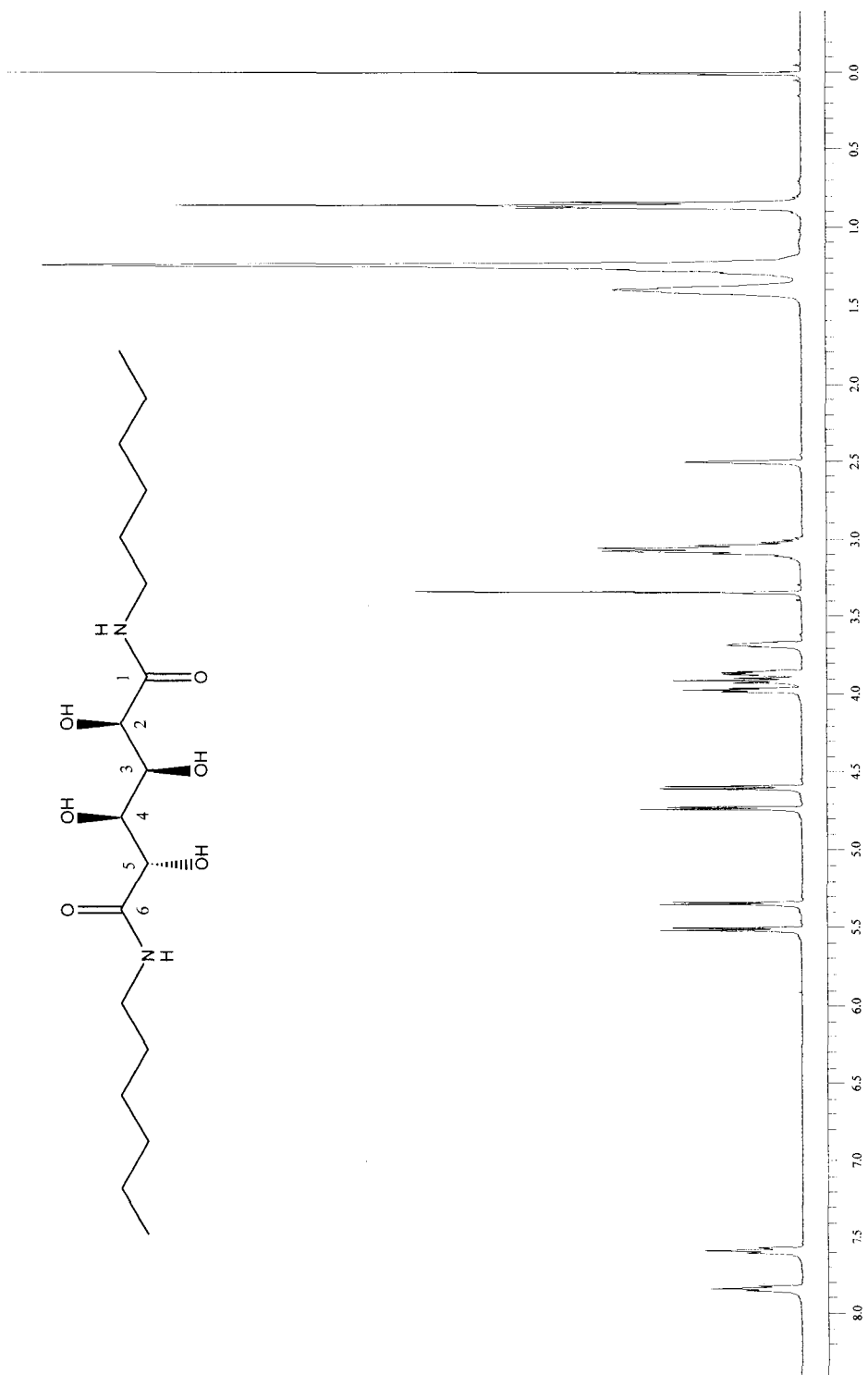


**Figure 5.** <sup>1</sup>H NMR (DMSO-d<sub>6</sub>) spectrum of *N,N'*-dihexyl-D-glucaramide (4).

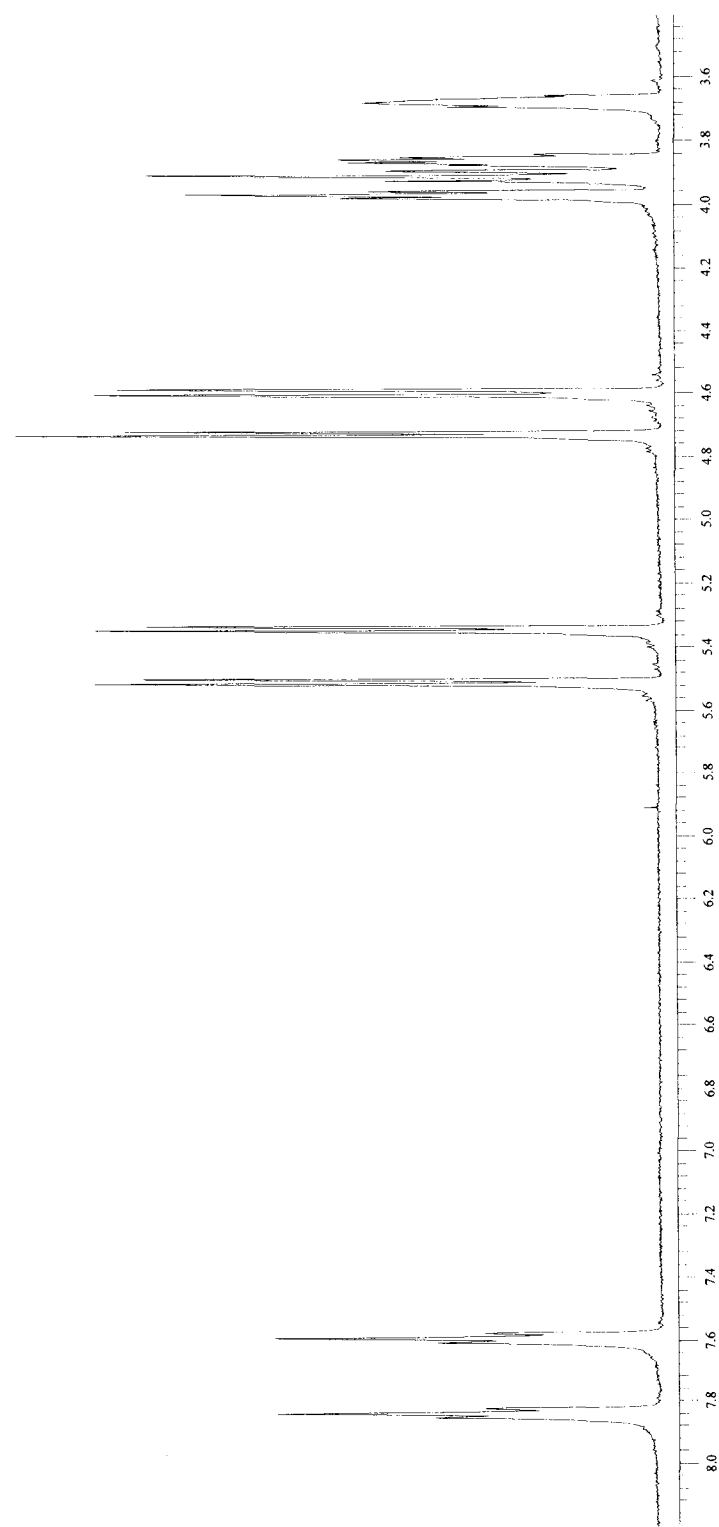
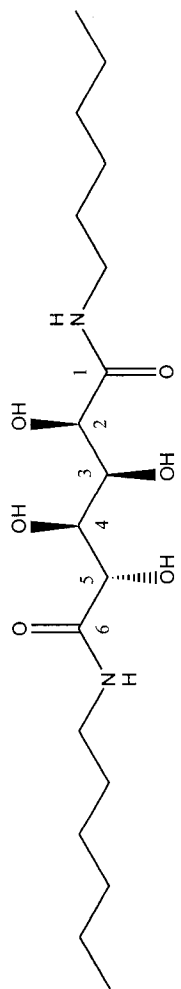


**Figure 6.**  $^1\text{H}$  NMR (DMSO- $d_6$ ) spectrum of *N,N'*-dihexyl-D-glucaramide (4) 3.4 – 8.2 ppm.

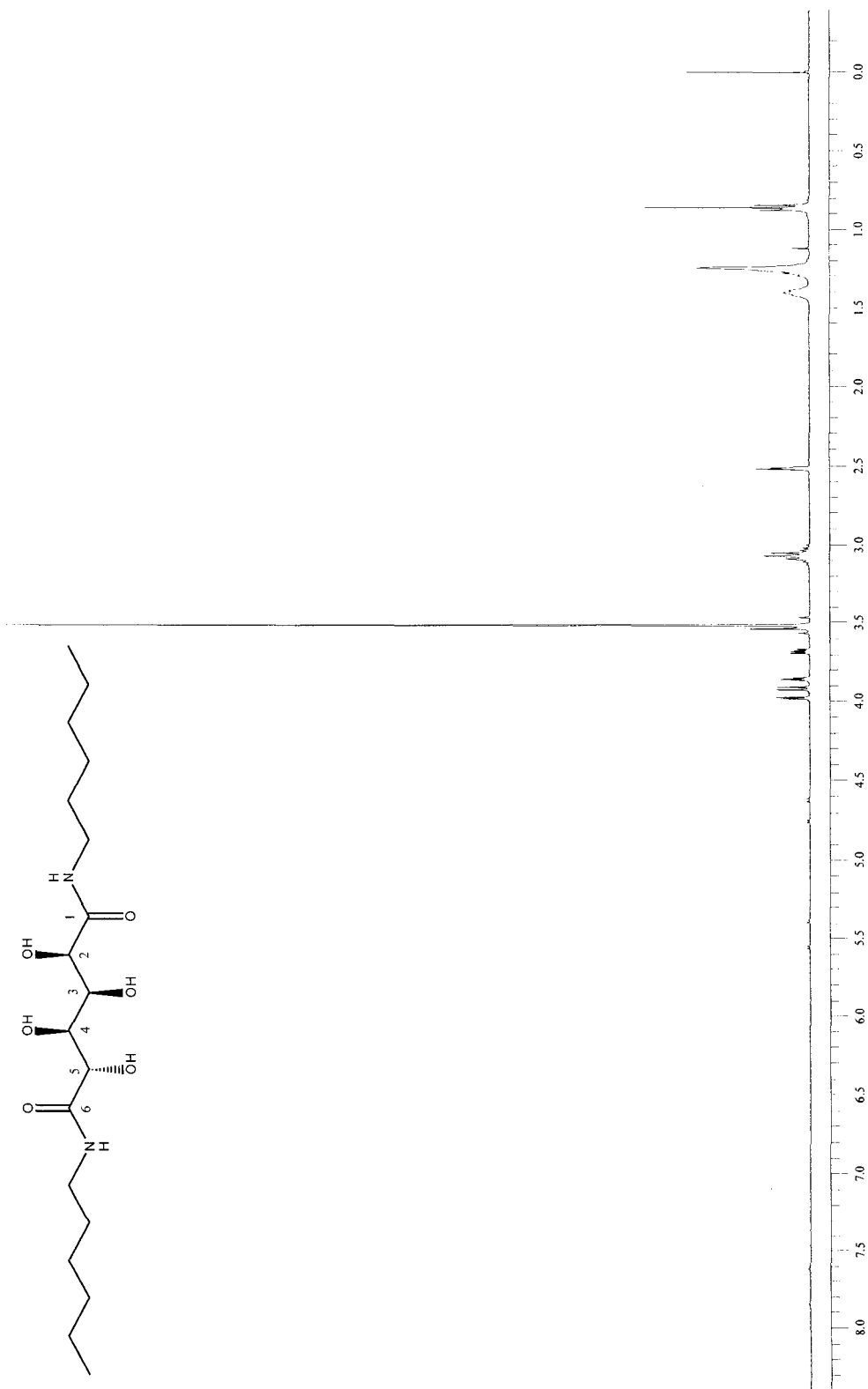


**Figure 7.** <sup>1</sup>H NMR (DMSO-d<sub>6</sub>) spectrum of *N,N'*-dihexyl-D-glucaramide (4, add 2 drops D<sub>2</sub>O).

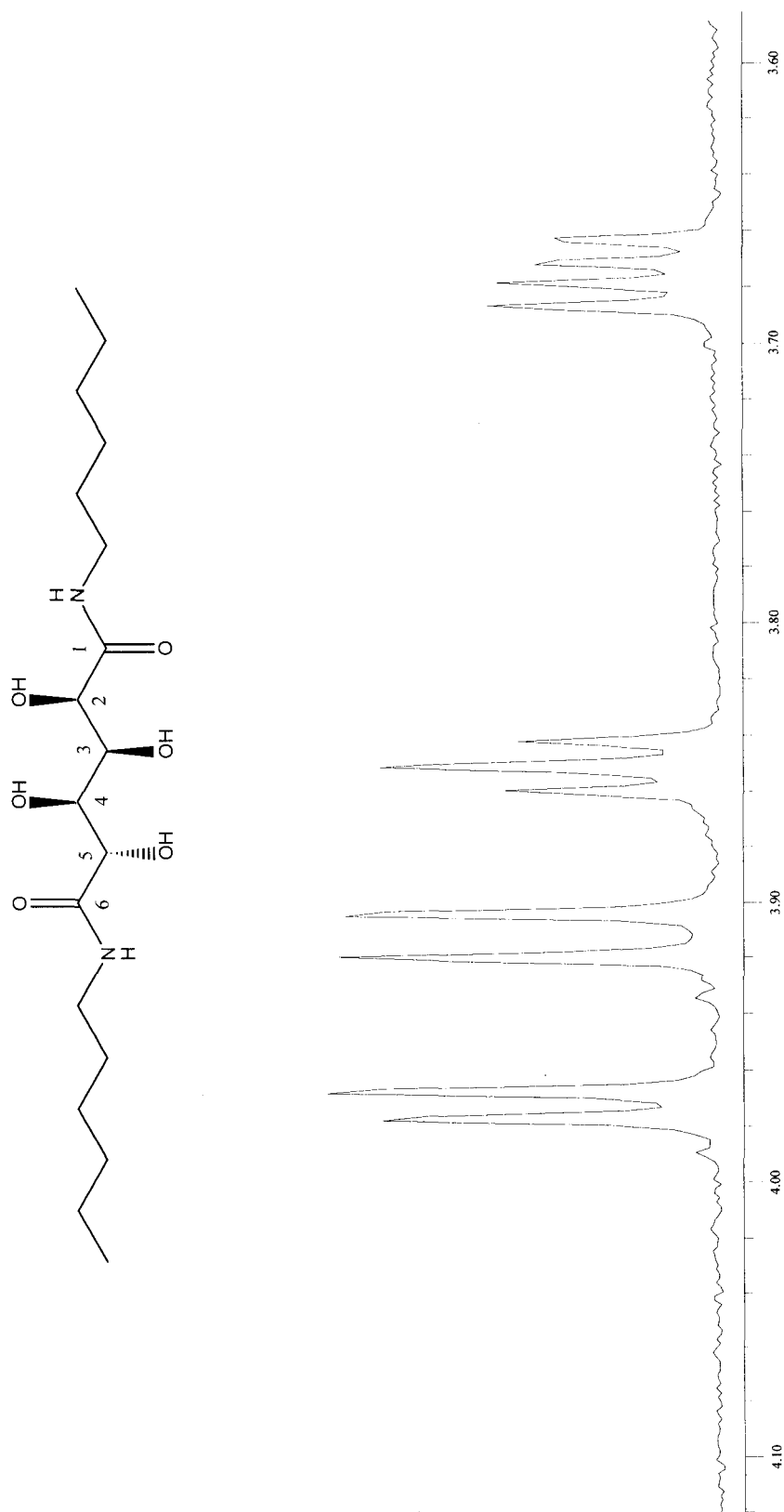


**Figure 8.** <sup>1</sup>H NMR (DMSO-d<sub>6</sub>) spectrum of *N,N'*-dihexyl-D-glucaramide (**4**, add 2 drops D<sub>2</sub>O) 3.58 – 4.12 ppm.

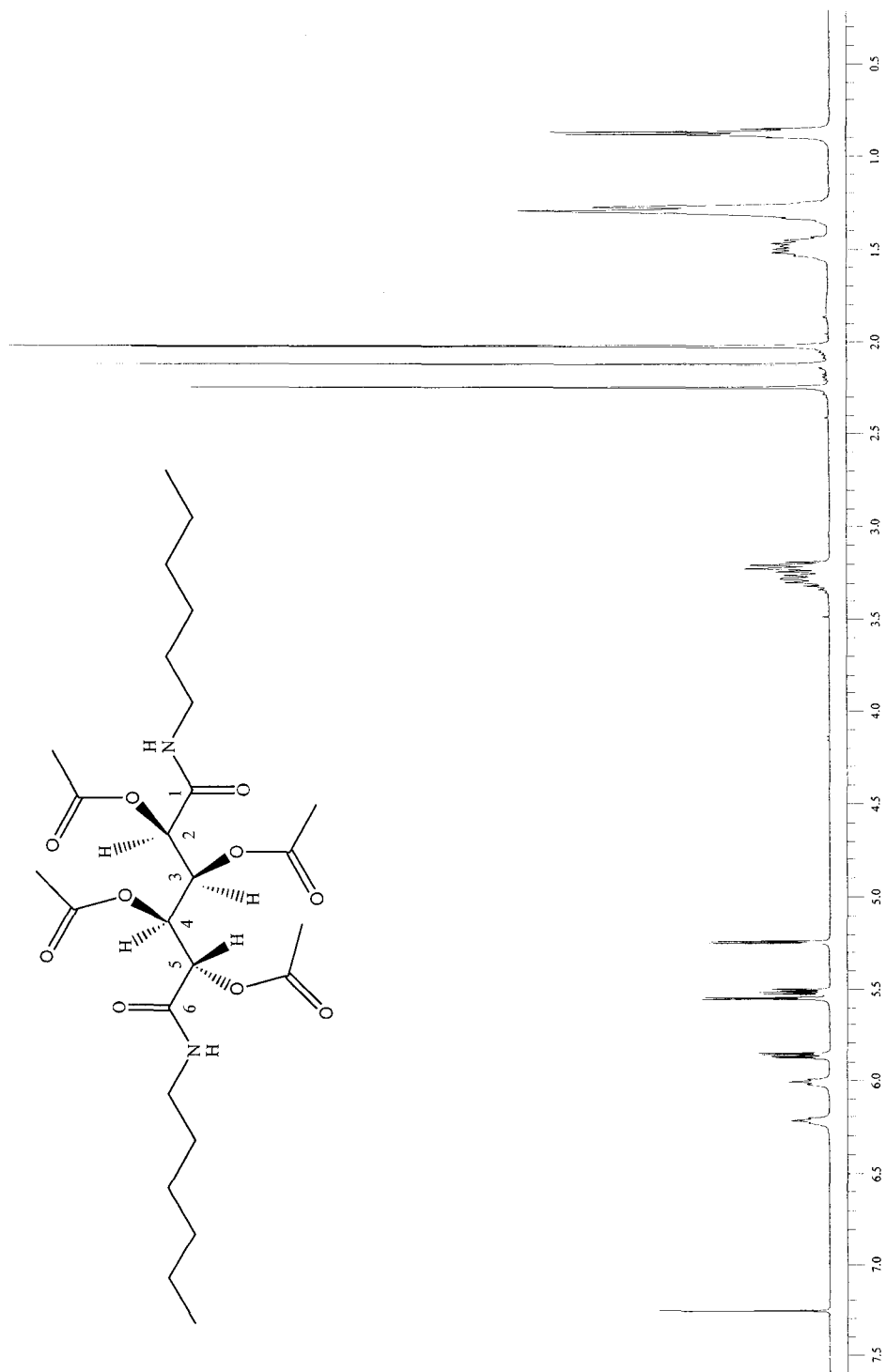


**Figure 9.** <sup>1</sup>H NMR (CDCl<sub>3</sub>) spectrum of tetra-*O*-acetyl-*N,N'*-dihexyl-D-glucaramide (**5a**)



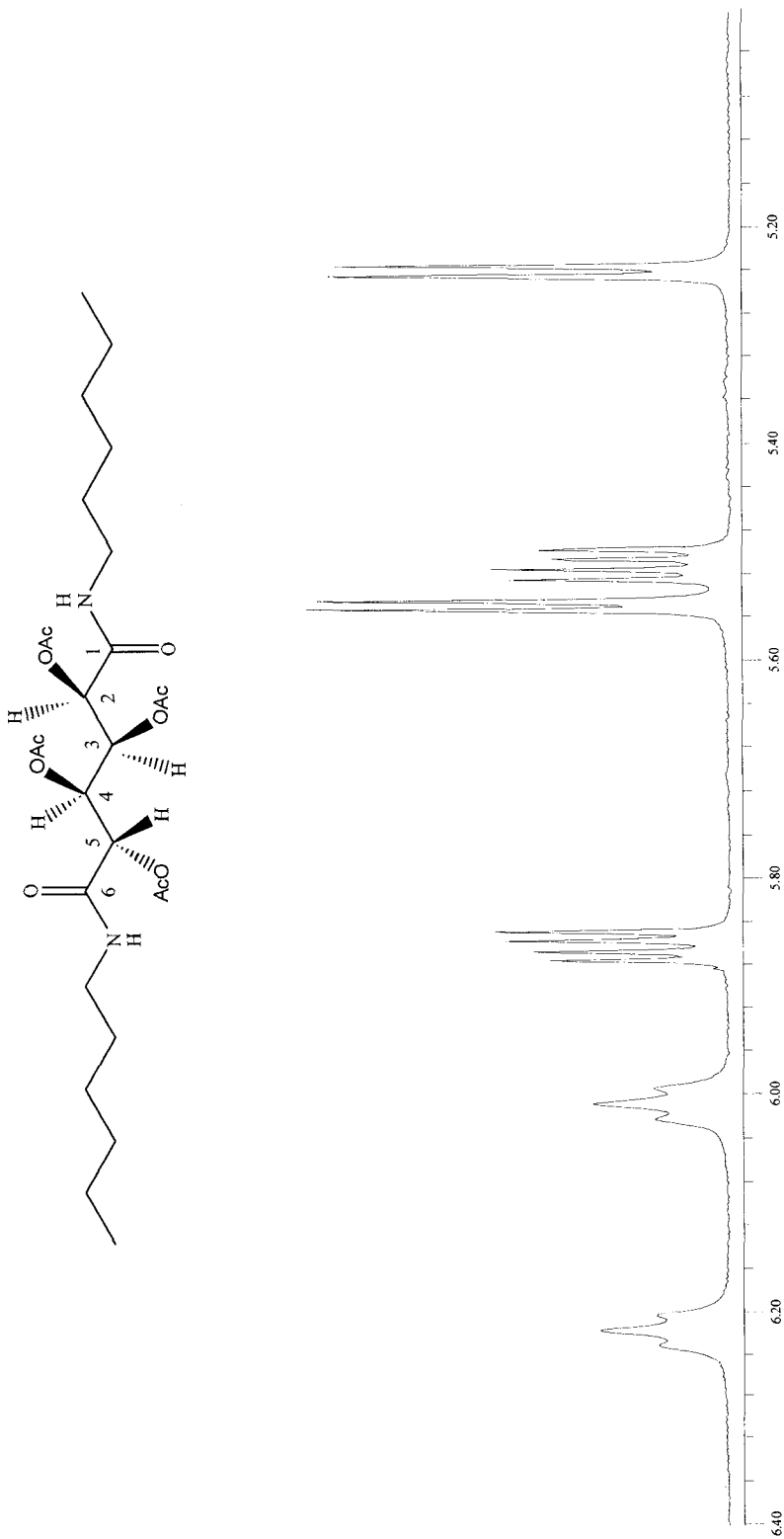


**Figure 10.** <sup>1</sup>H NMR (CDCl<sub>3</sub>) spectrum of tetra-O-acetyl-L,N,N'-dihexyl-D-glucaramide (**5a**) 5.00 – 6.40 ppm.

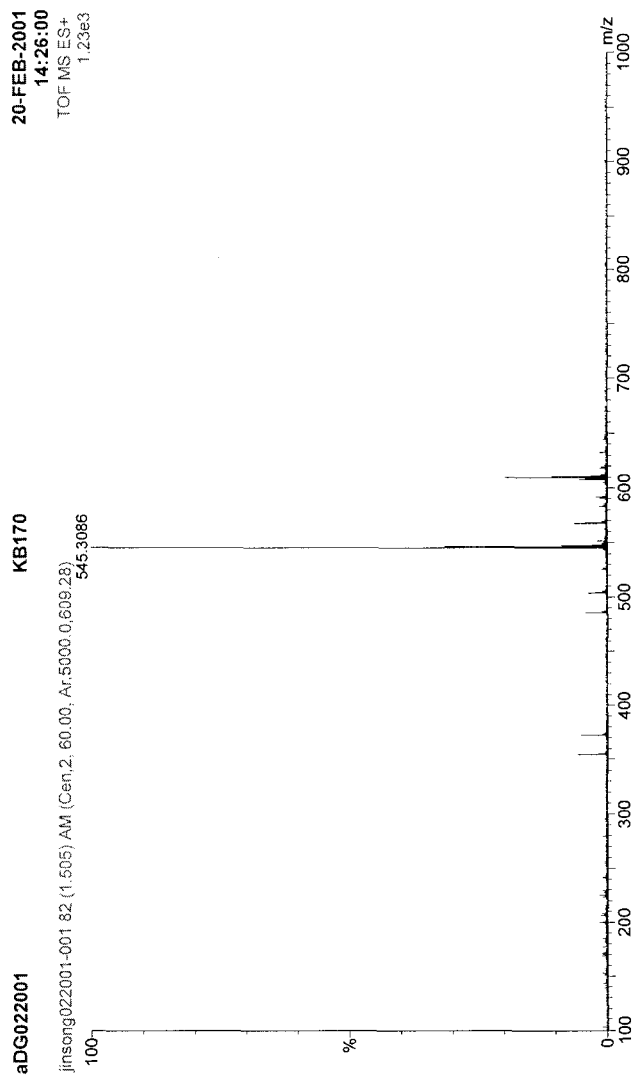
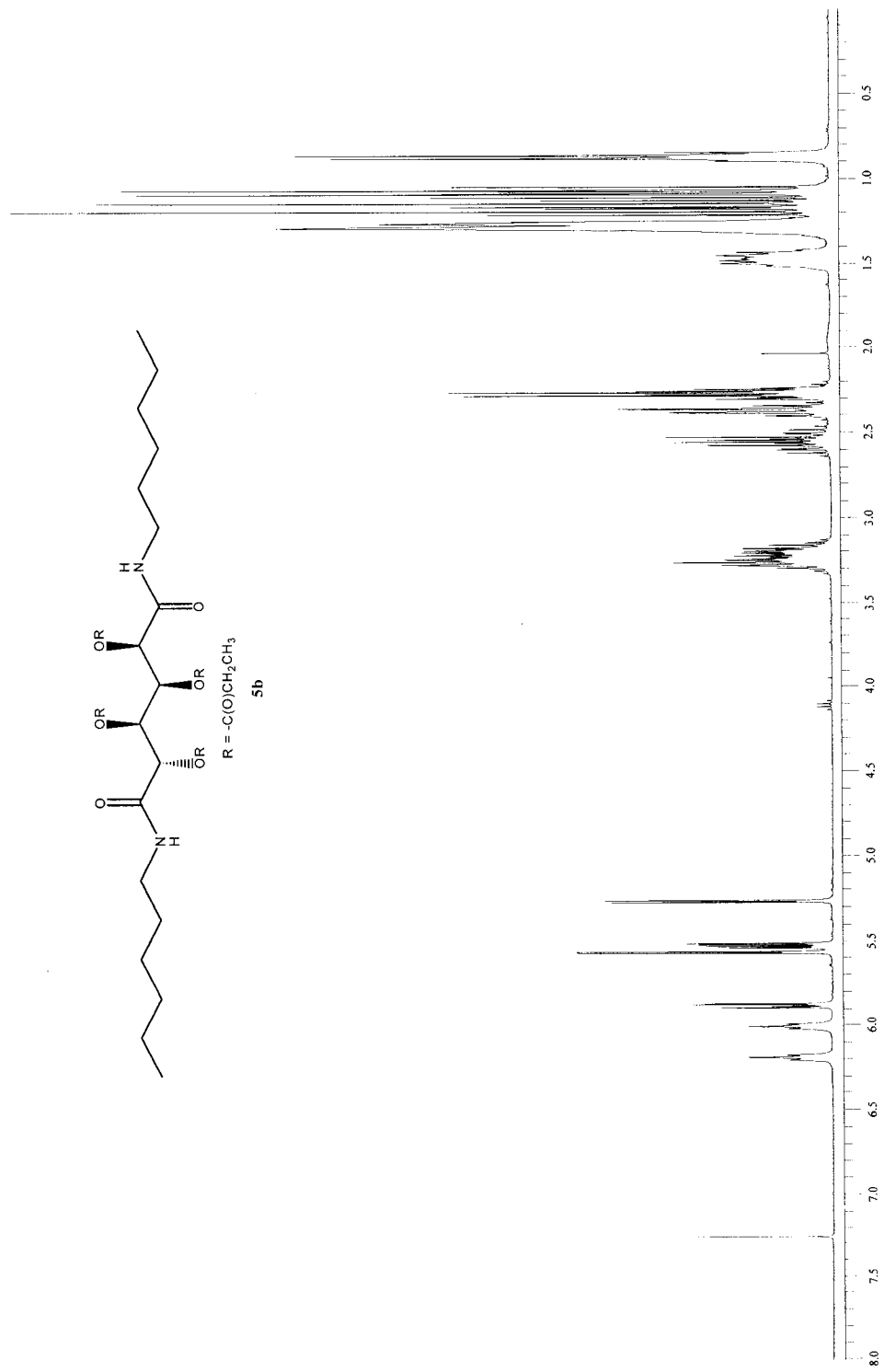
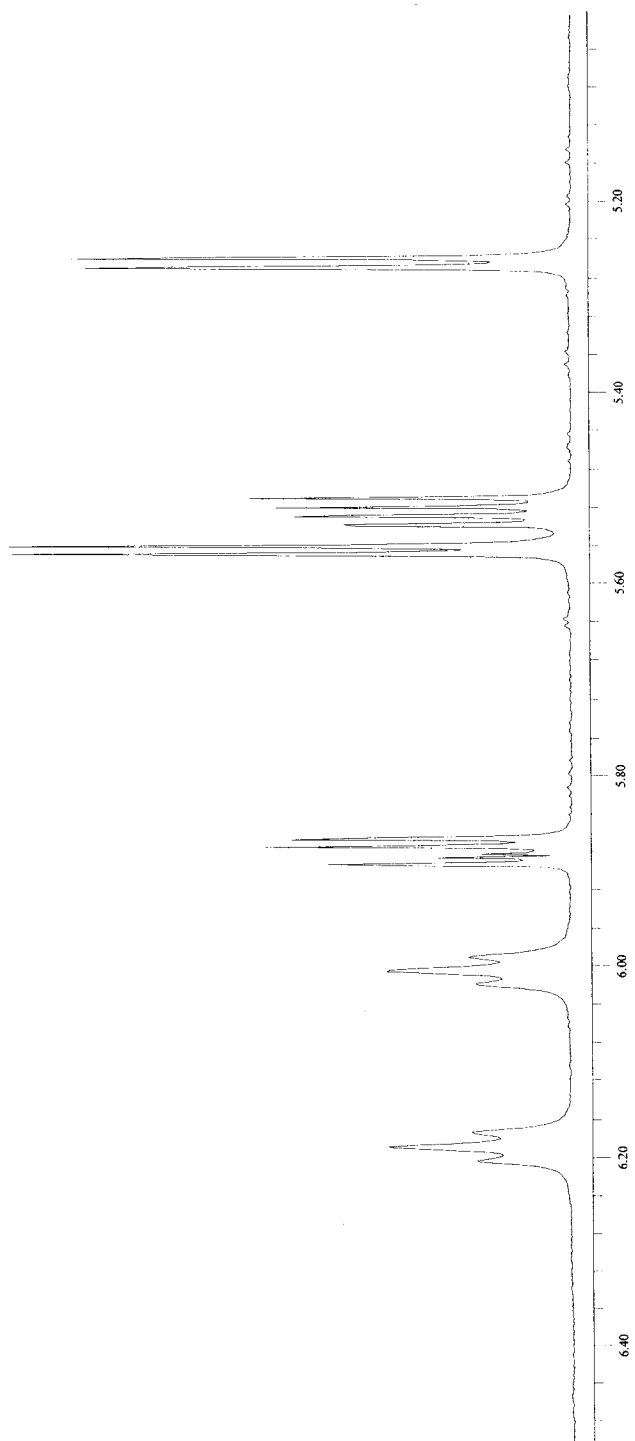
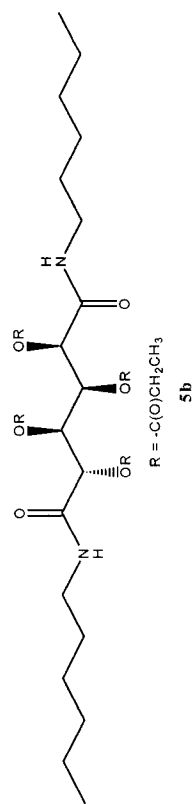


Figure 11. Mass (TOF electron spray) spectrum of tetra-*O*-acetyl-*N,N'*-dihexyl-*D*-glucaramide (**5a**).



**Figure 12.**  $^1\text{H}$  NMR (CDCl<sub>3</sub>) spectrum of tetra-*O*-propanyl-*N,N'*-dihexyl-D-glucaramide (**5b**).



**Figure 13.**  $^1\text{H}$  NMR ( $\text{CDCl}_3$ ) spectrum of tetra-*O*-propanyl-*N,N'*-dihexyl-D-glucaramide (**5b**) 5.00 – 6.50 ppm.

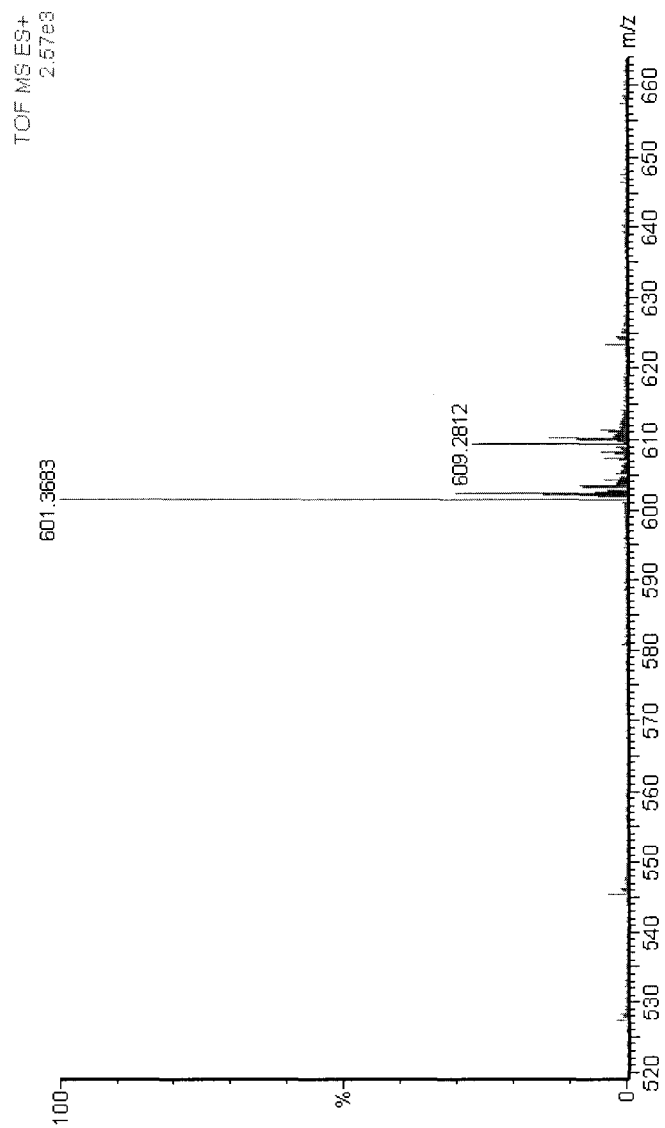


**Figure 14.** Mass (TOF electron spray) spectrum of tetra-*O*-propanyl -*N,N'*-dihexyl-D-glucaramide (**5b**).

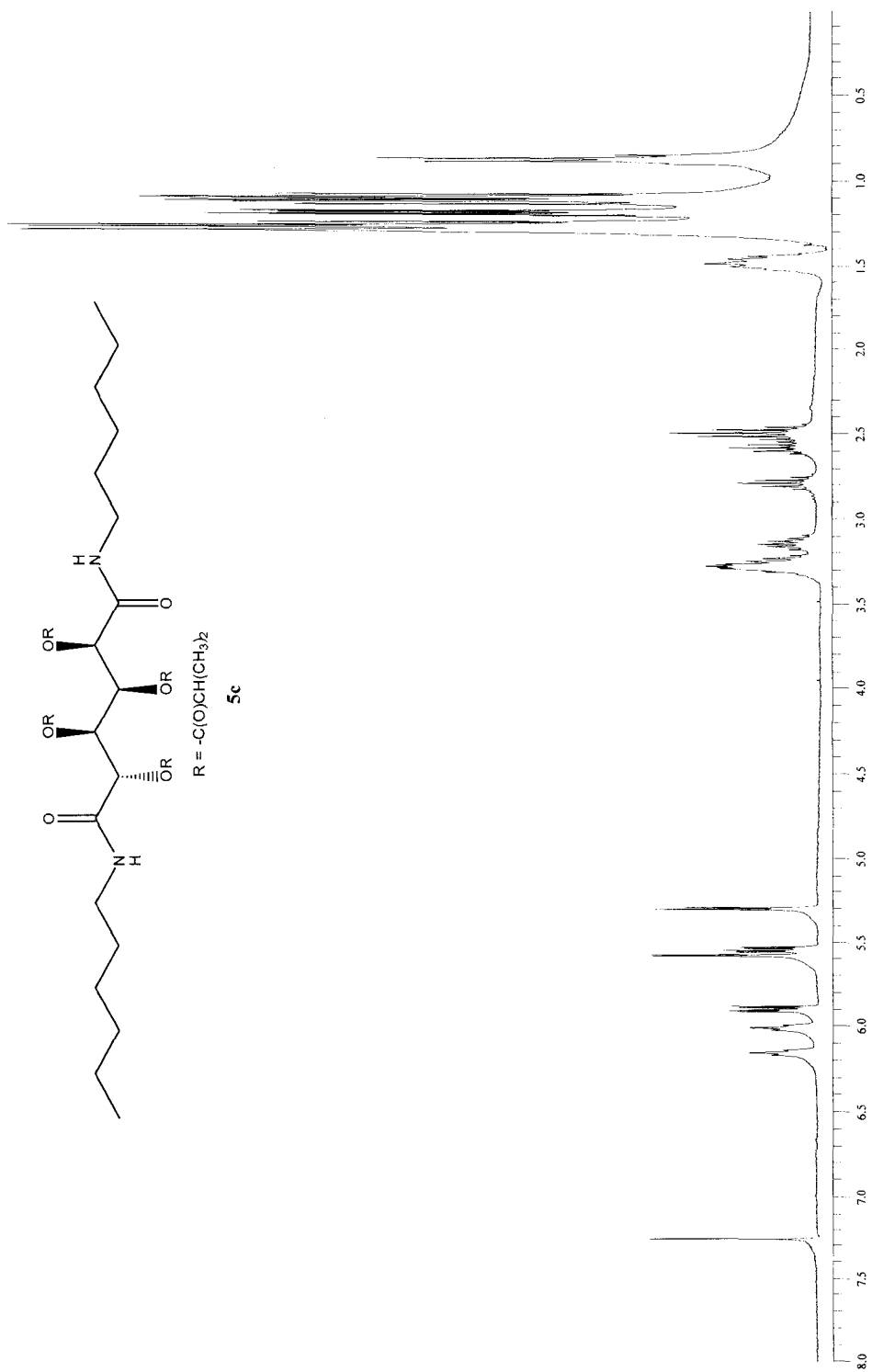


**Figure 15.**  $^1H$  NMR (CDCl<sub>3</sub>) spectrum of tetra-*O*-methylpropanyl-*N,N'*-dihexyl-D-glucaramide (**5c**).

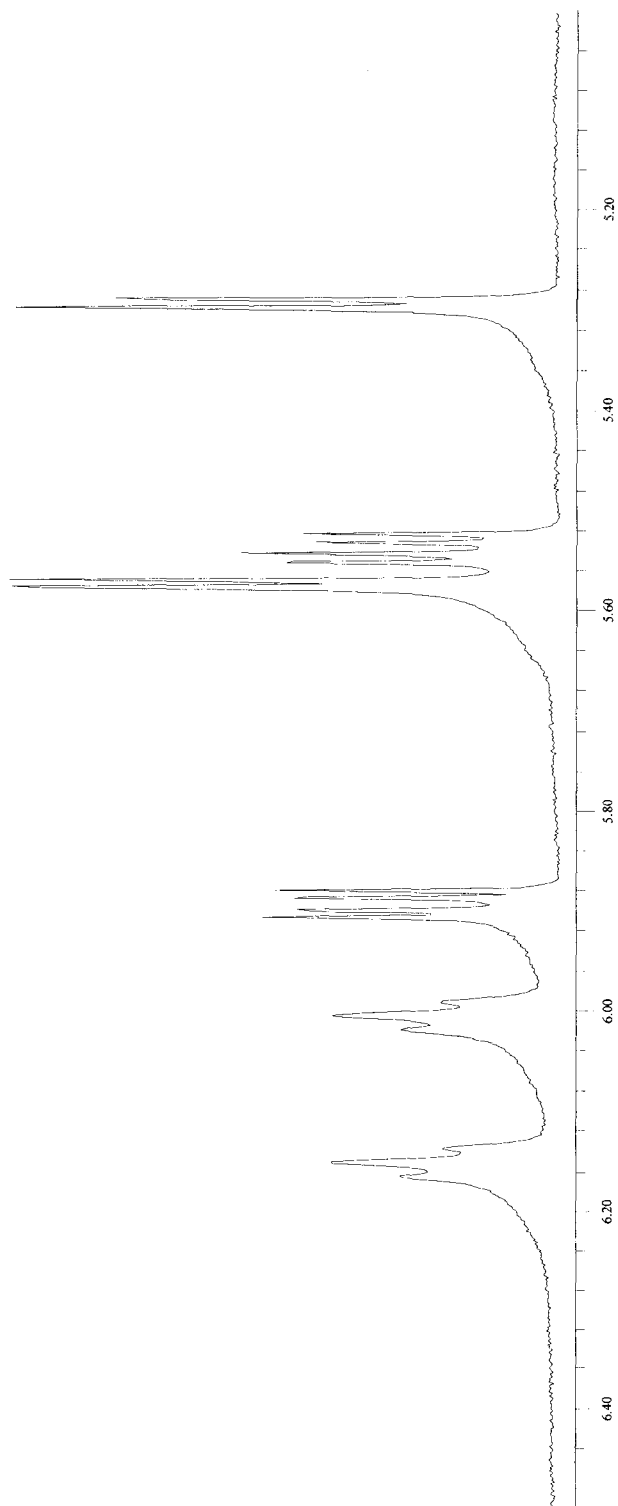
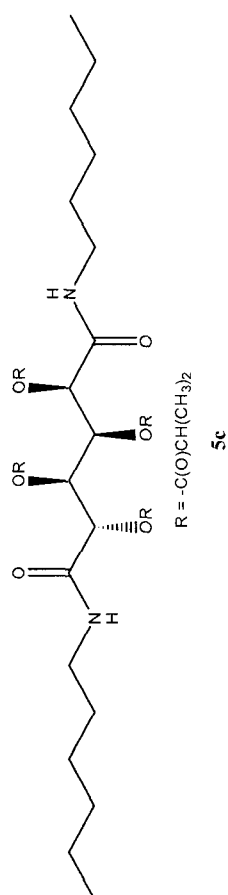


**Figure 16.**  $^1H$  NMR ( $CDCl_3$ ) spectrum of tetra-*O*-methylpropanyl-*N,N'*-dihexyl-*D*-glucaramide (**5c**) 5.00 – 6.50 ppm.

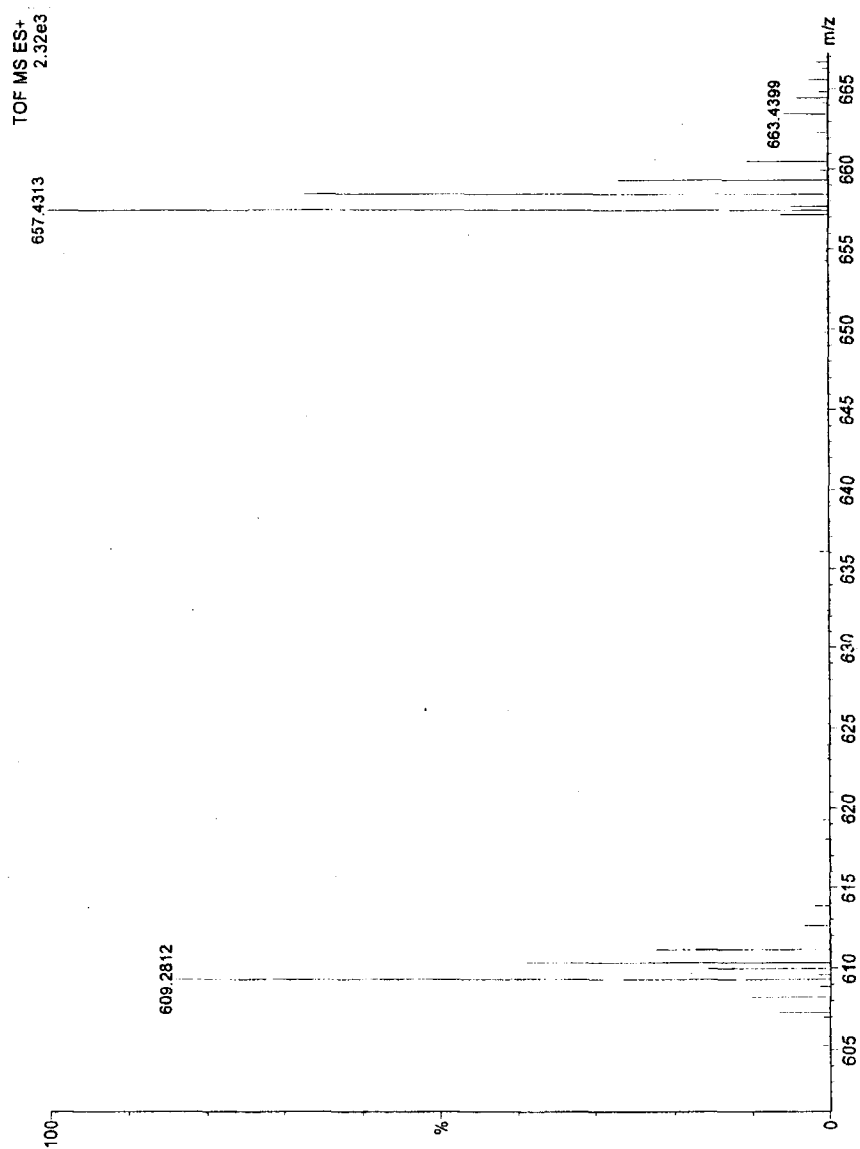


**Figure 17.** Mass (TOF electron spray) spectrum of tetra-*O*-methylpropyl-*N,N'*-dihexyl-*D*-glucaramide (**5c**).



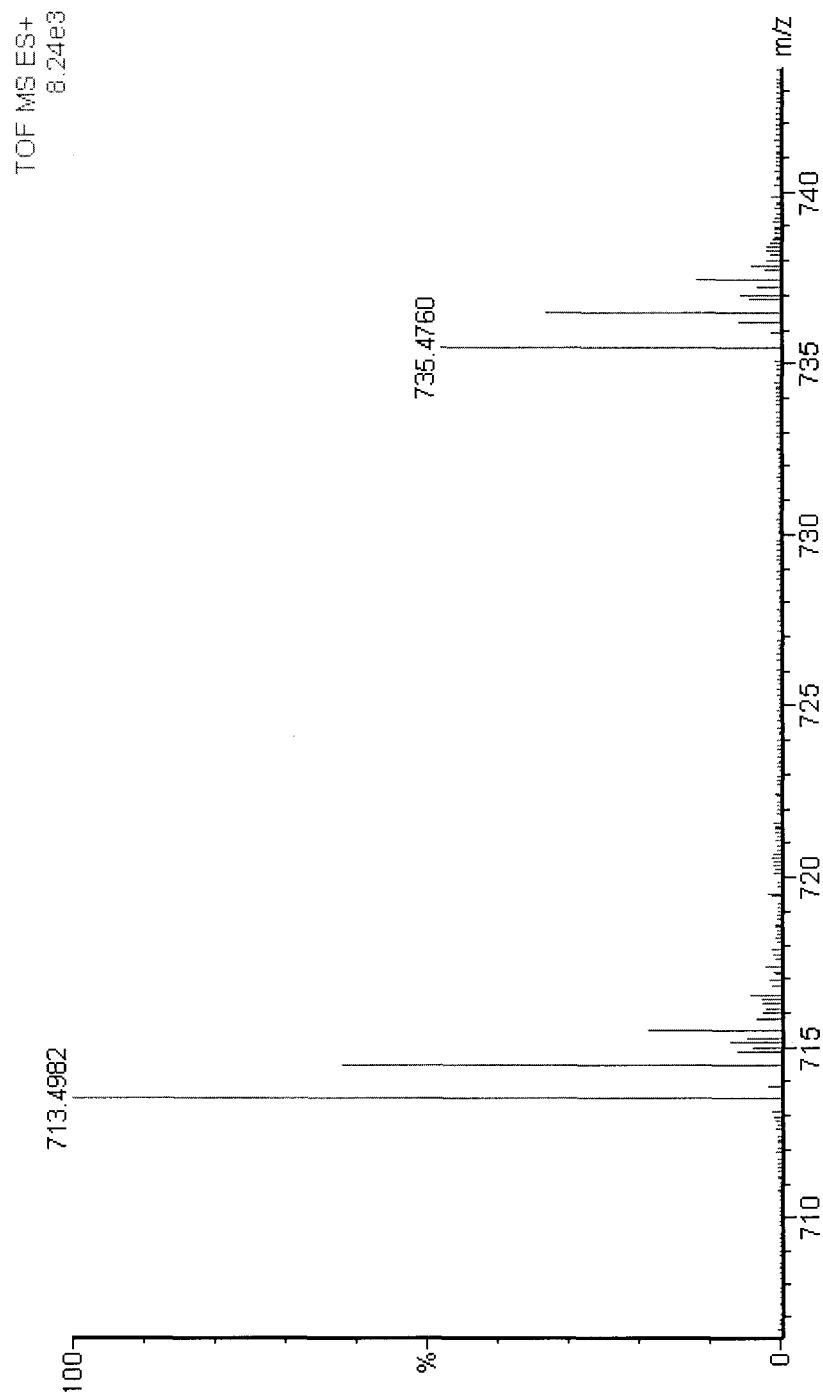


**Figure 18.** Mass (TOF electron spray) spectrum of tetra-*O*-dimethylpropanyl -*N,N'*-dihexyl-D-glucaramide (**5d**).

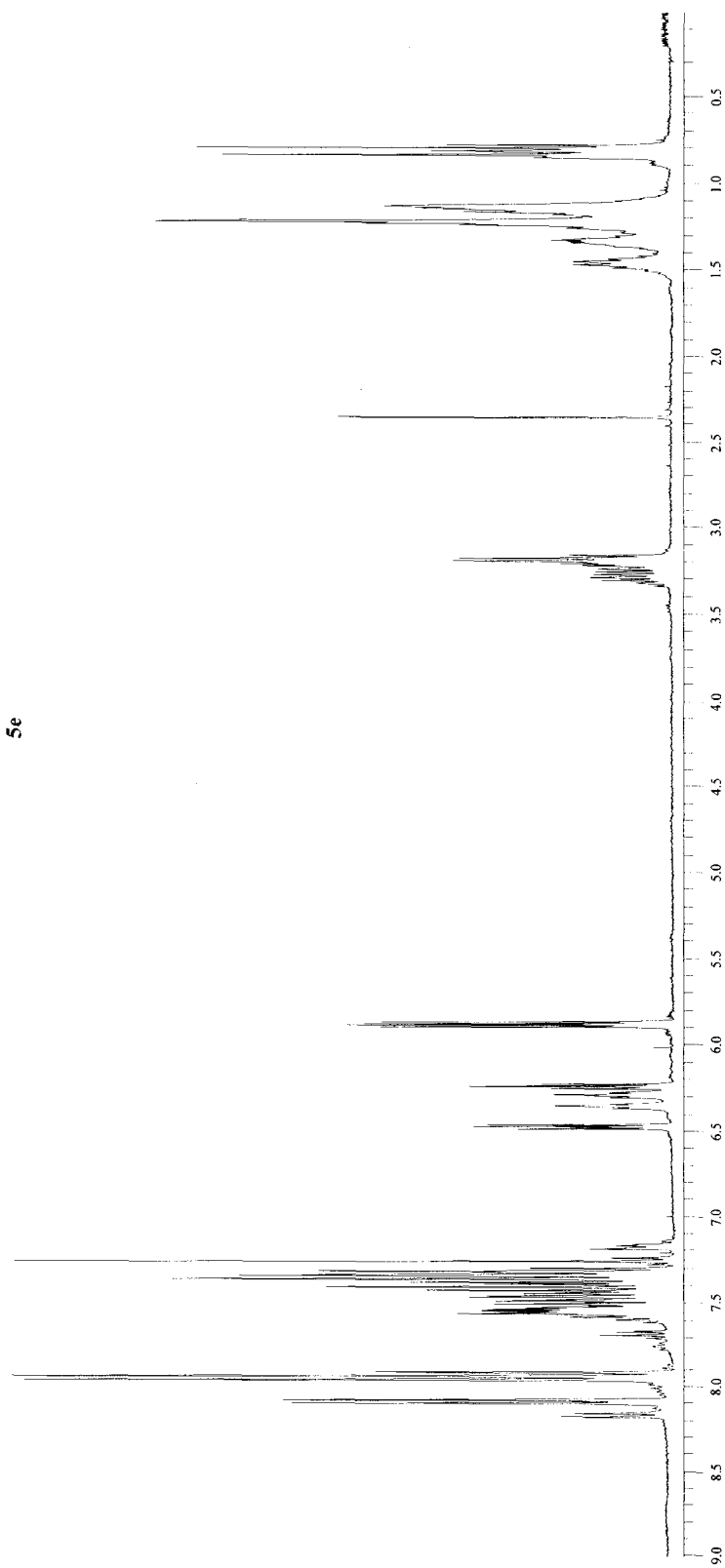
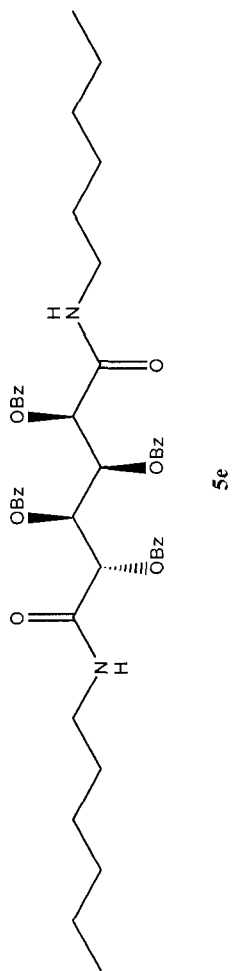


**Figure 19.**  $^1\text{H}$  NMR ( $\text{CDCl}_3$ ) spectrum of tetra-*O*-benzoyl-*N,N'*-dihexyl-*D*-glucaramide (**5e**).

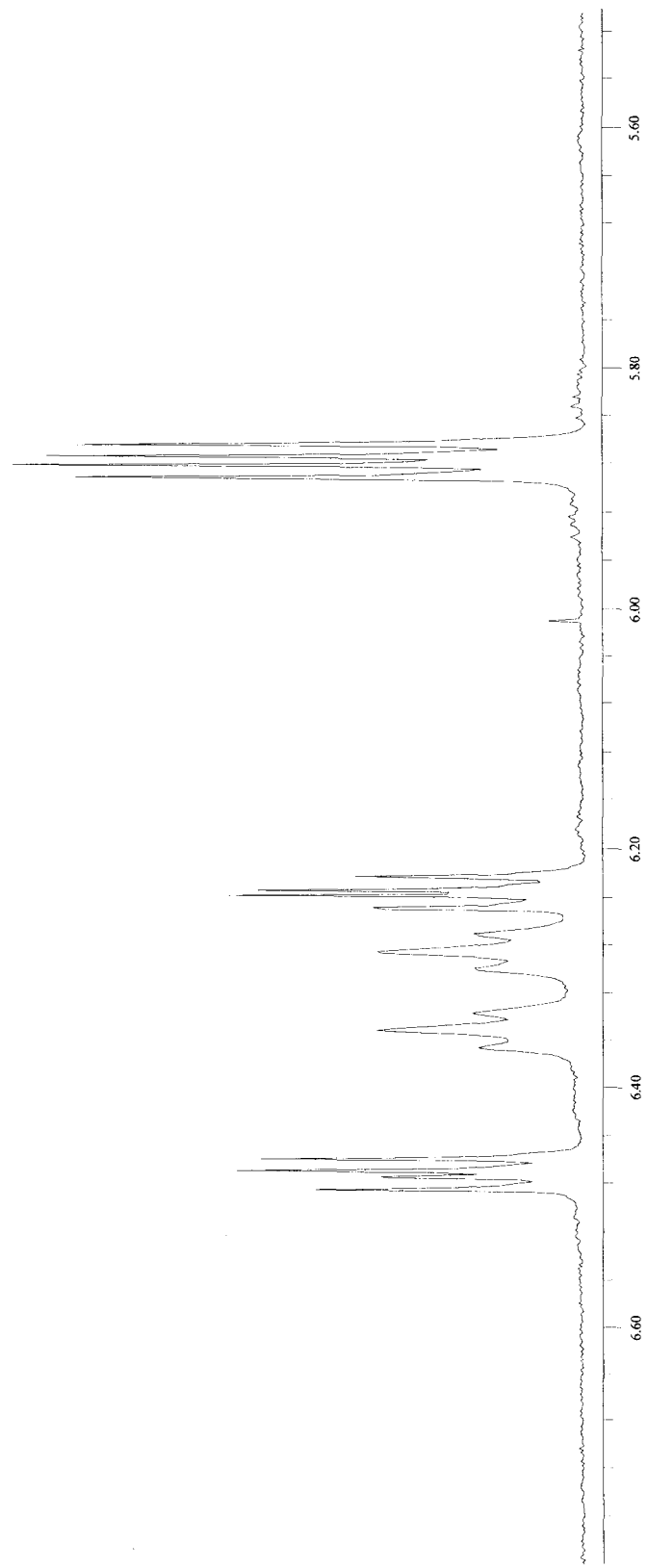
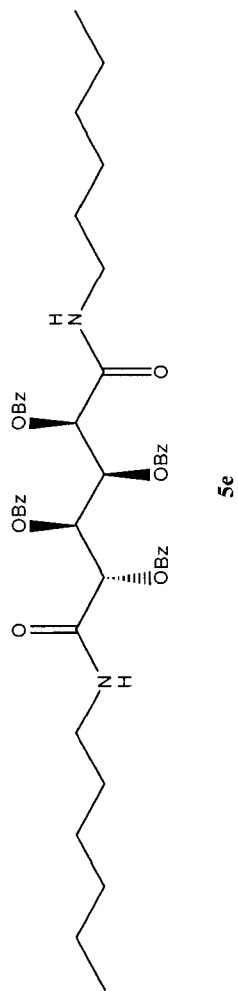


**Figure 20.**  $^1\text{H}$  NMR ( $\text{CDCl}_3$ ) spectrum of tetra-*O*-benzoyl-*N,N'*-dihexyl-D-glucaramide (**5e**) 5.50 – 6.80 ppm.

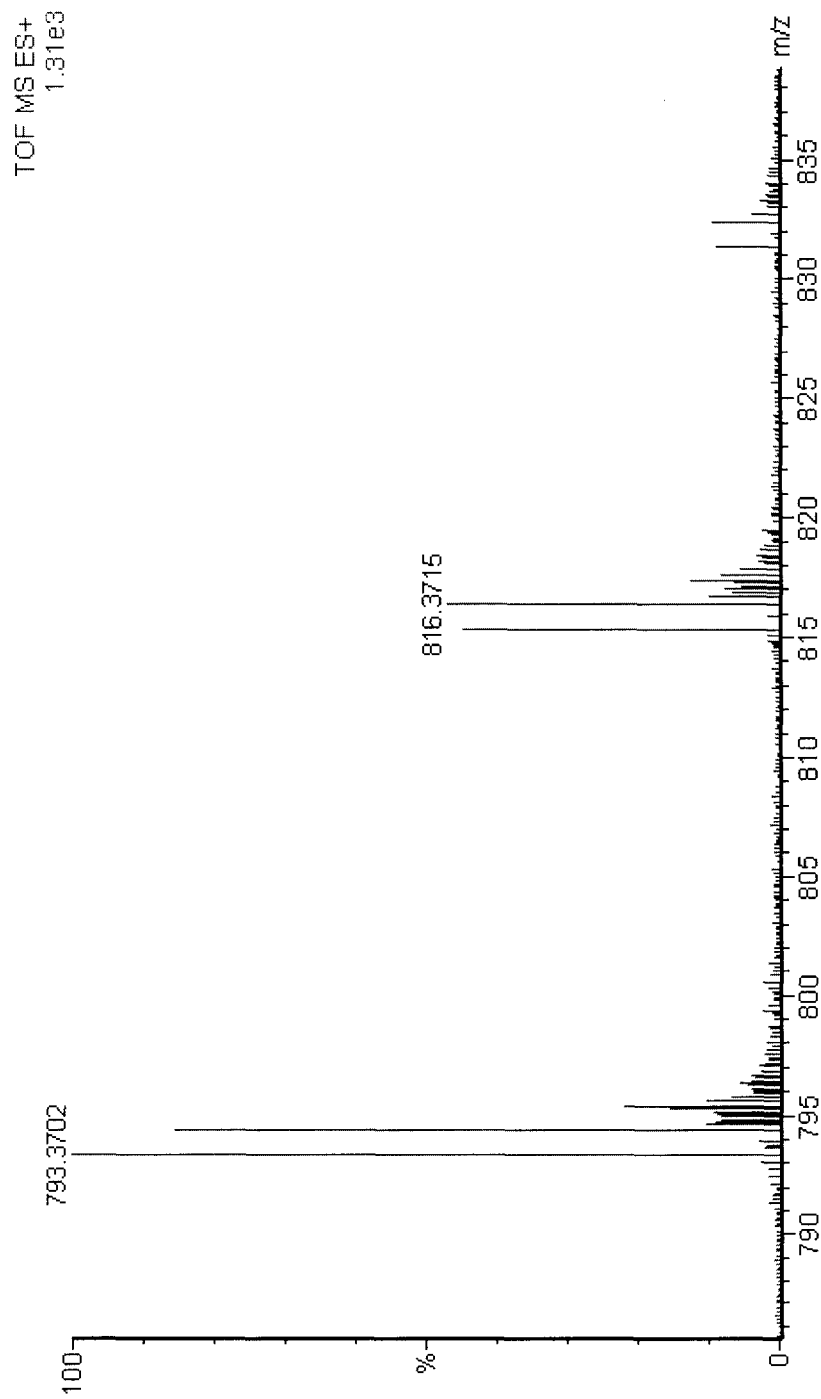


**Figure 21.** Mass (TOF electron spray) spectrum of tetra-*O*-benzoyl -*N,N'*-dihexyl-D-glucaramide (**5e**).

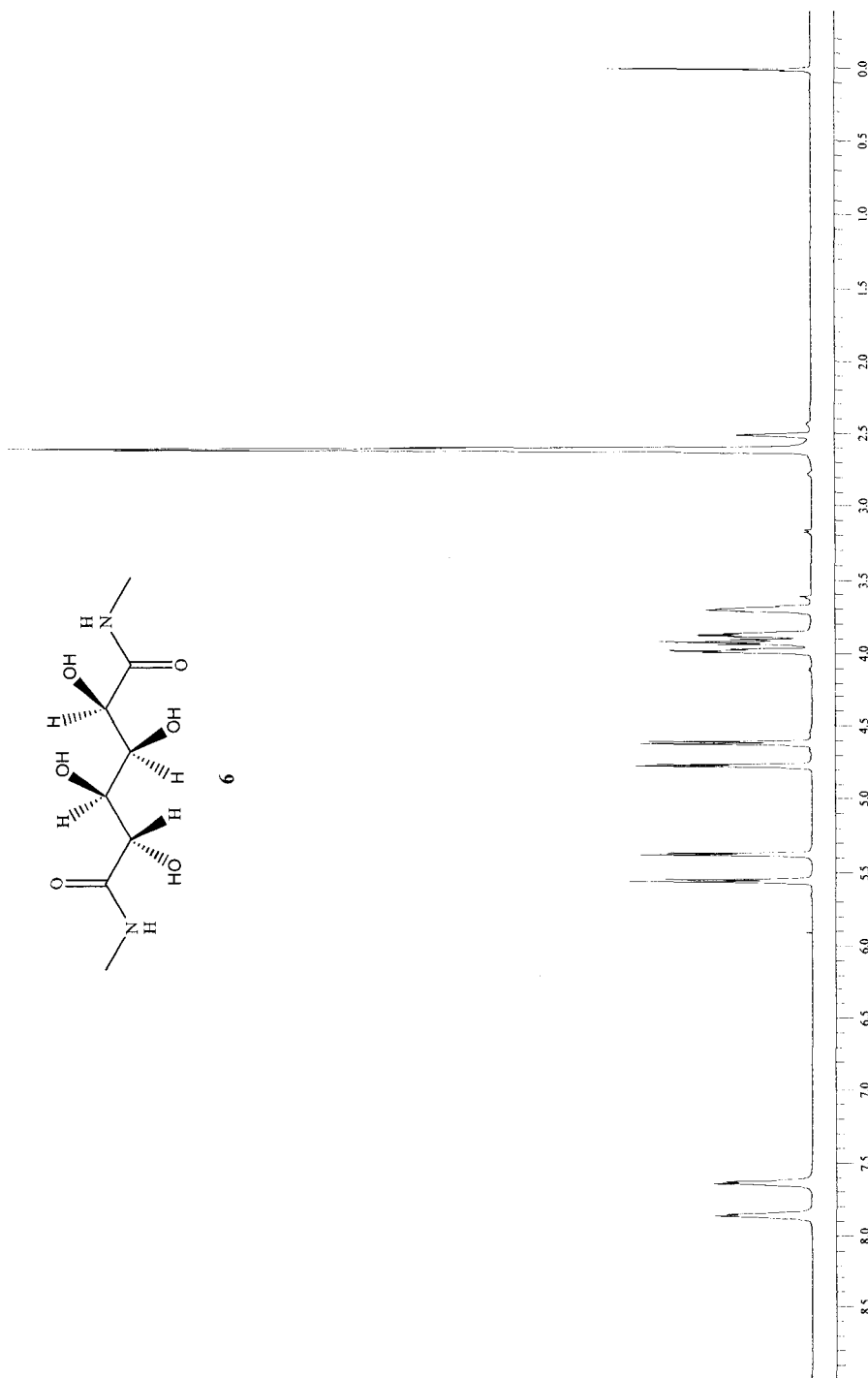
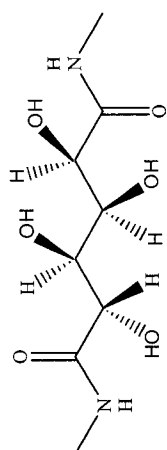


**Figure 22.**  $^1\text{H}$  NMR (DMSO- $d_6$ ) spectrum of dimethyl-L-D-glucaramide (6).



6

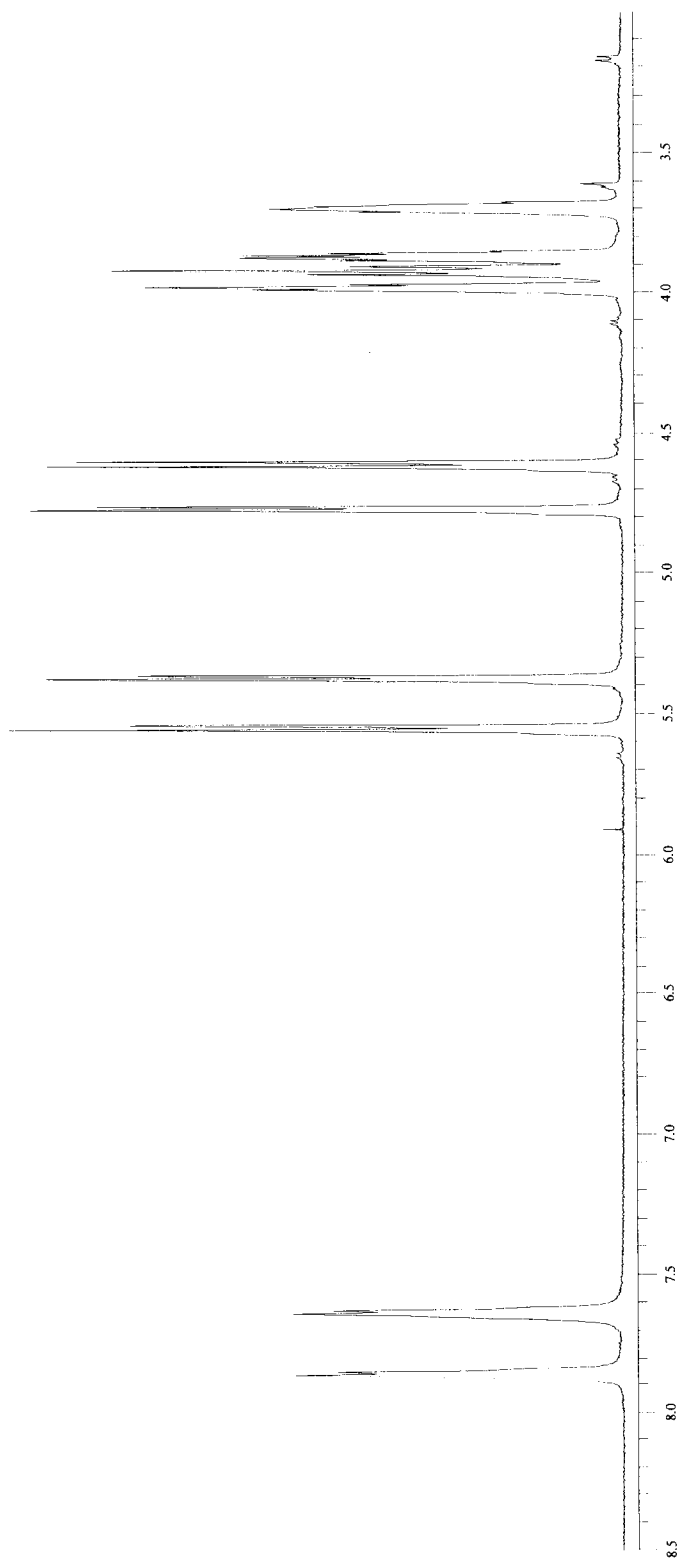
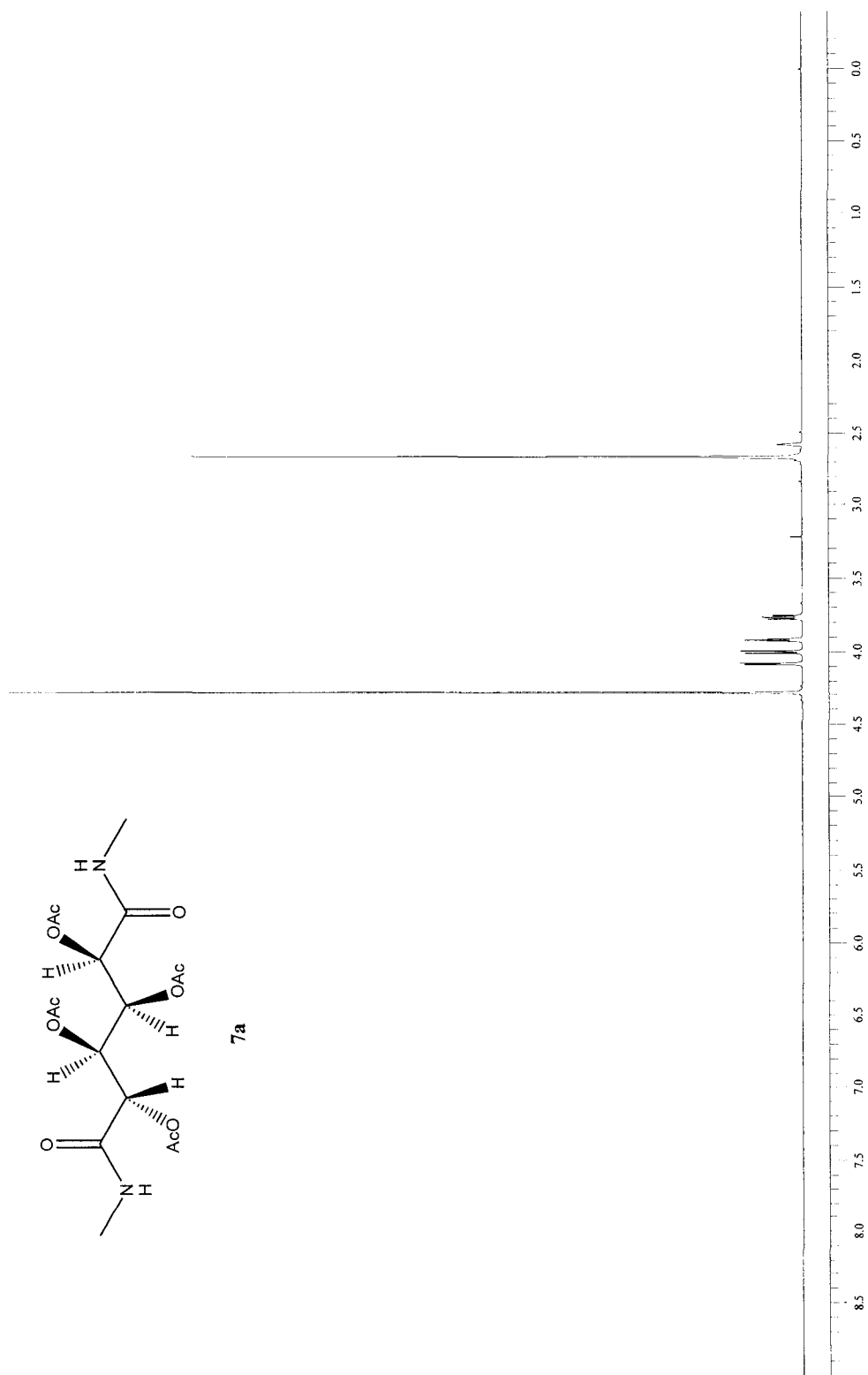
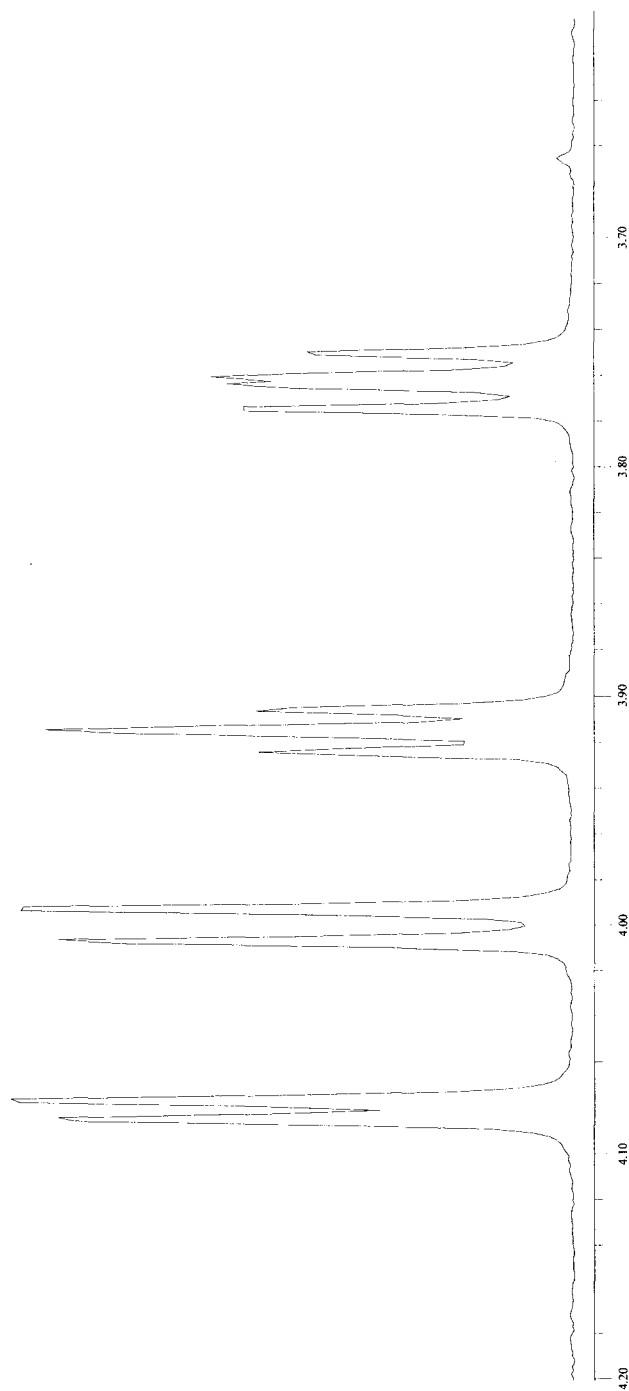
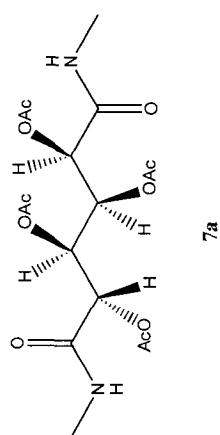


Figure 23. <sup>1</sup>H NMR (DMSO-d<sub>6</sub>) spectrum of dimethyl-D-glucaramide (6) 3.00 – 8.50 ppm.



**Figure 24.** <sup>1</sup>H NMR (DMSO-d<sub>6</sub>) spectrum of dimethyl-D-glucaramide (6, add 6 drops D<sub>2</sub>O).



**Figure 25.**  $^1\text{H}$  NMR (DMSO- $d_6$ ) spectrum of dimethyl-D-glucaramide (6, add 6 drops  $\text{D}_2\text{O}$ ) 3.60 – 4.20 ppm.



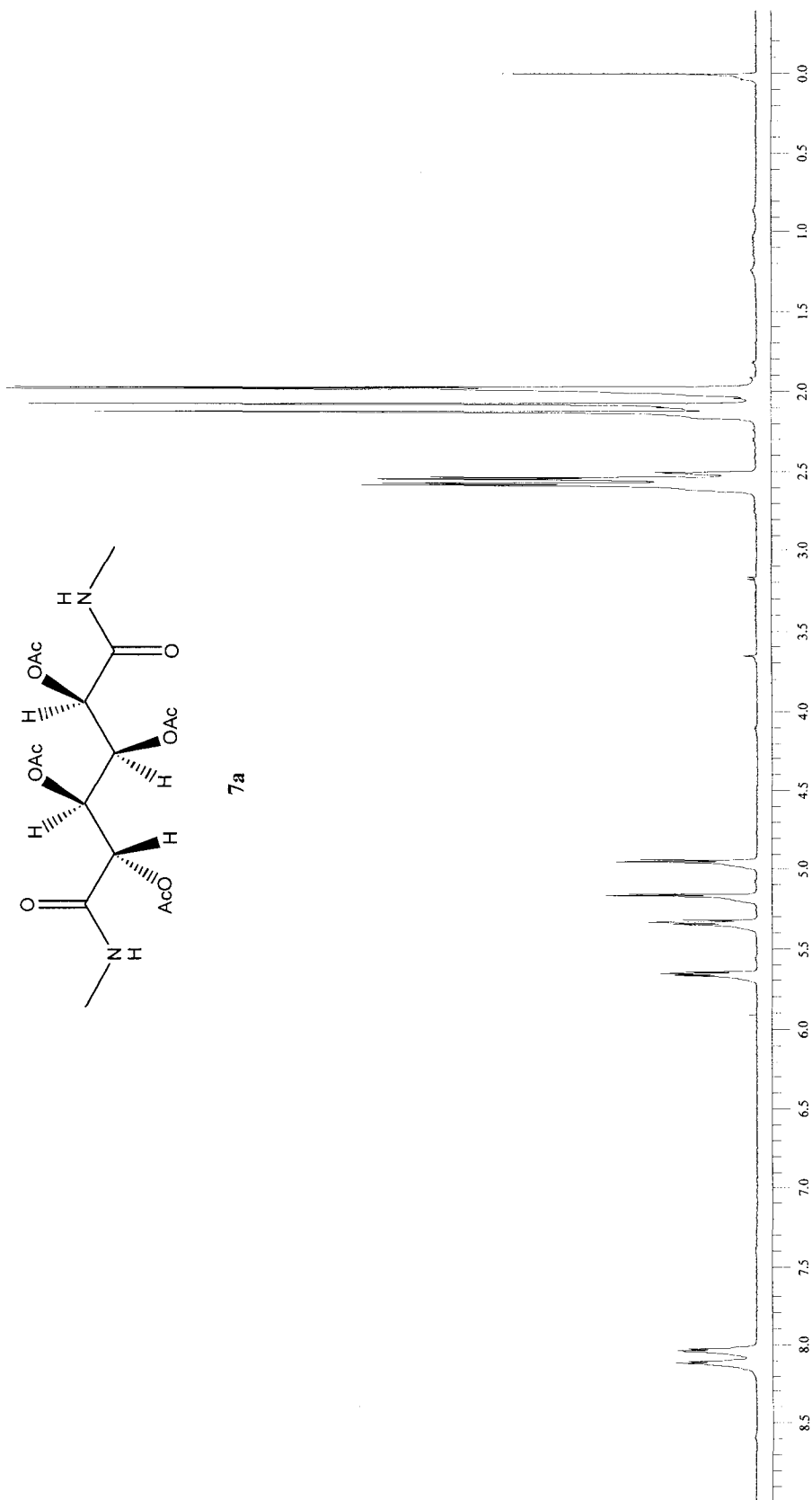


**Figure 26.** <sup>1</sup>H NMR (DMSO-d<sub>6</sub>) spectrum of tetra-*O*-acetyl-*N,N'*-dimethyl-*D*-glucaramide (**7a**).

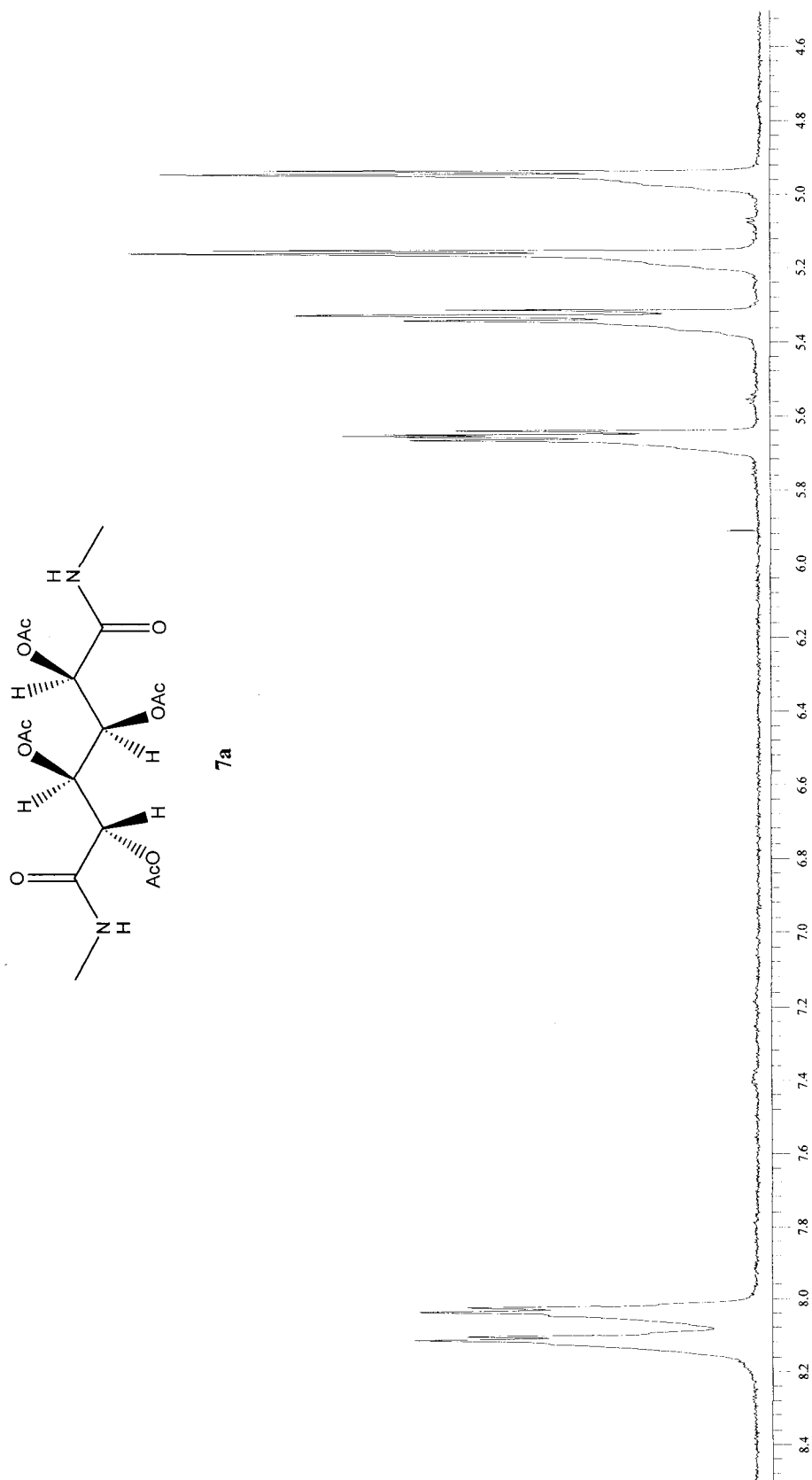


**Figure 27.**  $^1\text{H}$  NMR ( $\text{DMSO-}d_6$ ) spectrum of tetra-*O*-acetyl-*N,N'*-dimethyl-*D*-glucaramide (**7a**) 4.50 – 8.50 ppm.

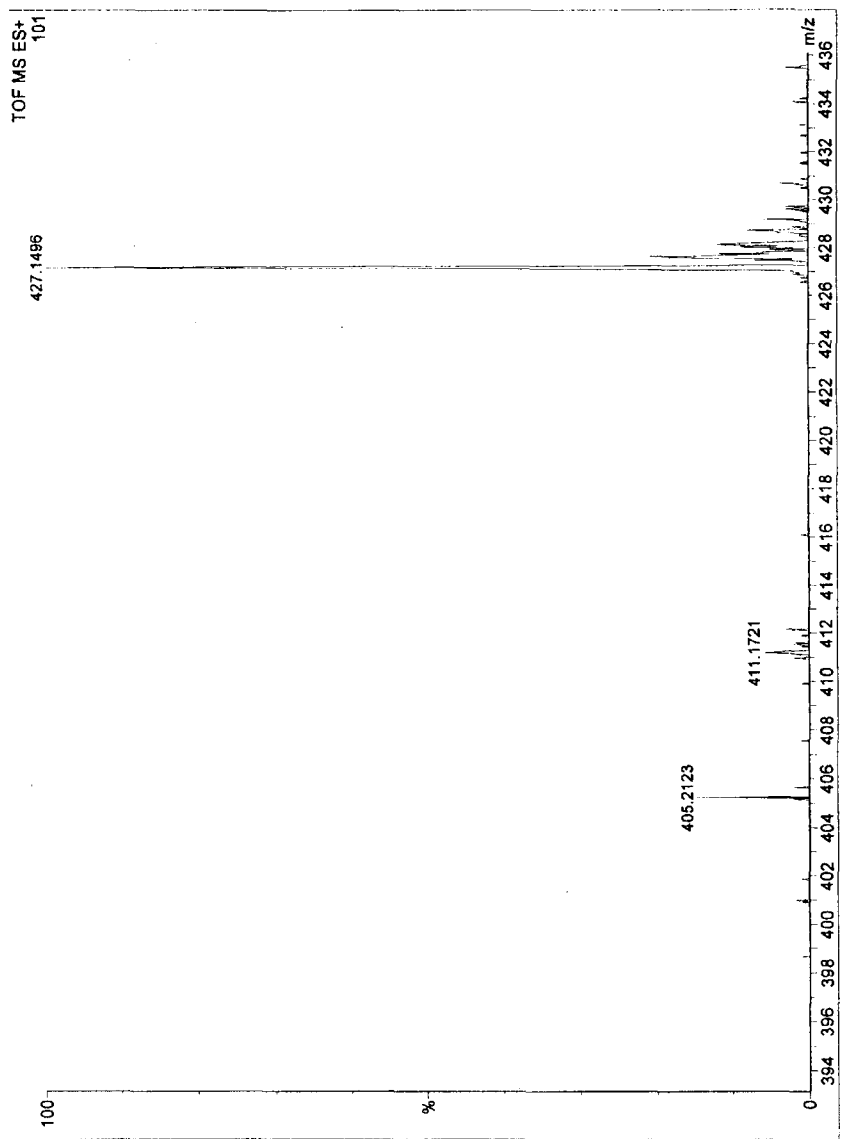


**Figure 28.** Mass (TOF electron spray) spectrum of tetra-*O*-acetyl-*N,N'*-dimethyl-*D*-glucaramide (**7a**).

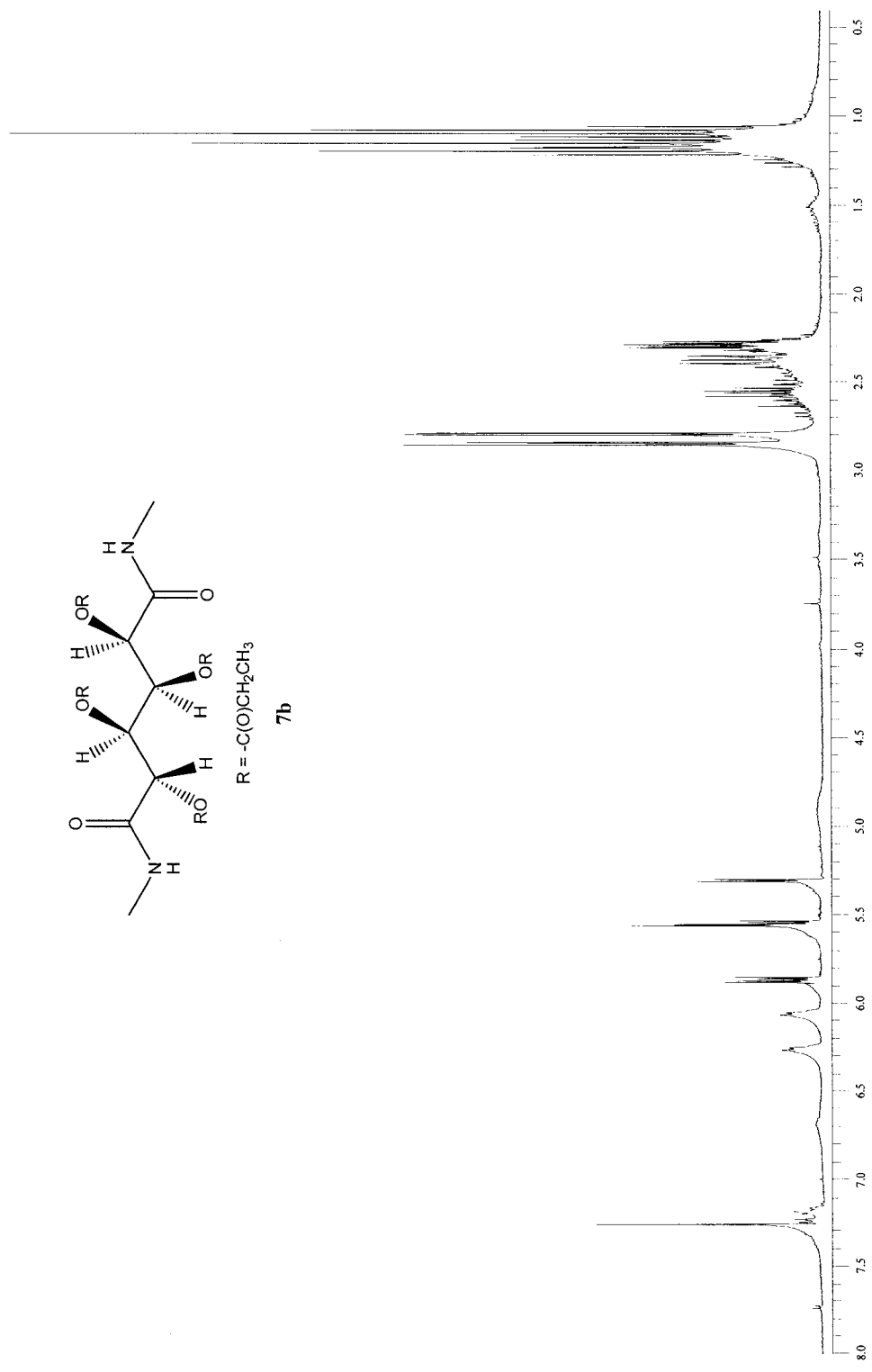


**Figure 29.** <sup>1</sup>H NMR (CDCl<sub>3</sub>) spectrum of tetra-O-propanyl-N,N'-dimethyl-D-glucaramide (7b).

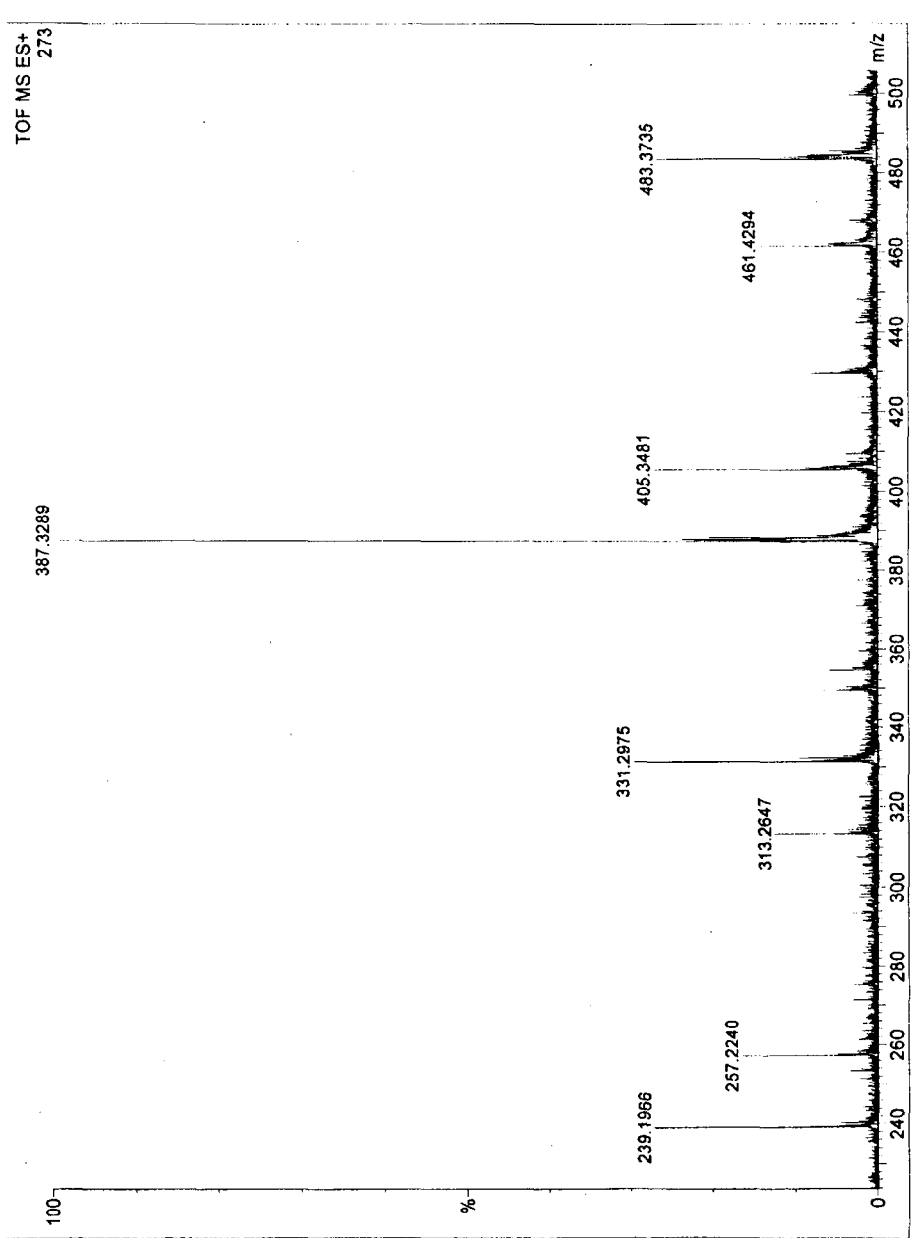


**Figure 30.** Mass (TOF electron spray) spectrum of tetra-*O*-propanyl-*L,N,N'*-dimethyl-*D*-glucaramide (**7b**).

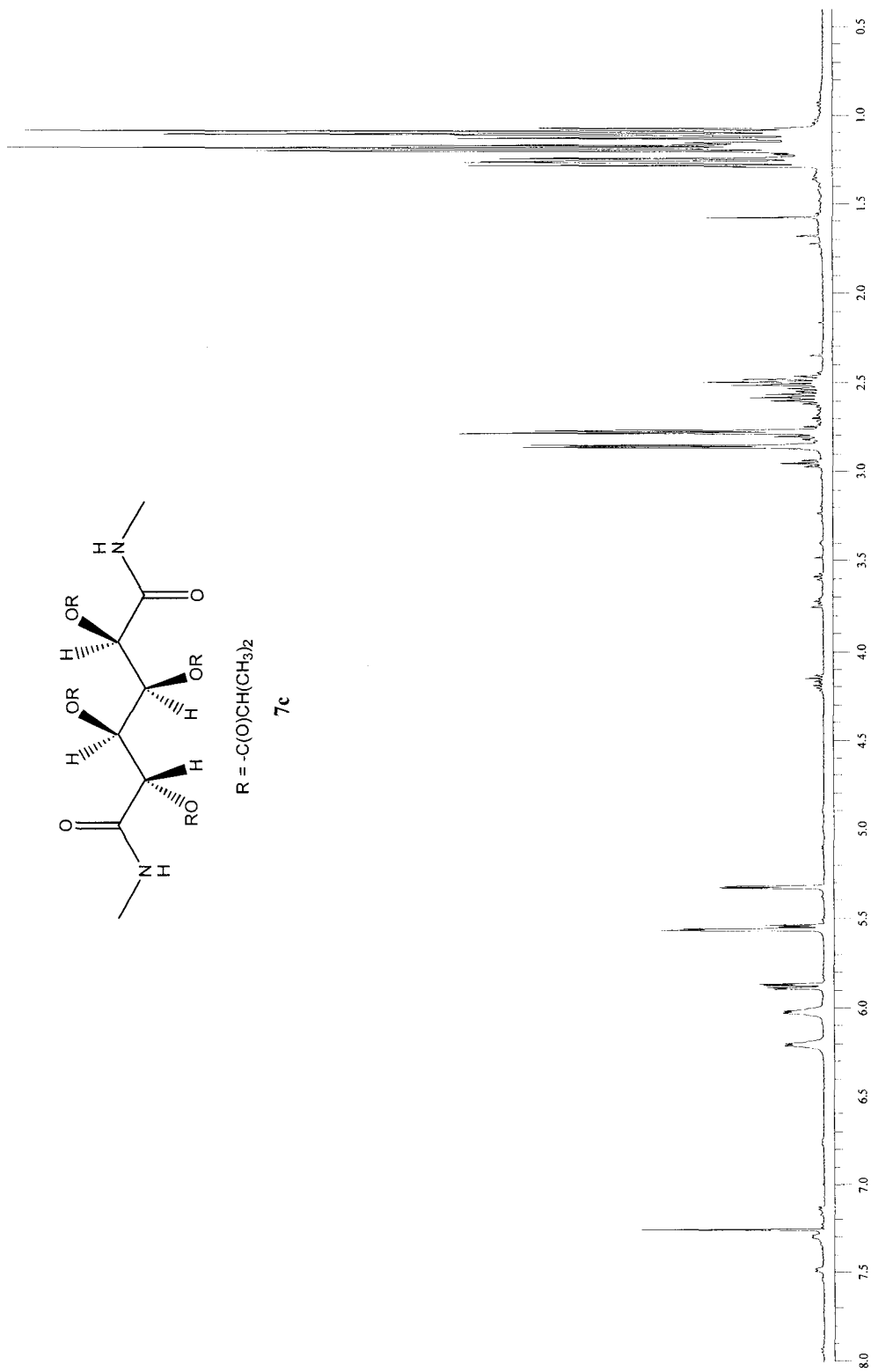


**Figure 31.**  $^1\text{H}$  NMR ( $\text{CDCl}_3$ ) spectrum of tetra-*O*-methylpropargyl-*N,N'*-dimethyl-D-glucaramide (**7c**).

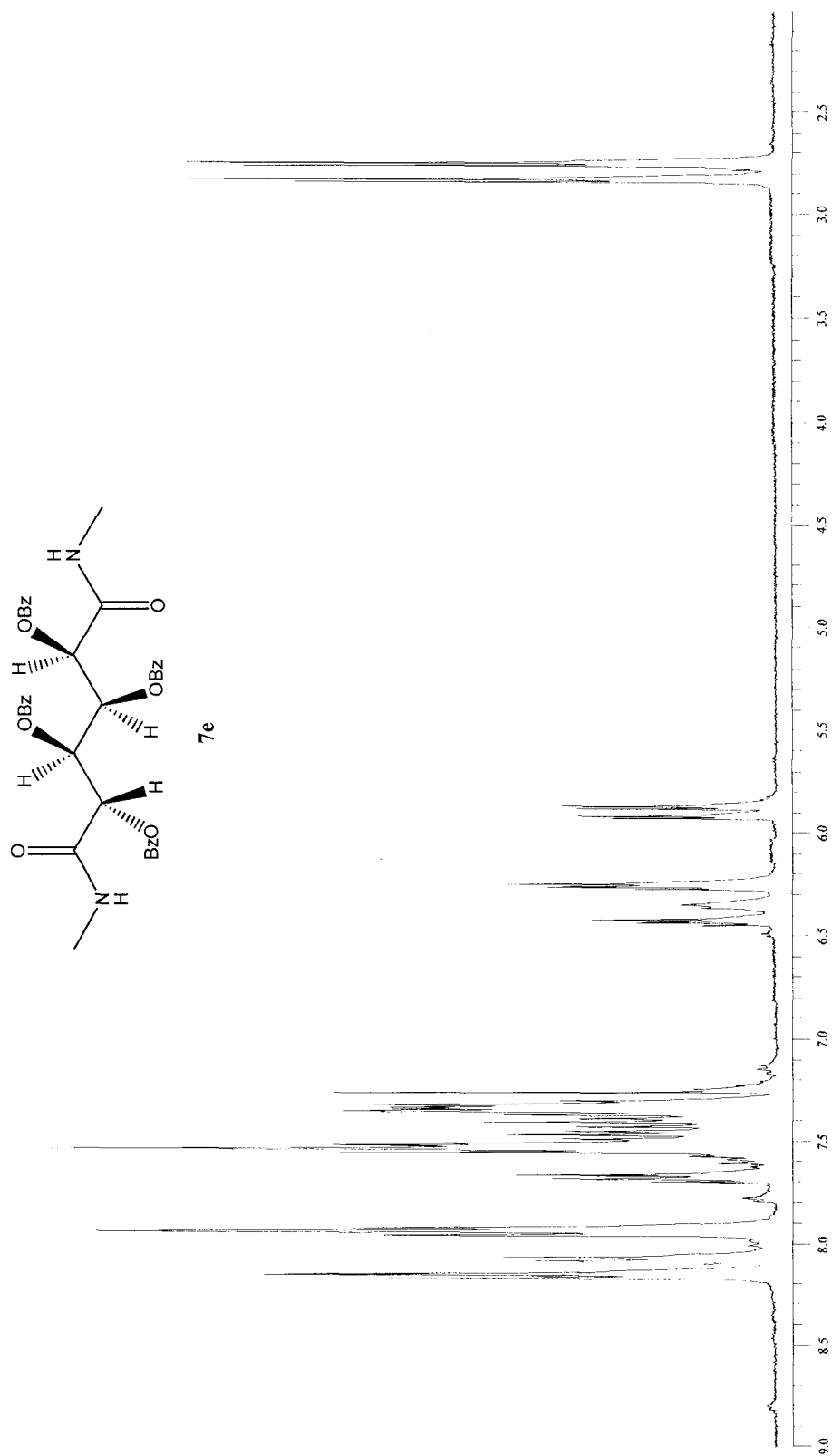


**Figure 32.** <sup>1</sup>H NMR (CDCl<sub>3</sub>) spectrum of tetra-*O*-benzoyl-*N,N'*-dimethyl-D-glucaramide (**7e**).

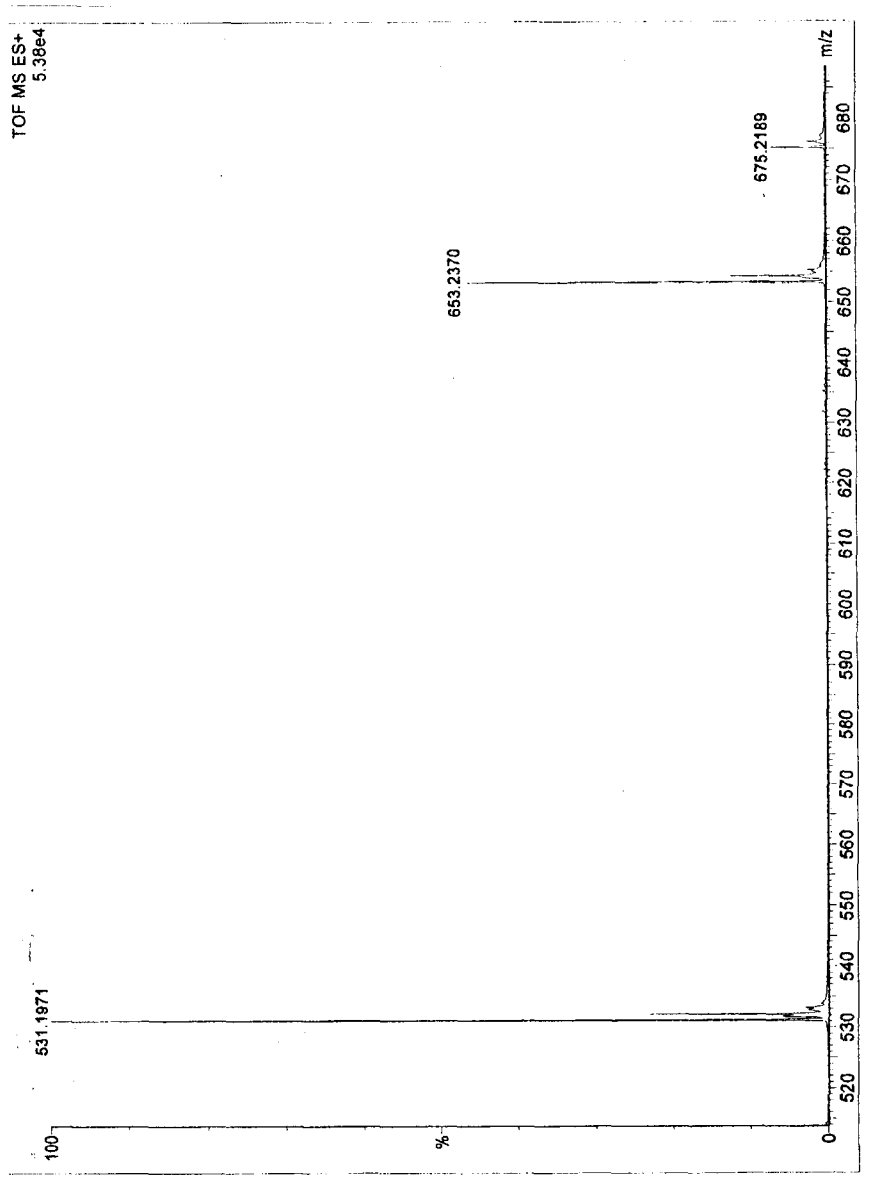


**Figure 33.** Mass (TOF electron spray) spectrum of tetra-*O*-benzoyl-*N,N'*-dimethyl-D-glucaramide (**7e**).



## Appendix 2. Spectra of Compounds in Chapter 3

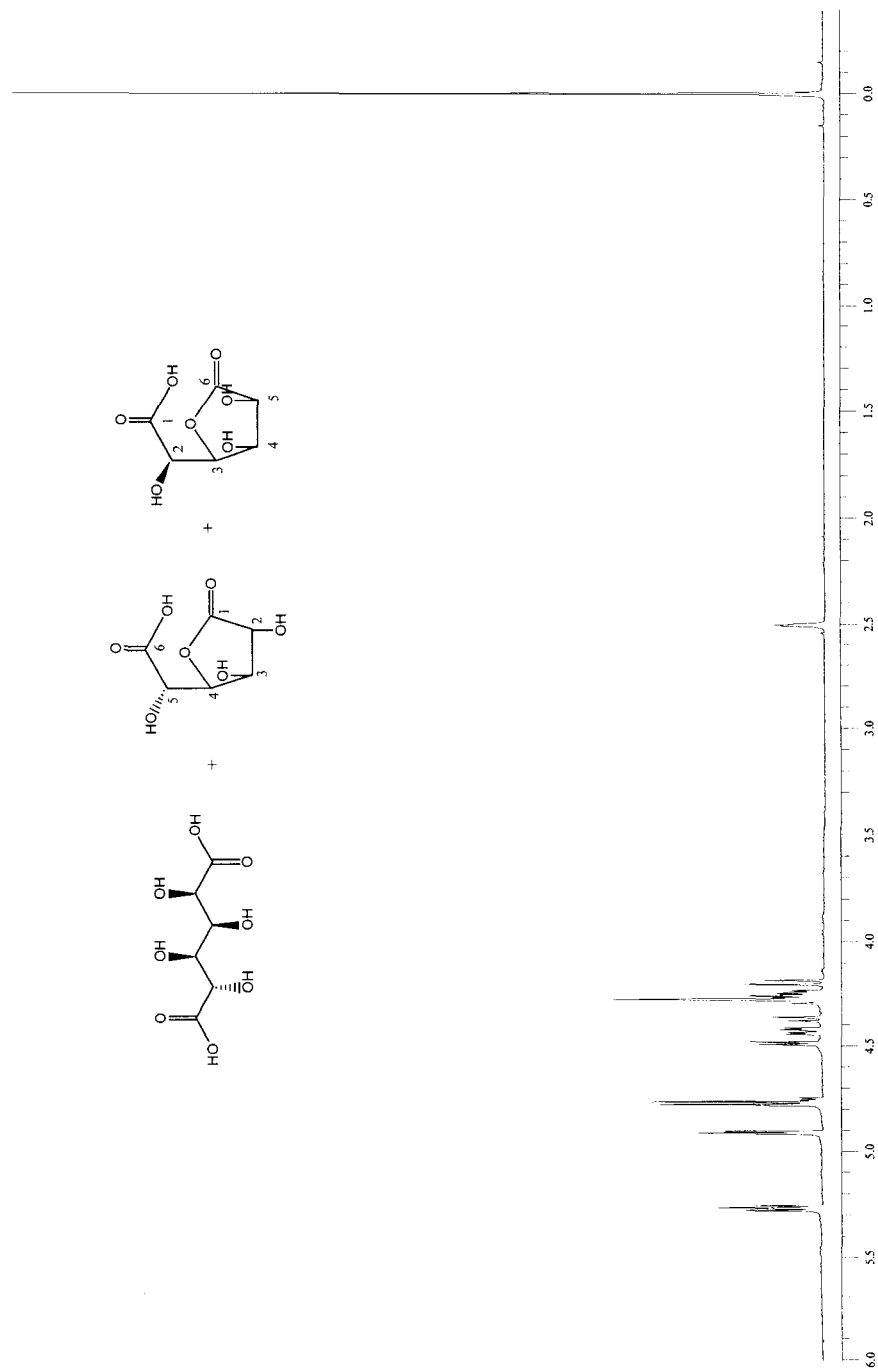


**Figure 1.**  $^1\text{H}$  NMR ( $\text{DMSO-}d_6$ ) spectrum of D-glucaric acid, D-glucaro-6,3-lactone and D-glucaro-1,4-lactone mixture (**1**).

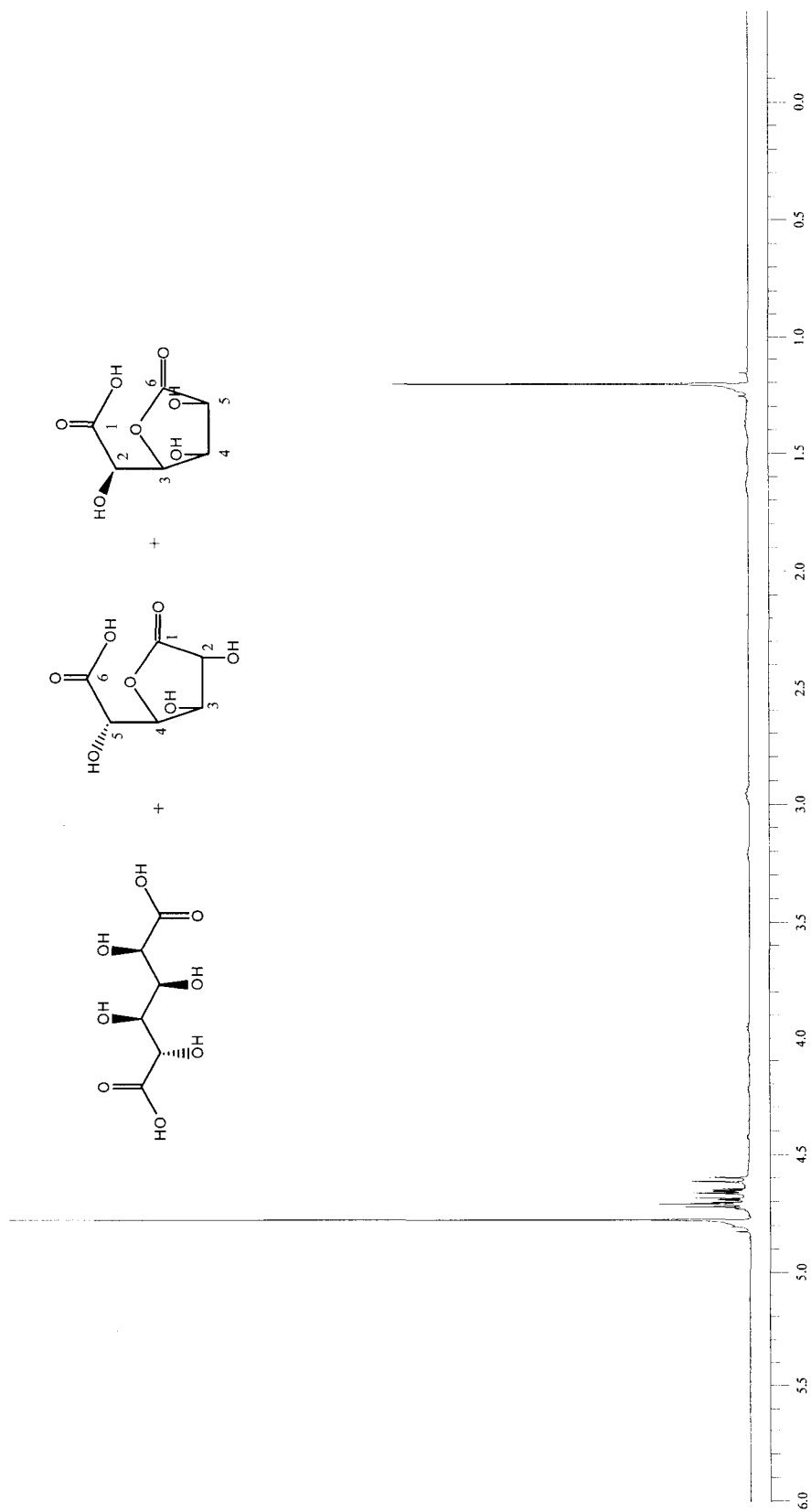


**Figure 2.**  $^1\text{H}$  NMR ( $\text{D}_2\text{O}$ ) spectrum of D-glucaric acid, D-glucaro-6,3-lactone and D-glucaro-1,4-lactone mixture (**1**).

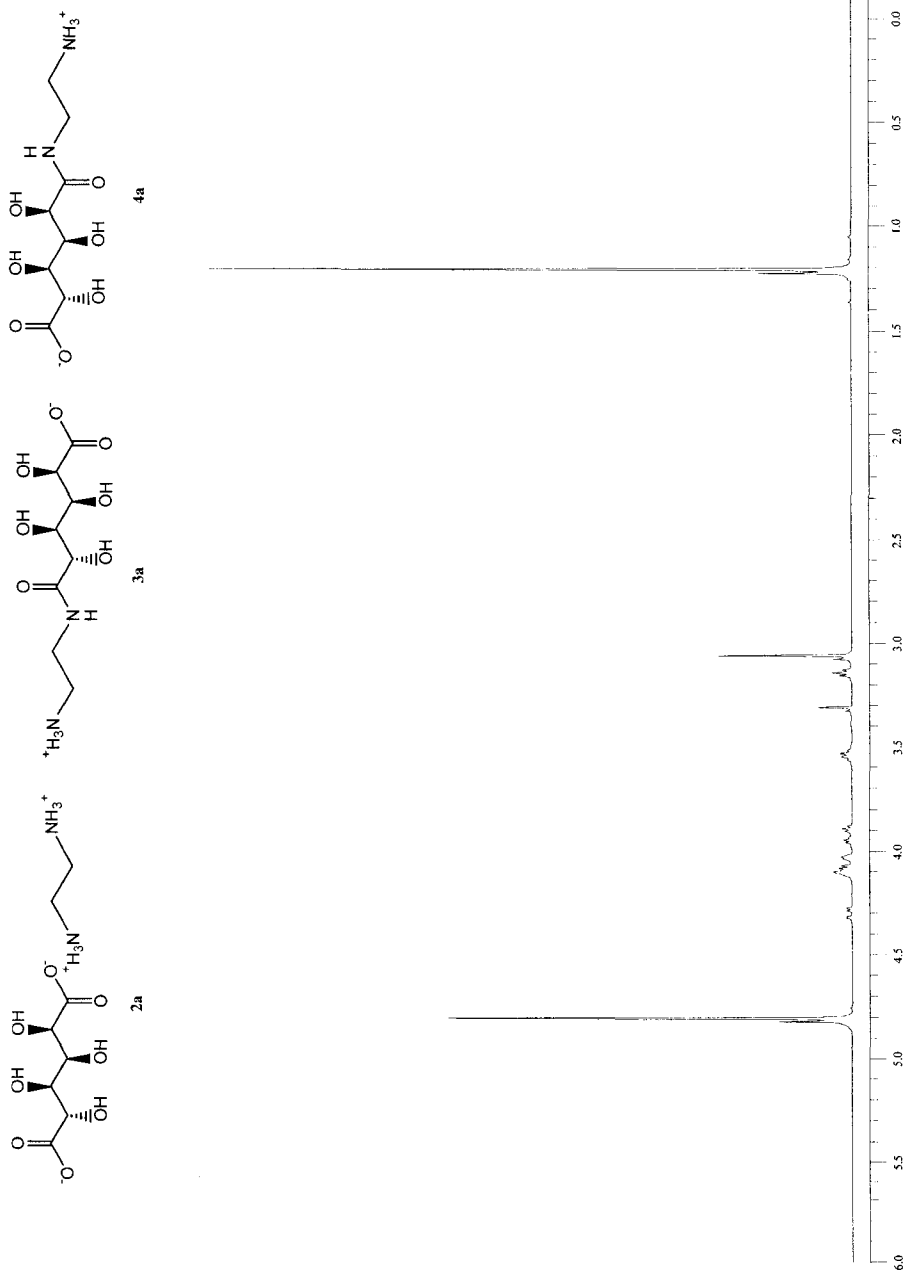


**Figure 3.** <sup>1</sup>H NMR (D<sub>2</sub>O) spectrum of ethylenediammonium D-glucurate (**2a**) / N-(2-aminoethyl)-D-glucar-6-amic acid salt (**3a**) / N-(2-aminoethyl)-D-glucar-1-amic acid salt (**4a**) mixture.

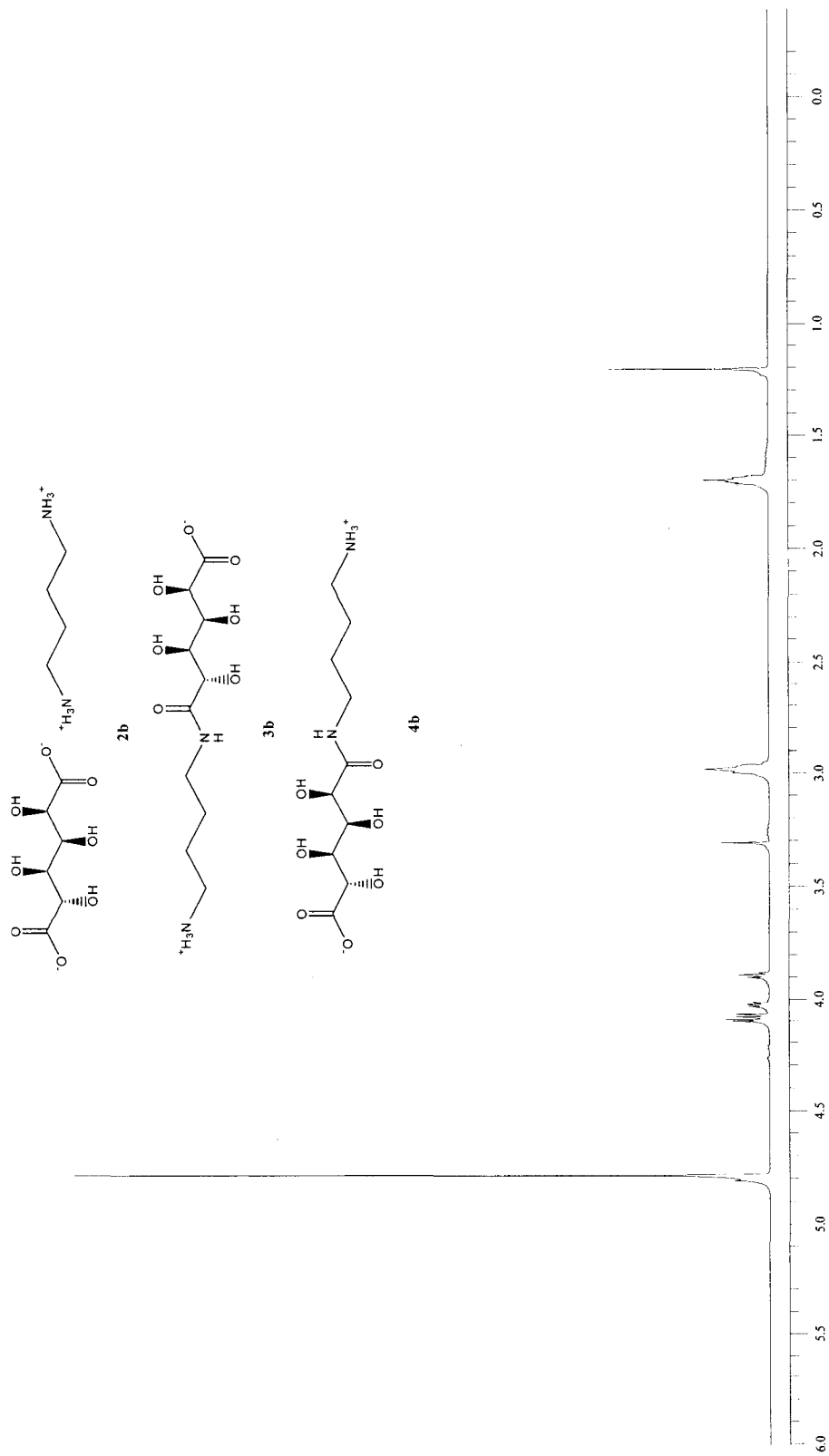


**Figure 4.**  $^1\text{H}$  NMR ( $\text{D}_2\text{O}$ ) spectrum of tetramethylethylenediammonium D-glucarate (**2b**) / *N*-(4-aminobutyl)-D-glucar-6-amic acid salt (**3b**) / *N*-(4-aminobutyl)-D-glucar-1-amic acid salt (**4b**) mixture.

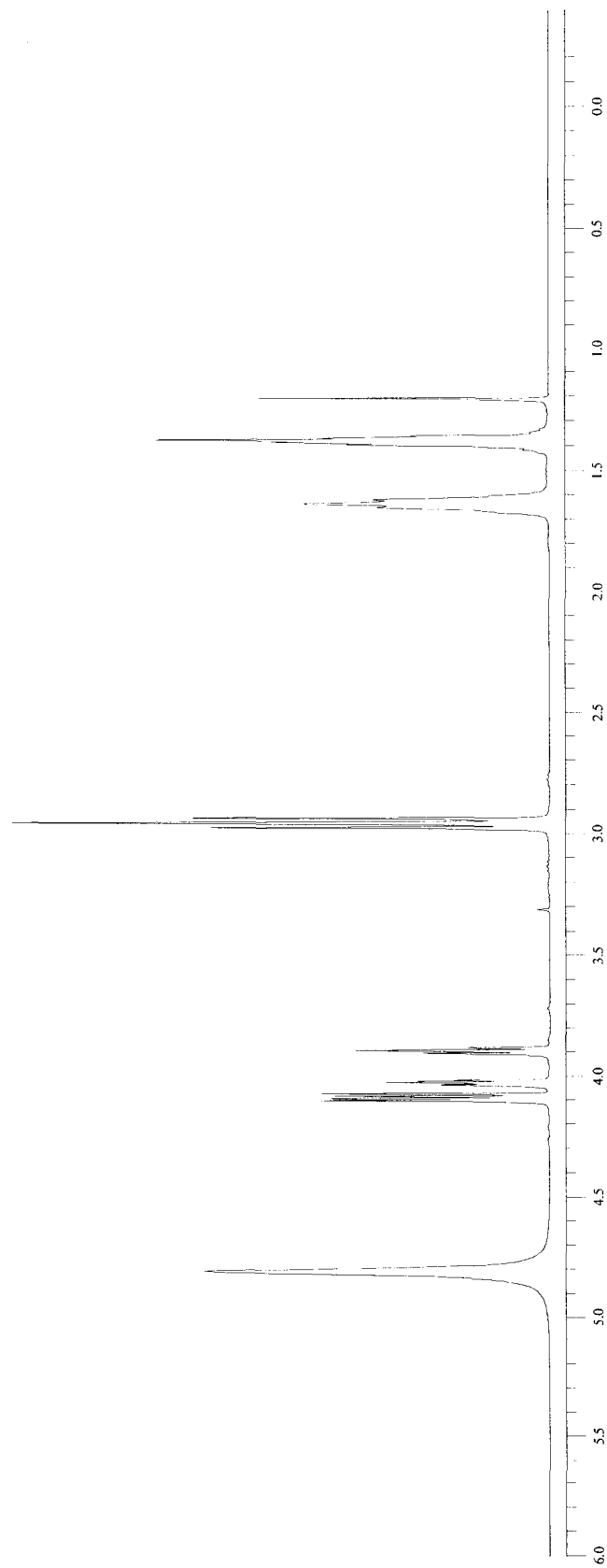
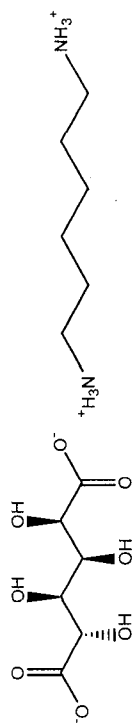


**Figure 5.** <sup>1</sup>H NMR (D<sub>2</sub>O) spectrum of hexamethylenediammonium D-glucuronate (**2c**).

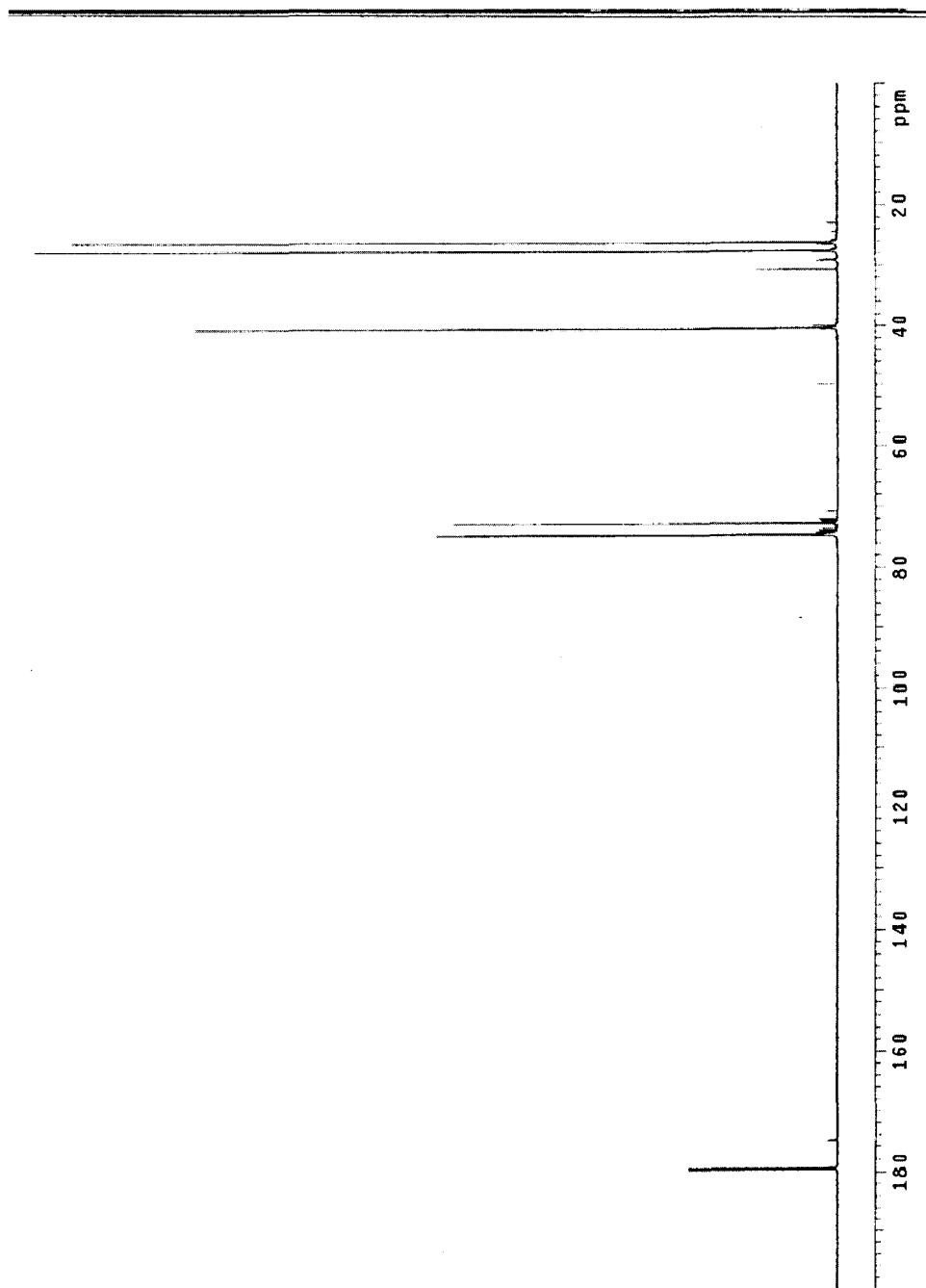


**Figure 6.**  $^{13}\text{C}$  NMR ( $\text{D}_2\text{O}$ ) spectrum of hexamethylenediammonium D-glucarate (**2c**).

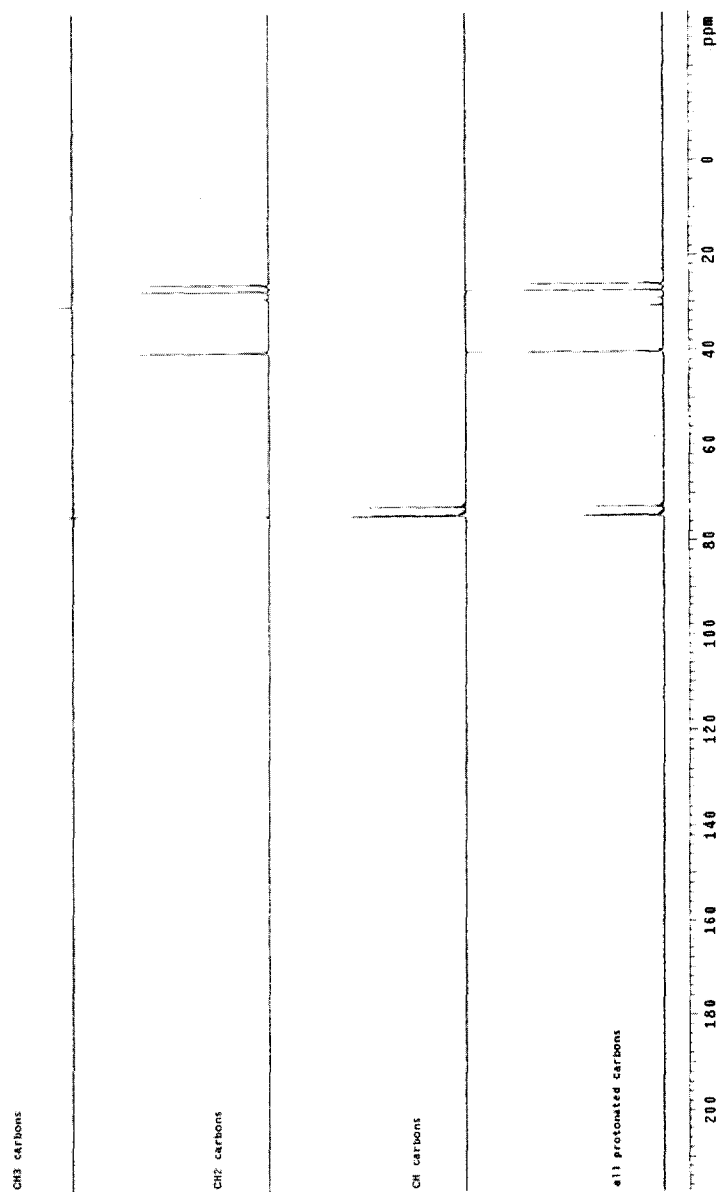


**Figure 7.**  $^{13}\text{C}$  NMR DEPT ( $\text{D}_2\text{O}$ ) spectrum of hexamethylenediammonium D-glucarate (**2c**).

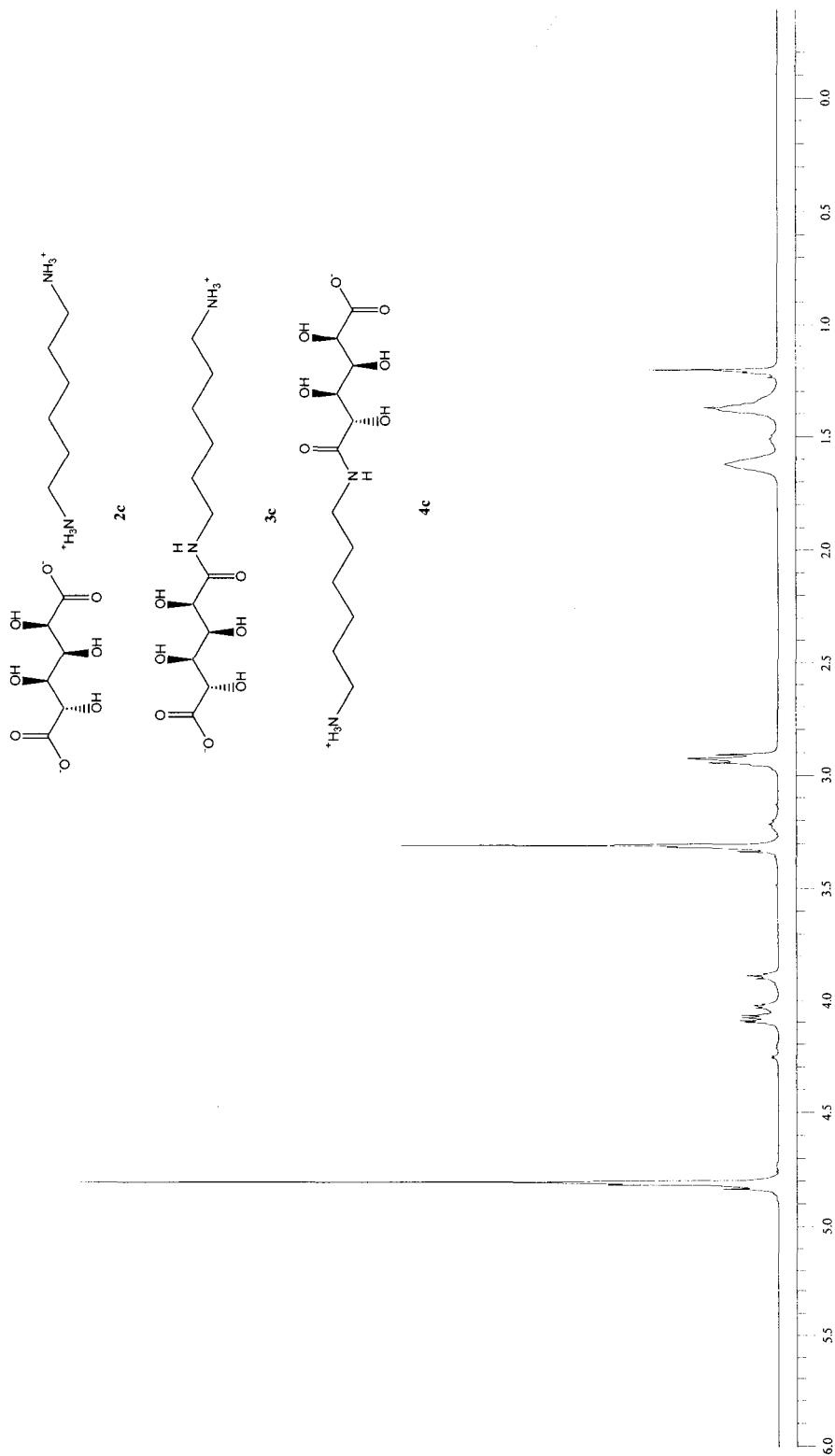


**Figure 8.**  $^1\text{H}$  NMR ( $\text{D}_2\text{O}$ ) spectrum of hexamethylenediammonium D-glucarate (**2c**) / *N*-(6-aminobutyl)-D-glucar-6-amic acid salt (**3c**) / *N*-(6-aminobutyl)-D-glucar-1-amic acid salt (**4c**) mixture.



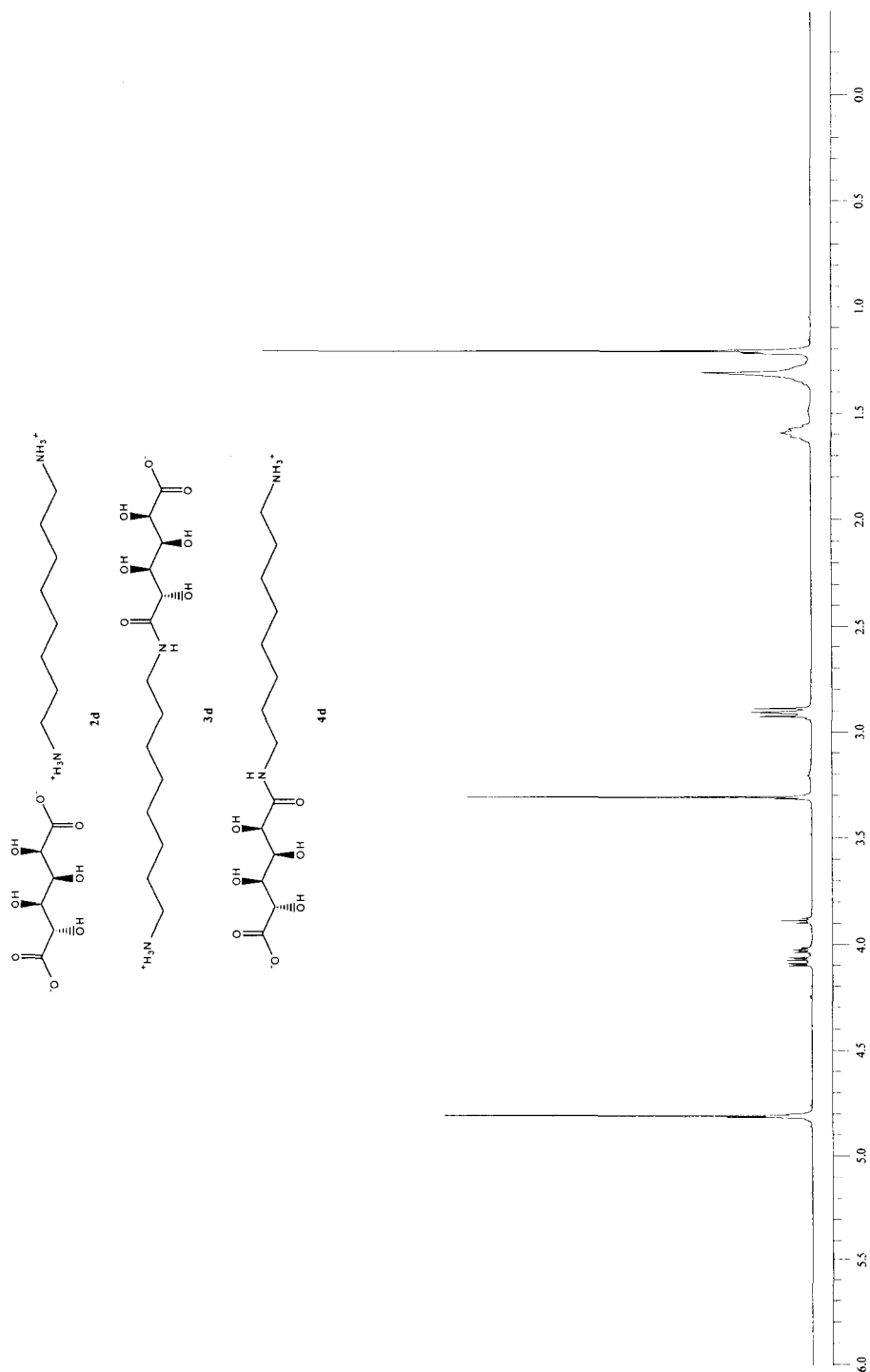


**Figure 9.** <sup>1</sup>H NMR (D<sub>2</sub>O) spectrum of octamethylenediammonium D-Glucarate (**2d**) / N-(8-aminobutyl)-D-glucar-6-amic acid salt (**3d**) / N-(8-aminobutyl)-D-glucar-1-amic acid salt (**4d**) mixture.

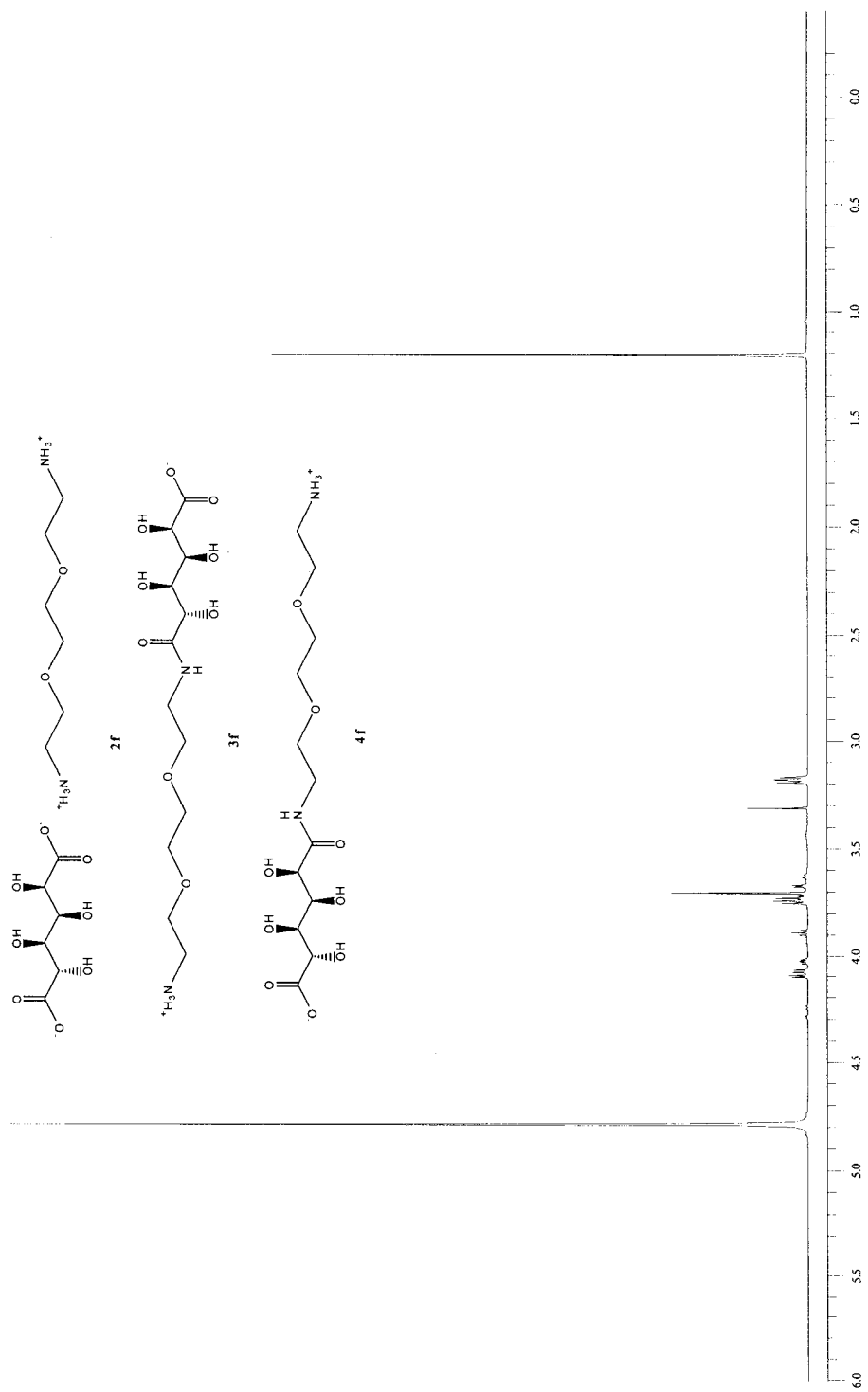


**Figure 10.** <sup>1</sup>H NMR (D<sub>2</sub>O) spectrum of 3,6-dioxaoctamethylenediammonium D-glucarate (**2f**) / *N*-(8-amino-3,6-dioxa-octyl)-D-glucaro-1-amic acid salt (**3f**) / *N*-(8-amino-3,6-dioxa-octyl)-D-glucaro-1-amic acid salt (**4f**) mixture.

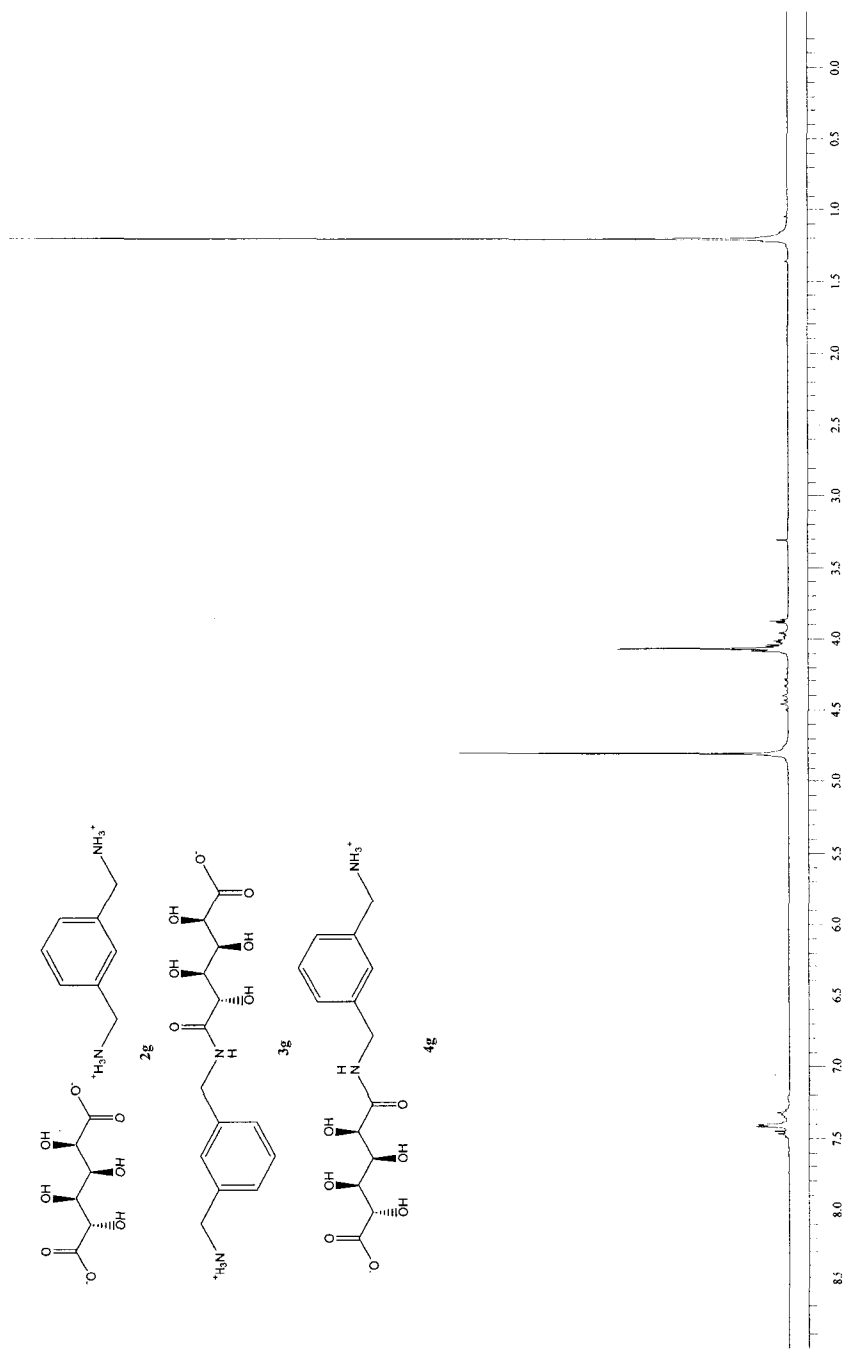


**Figure 11.** <sup>1</sup>H NMR (D<sub>2</sub>O) spectrum of *m*-xylylenediammonium D-glucarate salt (**2g**) / *N*-(*m*-amino-xylylene)-D-glucara-6-amic acid salt (**3g**) / *N*-(*m*-amino-xylylene)-D-glucara-1-amic acid salt (**4g**) mixture.

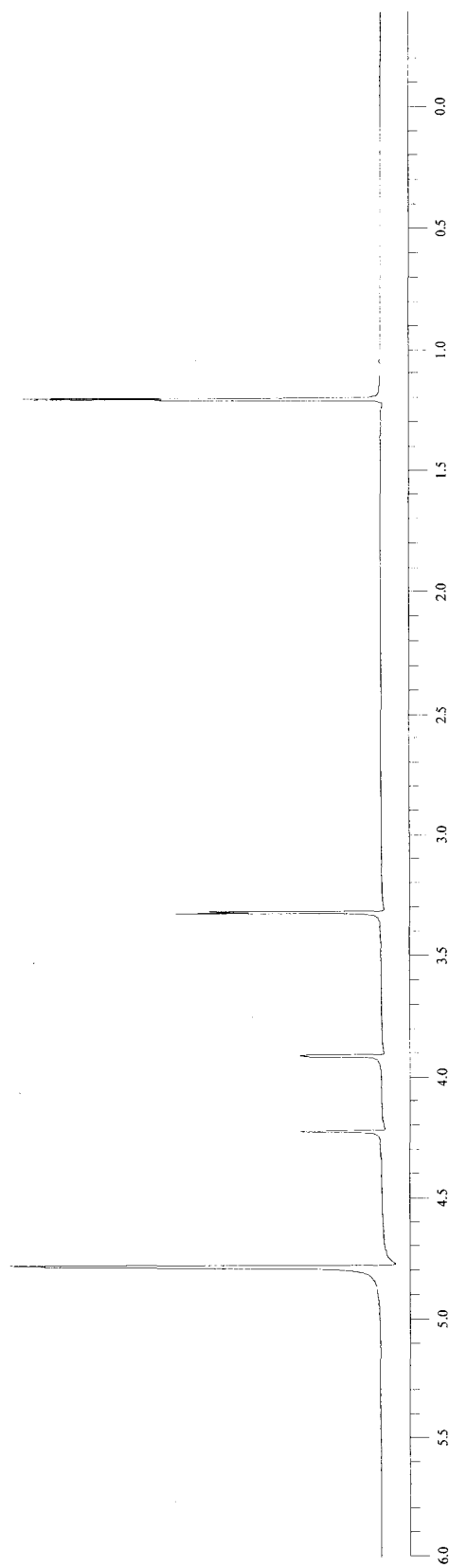
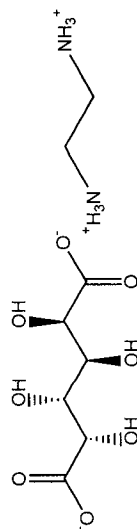


**Figure 12.** <sup>1</sup>H NMR (D<sub>2</sub>O) spectrum of ethylenediammonium D-galactarate (**5a**).

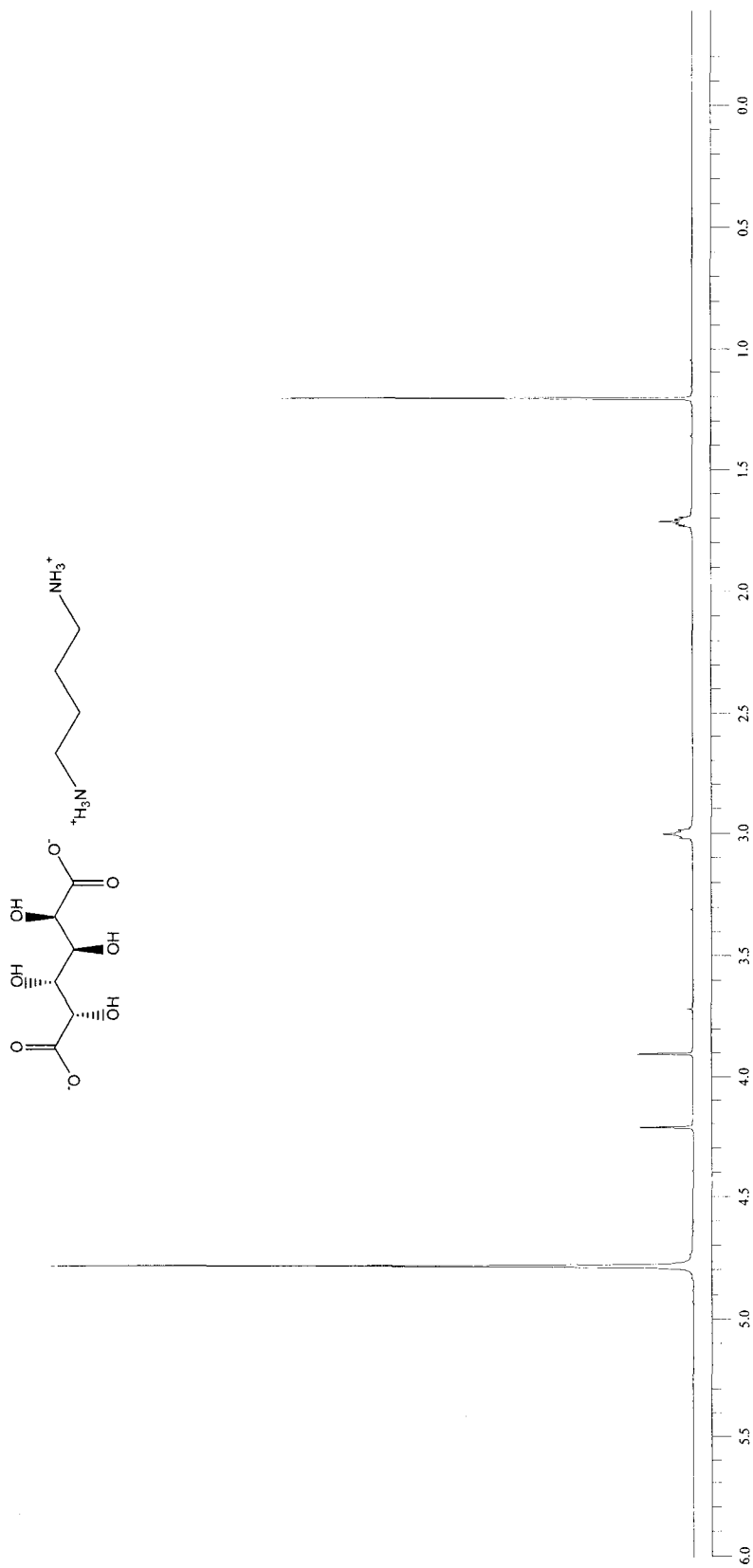


**Figure 13.** <sup>1</sup>H NMR (D<sub>2</sub>O) spectrum of tetramethylethylenediammonium D-galactarate (**5b**).

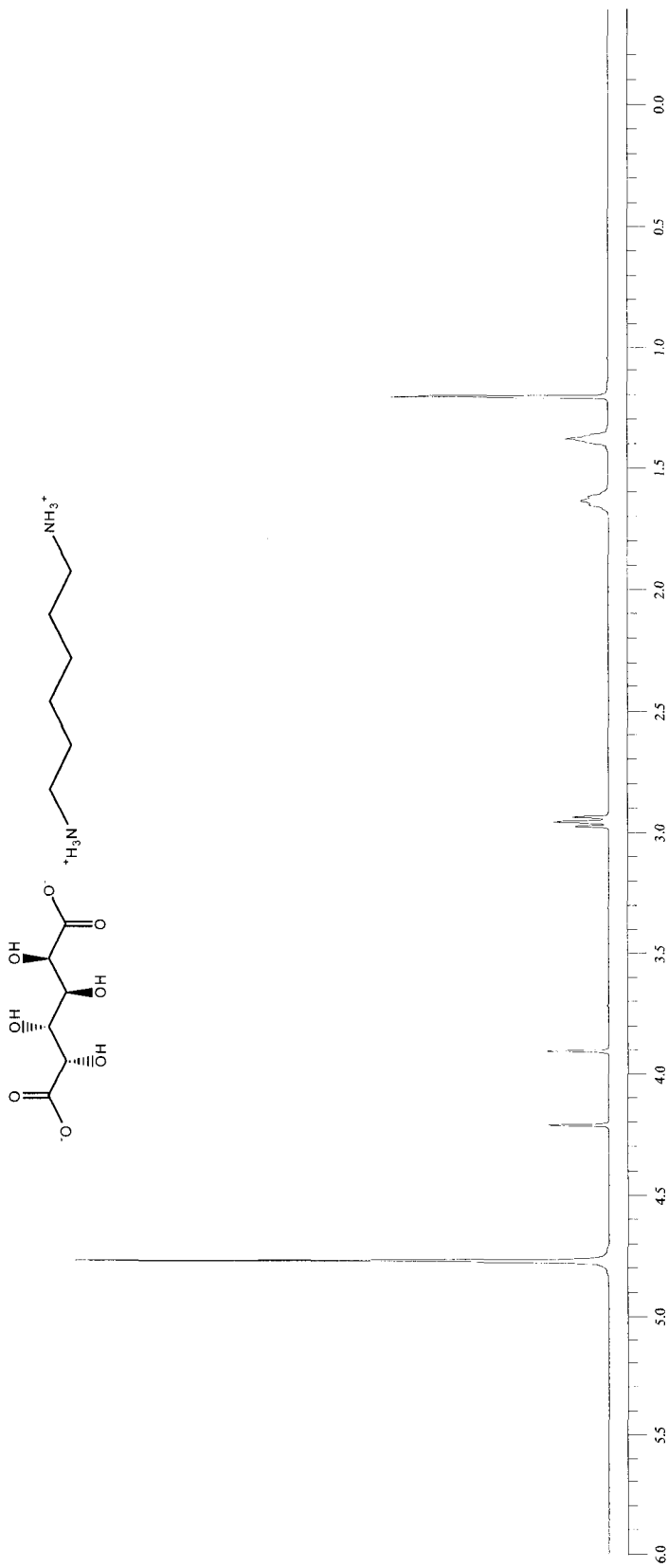


**Figure 14.** <sup>1</sup>H NMR (D<sub>2</sub>O) spectrum of hexamethylenediammonium D-galactarate (**5c**).

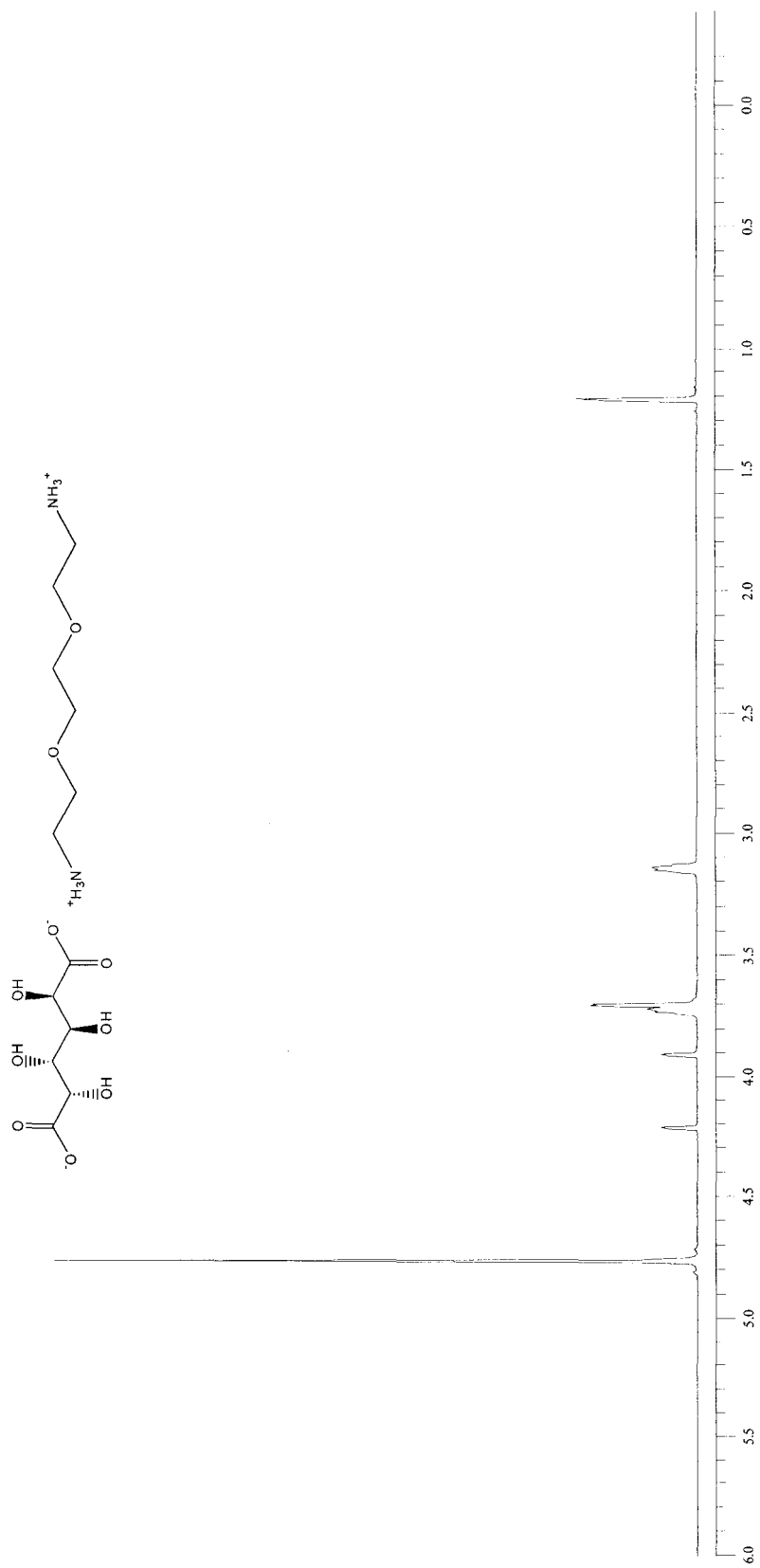


**Figure 15.** <sup>1</sup>H NMR (D<sub>2</sub>O) spectrum of 3,6-dioxaoctamethylenediammonium D-galactarate (**5f**).

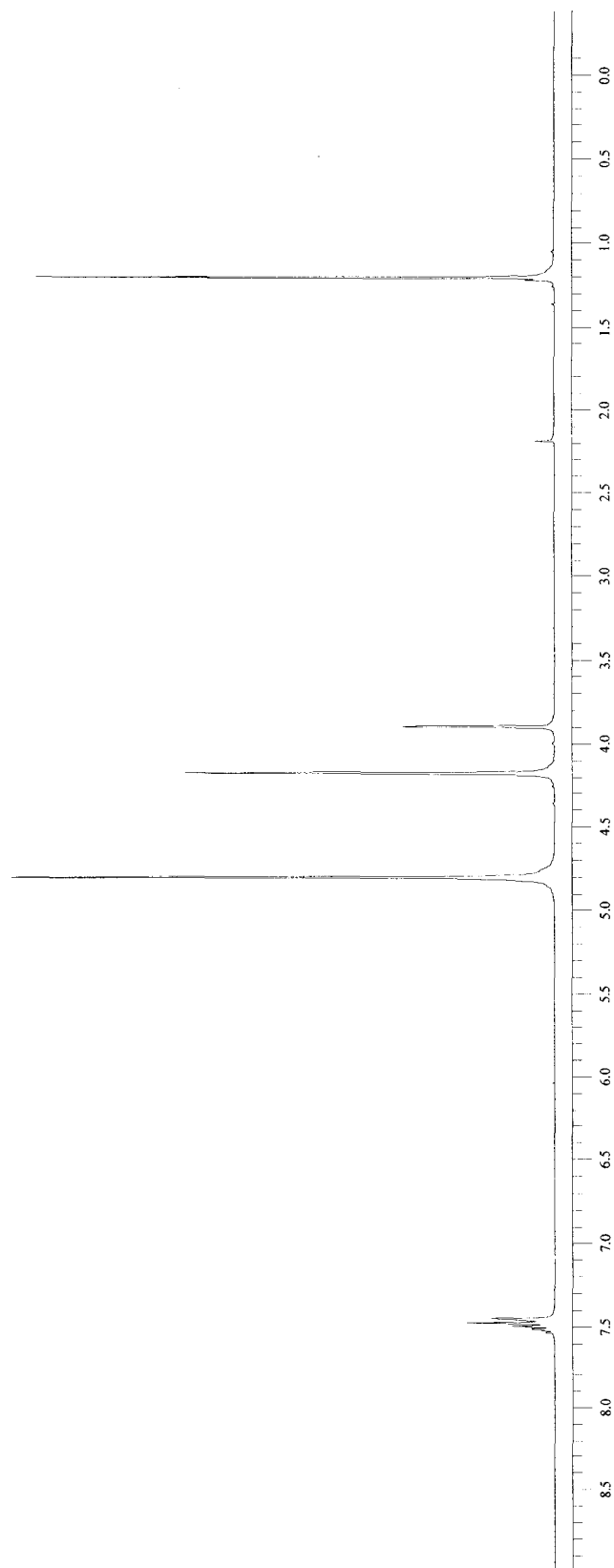
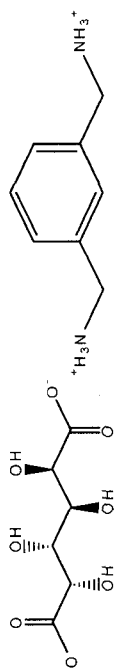


**Figure 16.** <sup>1</sup>H NMR (D<sub>2</sub>O) spectrum of *m*-xylylenediammonium D-galactarate (**5g**).



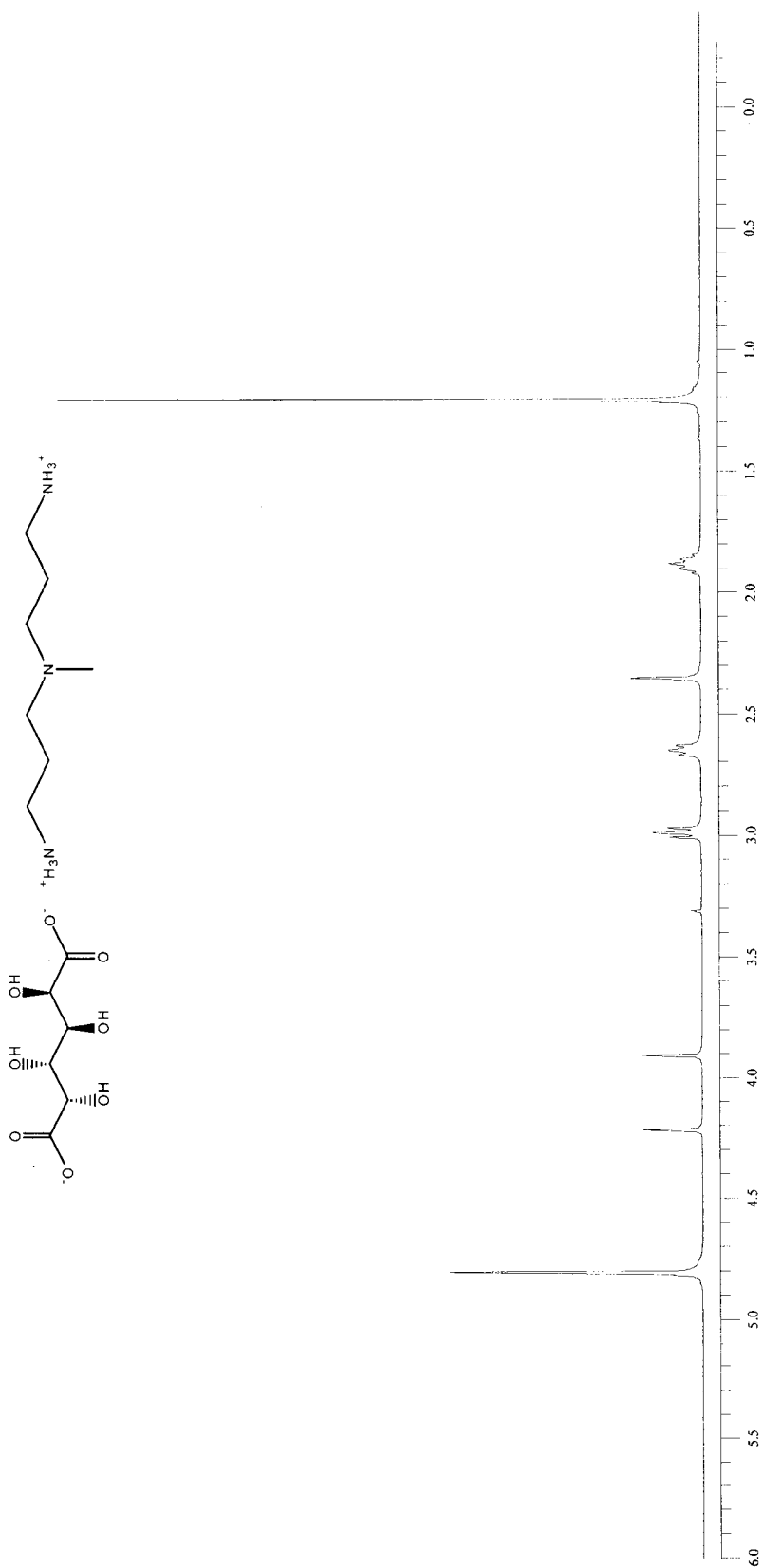


**Figure 17.** <sup>1</sup>H NMR (D<sub>2</sub>O) spectrum of 3,3'-diamino-N-methyl dipropylammonium D-galactarate (**5h**).

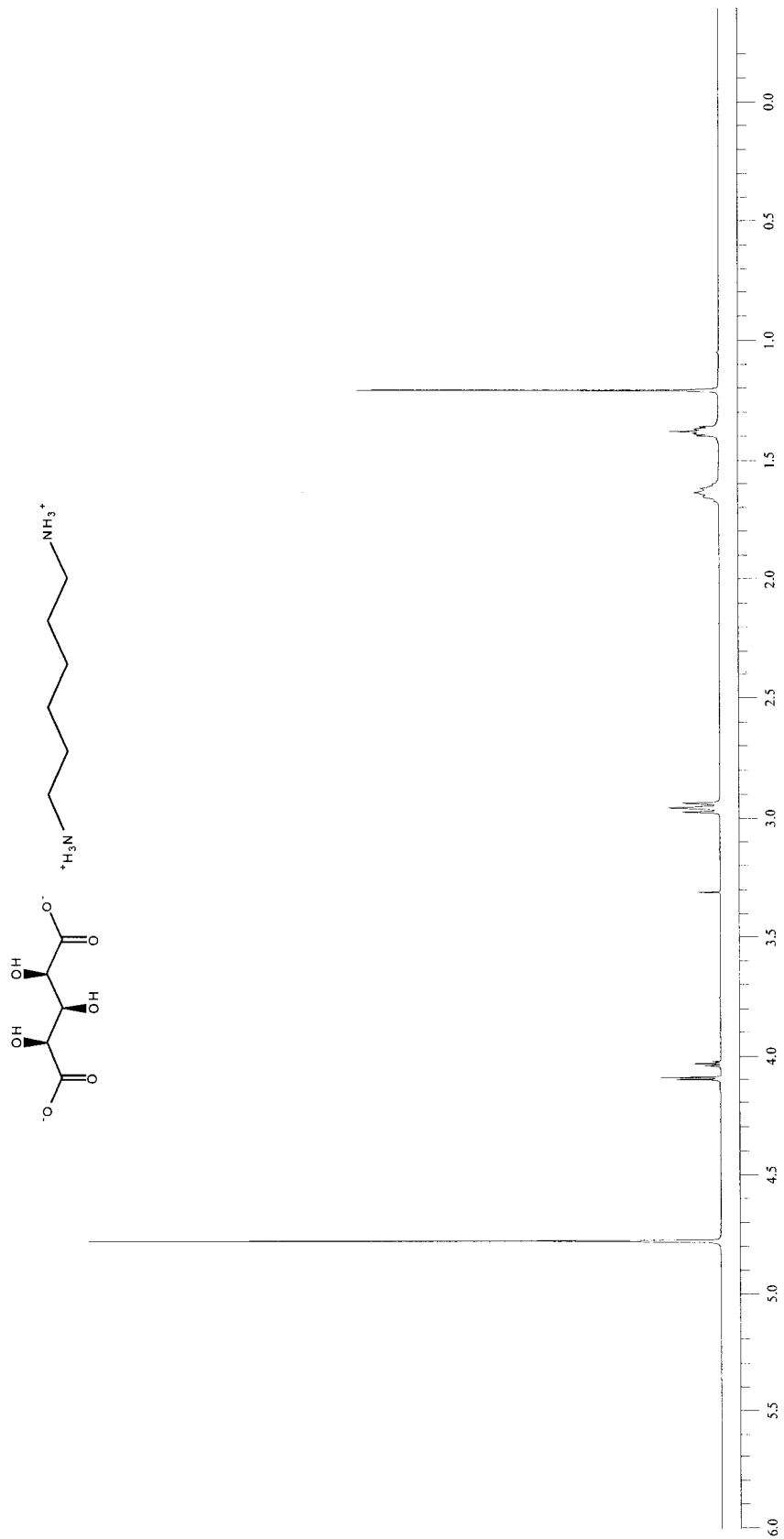


**Figure 18.** <sup>1</sup>H NMR (D<sub>2</sub>O) spectrum of hexamethylenediammonium D-xylarate (**6c**).

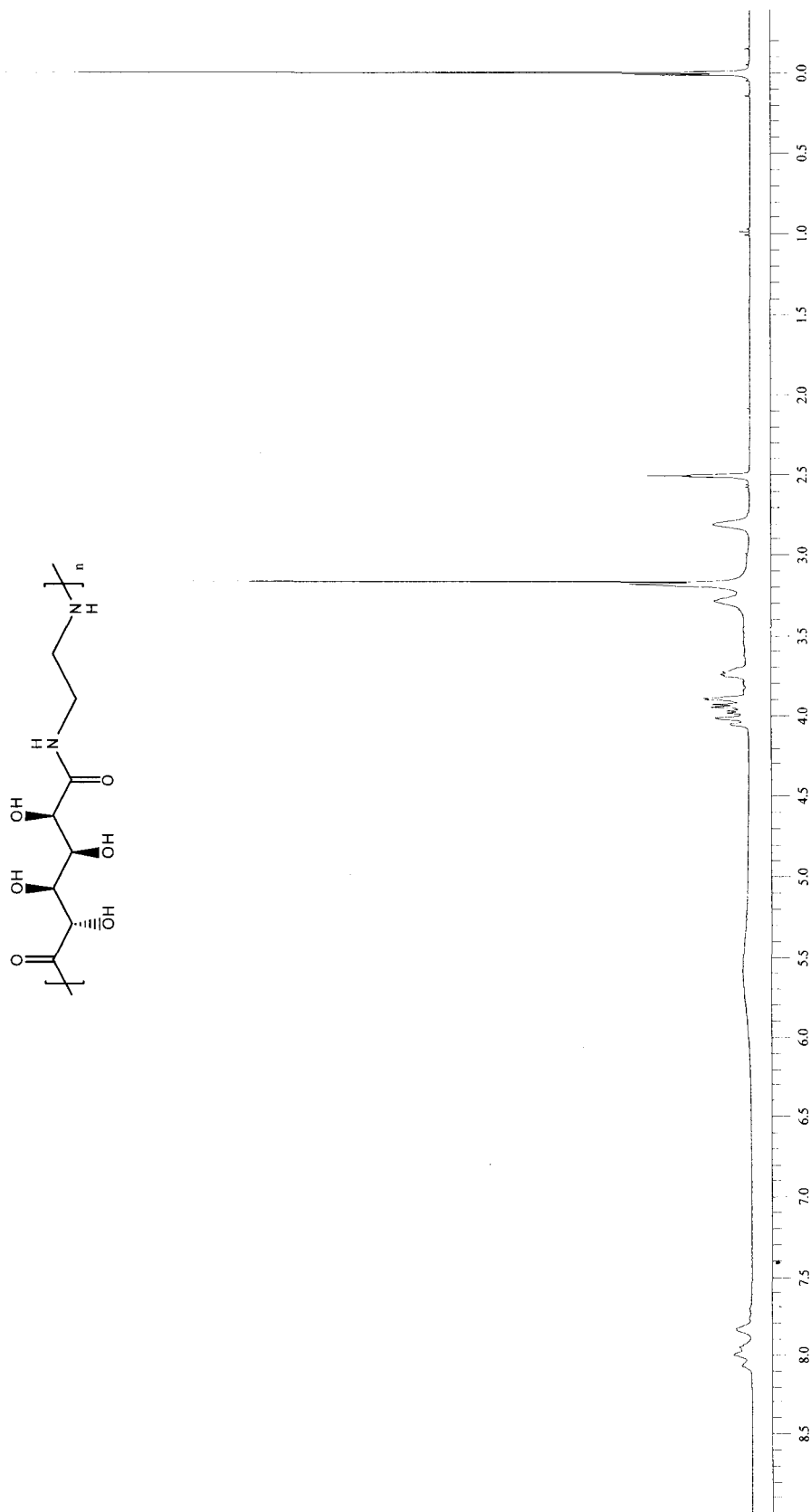


**Figure 19.**  $^1\text{H}$  NMR (DMSO- $d_6$ ) spectrum of *random* poly(ethylene D-glucaramide) (**7a**) prepolymer.

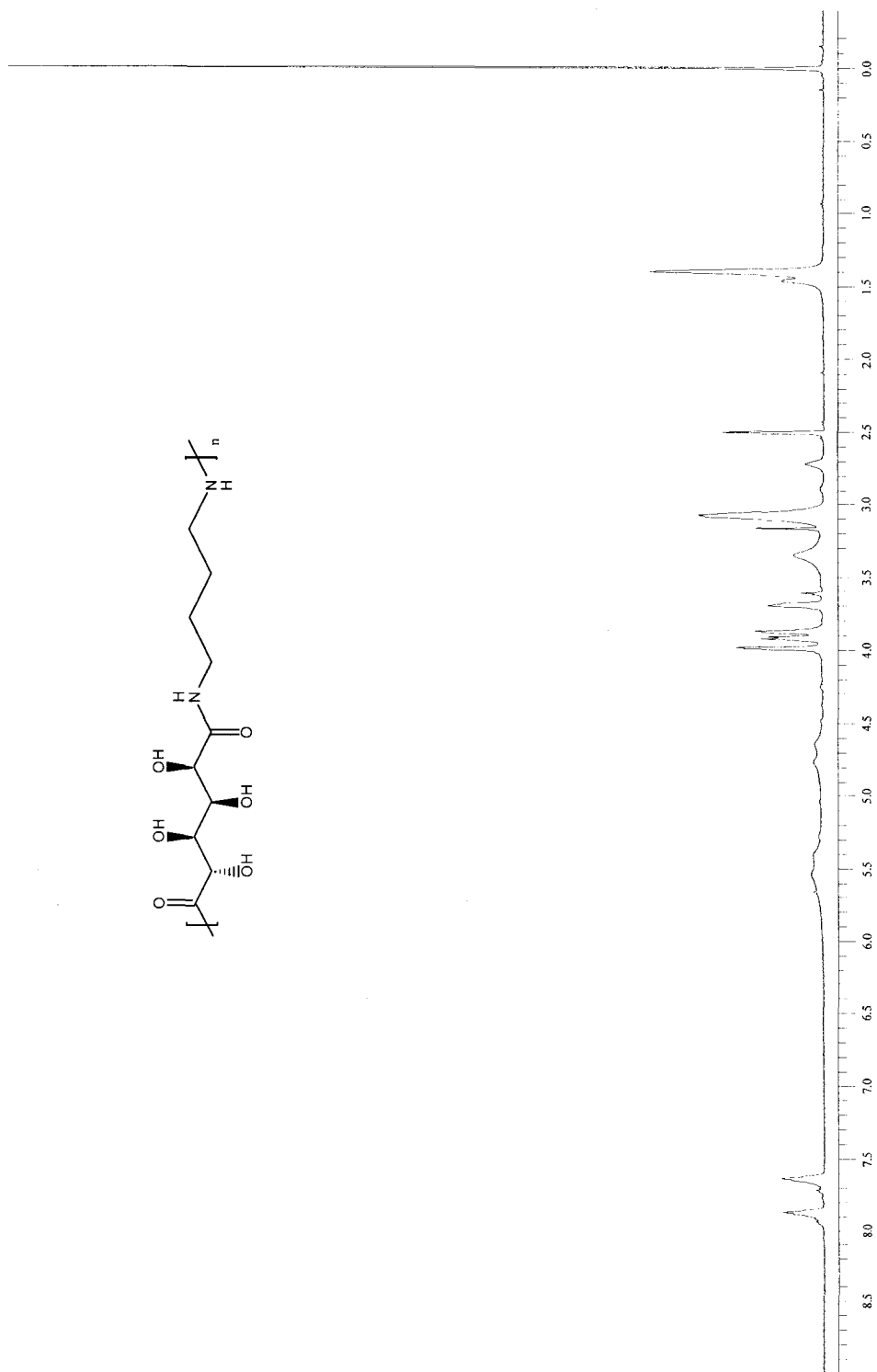


**Figure 20.** <sup>1</sup>H NMR (DMSO-d<sub>6</sub>) spectrum of *random* poly(tetramethylene D-glucaramide) (**7b**) prepolymer.

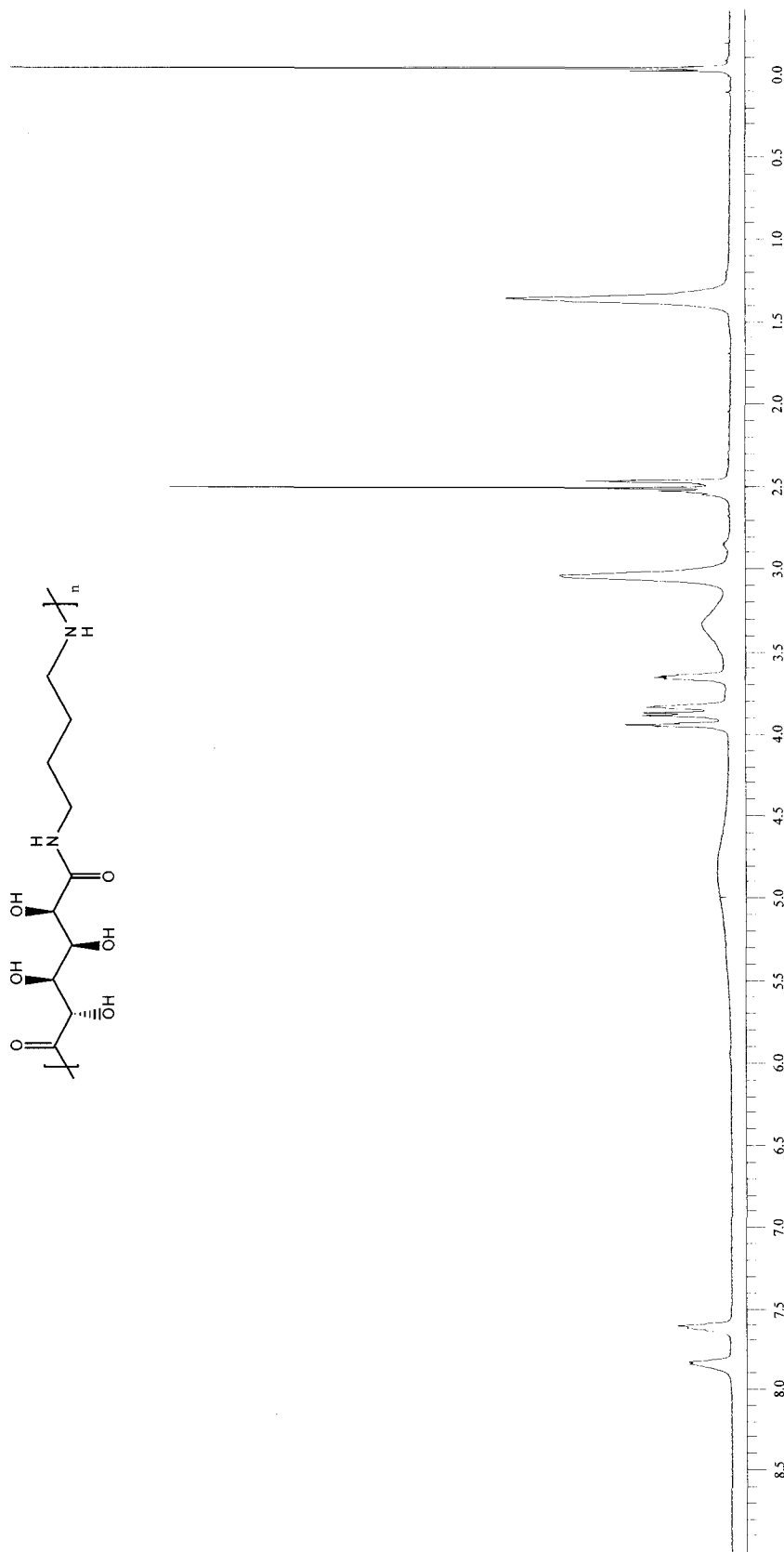


**Figure 21.** <sup>1</sup>H NMR (DMSO-d<sub>6</sub>) spectrum of *random* poly(tetramethylene D-glucaramide) (**7b**) postpolymer.

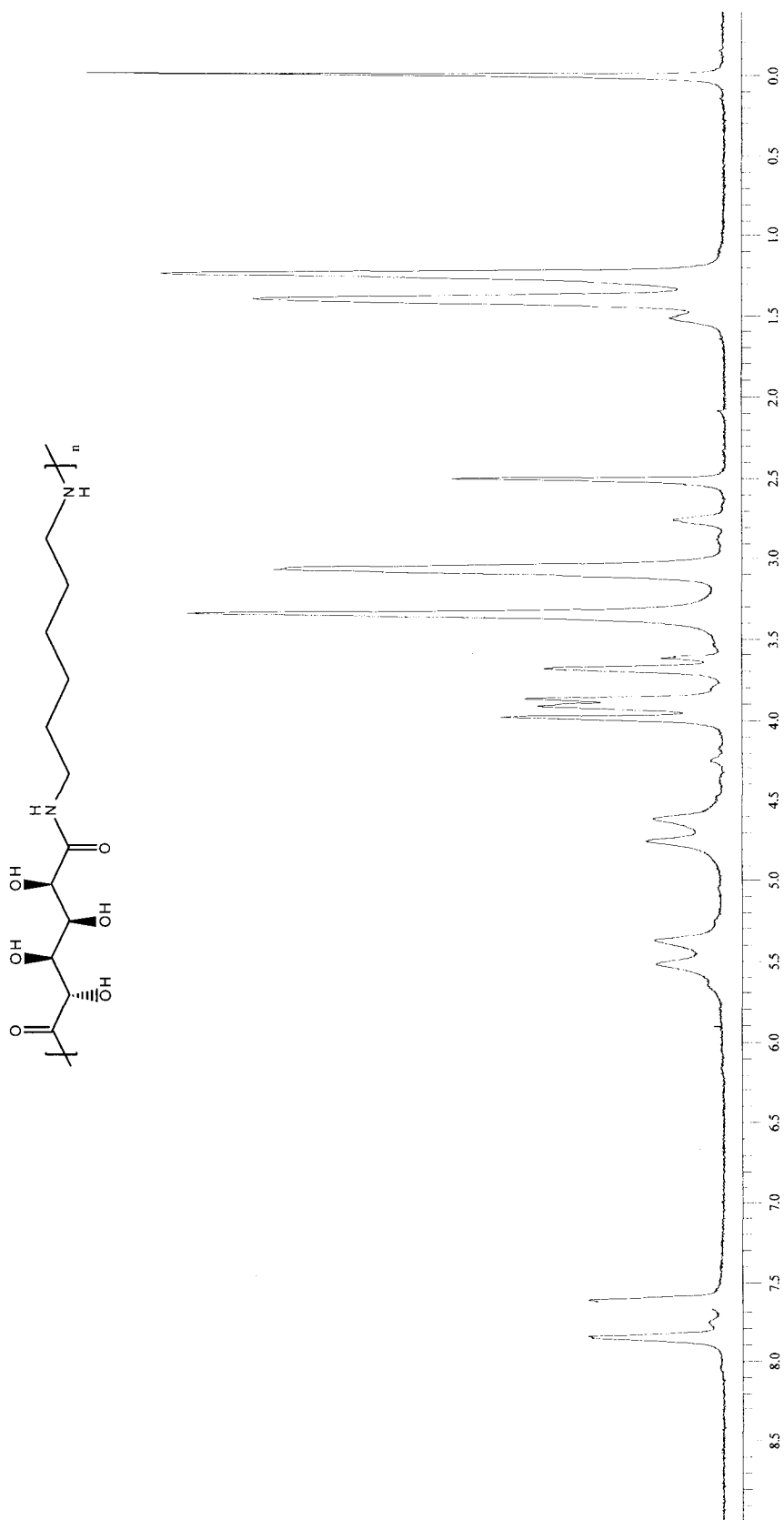


**Figure 22.** <sup>1</sup>H NMR (DMSO-d<sub>6</sub>) spectrum of *random* poly(hexamethylene D-glucaramide) (**7c**) prepolymer.

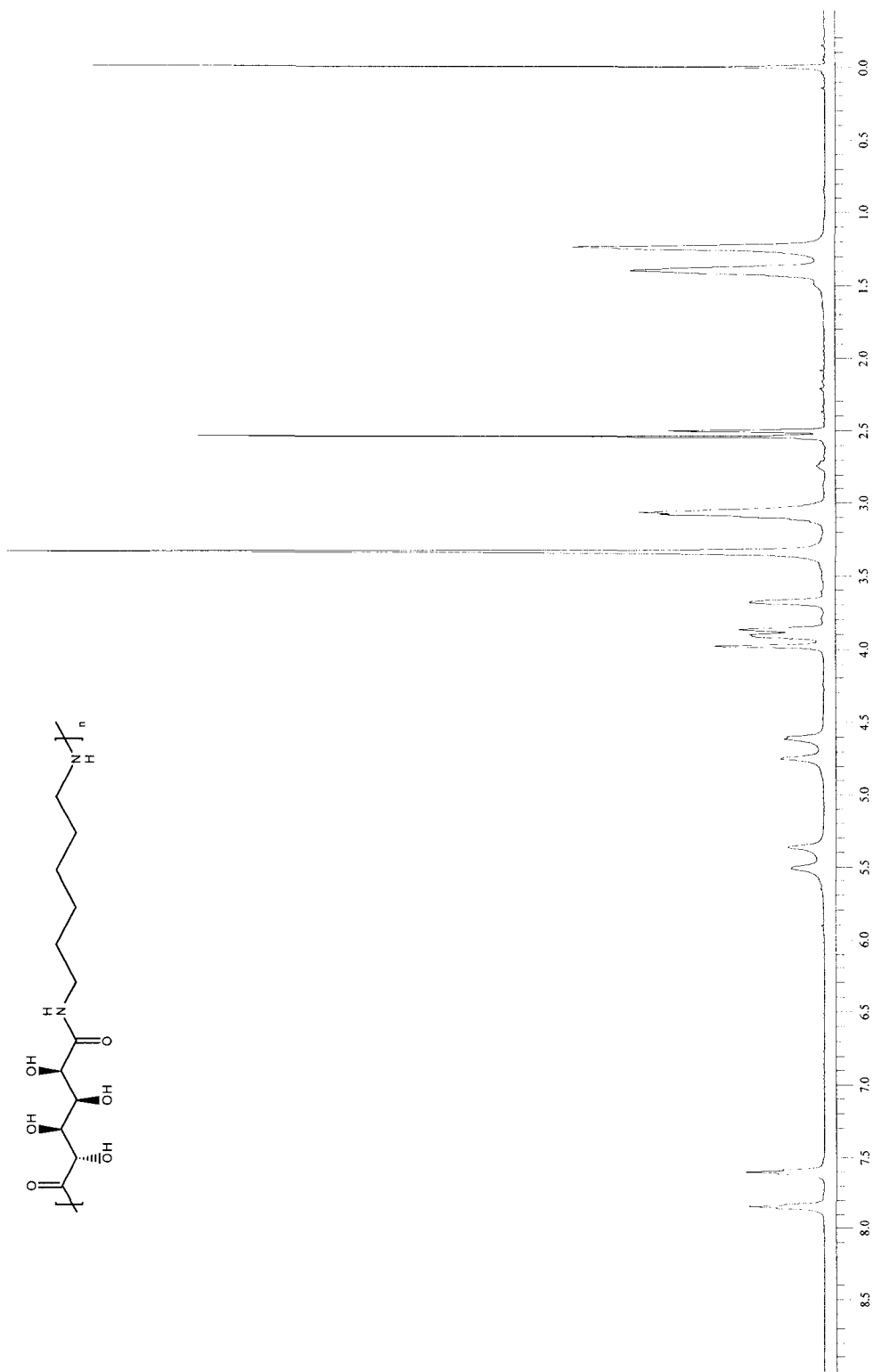


**Figure 23.** <sup>1</sup>H NMR (DMSO-d<sub>6</sub>) spectrum of *random* poly(hexamethylene D-glucaramide) (7c) postpolymer.

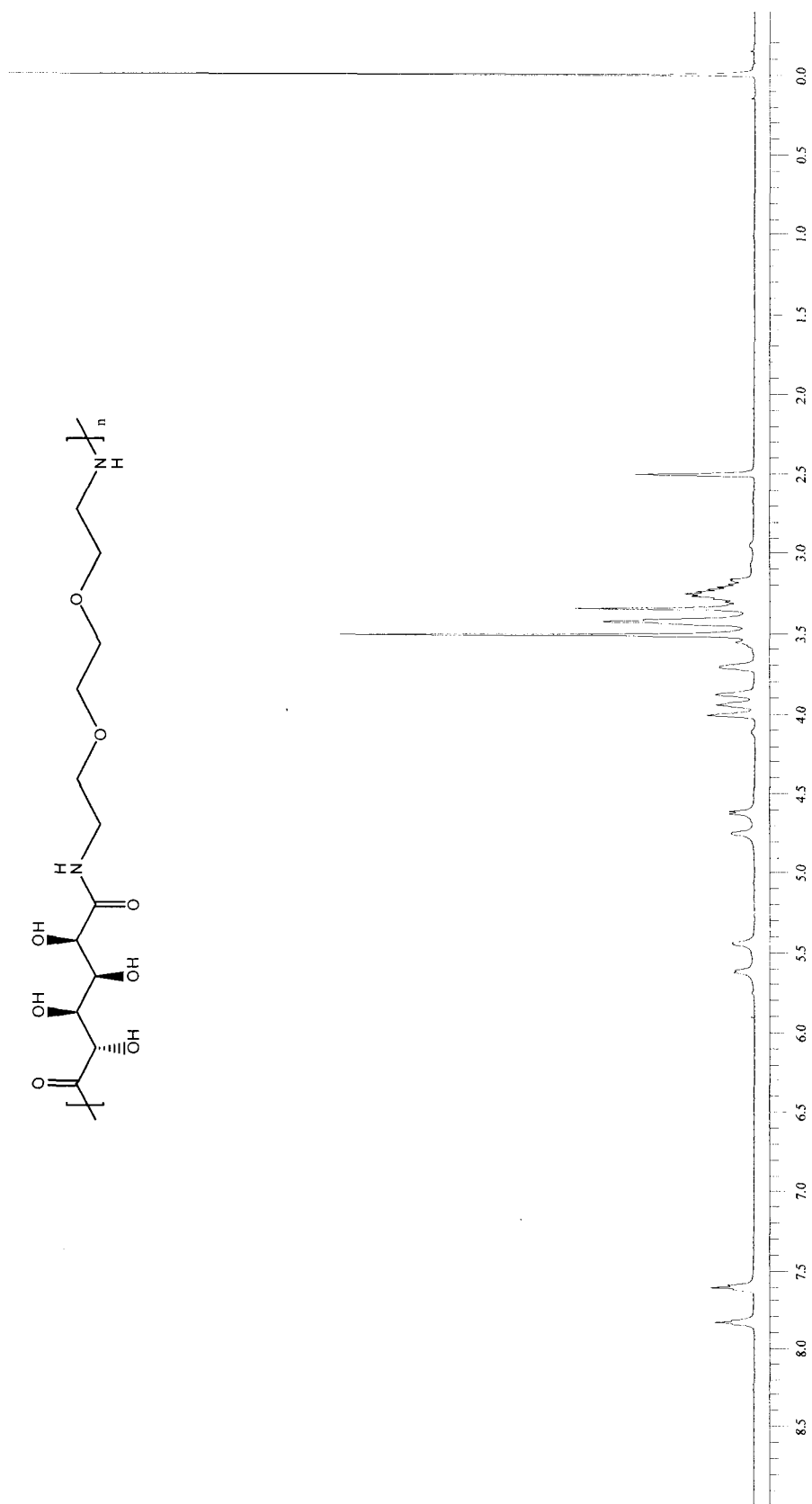


**Figure 24.** <sup>1</sup>H NMR (DMSO-d<sub>6</sub>) spectrum of *random* poly(3,6-dioxo-1,8-octamethylene D-glucaramide) (7f) prepolymer.



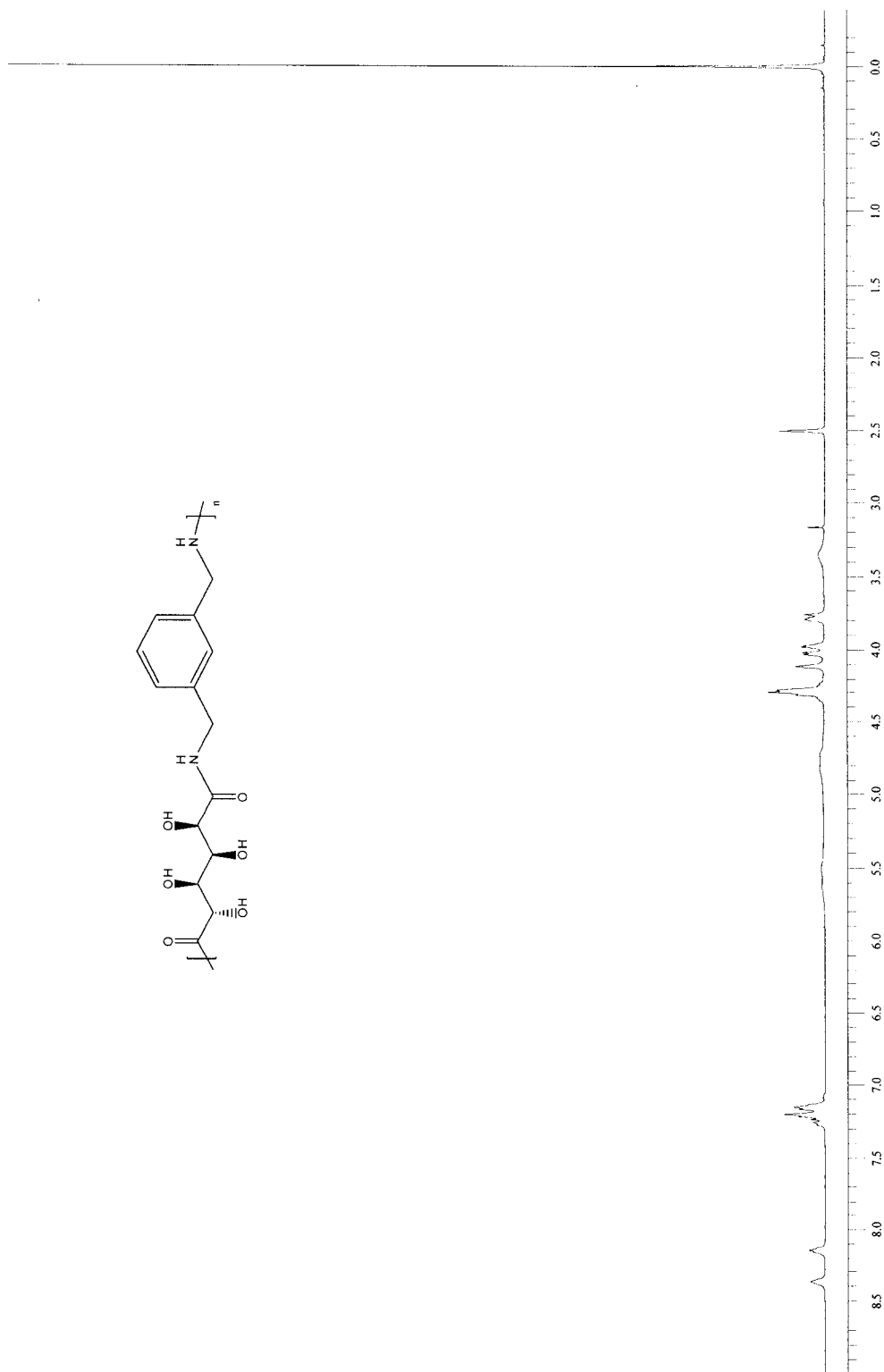


**Figure 25.** <sup>1</sup>H NMR (DMSO-d<sub>6</sub>) spectrum of *random* poly(*m*-xylylene D-glucaramide) (7g) prepolymer.

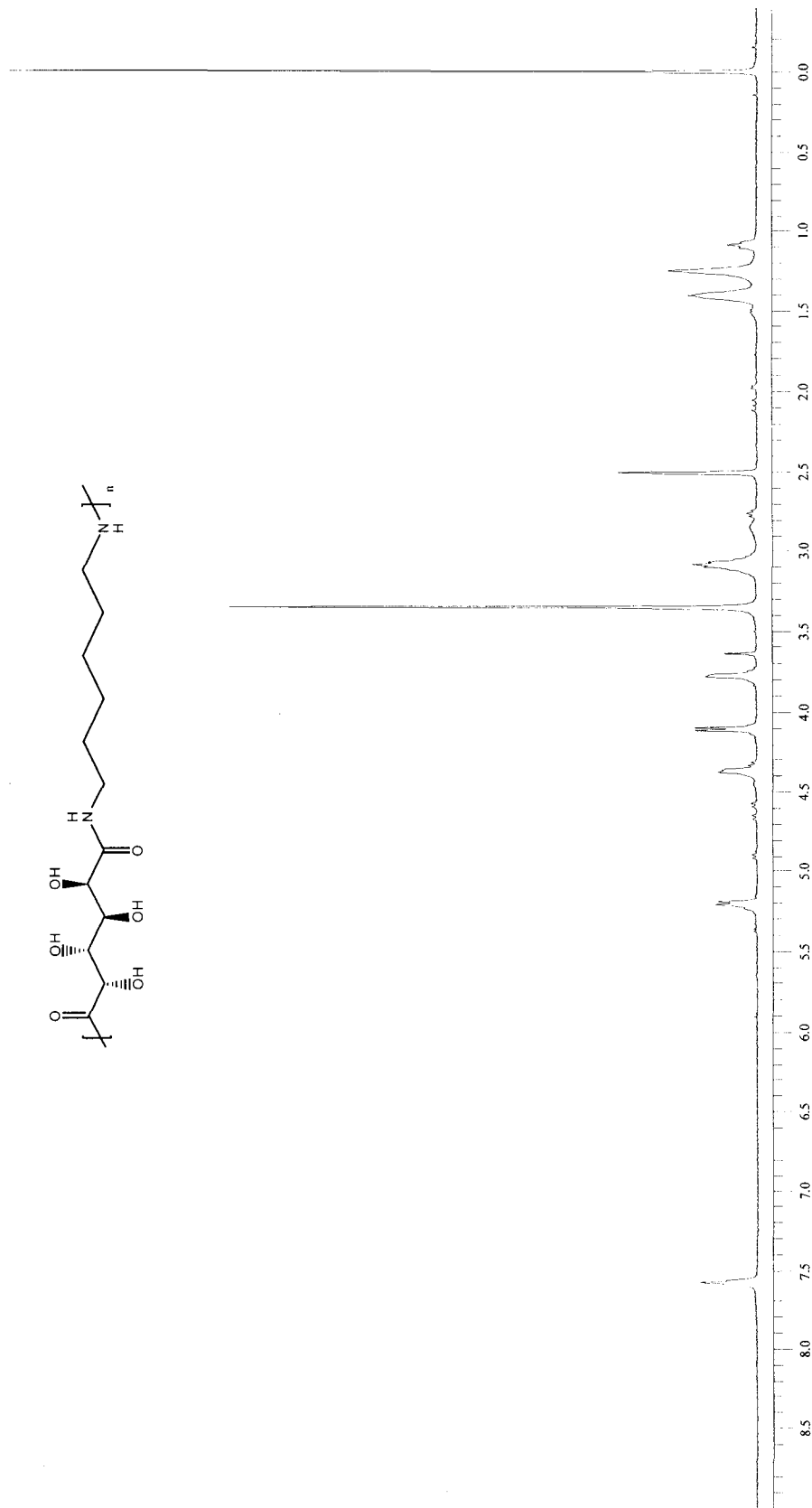


**Figure 26.** <sup>1</sup>H NMR (DMSO-d<sub>6</sub>) spectrum of *random* poly(hexamethylene D-galactaramide) (**8c**) prepolymer.

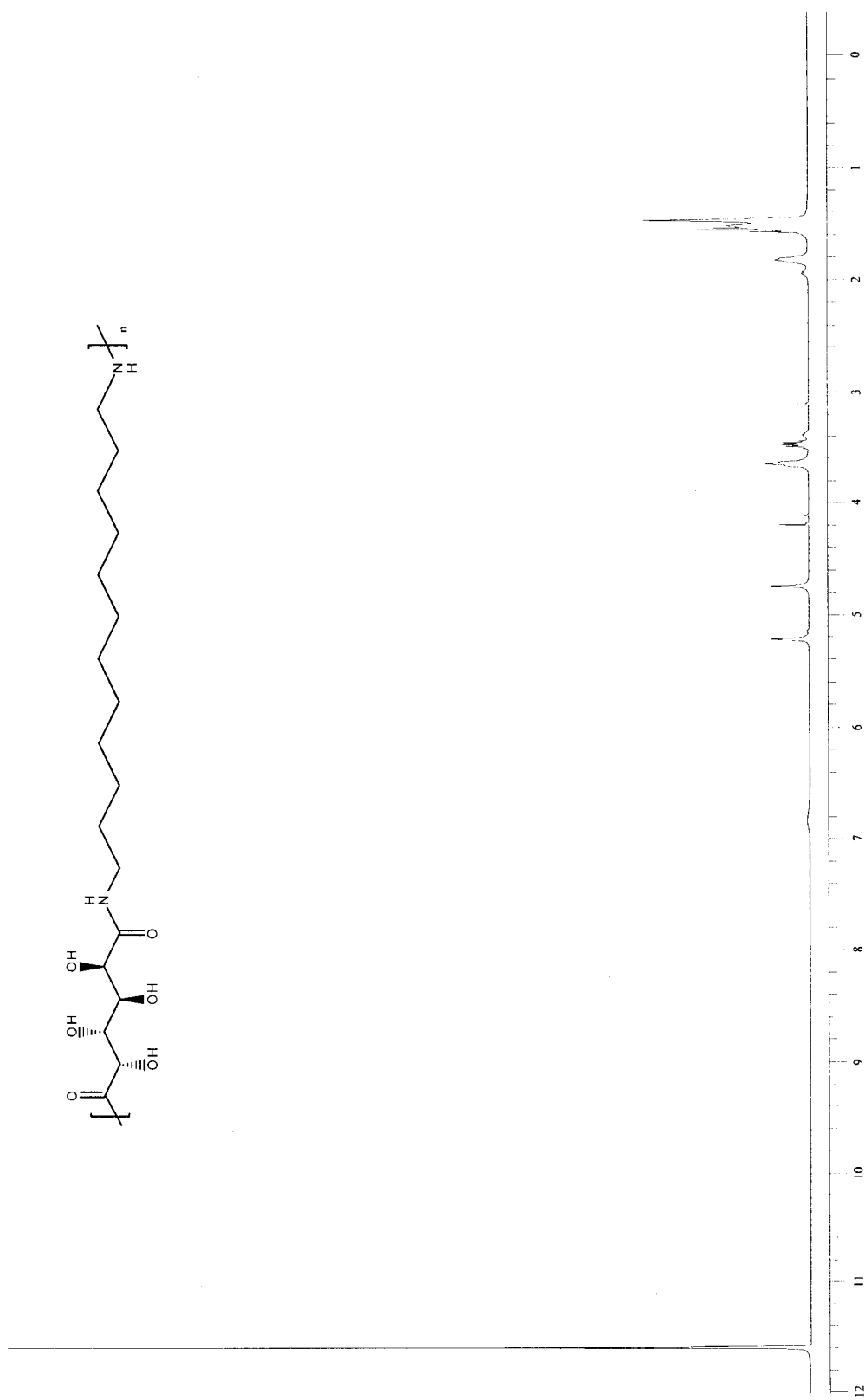


**Figure 27.** <sup>1</sup>H NMR (D<sub>2</sub>O) spectrum of *random* poly(dodecamethylene D-galactaramide) (**8e**) prepolymer.

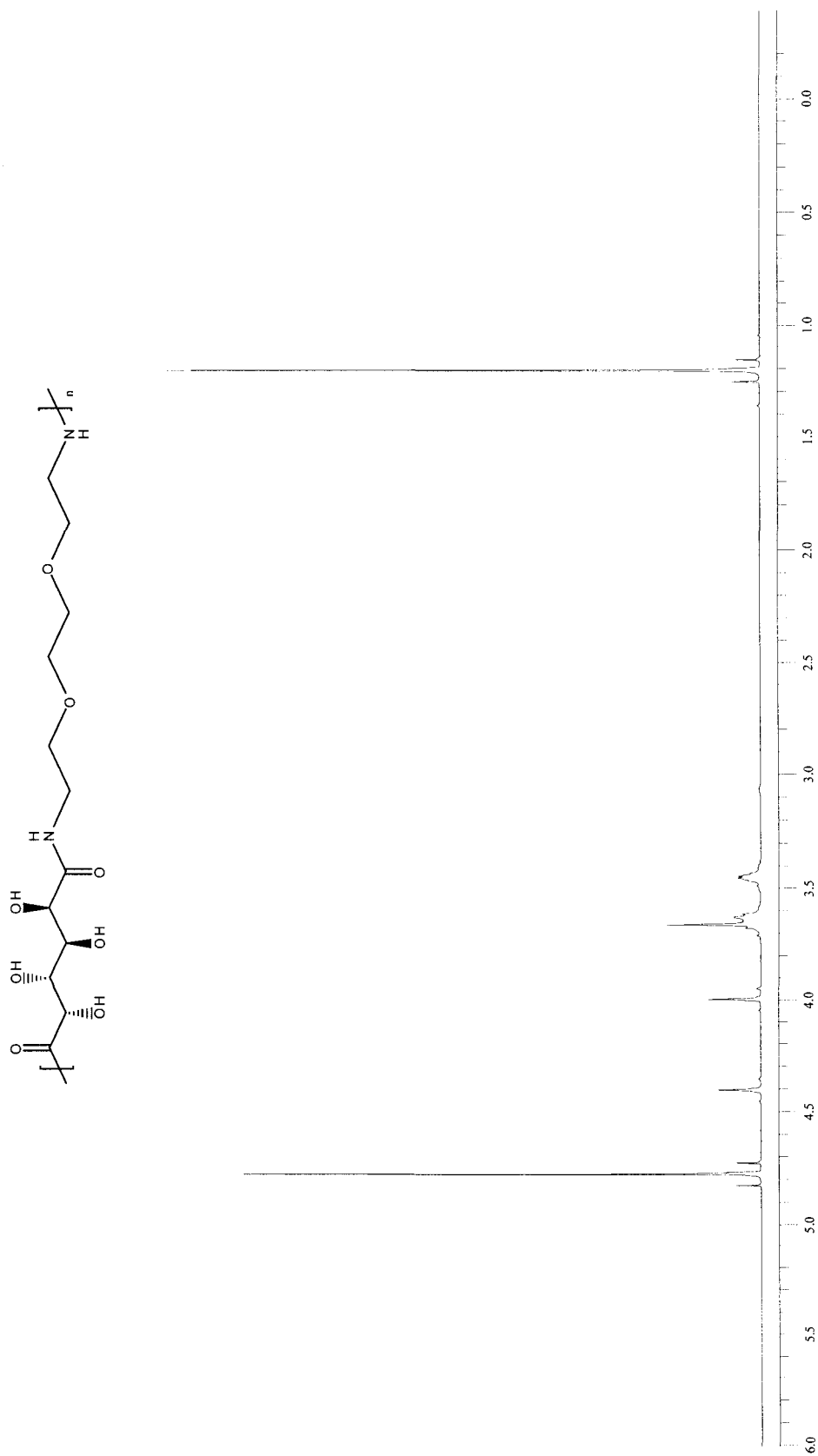


**Figure 28.** <sup>1</sup>H NMR (D<sub>2</sub>O) spectrum of *random* poly(3,6-dioxo-1,8-octamethylene D-galactaramide) (**8f**) prepolymer.